Platform of supramolecular assemblies of hydrogen bonding synthetic copolymers

Laura Vasilica Arsenie

THÈSE POUR OBTENIR LE GRADE DE DOCTEUR DE L'UNIVERSITÉ DE MONTPELLIER

En Chimie et Physico-Chimie des Matériaux

École doctorale Sciences Chimiques Balard

Unité de recherche de l'Institut Charles Gerhardt de Montpellier, UMR 5253

Plateforme d'assemblages supramoléculaires de copolymères synthétiques promoteurs de liaisons hydrogènes

Présentée par Laura Vasilica ARSENIE

Le 26 septembre 2022

Sous la direction de Vincent LADMIRAL et Sylvain CATROUILLET

Devant le jury composé de

Catherine LADAVIÈRE, DR, Université Claude Bernard Lyon 1	Président du Jury
Sébastien PERRIER, PU, University of Warwick/ Monash University, United Kingdom	Rapporteur
Olivier COLOMBANI, MCF, Université du Maine	Examinateur
Marie MORILLE, MCF, Institut Charles Gerhardt Montpellier (ICGM)	Examinatrice
Anja TRAEGER, AP, Friedrich-Schiller University of Jena, Germany	Invitée
Johannes C. BRENDEL, AP, Friedrich-Schiller University of Jena, Germany	Invité
Mona SEMSARILAR, CR, Institut Européen des Membranes Montpellier (IEM)	Invitée
Vincent LADMIRAL, DR, Institut Charles Gerhardt Montpellier (ICGM)	Directeur de thèse
Sylvain CATROUILLET, MCF, Institut Charles Gerhardt Montpellier (ICGM)	Co-encadrant

UNIVERSITÉ DE MONTPELLIER

Remerciements

Ces travaux de thèse ont été réalisés au sein de l'équipe Chimie et Matériaux Macromoléculaires (C3M) de l'Institut Charles Gerhardt (UMR 5253) de Montpellier et ont été financés par le Ministère de l'Education Nationale de l'Enseignement Supérieur et de la Recherche, ainsi que par l'Office allemand d'échanges universitaires (DAAD).

Tout d'abord, mes profonds remerciements sont exprimés à mes encadrants, M. Sylvain Catrouillet et M. Vincent Ladmiral, qui ont dirigé les travaux de ma thèse. Je tiens à vous remercier pour votre soutien dans chaque étape de cette thèse, votre grande disponibilité, votre esprit critique et votre aide dans tous les secteurs qui couvrent un projet de thèse (recherche scientifique, publications scientifiques, participations aux congrès, dépôt des projets scientifiques, ouverture de carrière après la thèse). Je vous remercie pour tout ce que vous m'avez appris pendant ces trois ans.

Je tiens à remercier M. Patrick Lacroix-Desmazes de m'avoir accueilli au sein de l'équipe C3M où j'ai effectué mes travaux de thèse, ainsi que pour ses conseils précieux et son participation active au sein des publications issues de cette thèse.

Je remercie particulièrement Mme. Catherine Ladavière et M. Sébastien Perrier qui me font l'honneur d'accepter d'être rapporteurs de ma thèse.

Je remercie également Mme. Marie Morille ainsi que M. Olivier Colombani qui ont accepté de juger ces travaux de thèse en qualité d'examinateurs.

Je tiens à remercier profondément Mme. Mona Semsarilar, Mme. Anja Traeger et M. Johannes C. Brendel d'avoir accepté de participer à ce jury de thèse en tant que membres invités.

Ainsi, je tiens à remercier particulièrement Mme. Mona Semsarilar pour le temps qu'elle m'a accordé à la préparation d'échantillons pour les analyses TEM, ainsi que pour sa collaboration au sein des publications sorties de ce projet de thèse.

Je tiens à exprimer mes sincères et profonds remerciements à Mme. Anja Traeger et à M. Johannes C. Brendel, pour leur grande disponibilité, leur soutien et leur conseils précieux qu'ont ouvert des perspectives prometteuses à ce projet de thèse dans les sciences biologiques. Merci de m'avoir accueilli dans votre laboratoire à Iéna (Allemagne) pendant le stage de

recherche dédiée aux essaies biologiques, qui a été une belle expérience professionnelle dans un milieu culturel international. *Mit freundlichen Grüßen*!

J'associe à mes remerciements Mme. Bénédicte Prélot et M. Amine Geneste pour leur conseils concernant les expériences de titrage calorimétrique isotherme, une analyse qui a constitué une partie importante de ces travaux de thèse. Je remercie M. Philippe Gonzales pour les mesures d'indice de réfraction, nécessaires lors de quelques études qui font partie de cette thèse. Je remercie l'équipe des biologistes du laboratoire IOMC (Iéna, Allemagne) de m'avoir accueilli dans leur groupe pendant trois mois, et de m'avoir formé avec professionnalisme pour travailler en biologie cellulaire : Carolin, Elisabeth, Lien et Friederike.

Je remercie particulièrement Maxime Colpaert, pour tout ce qu'il m'a appris en ce qui concerne les aspects techniques des manips de laboratoire, ainsi que pour son implication active dans un projet de recherche qu'on a mené ensemble sur la chimie du bore, en utilisant des polymères de cette thèse, projet qui aboutira à ses fins dans les prochains mois.

Je remercie les membres de l'équipe C3M, permanents comme non-permanents, nouveaux et anciens, pour leur aide et l'agréable environnement de travail dans lequel j'ai effectué mes travaux de thèse pendant ces trois ans.

De sincères remerciements aux anciens encadrants (des différentes stages) avec qui j'ai travaillé avant de commencer cette thèse. C'est en travaillant avec vous, que j'ai pris la décision de poursuivre une thèse et une carrière dans la recherche : Mme. Coline Pinese, Mme. Florina Dumitru, M. Mihai Barboiu, Mme. Nicoleta Badea, Mme. Ioana Lacatusu, Mme. Ionela Neacsu et M. Anton Ficai.

Il faut aussi vivre hors d'une thèse ! Dans ce contexte, merci à mes amies, Samantha, Ioana et Elodie, pour votre écoute, votre soutien et les inoubliables soirées cocktail- détente.

Mes plus profonds remerciements s'adressent à mes parents, qui m'ont toujours encouragé et aidé. Vous avez été toujours là, pour moi, et vous m'avez soutenu, dans chaque étape de ma vie. Votre amour me guide chaque jour. Également, j'associe mes vifs remerciements à ma belle-famille, que j'apprécie beaucoup.

Enfin, je tiens à remercier à mon compagnon, Richard, pour son soutien moral, son écoute, sa patience énorme et son amour, qui m'ont été d'une aide profonde durant ces années. Merci d'être à mes côtés, toujours, dans toutes les circonstances !

A ma grande-mère, Veronica

Préface

Abréviations

Polymers

PNIPAM	Poly(N-isopropylacrylamide)
PMA	Poly(methyl acrylate)
PS	Polystyrene
PEG	Poly(ethylene glycol)
PPMA	Poly(propargyl methacrylate)
PCL	Polycaprolactone
PC	Polycarbazole
PC-T	Polycarbazole-thymine
PPG	Polypropylene glycol
BU-PPG	telechelic uracyl-functionalized polypropylene glycol
BA-PEG	Adenine difunctionalized polyethylene glycol
A-PEG	Adenine monofunctionalized polyethylene glycol
T-PEG	Thymine functionalized polyethylene glycol
POEGMA	Poly(oligoethylene glycol methacrylate)
PMBA	Poly(n-butyl methacrylate)
POEGMA-b-PMBA	Poly(oligoethylene glycol methacrylate-b-n-butyl methacrylate)
A-PCL	Adenine functionalised polycaprolactone
U-PCL	uracil functionalized polycaprolactone
PNAM	Poly(4-acryloylmorpholine)
PMMA-b-PTMA	Poly(methyl methacrylate)-b-poly(thymine methacrylate)
PMMA-b-PAMA	Poly(methyl methacrylate)-b-poly(adenine methacrylate)
PNAM-b-PTAm	Poly (N-acryloil morpholine)-b-Poly(acryl amide thymine)
PNAM-b-PAAm	Poly (N-acryloil morpholine)-b-Poly (acryl amide adenine)
P(NAM)-g-S	galactose grafted Poly (N-acryloil morpholine)
PAEFC	Poly(2-acryloyloxyethyl ferrocenecarboxylate)
PLA	polylactic acid/polylactide
PAH	Poly (N-acryloil azocane)
PMEMA	Poly[2-(N-morpholino)ethyl methacrylate])
PNEMA	Poly(N-ethylmorpholine methacrylamide)

PAZd	Poly(N-acryloyl-2,5-dimethylpiperazine)
PIPAAm	Poly(N-isopropylacrylamide)
PDA	Polydopamine
PVDF	Poly(vinylidene fluoride)
PEG	Poly(ethylene glycol)
PEG-DA	Poly(ethylene glycol) diacrylate
RAFT	Reversible addition-fragmentation chain transfer polymerization
ATRP	Atom transfer radical polymerisation
PAGA	Poly (2-acrylamidoglycolic acid)
PNAM-MA	Poly(acryloyl morpholine) methacrylate
PVP	Poly(N-vinyl pyrrolidone)
PNAM	Poly(N-acryloil morpholine)
P(NAM-NAS)	Poly(N-acryloil morpholine-co-N-accryloxysuccinimide)
P(NAM-HEMA)	Poly(N-acryloil morpholine-co-hydroxyethylmethacrylate)
P(NAM-GLA)	Poly(acryloil morpholine – co-glycerol acrylate)
PNAM- b-PIPAAm	Poly(acryloyl morpholine)-b-Poly(N-isopropylacrylamide)
P(NAM-b-NAT)	Poly(acryloil morpholine)-b- Poly(acryloyl thiomorpholine)
(PNAM-b-PDA)	Poly(acryloyl morpholine) -b-Poly(glycyl tertbutyl ester bearing catechol)
P($UrMA_n$-*stat*-$THOXMA_m$)	Poly((3-(uracil-1-yl) propyl methacrylate) -*stat*-(2-ethyl thiomorpholine oxide methacrylate))
PEG_{112}-*b*-P($AdMA_n$-*stat*-$THOXMA_m$)	Poly(ethylene glycol)-*b*-Poly((3-(adenine-9-yl) propyl methacrylate)-*stat*-(2-ethyl thiomorpholine oxide methacrylate))
P($AdMA_n$-*stat*-$THOXMA_m$)	Poly((3-(adenine-9-yl) propyl methacrylate) -*stat*-(2-ethyl thiomorpholine oxide methacrylate))
PPG	Poly(propylene glycol)
PEI	Poly(ethylene imine)

Organic molecules and monomers

βCD	beta cyclodextrin
HNE	4-hydroxy-2-nonenal
HEMA	2-hydroxyethyl methacrylate
NEMA	N-ethylmorpholine methacrylamide
NAM	N-acryloil morpholine

IPAAm	N-isopropylacrylamide
AG	argatroban
BMA	butyl methacrylate
NAT	N-acryloil thiomorpholine
VDF	vinylidene fluoride
NAS	N –acryloxy succinimide
BA	n butyl acrylate
ManEA	mannosyl ethyl acrylate
AEM	aminoethyl morpholine
PBA	phenyl boronic acid
AA	acrylic acid
MMA	methyl methacrylate
THMA	2-ethyl thiomorpholine methacrylate
THOXMA	2-ethyl thiomorpholine oxide methacrylate
UrMA	3-(uracil-1-yl)propyl methacrylate
AdMA	3-(adenin-9-yl)propyl methacrylate

Genetic material and Nucleobases

DNA	deoxyribonucleic acid
RNA	ribonucleic acid
siRNA	small interfering RNA
pDNA	plasmid DNA
mRNA	messenger RNA
poly(A)	poly(adenylic acid)
T	Thymine
A	Adenine
U	Uracil
G	Guanine
C	Cytosine
BU	Bi-uracil
BA	Bi-adenine
UPy	2-ureido-4-pyrimidinone
H-bonds	Hydrogen bonds
RNAse A	Ribonuclease A (an enzyme)

Organic Dyes

LY	Lucifer yellow

Organic ligands

NTA	Nitriloacetic acid

Cells

MC7	Human breast carcinoma cells
ECM	Extracellular matrix
L929	Mouse cell line

Aminoacids

Gly	Glycine
Ile	Isoleucine
His	Histidine

Inorganic molecules

NO	Nitric oxide

Drugs

PTX	Paclitaxel
DOX	Doxorubicin
ADT-OH	Anethole dithiolethione
Ibu	Ibuprofen

Proteins

ConA	Concanavalin A
CT	Cholera toxin
BSA	Bovin serum albumin
SA	Streptadivin

Biological receptors

CRGD (or cRGD)	Protein receptor

Pharmacology

IC_{50}	Inhibitory concentration

Oxydation sensitive materials

ROS	Reactive oxygen species

Solvents and buffers

THF	Tetrahydrofuran
PBS	Phosphate buffer solution
DMSO	Dimethyl sulfoxide
DMF	Dimethylformamide

$CHCl_3$	Chloroform
HEPES	4-(2-hydroxyethyl)-1-piperazineethanesulfonic acid buffer

Other abbreviations

LCST	Lower critical solution temperature
CMC	Critical Micellar Concentration
NPs	Nanoparticles
SN	Nucleophilic Substitution
T_g	Glass transition temperature
NMR	Nuclear Magnetic Resonance
DLS	Dynamic Light Scattering
SLS	Static Light Scattering
TEM	Transmission Electron Microscopy
SEC	Size Exclusion Chromatography
FTIR	Fourier Transform Infrared Spectroscopy
ITC	Isothermal Titration Calorimetry
CD	Circular Dichroism
N_{agg}	Aggregation Number
Z_{ave}	Particle size
R_g	Radius of gyration
R_h	Hydrodynamic diameter
q	Wave vector
n	Refractive index
M_w	Weight average molecular weight
M_n	Number average molecular weight
Đ	Dispersity
DP	Degree of polymerisation
N_A	Avogadro's number

Table des matières

Table des matières

Introduction générale

Introduction générale

Dans les systèmes vivants, l'organisation du matériel génétique (ADN et ARN) en simple brin, double brin et double hélice, est le résultat de nombreuses interactions supramoléculaires sélectives (liaisons hydrogène, interactions $\pi - \pi$, etc.) qui guident la formation des structures hiérarchiques du matériel génétique.[1]

Toutefois, la structure des bases azotés à base de noyaux aromatiques est hydrophobe. Ces interactions de nature hydrophobe sont classiquement à l'origine de nombreuses structures auto-assemblées en solution avec de nombreuses morphologies obtenues (micelles, cylindres, etc.). Ces interactions hydrophobes sont nécessaires pour obtenir des auto-assemblages supramoléculaires dans l'eau avec des liaisons hydrogène (par exemple à base de bisurées ou de peptide cycliques). Mais, il est difficile de moduler la balance hydrophile/hydrophobe ainsi que le nombre de liaisons hydrogènes dans ces systèmes.

Le principe de la reconnaissance moléculaire entre les bases nucléiques (aussi appelées nucléobases ou bases azotées) complémentaires (*i. e.*, adénine - thymine A – T, dans l'ADN, adénine-uracile A - U, dans l'ARN ou cytosine – guanine C – G dans l'ADN et l'ARN) a inspiré la synthèse de copolymères contenant des nucléobases. Ces travaux occupent une place significative dans la littérature ces dernières années.[2] Ces polymères ont notamment été utilisés dans la formation d'assemblages supramoléculaires organisés mimant l'ADN, un domaine qui ouvre de nombreuses applications à l'interface entre la chimie et la physico-chimie des polymères et la biologie (systèmes de délivrance des principes actifs, thérapie génique, etc.).

Les polymères contenant des bases nucléiques présentent des particularités structurales spécifiques qui expliquent leur capacité à s'organiser dans des architectures supramoléculaires. Tout d'abord, ils contiennent des unités nucléobases (adénine, cytosine, thymine, uracile etc.) qui sont les motifs structuraux clés du matériel génétique. Elles interviennent dans l'organisation et la réplication de l'ADN *via* la reconnaissance moléculaire par liaisons hydrogène entre nucléobases complémentaires. Un autre avantage de ces polymères consiste dans la possibilité de moduler la balance du caractère hydrophile/hydrophobe, en variant le synthon polymérisable (acrylate, acrylamide, méthacrylate, méthacrylamide, vinyle, etc.), l'espaceur qui relie l'unité polymérisable à la nucléobase, ou bien en utilisant des co-monomères avec une hydrophilie différente.[3] Contrôler la balance hydrophile/hydrophobe est important afin de maitriser l'équilibre entre les interactions hydrophobes (forces de Van der

Waals, etc.) et les liaisons d'hydrogène, qui sont les interactions majeures responsables de l'organisation supramoléculaire de ces polymères. Malgré leurs potentielles propriétés structurales uniques inspirés de l'ADN, les copolymères contenant des nucléobases n'ont été étudiés que dans des solvants organiques (DMF, DMSO, ou $CHCl_3$) jusqu'à présent dans la littérature.[4] La non-solubilité dans l'eau (ou dans des systèmes tampon à pH physiologique) de ces polymères représente l'un des verrous majeurs afin d'être utilisés en biologie.

Grâce à leurs particularités structurales, les copolymères synthétiques porteurs des bases nucléiques forment des co-assemblages supramoléculaires avec différentes morphologies (sphères, cylindres ou vésicules).[2,3,4] Les morphologies adaptables présentées dans les travaux de la littérature sont influencées surtout par l'architecture des copolymères de départ (le dégrée de polymérisation, le nombre de nucléobases dans le polymère), et donc la balance hydrophile/hydrophobe du système. Ainsi, quelques travaux ont montré la dépendance des morphologies formées en fonction du solvant due à leur capacité à former ou limiter la formation des liaisons hydrogène.[5] Globalement, les exemples illustrés dans la littérature ont montré que ces morphologies résultent des équilibres entre les interactions supramoléculaires (liaisons hydrogènes, forces van der Waals, interactions $\pi - \pi$) et sont influencés par les paramètres structuraux des polymères. Ces premiers travaux apportent une preuve de concept sur l'autoassemblage des copolymères contenant des bases nucléiques, mais ils n'ont pas étudié précisément les paramètres qui influent sur ces co-assemblages, ni leurs limites.

La connaissance de l'origine des autoassemblages obtenues (*i.e.,* liaisons hydrogène complémentaires ou interactions hydrophobe) est d'une importance majeure pour maitriser la dynamique d'auto-assemblage : obtenir des auto-assemblages réversibles ou irréversibles, et pour contrôler la cinétique de l'auto-association. Des travaux antérieurs sur les oligonucléotides ont montré que l'organisation hélicoïdale de l'ADN pouvait être la conséquence d'échanges dynamiques de liaisons H entre les nucléobases complémentaires, tandis que les interactions hydrophobes (c'est-à-dire l'empilement entre les régions aromatiques des nucléobases) étaient impliquées dans la stabilisation de l'hélice d'ADN.[6] D'autres études menées sur les autoassemblages des polymères contenant de l'urée ont montré que la dynamique d'association par des liaisons hydrogène est liée à la morphologie des autoassemblages.[7] Dans ce cas, des morphologies complexes de type cylindres ont été le résultat d'un échange dynamique des liaisons hydrogène, mais avec une cinétique lente, tandis qu'une cinétique rapide d'échange a conduit à la formation des morphologies sphériques.

Néanmoins, l'investigation de la cinétique ou de la dynamique d'auto-association n'a jamais été explorée auparavant dans le cas des autoassemblages de copolymères contenant des nucléobases. En pratique, la maitrise de la cinétique d'association/dissociation des liaisons hydrogène peut-être un outil précieux dans des applications comme des vecteurs des substances actives et du matériel génétique. Des études menées dans le cadre des vecteurs de siARN ont montré que les interactions supramoléculaires (particulièrement les liaisons H) sont responsables de la durée requise pour l'expression des gènes dans les cellules vivantes.[8] Comme les nucléobases présentes dans la structure des assemblages se trouvent aussi dans le matériel génétique, connaître quels sont les paramètres qui contrôlent la cinétique d'échange dévient intéressant pas uniquement pour prouver le concept théorique, mais aussi pour trouver une application aux assemblages décrits en généralisant les résultats obtenus au matériel génétique.

Malgré leurs propriétés structurales uniques et leur potentiel accru à s'auto-associer dans des architectures supramoléculaires avec des morphologies contrôlées inspirées par le vivant, les copolymères synthétiques porteurs de bases nucléiques n'ont pas encore attiré tout l'intérêt qui leur est dû. Un aspect sur lequel ces polymères n'ont jamais été étudiées à notre connaissance, c'est l'interaction avec le matériel génétique. Etudier le comportement de ces polymères vis-à-vis du matériel génétique est d'une importance primordiale afin de valider le concept d'association par des liaisons hydrogène entre ces architectures synthétiques et l'ADN, et envisager de nouveaux vecteurs du matériel génétique avec une action thérapeutique.

Cette thèse vise à explorer et saisir ces problématiques majeures concernant les autoassemblages des copolymères contenant des bases nucléiques, en développant de nouvelles plateformes supramoléculaires hydrosolubles, avec une dynamique contrôlable et sensible à différents stimuli, et visant des applications en complexation du matériel génétique.

Ce mémoire de thèse a été centré sur trois axes :

1er axe : le développement des polymères hydrosolubles contenant des nucléobases et l'étude des co-assemblages de ces polymères en conditions physiologiques (Chapitres II et Chapitre III)

2eme axe : Co-assemblages supramoléculaires de polymères comportant des nucléobases sensibles aux changements de pH et avec une cinétique d'assemblage contrôlable (Chapitre IV)

3eme axe : L'étude de la complexation *via* des liaisons hydrogène entre les polymères comportant des nucléobases et différents types de matériel génétique, pour la conception des vecteurs de ARNm (Chapitre V).

Le projet de thèse a été effectué au sein du département D2 de l'Institut Charles Gerhardt de Montpellier (ICGM) qui possède une maîtrise particulière dans la polymérisation radicalaire contrôlée et dans la physico-chimie des assemblages supramoléculaires. Des collaborations ont été réalisées avec le Dr. Johannes Brendel et le Dr. Anja Traeger (laboratoire IOMC, Iéna, Allemagne) dans le cadre des expériences biologiques avec différents types de matériel génétique, ainsi qu'avec le Dr. Mona Semsarilar (IEM, Montpellier, France) pour les analyses de microscopie électronique en transmission (TEM) et le Dr. Bénédicte Prélot (ICGM, Montpellier, France) pour les suivis de la cinétique supramoléculaire par titrage calorimétrique isotherme (ITC).

Cette thèse est divisée en cinq chapitres (*Fig. 0-1.*). Le premier chapitre présente un état de l'art, *via* une revue exhaustive, sur les autoassemblages des polymères contenant des nucléobases en relation avec la structure des polymères utilisés, ainsi qu'en relation avec d'autres paramètres tel que le solvant, la température, ou le pH. Les objectifs de cette première partie sont 1) de faire le résumé des copolymères synthétiques contenant des nucléobases qui sont cités jusqu'à présent dans la littérature, en différenciant leur méthode de synthèse, leurs avantages et inconvénients et 2) le focus sur l'influence des différents paramètres sur la variété des morphologies issues de l'autoassemblage de ces polymères. Une attention particulière est portée sur le rôle des liaisons hydrogène et des effets hydrophobes sur la formation des autoassemblages décrits.

Comme précisé précédemment, les polymères contenant des nucléobases sont insolubles dans l'eau. Or, un des objectifs de cette thèse est d'obtenir une architecture macromoléculaire hydrosoluble. Afin d'accomplir cet objectif, nous avons développé un nouveau monomère méthacrylate hydrosoluble contenant un groupement thiomorpholine oxide qui, par copolymérisation avec les monomères méthacrylate de base nucléique, conduit à l'obtention de copolymères hydrosolubles. Le choix de la thiomorpholine oxide comme groupement hydrophile a été inspirée par une 2eme revue synthétique qui fait partie du 2eme Chapitre, portant sur les relations structure-activité biologique des polymères à base de morpholine et thiomorpholine. Ce chapitre porte sur les avantages d'utilisation en biologie (immunologie, transfection cellulaire, délivrance de principes actifs, etc.) des composés dérivés de la morpholine vis-à-vis les dérivés classiques de PEG. En complément de cette revue, le 2eme

Chapitre inclue un article de recherche sur les nouveaux polymères à base de thiomorpholine oxide qui ont été développés, leur sensibilité au pH et à la température, ainsi que leur potentielle utilisation comme matériaux hémocompatibles.

Le troisième chapitre de cette thèse est présenté sous la forme d'un article de recherche qui présente le développement des copolymères hydrophiles comportant des nucléobases et unités thiomorpholine oxide, ainsi que leurs propriétés d'autoassemblage en conditions physiologiques. Cet article vise : 1) à présenter la synthèse et la caractérisation de nouveaux polymères de nucléobases (solubles à pH physiologique) avec une architecture contrôlée par RAFT ; 2) à étudier l'influence des paramètres structuraux (le nombre et le type des nucléobases, le degré de polymérisation, les ratios entre les co-monomères, les ratios entre les nucléobases complémentaires) sur la formation des autoassemblages en conditions physiologiques ; 3) à mettre en évidence la contribution des liaisons hydrogène complémentaires sur la formation d'assemblages supramoléculaires (par des expériences avec des molécules compétitrices des liaisons hydrogène) ; 4) à étudier les propriétés biologiques *in-vitro* (évaluation de la cytotoxicité et de l'hémocompatibilité) des polymères développés.

Le quatrième chapitre de ce mémoire de thèse est centré sur l'influence du pH sur les co-assemblages à partir des copolymères à bases nucléiques. L'article de recherche compris dans ce chapitre illustre les transitions induites par différents pH sur les morphologies (sphères denses texturés, dendrites ou flocons de neiges) des co-assemblages. Les morphologies obtenues sont similaires à celles observées pour des systèmes bio-inspirés auto-associées à base de peptides et de nucléopeptides. Mais, elles sont uniques dans le cas des copolymères de nucléobases. Une corrélation entre les morphologies obtenues et les intéractions supramoléculaires qui guident la formation de ces assemblages a été mise en évidence.

Le 5eme et dernier chapitre de la thèse, présente l'utilisation des polymères contenant des nucléobases dans la complexation sélective du matériel génétique, dans la perspective d'introduire et transporter l'ARN dans les cellules et donc de réaliser de la transfection cellulaire. L'article de recherche de ce chapitre vise à investiguer : 1) l'interaction entre les polymères contenant des fonctions uracile (comme nucléobase) et différents types de matériel génétique (ADN plasmidique, acide poly adénylique polyA et ARNm), 2) les propriétés physico-chimiques des hybrides polymères-matériel génétique obtenus, 3) la résistance des hybrides aux RNAses et au sérum physiologique.

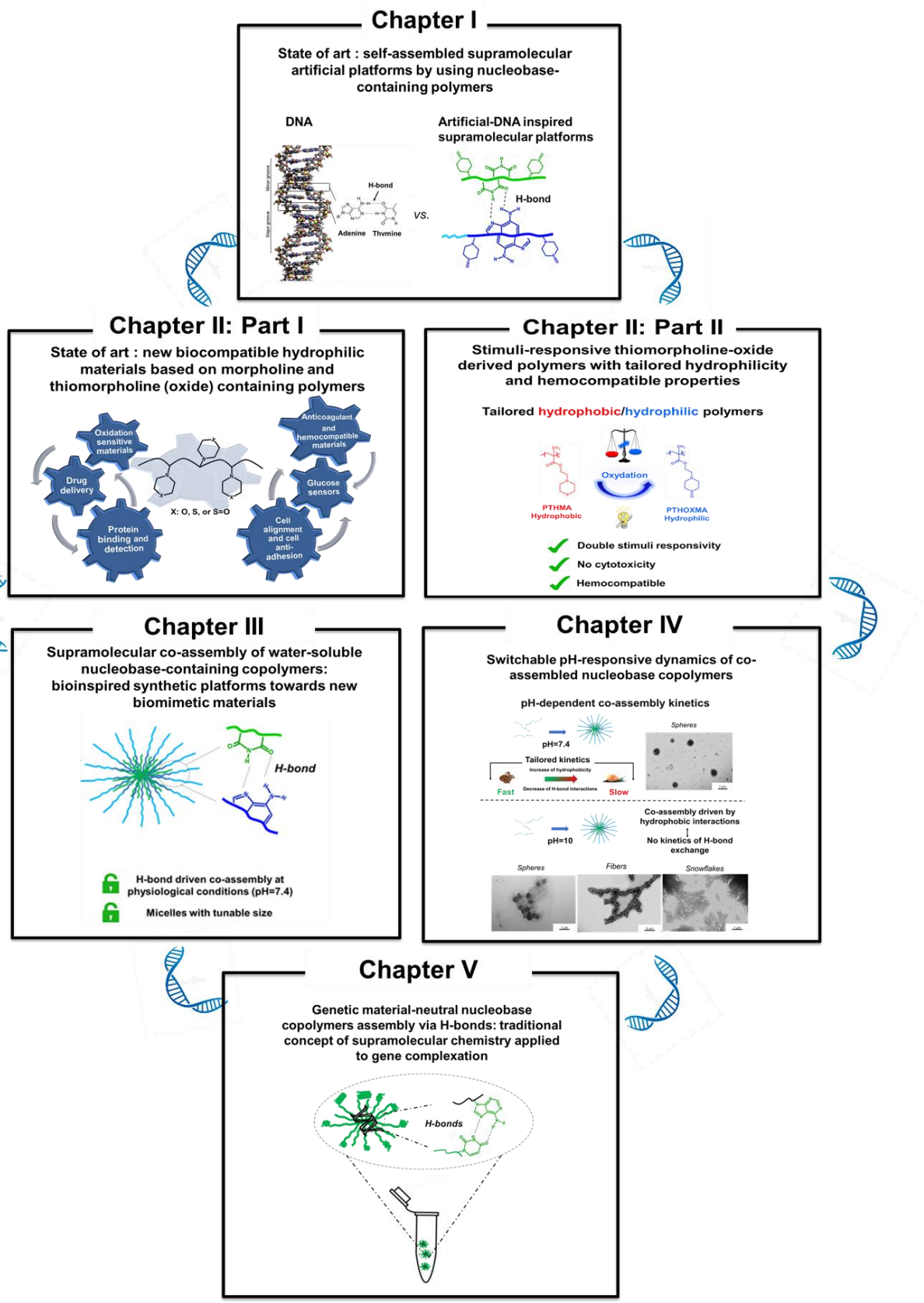

Fig. 0-1. Représentation globale des chapitres de thèse

Références bibliographiques

1. J. Lehn, *PNAS*, 2002, **99(8)**, 4763-4768.

2. Z. Hua, A. Pitto-Barry, Y. Kang, N. Kirby, T. R. Wilks, R. K. O'Reilly, *Polym. Chem.*, 2016, **7**, 4254–4262.

3. Z. Hua, R. Keogh, Z. Li, T. R. Wilks, G. Chen, R. K. O'Reilly, *Macromolecules*, 2017, **50**, 3662–3670.

4. M. Wang, B. Choi, Z. Sun, X. Wei, A. Feng, S. H. Thang, *Chem. Commun.*, 2019, **55**, 1462–1465.

5. Y. Kang, A. Pitto-Barry, A. Maitland, R. K. O'Reilly, *Polym. Chem.*, 2015, **6**, 4984-4992.

6. E. Largy and V. Gabelica, *Anal. Chem.*, 2020, **92(6)**, 4402-4410.

7. G. Mellot, J-M. Guigner, J. Jestin, L. Bouteiller, F. Stoffelbach, J. Rieger, *Macromolecules*, 2018, **51(24)**, 10214-10222.

8. K. L. Luo, D. C. Chang, *Biochem Biophys Res Comms.*, 2004, **318**, 303-310.

Chapitre I : Etat de l'art sur la synthèse et l'auto-assemblages des copolymères contenant des nucléobases

Chapitre I : Etat de l'art sur la synthèse et l'auto-assemblages des copolymères contenant des nucléobases

Introduction Chapitre I

L'autoassemblage (supra)moléculaire est un processus qui implique l'organisation spontanée et autonome d'entités moléculaires dans des architectures organisées bien définies. Les interactions impliquées dans la formation de l'autoassemblage sont des liaisons non covalentes faibles (*i.e.*, interactions de Van der Waals, interactions solvophobes, liaisons hydrogène, etc.).

Dans les systèmes vivants, la formation de l'ADN utilise les principes de la chimie supramoléculaire. L'assemblage par liaisons hydrogène de l'ADN en double hélice a inspiré ensuite l'utilisation des liaisons hydrogène comme force motrice des auto-assemblages en chimie supramoléculaire, formées à partir des polymères contenant de l'ADN, des bisurées ou bien des peptides cycliques.

Quelques exemples notables reposent sur le développement de copolymères hybrides d'ADN qui sont formés par la copolymérisation à bloc des monomères commerciaux avec de l'ADN contenant des fonctions polymérisables. Malgré la diversité morphologique obtenue dans le cas de ces systèmes (de type ''bottle-brush'', ou nano-fibre), un inconvénient des copolymères amphiphiles contenant de l'ADN est la difficulté et le coût de la synthèse de l'ADN et de son couplage avec le polymère. C'est pourquoi, les polymères synthétiques contenant des nucléobases ont ensuite reçu un intérêt particulier.

Cependant, le nombre d'exemples des polymères contenant des nucléobases dans la littérature est très limité. La structure de type copolymères à bloc contenant des nucléobases permet d'obtenir des structures polymériques amphiphiles, en combinant des blocs de polymères hydrophiles avec des blocs de polymères hydrophobes (contenant les nucléobases). Néanmoins, un désavantage majeur des copolymères à bloc contenant des nucléobases consiste en l'impossibilité d'obtenir un contrôle de la séquence des nucléobases, aspect qui est possible dans le cas de la technologie de la synthèse artificielle de l'ADN. De plus, un autre inconvénient est la difficulté de synthèse des monomères contenant les fonctions nucléobases (avec des rendements de réactions assez faibles), qui sont ensuite impliqués dans la polymérisation

RAFT. Un dernier désavantage est l'insolubilité de ces polymères dans l'eau, car ils sont solubles uniquement dans des solvants organiques ($CHCl_3$, DMF ou DMSO). A long terme, la non-solubilité en milieu aqueux limite les applications de ces polymères notamment en biologie.

En dépit de ces inconvénients liés plutôt à la chimie des monomères et polymères à bases nucléiques, l'auto-assemblage de ces structures polymériques a mené à des morphologies très diverses (micelles, vésicules, cylindres, ou de type ''worm'') dans différents solvants organiques. Les précédentes études ont indiqué que les morphologies obtenues sont contrôlées par la structure des polymères (le nombre et le rapport de nucléobases, les ratios de blocs hydrophiles/hydrophobes, la longueur des chaines polymères etc.), ou des paramètres tels que le type de solvant (qui favorise ou limite la formation des liaisons hydrogène). Ces morphologies ont été obtenues suite à un cumul entre les liaisons hydrogène entre les nucléobases complémentaires et les interactions hydrophobes. Cependant, ces études n'arrivent pas à délimiter avec exactitude quelle est la principale interaction (liaisons hydrogène ou interactions hydrophobes) qui est à l'origine des morphologies des auto-assemblages obtenues.

Savoir quelles interactions (effets hydrophobes ou liaisons hydrogène) guident majoritairement l'autoassemblage est important afin de développer des futurs systèmes intelligents répondant aux stimuli, qui peuvent trouver un jour un faisable approche aux systèmes naturels telles que l'ADN. Ce défi peut être réalisable en réalisant des autoassemblages dirigées majoritairement par liaisons hydrogène, en utilisant comme outil les polymères contenant des nucléobases. La plupart des systèmes auto-assemblés guidées par des interactions hydrophobes sont gelés (irréversibles), dans leur grande majorité. Cependant, des systèmes auto-assemblés par liaisons H principalement dans l'eau sont très rares. En utilisant des liaisons hydrogène comme force motrice de la réalisation de l'autoassemblage, on s'attend à ce qu'ils soient dynamiques, ainsi que sensibles aux stimuli tels que la température ou le pH, ce qui est rare.

Ce premier chapitre est une revue de la littérature qui est organisée sur deux parties. Tout d'abord, les défis liés à la synthèse des monomères contenant des nucléobases sont présentés, et une mise à jour des méthodes de synthèse des structures de copolymères comportant des nucléobases est réalisée. Dans une seconde partie, cette revue explique comment les interactions supramoléculaires (et particulièrement les liaisons hydrogène) à l'origine de l'auto-assemblage des polymères contenant des nucléobases permettent d'adopter une morphologie particulière. Cette revue a été publiée dans le journal **Polymer Chemistry** (**IF : 5.582**).

Publication scientifique : Revue de littérature numéro 1

Nucleobase-polymer architectures controlled by supramolecular interactions: the key to achieve biomimetic platforms with various morphologies

Laura Vasilica Arsenie,[1] *Vincent Ladmiral,*[1] *Patrick Lacroix-Desmazes*[1] *and Sylvain Catrouillet* [1]

[1]*ICGM, University of Montpellier, CNRS, ENSCM, 34095 Montpellier, France*

I. Graphical abstract

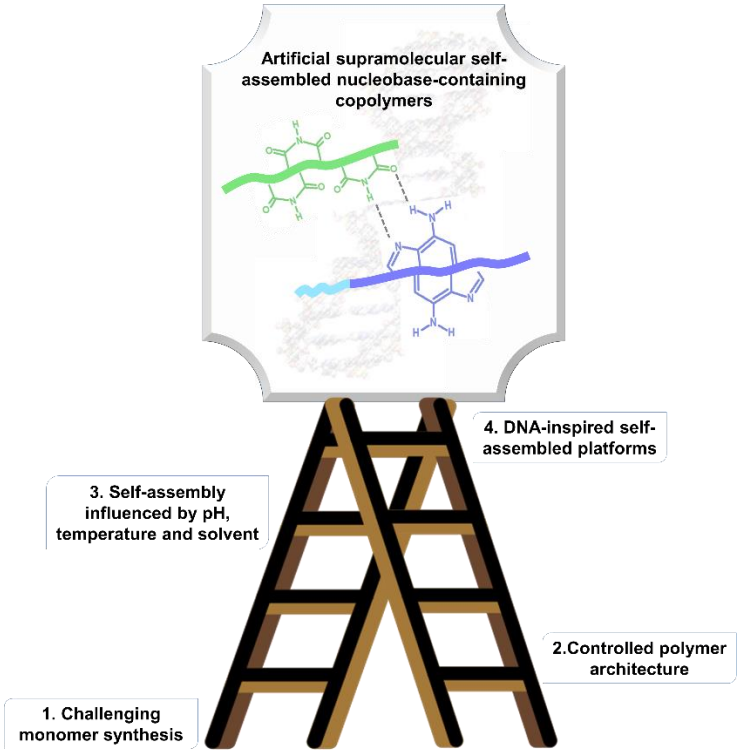

II. Abstract

In biological systems, DNA formation occurs due to complementary H-bond interactions between nucleobases, as well as hydrophobic supramolecular interactions. It inspired polymer chemists in the development of supramolecular artificial platforms based on nucleobase-containing polymers. Despite their biomimetic nature and their huge potential to develop

bioinspired supramolecular assemblies, nucleobase-containing polymers are in their infancy. The first part of this review aims to highlight the synthetic challenges related to the synthesis of nucleobase-containing monomers and polymers. The second part illustrates how to guide supramolecular interactions of nucleobase-containing copolymer architectures in order to obtain particular morphologies of the resulting supramolecular systems.

III. Introduction

Self-assembly describes a process in which a disordered system becomes ordered as a result of interactions within itself.[1] In other words, this phenomenon involves the spontaneous organization of molecular entities into well-defined organized architectures. The interactions involved in self-assembly are weak non-covalent bonds (*e.g.*, Van der Waals forces, solvophobic interactions, H-bonds, crystallization, etc.).

Historically, the first self-assemblies were obtained from small amphiphilic molecules such as surfactants.[2] These self-assemblies originated from solvophobic interactions between the aliphatic moieties of the surfactant-active chains and led to the formation of various morphologies including spheres or vesicles.[3] Later, amphiphilic block copolymers were used to perform self-assembly as they present a lower critical micellar concentration (CMC) and were also shown to be able to self-assemble into various morphologies. As for small surfactant molecules, the main interactions controlling the self-assembly of block copolymers were the solvophobic interactions. Similarly to surfactants, these polymers include a solvophilic and a solvophobic block which self-assemble in a selective solvent. By adjusting the volume fraction of the blocks, not only spherical structures, but also cylindrical and lamellar ones become accessible. [4–6]

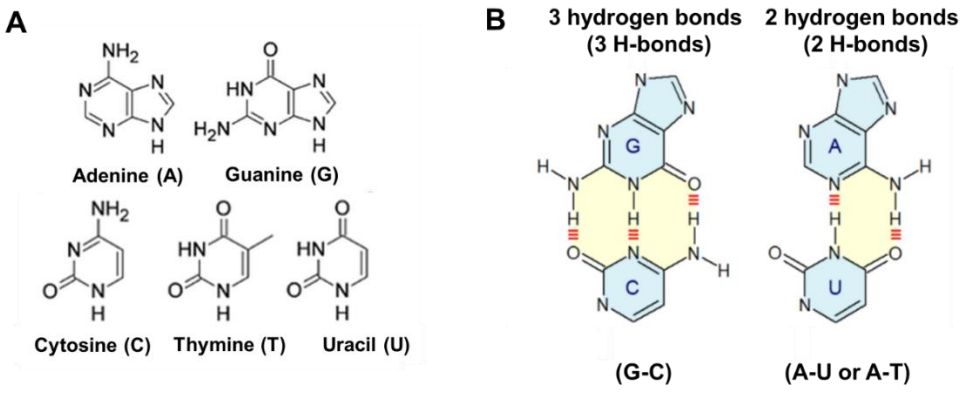

Fig. 1. (A) Structures of nucleobases; (B) Pairing of complementary nucleobases: G and C involves three H-bonds, while pairing of A and U or A and T involves two H-bonds.

Other non-covalent interactions such as H-bonds can also be used when performing the self-assembly of amphiphilic block copolymers. Most processes taking place in nature involve H-bonds. For example, genetic replication requires H-bond recognition between complementary nucleobases (*Fig.1.*).[7] Nucleobases were key motifs used to develop various biomimetic self-assembled systems.[8–10] However, most of these self-assembled architectures were constructed by using small organic molecules containing nucleobases, oligonucleotides or DNA-containing polymers.[8–10] Some interesting examples of DNA-containing triblock copolymer conjugates were reported to illustrate the influence of H-bond recognition between nucleobases on the morphological transition from spheres to cylinders when increasing the length of the DNA (*Fig. 2*).[13,14]

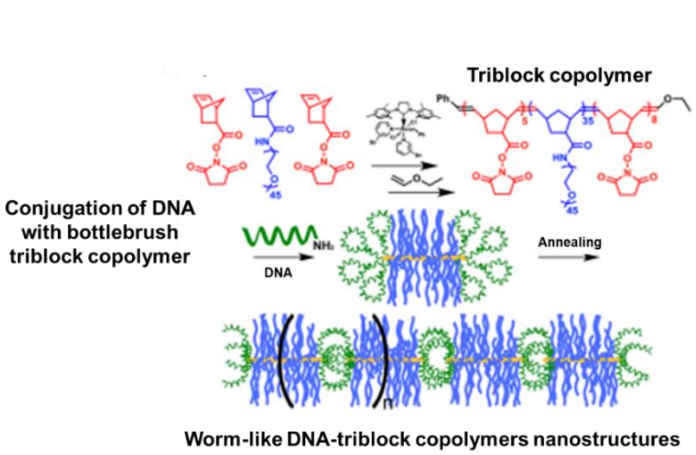

Fig. 2. The design of worm-like nanostructures via the conjugation of triblock bottlebrush copolymers with DNA. Reprinted with permission from Ref.14 Copyright (2014) American Chemical Society.[14]

Although these systems present a huge potential for the control of self-assemblies in solution state, an important drawback of amphiphilic DNA-containing copolymers lies in the difficulty of DNA synthesis and of the complete coupling with polymer. Therefore, in order to mimic DNA, chemists have developed nucleoside-containing polymers.[15] First significant attempts were reported by Haddleton *et al.*[16] to prepare nucleoside-containing polymers (*i.e.*, with adenosine or uridine) by using Atom Transfer Radical Polymerization (ATRP). Moreover, Ring Opening Polymerization (ROP) was applied to develop a range of thymidine-containing polymers.[17] Furthermore, using nucleobase motifs instead of nucleosides in the development of polymers was reported to be more advantageous in terms of difficulties associated to the organic synthesis.[15] For example, the group of Van Hest *et al.*[18] prepared polymethacrylates containing adenine, thymine or cytosine by ATRP. Moreover, monomers of styrene functionalized by

adenine and thymine were used in the NMP polymerization, as stated by Long and collaborators.[19] Other significant contributions were made by Rowan *et al.*,[20] Leibler *et al.*[21] as well as Binder *et al.*[22] in the field of adenine and thymine-containing telechelic polymers. These supramolecular systems using nucleobases have been the subject of some recently published comprehensive reviews.[23,24] The nucleobase-containing polymer structures reported so far for self-assembly applications in solution are based on either commercial polymers modified with nucleobases, or more often on nucleobase-containing block copolymers prepared particularly by RAFT polymerization of nucleobase-containing monomers.[17,25] Professor O'Reilly performed pioneer works in the field of self-assembly in solution state of nucleobase-containing polymers prepared by RAFT.[26] In this context, a block topology was generally chosen in order to access an amphiphilic behavior. In this case the nucleobase containing block was hydrophobic and was combined with a hydrophilic block mainly of poly(*N*-acryloyl morpholine). These block copolymers led to architectures able to self-assemble mainly *via* H-bond recognition between the nucleobases. Nevertheless, a disadvantage of nucleobase-containing copolymers is the impossibility to achieve the perfect sequence control of nucleobases that nature possesses in the case of DNA, because these structures are prepared by chain polymerization. Few studies indicated that, by modifying the nucleobase containing block (*i.e.*, the number and the ratio of nucleobases, the addition of hydrophilic or hydrophobic co-monomers etc.), different self-assembled morphologies can be obtained.[26] These studies also showed that the obtained type of morphology can vary when some parameters including the pH or solvent type are changed.[26] Indeed, these parameters affected the H-bonds between nucleobases responsible for the self-assembly and in consequence the self-assembled morphology. The correlation between complementary H-bonds in nucleobase-containing copolymers and their morphology is still under investigation. So far, few papers (~25) studied different ways to modulate the morphology of self-assembled nucleobase-containing copolymers by changing a range of parameters. This review will highlight how to guide supramolecular interactions of nucleobase-containing copolymer architectures towards a particular morphology, by summarizing the main observations reported so far. First, synthetic challenges associated with nucleobase-containing monomers will be presented, and a brief update of the synthesis methods of nucleobase-containing copolymer structures will be presented. Then, the second part of this review will explain how changes in the supramolecular interactions in nucleobase-containing polymers enable the resulting self-assembled architectures obtained in solution state to adopt a particular morphology.

IV. Nucleobase-containing monomers and polymers

A. Nucleobase-containing monomers

This section focused on the synthesis of nucleobase-containing monomers polymerizable by radical polymerization. Radical polymerization is a versatile and compatible polymerization technique with the functional groups contained in the nucleobases. The synthesis of nucleobase-containing vinyl monomers has been seldomly described so far. The most common and cited method to synthesize nucleobase-containing vinyl monomers is nucleophilic substitution (SN) reactions.[24] This method was mainly used to prepare adenine and thymine (or uracil)-containing monomers. Previous reports mentioned that in the case of cytosine- and guanine-containing vinylic monomers this method is challenging due to side reaction products and low reaction yields (below 48%).[18] Similar to the vinylic monomers, the synthesis of cytosine and guanine-containing nucleobase copolymers is very complex, and the number of examples of self-assembled architectures made from these polymers are in consequence very limited.[15,26,27] Since most of the examples of self-assembled nucleobase-containing copolymers concern adenine and/or thymine (uracil) derivatives,[26,28] the discussion of this section will focus on monomers containing these nucleobases prepared by SN reactions.

A.1. Reactivity of nucleobases in nucleophilic substitution reactions

The synthesis of nucleobase-containing vinylic monomers reported in the literature takes place in anhydrous polar aprotic solvents. The main strategy used to synthesize these monomers comprises two steps: deprotonation of the nucleobase (Step 1) and bimolecular nucleophilic substitution (SN_2) of the deprotonated nucleobase with a primary alkyl halide (Step 2). The nucleobases are nucleophilic agents in nucleophilic substitution reactions since they contain electron donor amino groups. To increase the nucleophilicity of nucleobases in SN_2 type reaction, the treatment of nucleobases with inorganic bases (*i.e.*, NaH, or K_2CO_3) is preferentially performed. The inorganic bases deprotonate the amino functions of nucleobases, which results in strong nucleophilic anions, appropriate for SN_2 reaction.[29]

A.2. Synthesis of nucleobase-containing monomers

- **Adenine-containing monomers**

The adenine presents a primary amino group which is involved in the H-bonds with thymine (or uracil). Therefore, in order to perform a nucleophilic substitution with adenine, the primary amino group should be preserved, while substituting the NH group in the imidazole ring. Thus, the NH group of the imidazole ring should be deprotonated by inorganic bases to form a strong

nucleophilic agent (*Fig. 3A*). Strong inorganic bases such as NaH are used to deprotonate the secondary cyclic amine structure of the adenine. The secondary amine proton of the imidazole ring presents a $pK_a \sim 9.8$ (of the non-protonated form),[29] so it can be deprotonated by strong bases. Then, the deprotonated adenine reacts with primary alkyl bromo halides containing polymerizable synthons (acrylamide-, acrylate- or methacrylate-), leading to the final monomer (*Fig. 3B*). Acrylamide-, acrylate- and methacrylate- derived adenine containing monomers were reported in the literature with low or moderate reaction yields (*Fig. 3C*). For example, acrylamide-alkyl monomers containing adenine were previously obtained by Hua *et al.*[30] with low yield and small scale (52%, 1 g) due to an undesired attack of NaH on the amide of acrylamide region of the bromo alkyl halide, which led to secondary substitution products. Then, Zhang *et al*.[31] synthesized an adenine-containing acrylate as polymerizable synthon. However, the authors reported a global yield of the reaction of 31%. Compared to the example of the acrylamide adenine-containing monomers,[30] the low reaction yield was a consequence of the structure of the bromo-derivative used in the SN reaction (*i.e.*, where the halogen group was placed at the β position of an ester), as illustrated by Zhang *et al.*[31] Moreover, Kang *et al.*[28] reported the successful synthesis of adenine-containing methacrylates, in moderate yield and small scale (75%, 3.5 g). The higher yield (compared to that of acrylate or acrylamide type monomers) was explained by the activation of the halogen group which was situated at the α position of an ester.[28]

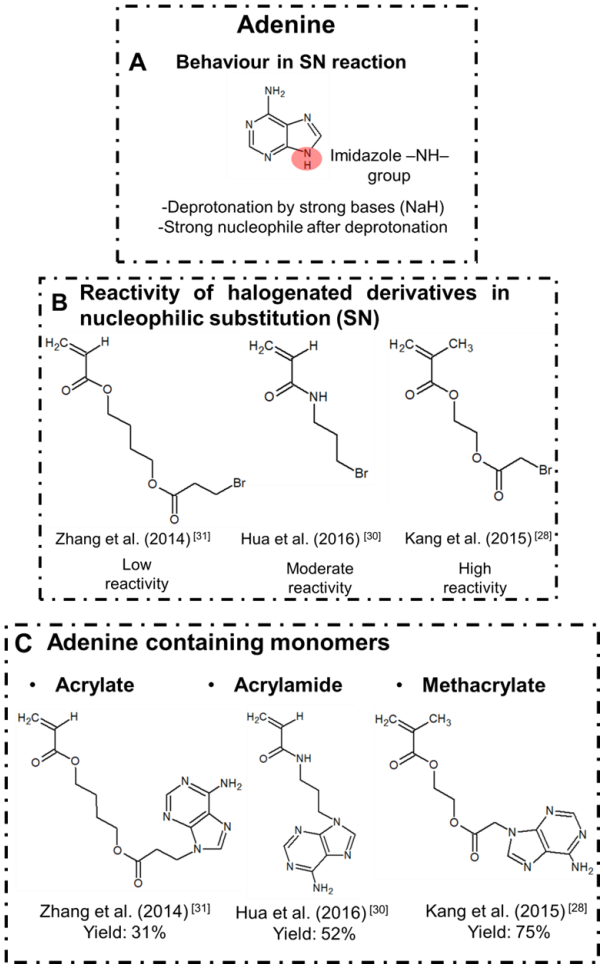

Fig. 3. (A) Acid–base properties of adenine and behavior in SN reaction; (B) reactivity of alkyl halides in the nucleophilic substitution; (C) structures of adenine-containing monomers.

- **Thymine containing monomers**

The deprotonation of thymine molecules to be further used in nucleophilic substitution reactions is different due to the presence of two –NH– groups with different reactivities: one imide group (1) and a secondary cyclic amide (2) (*Fig. 4A*). In order to achieve the complementary H-bonds with adenine synthon as in the biological systems, the imide group should be free. Thus, the secondary cyclic amide proton (2) should be selectively targeted to perform the substitution reactions. The approach used by Hua *et al.*[30] to prepare thymine-containing acrylamide monomers was to protect the imide group (1) of thymine with benzoyl chloride in the presence of K_2CO_3. By this way, the cyclic amide group (2) of thymine was deprotonated by NaH and then involved in the SN reaction with the bromo alkyl acrylamide derivative (*Fig. 4B and C*).[30] The protection of the imide group was required since its pK_a (*i.e.*, 9.5) makes it sensitive to NaH attack. Then, deprotection of the benzoylated imide group was performed using TFA. The global yield of the three-steps synthesis of acrylamide-alkyl thymine was 35%. As stated by the

authors, the decreased yield compared to the adenine derivative was mainly due to the protection/deprotection steps of thymine. Thymine-containing methacrylate were synthesized by Kang *et al.*[28] using an iodide derivative to perform the SN with deprotonated thymine (deprotonation realized with K_2CO_3). In this case, the use of a softer base for the deprotonation of the thymine prevents the protection/deprotection steps. A 60% reaction yield was reported by the authors. Compared to the yield of thymine-containing acrylamide and acrylate, the increased yield was a consequence of the increased reactivity of iodide group compared to the bromo group in the SN, as well as due to the absence of protection/deprotection steps during synthesis (*Fig. 4B and C*). To summarize, the low reaction yields (31–75%) and the difficulty to scale up the synthesis protocols (a few grams) are the main challenges of nucleobase-containing monomers reported until now in the literature.

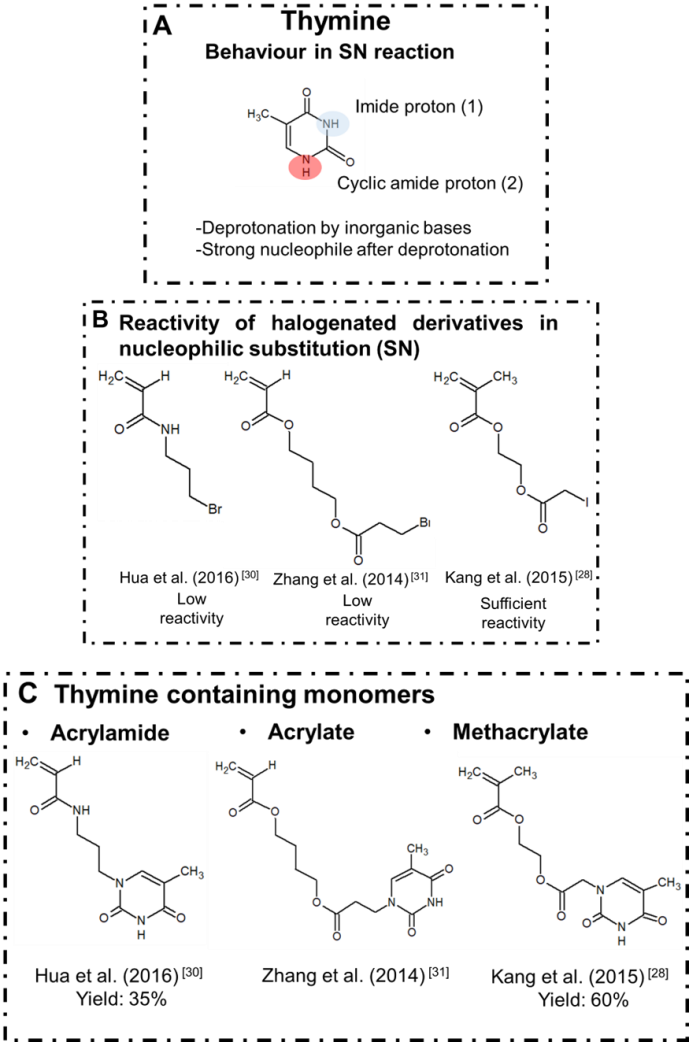

Fig. 4. (A) Acid–base properties of thymine and behavior in SN reaction; (B) reactivity of halogeno intermediary products in the nucleophilic substitution; (C) structures of thymine-containing monomers.

B. Nucleobase-containing polymers

A first approach to obtain nucleobase-containing polymers consists in the polymerization of nucleobase-containing monomers. While the synthesis of nucleobase-containing monomers can be difficult as shown in the previous section, the synthesis of the corresponding nucleobase-containing (co) polymers is easy in high yields. The polymer synthesis can be performed using radical controlled polymerization techniques which allow the synthesis of well-defined statistical copolymers or block copolymers containing predetermined numbers of nucleobases.

Controlling the position, proportion and the number of nucleobase units in each polymer chain is key to obtain desired H-bond recognition during self-assembly. Among the well-known radical controlled polymerization techniques, RAFT is the most often reported technique to prepare nucleobase-containing copolymers (and in particular nucleobase-containing block copolymers).

The pioneering works of the O'Reilly group described the synthesis of amphiphilic block copolymers by RAFT polymerization of adenine-acrylamide (AM-A), thymine-acrylamide (AM-T), *N*-isopropylacrylamide (NIPAM) and *N*-acryloylmorpholine (NAM) (*Fig. 5A*). The strategy consisted in the synthesis of a thermoresponsive poly(NIPAM-*co*-NAM) macro-CTA followed by chain extension using the nucleobase-containing AM-A monomers.[32] The same strategy was employed by Kang *et al.*[28] to synthesize poly(methyl methacrylate)-*b*-poly(adenine methacrylate) (PMMA-*b*-PAMA) and poly(methyl methacrylate)-*b*-poly(thymine methacrylate) (PMMA- *b* -PTMA) block copolymers containing from 20 to 200 nucleobase units per polymer chain (*Fig. 5B*).

Longer chains (*Fig. 5C*)[32] were reported for poly(*N*-acryloyl morpholine)-*b*-poly (thymine acrylamide) (PNAM-*b*-PTAm) block copolymers containing up to 300 thymine units. Wang *et al*.[33] and Kim *et al*.[34] reported the RAFT polymerization of nucleobase-containing monomers providing rigid backbones, such as poly(vinyl benzyl-adenine) (PA) and poly(vinyl benzyl-thymine) (PT) (*Fig. 6A*).[33,34] Furthermore, multiblock amphiphilic copolymers were designed by the sequential RAFT polymerization of thymine acrylate, n-butyl acrylate, and adenine acrylate using a bifunctional macro-CTA agent (*Fig. 6B*).[35]

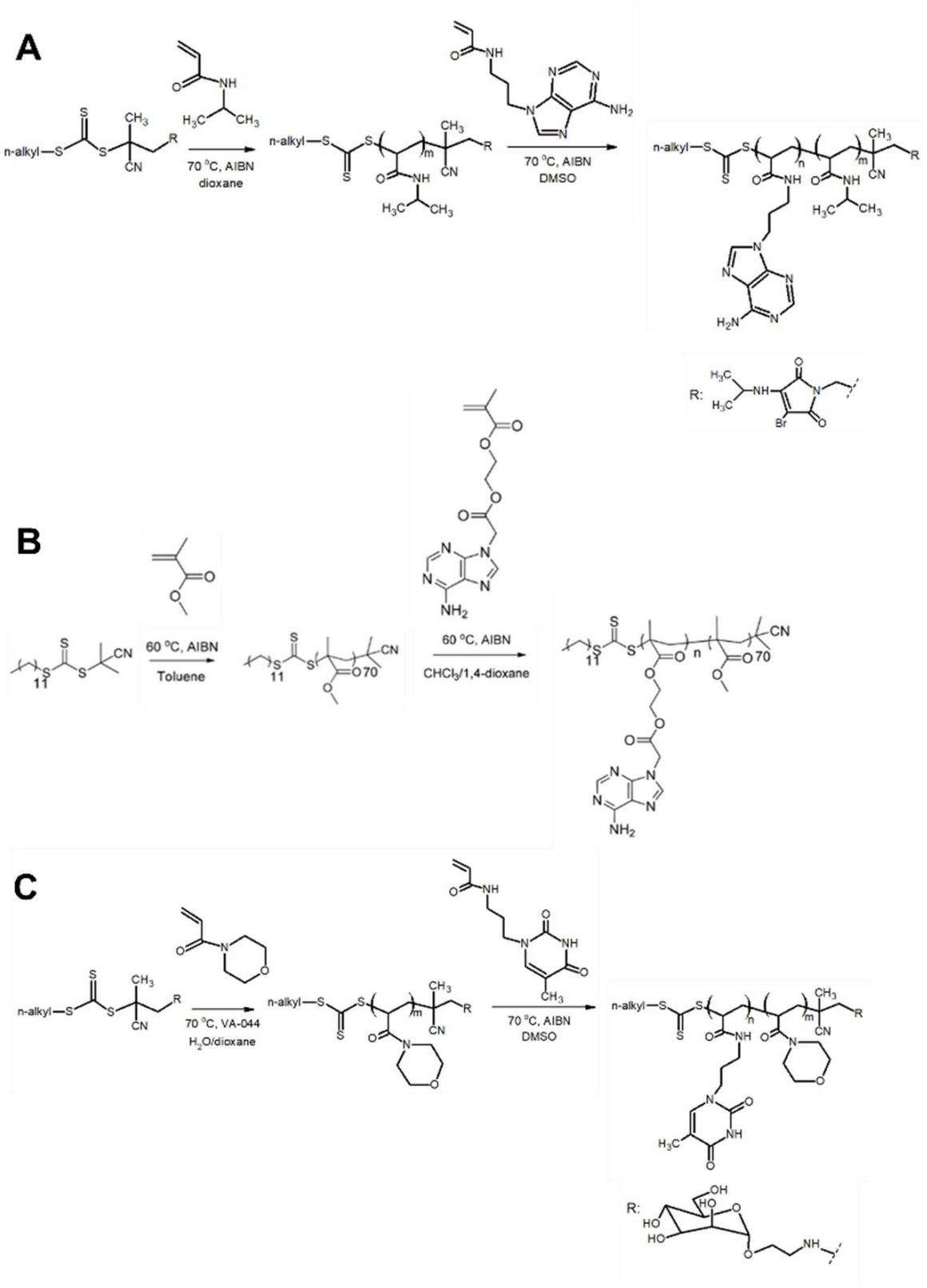

Fig. 5. (A) Synthesis of adenine-containing copolymers based on acrylamide type backbone [32] *and (B) methacrylate type backbone;*[28] *(C) synthesis of thymine-containing copolymers based on acrylamide type backbone.*[32]

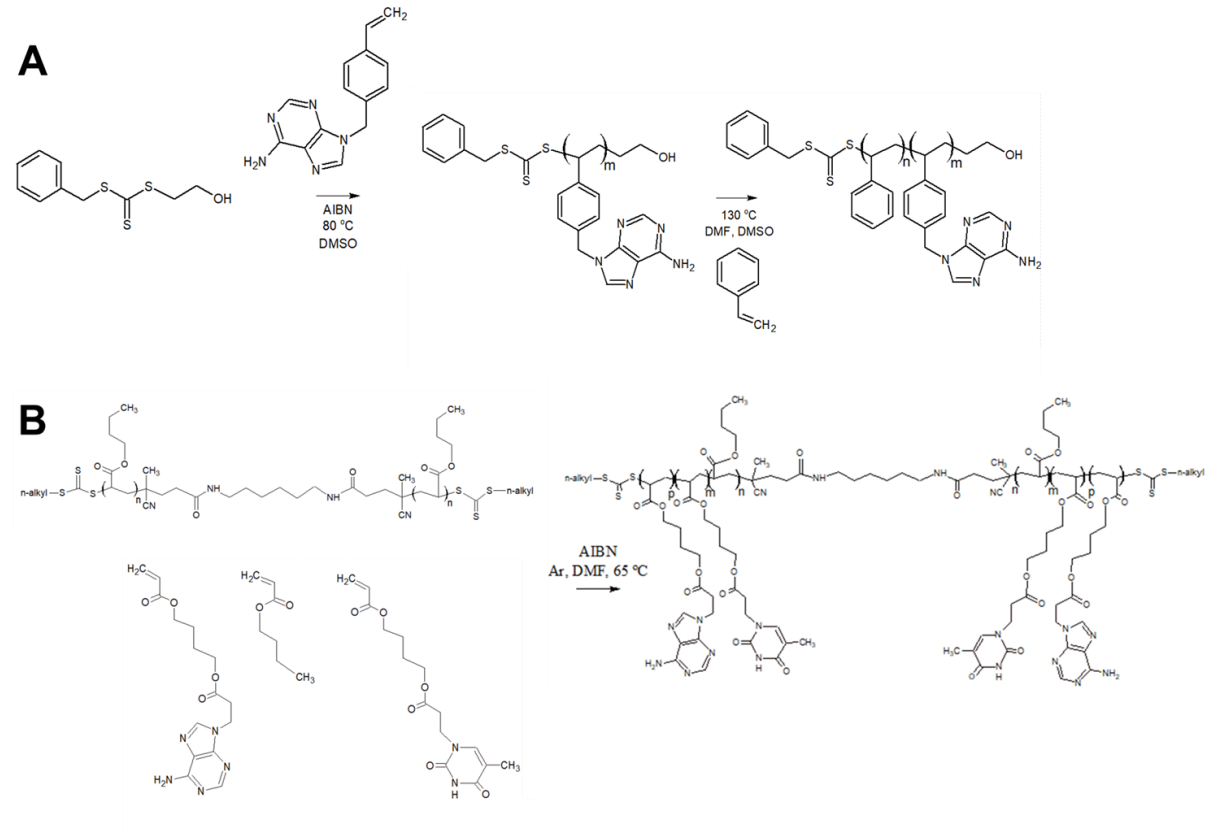

Fig. 6. (A) Synthesis of poly(adenine-styrene)-b-poly(styrene) copolymers[34] *and of (B) poly(butylacrylate)-b-poly(thymine-methacrylate-coadenine-methacrylate) copolymers.*[35]

Overall, the previous examples consisted in the RAFT polymerization of nucleobase-containing monomers. In addition, the RAFT agent used in the polymerization can be modified with nucleobases prior to perform the RAFT polymerization. For example, in the study reported by Wang *et al.*,[36] a RAFT chain transfer agent (CTA) possessing a carboxylic acid end-group was esterified with adenine or thymine bearing 2-hydroxyethyl groups (with yield up to 85%). Then, the resulting modified RAFT agent was used to copolymerize oligo(ethylene glycol) methacrylate and n-butyl methacrylate, in order to obtain poly(oligo(ethylene glycol) methacrylate)-*b*-poly(n-butyl methacrylate) (POEGMA-*b*-PMBA) block copolymers with adenine (A) or thymine (T) end-groups (*Fig. 7*).

The second approach to obtain nucleobase-containing polymers consists in the post-functionalization of commercial polymers with nucleobases. In order to post-functionalize macromolecular architectures, click-chemistry is an efficient option owing to the simplicity in experimental setup, the versatility of this class of reaction both in terms of reaction conditions and in variety of substrates.[37–39] Copper(I)-catalyzed alkyne–azide cycloaddition (CuAAC) was used by Huang *et al.*[40] to produce thymine-containing poly(carbazole) (PC-T) and thymine-

functionalized carbazole-triphenyl aniline copolymers (PTC-T) in high yields (up to 95%) (*Fig. 8A*).

The same strategy was applied to graft uracil-bearing propargyl moieties on azide-functionalized poly(*ε*-caprolactone) (PCL) with 71% yield (*Fig. 8B*).[41,42] This relatively low yield for a click-chemistry reaction was ascribed to the hindered azide-PCL structure. Another example of click chemistry is the aza-Michael addition (*Fig. 9*), successfully used for the synthesis of telechelic uracil-functionalized poly(propylene glycol) (BU-PPG)[43] (*Fig. 9A*) and telechelic adenine-functionalized poly(ethylene glycol) (BA-PEG) (*Fig. 9B*) in high yields (96%).[42]

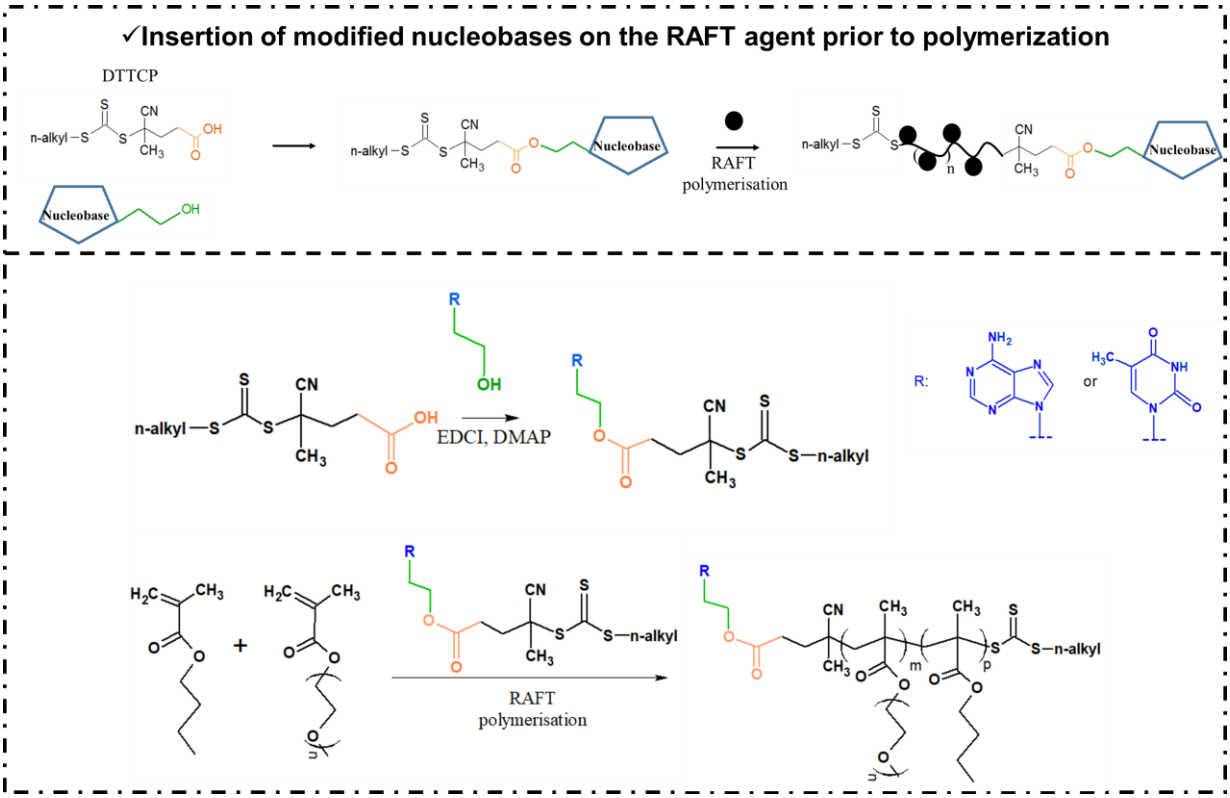

Fig. 7. Synthesis of nucleobase-containing copolymers by the functionalization of the RAFT agent with nucleobases prior to polymerization.[36]

Another type of reaction used to functionalize commercial polymers with nucleobases is the esterification. Zhao *et al.*[44] applied a similar concept (*i.e.*, esterification as linkage reaction), to functionalize a poly(2-hydroxyethyl acrylate)-*b*-poly(*ε*-caprolactone) with an adenine bearing a 2-carboxyethyl group. This way, adenine-containing PCL amphiphilic block copolymers were obtained with 75% yield (*Fig. 10*).[44]

In conclusion, two different methods were used to prepare nucleobase-containing copolymers.

The first one consists in the controlled radical polymerization of nucleobase-monomers (*Fig. 11*). This method affords nucleobase-containing polymers with controlled architecture, degrees of polymerization and co-monomers ratios. Nevertheless, this method requires to synthesize the nucleobase-containing monomers, which involve challenging organic synthesis, as described in the previous section. Alternatively, nucleobase-ended polymers can be obtained by using a nucleobase-functionalized RAFT chain transfer agent, but only a single nucleobase is inserted in the polymer chain.

The second method consists in the post-functionalization of polymers, using click-chemistry reactions (CuAAC, aza-Michael Addition) or esterification for examples (*Fig. 12*). This method is advantageous since it allows to prepare libraries of polymers only different in their degree of functionalisation.

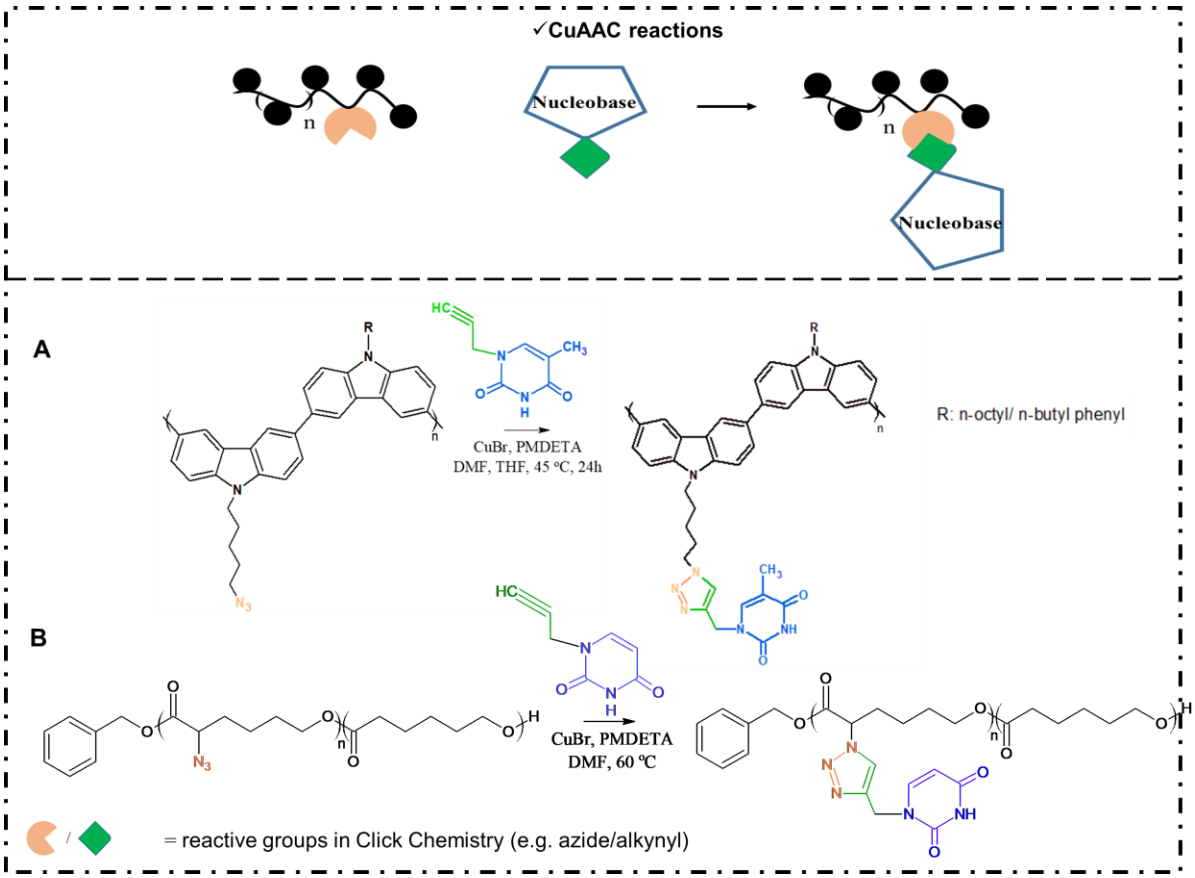

Fig. 8. CuAAC reactions for the nucleobase-functionalization of polymers.[40,42]

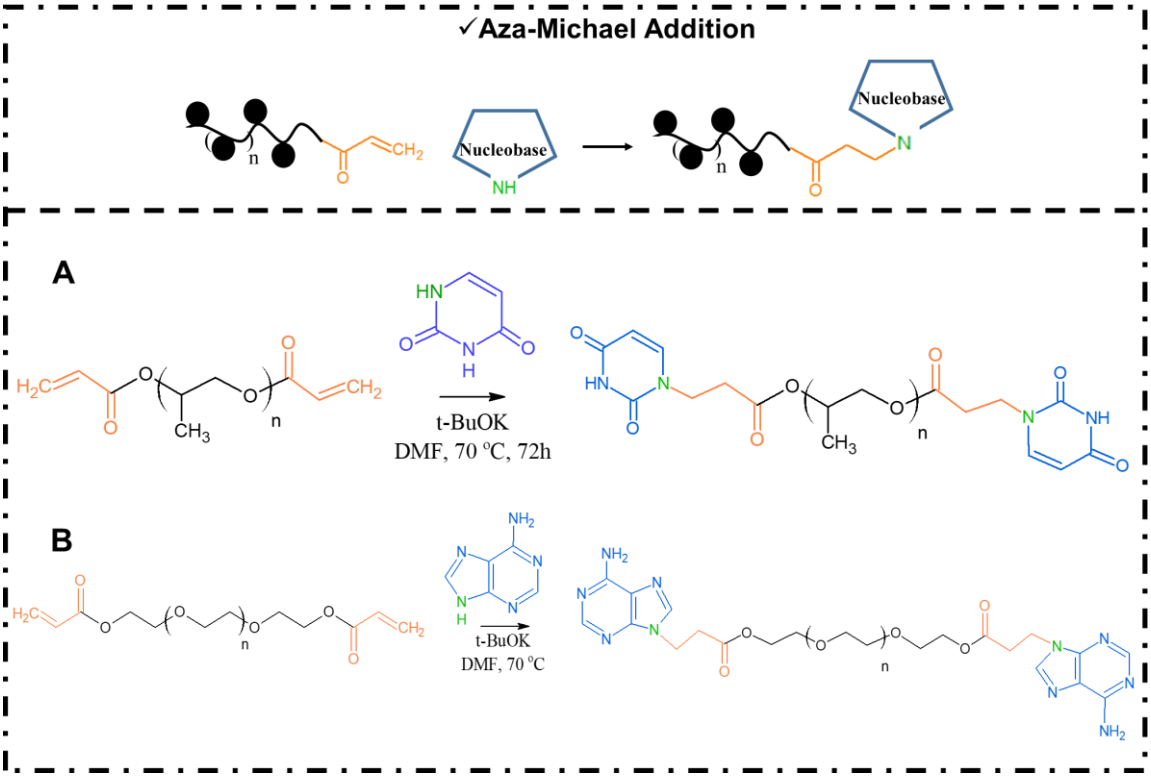

Fig. 9. Aza-Michael Addition for the nucleobase-functionalization of polymers.[42,43]

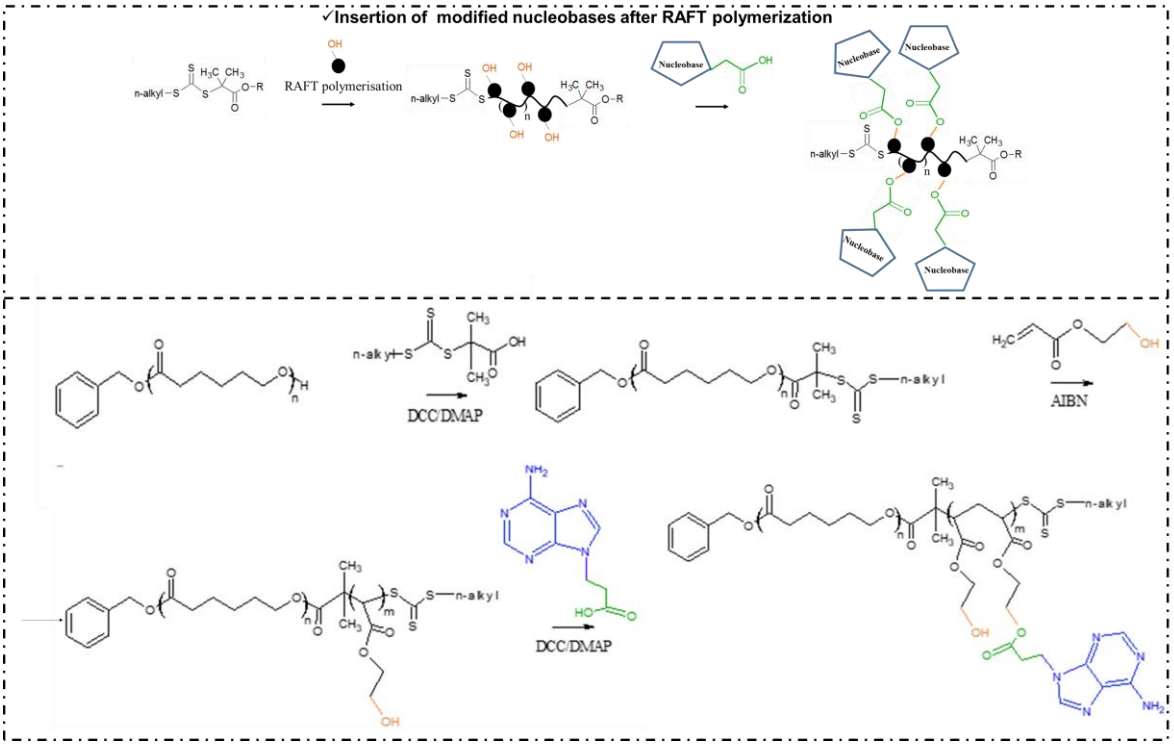

Fig. 10. Functionalization with nucleobases by insertion of modified nucleobases after RAFT polymerization.[44]

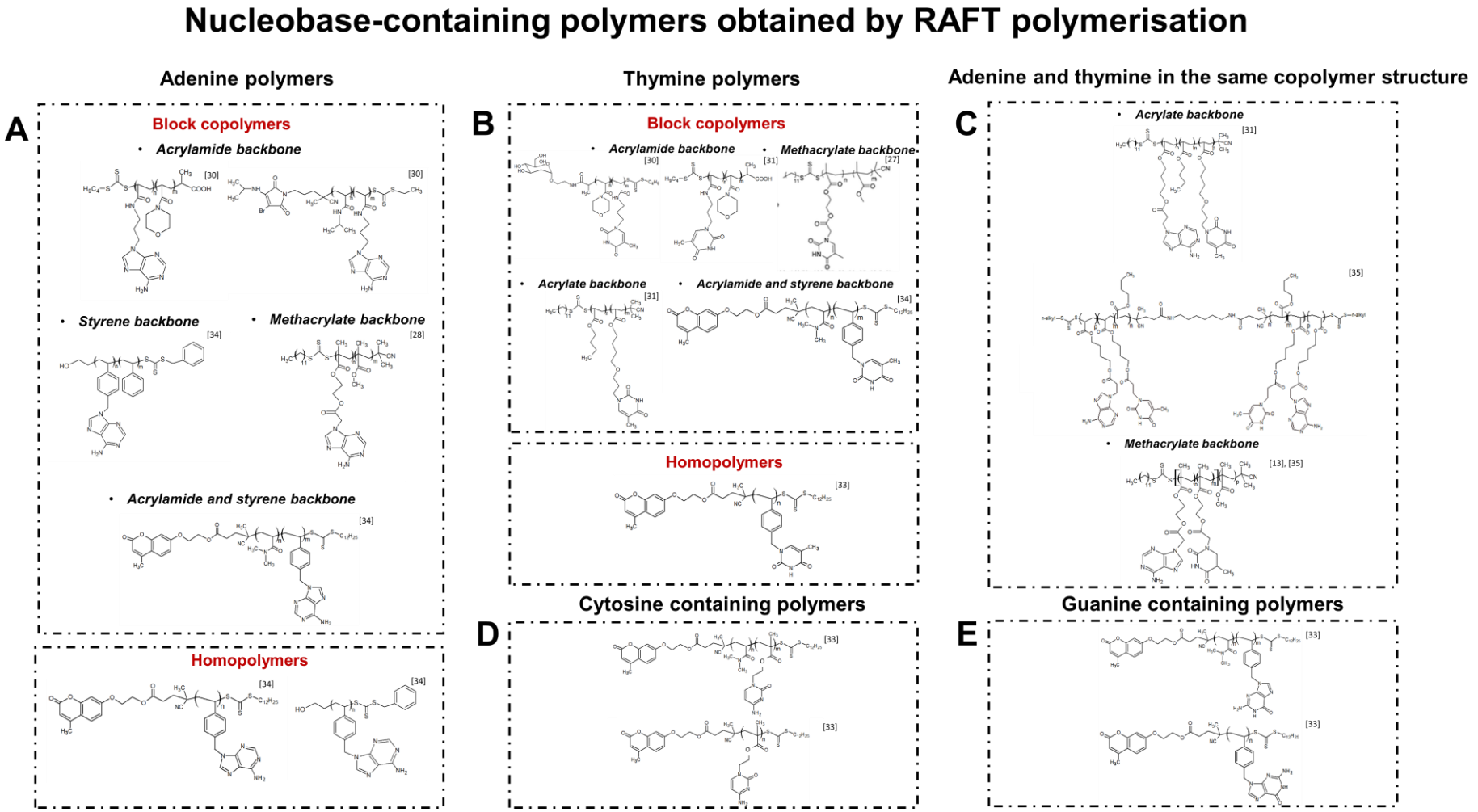

Fig. 11. Nucleobase-containing polymers obtained by RAFT polymerization: (A) Adenine-containing polymers; (B) thymine-containing polymers; (C) adenine- and thymine-containing polymers; (D) cytosine-containing polymers and (E) guanine-containing polymers.

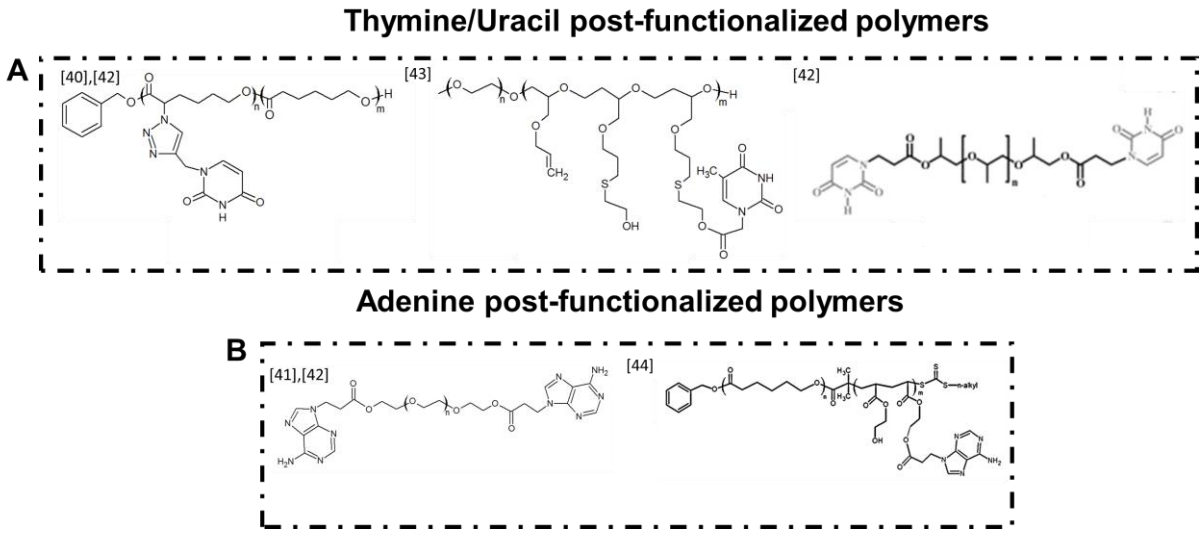

Fig. 12. Nucleobase-containing polymers obtained by post-functionalisation reactions.

V. Self-assembly of nucleobase-containing polymers

Few examples of self-assembled structures formed in solution state based on synthetic nucleobase-containing polymers have been reported so far, probably because the synthesis of these polymers is very labor-intensive, as presented in the previous section. Until now, the reported self-assembled nucleobase containing polymer architectures were formed from synthetic nucleobase-containing block copolymers or commercial polymers functionalized with nucleobases. Various parameters (internal: chain length, density and position of nucleobases on the macromolecular backbone, incompatibility of the blocks; or external: pH, temperature, solvent etc.) are known to influence the self-assembly of nucleobase-containing polymers.

While these parameters were many times reported to change the morphology (in terms of shape or size) of the self-assemblies, a clear correlation between the varied parameter and the obtained morphology has never been explained, to our knowledge. Most of the self-assembled nucleobase-containing polymers mentioned in the literature were prepared in organic solvents. The nucleobase-containing homopolymers reported so far were not water soluble. Indeed, in DNA or RNA, water-solubility comes from the charged backbone. To mimic DNA, water solubility is an important parameter. Only few water-soluble self-assemblies made of nucleobase-containing copolymers have been reported. In this section, the main properties of self-assembled nucleobase-containing polymers are classified according to the type of solvent used (organic solvent, mixture of organic solvent/water or water).

A. Self-assembled nucleobase-containing polymers prepared in organic solvents

According to Kang *et al*., distinct morphologies (*Fig. 13A*) could be obtained by changing the organic solvent used for the self-assembly of poly(2-(2-(thymine-1-yl) acetoxyl) ethyl methacrylate)-*b*-poly (methyl methacrylate) diblock copolymers (DP of thymine containing block = 100).[45] In non-polar solvents such as chloroform, well-defined spherical micelles were formed. This morphology was confirmed by Small Angle Neutron Scattering (SANS) indicating a total radius of 108.3 nm and a shell thickness of 38.3 nm. In a chloroform/1,4 -dioxane (75 vol% $CHCl_3$) binary mixture, the block copolymer self-assembled into complex morphologies of lamellae with tentacles presenting a hydrodynamic diameter of 300 nm confirmed by dynamic light scattering (DLS). The composition of the solvent had an influence on the observed morphologies. At 50 vol% of $CHCl_3$, long flexible cylinders (5 µm) were observed whereas short worm-like structures of 75 nm long were obtained at 12.5 vol% $CHCl_3$. In pure 1,4-dioxane, core–shell spherical morphologies with a mean diameter of 100 nm were obtained.

Changing the length of the thymine-containing block (*Fig. 13B*) led to unexpected results in 1,4-dioxane. Indeed, at DP = 50, disk like morphologies were observed, whereas at DP = 100 spherical core shell morphologies were noted and at DP = 200 disk like morphologies appeared again (*Fig. 13B*). In chloroform, an increase of the degree of polymerization of the thymine-containing block from 20 to 50 led to spherical micelles and cylinders respectively (*Fig. 13B*). According to the authors, the morphological transitions in the presence of a non-polar solvent occurred due to the poor solubility of the polymers in chloroform which increased the intra- and intermolecular chain interactions. In 1,4-dioxane, the nucleobase containing blocks of the polymers were more soluble than in chloroform and thus, the non-covalent chain interactions were limited and the morphology was kept constant.

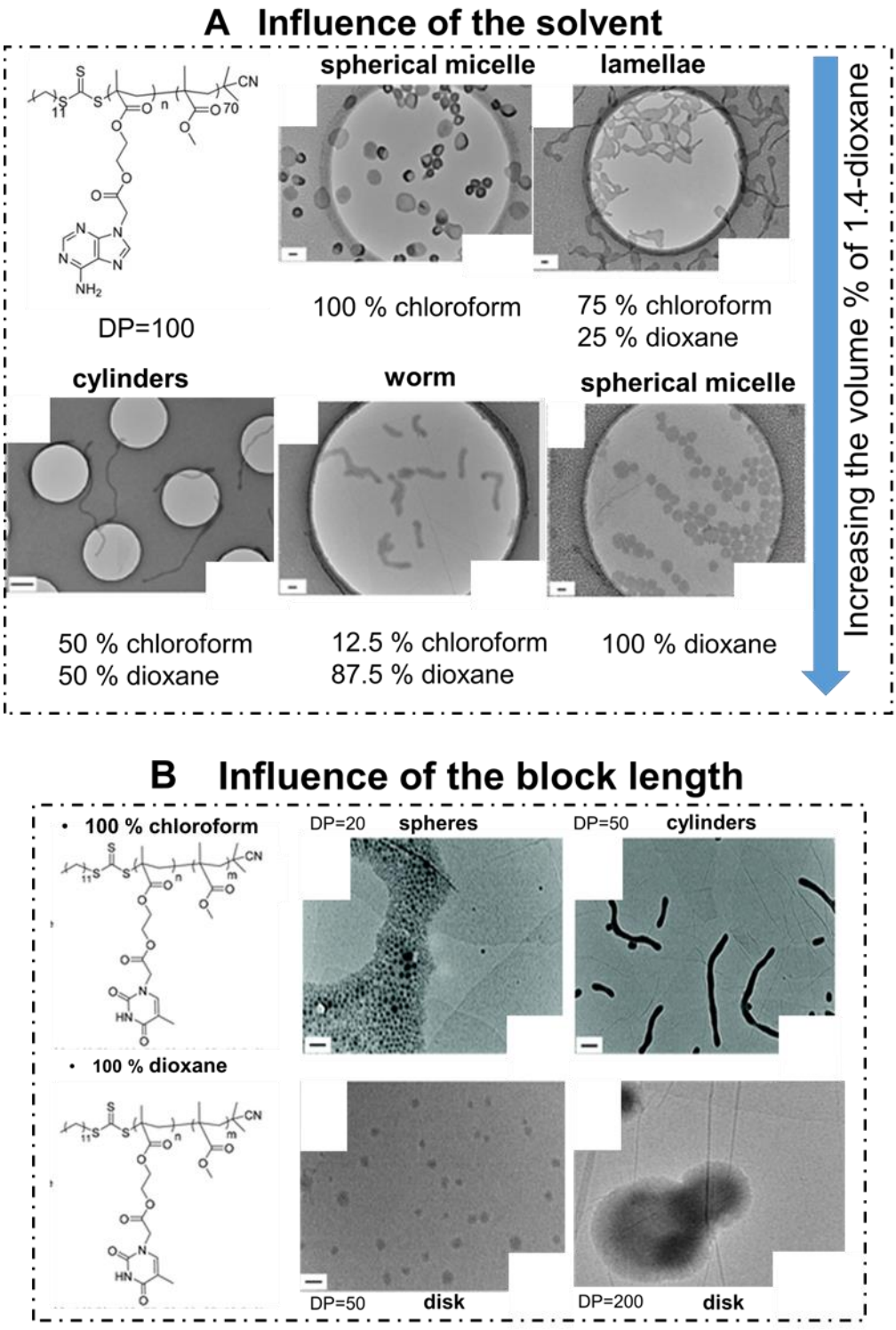

Fig. 13. (A) Morphologies of Poly(2-(2-(thymine-1-yl) acetoxyl) ethyl methacrylate)-b-Poly(methyl methacrylate) micelles at different compositions of solvents; morphologies of the micelles in chloroform (B) and in dioxane for different thymine-containing block length. Scale bar: 100 nm. Adapted from ref. 45 with permission from the Royal Society of Chemistry Copyright 2015.[45]

B. Self-assembled nucleobase-containing polymers prepared in organic solvent/water mixtures

- **The influence of the amount of complementary nucleobase-containing polymers**

In 2016, Cheng *et al.*[42] showed that the co-assembly in a THF/water mixture of uracil functionalized poly(*ε*-caprolactone) (U-PCL, M_n =37600 g mol^{-1}) with adenine-difunctionalized telechelic poly(ethylene glycol) (BA-PEG, M_n = 2000 g mol^{-1}) led to micelles with a pore-like morphology. The micelles were prepared by slow addition of the polymer solutions (prepared in THF) in water, under continuous stirring. The cores were composed of U-PCL units attached to the BA-PEG corona (*Fig. 14A*). An increase in the BA-PEG amount from 50 to 91 wt% led to a decrease of the micelle diameter from 176 to 97 nm due to a change in hydrophobic/hydrophilic balance (*Fig. 14B*). According to the authors, since the amount in BA-PEG increased, more U-PCL units were bound by H-bonds and the micelle became more compact. Changes in the amount of complementary nucleobase-containing polymer chain enabled modifications of the size of self-assembled spherical micelles obtained after self-assembly without shape modifications.

A

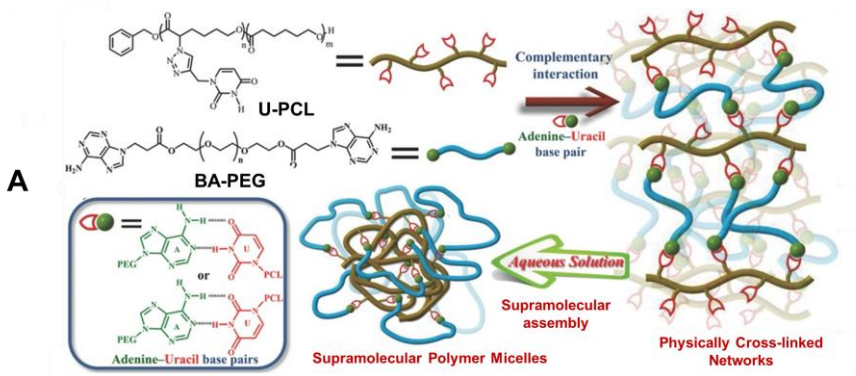

B

Sample (U-PCL/BA-PEG)	Size (nm)
1/1	176
1/5	114
1/10	97

Fig. 14 (A) Formation of micelles via the self-assembly of Uracil-poly (ε-caprolactone) (U-PCL) and biadenine-poly(ethylene glycol) (BA-PEG); (B) The size diameters of U-PCL/BA-PEG micelles depending on the weight ratios of the mixture. Adapted with permission from ref. 42 Copyright (2016) Wiley.[42]

- **Influence of chain length of nucleobase-containing block**

In the study described by Hua *et al.*,[30] an increase in the nucleobase-containing block length was key to obtain various morphologies. In their work, Hua *et al.* studied block copolymers consisting of a hydrophilic poly(4-acryloyl morpholine) (PNAM) block and a hydrophobic poly(thymine propyl acrylamide) (PTAm) block, as presented in *Fig. 15*. These block copolymers self-assembled in DMF/water mixture into spherical micelles with thymine-containing cores and hydrophilic PNAM shell. The authors stated that for short PTAm blocks (17 T to 34 T motifs), small micelles (N_{agg} ~ 13) were formed due to a low density of non-covalent interactions. Longer PTAm blocks (114 T to 301 T units) led to changes from spheres (114 T) to cylinders (160 T) and to smaller spheres (301 T). According to the authors, long chain thymine block enabled more non-covalent interactions inside the hydrophobic blocks that forced the structural packing in smaller micellar objects (*Fig. 15*).

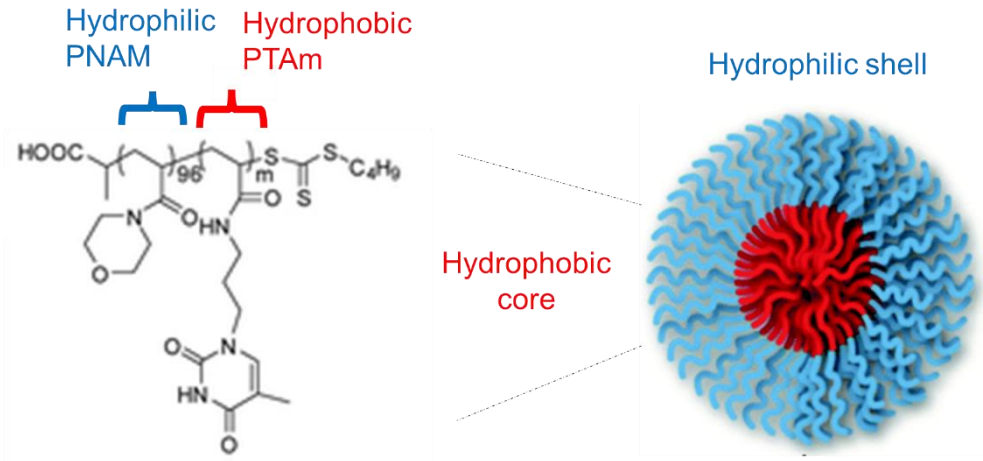

Fig. 15 Representation of Poly(4-acryloylmorpholine-b-poly(3-(thymine-9-yl)propyl acrylamide) diblock copolymer micelles. Adapted from ref. 30 with permission from the Royal Society of Chemistry Copyright 2015.[30]

- **Influence of the flexibility/rigidity of nucleobase-containing block**

Another way to modify hydrophobic/hydrophilic balance and hence the ability of nucleobase-containing copolymers to self-assemble in different morphologies is to use more flexible or more rigid polymer backbones. Wang *et al.*[33] reported the synthesis of different diblock copolymers with PNIPAM as the hydrophilic block. The hydrophobic block was either made of poly(styrene-adenine/thymine/guanine) ($P_sA/P_sT/P_sG$) as rigid block backbones (due to the presence of aromatic regions which create stacking effects), and hydrophobic poly(methacrylate-cytosine) (P_mC) as flexible block backbones (as a consequence of alkyl chains) (*Fig. 16A*).[33] All block copolymers (*i.e.*, P_sA-*b*-PNIPAM, P_sT-*b*-PNIPAM, P_mC-*b*-

PNIPAM, P_sG-*b*-PNIPAM) presented the same molar mass, around 9 kDa, while the DP of PNIPAM was ~30 and the DP of nucleobase-containing block was ~20. The co-assembly in DMSO/water of the rigid-rigid P_sA-*b*-PNIPAM and P_sT-*b*-PNIPAM (in 1: 1 molar ratio) mixture resulted in spindle-like aggregates. In contrast, the co-assembly of the flexible P_mC-*b*-PNIPAM with the rigid P_sG-*b*-PNIPAM led to a telophase-like structures (*Fig. 16B*).

According to the authors, these morphological differences were direct consequences of the steric confinement induced by the structure of the nucleobase-containing block. In the co-assembly formed by mixing P_sA-*b*-PNIPAM and P_sT-*b*-PNIPAM diblock copolymers, the hydrophobicity of poly(styrene) enabled the polymer chains to stack with each other, while the hydrophilic PNIPAM chains were displayed on both sides to reduce steric hindrance. According to the authors, these steric confinement effects explained the spindle-like morphology. The use of flexible P_mC, in copolymerization with PNIPAM, resulted in flexible P_mC-*b*-PNIPAM block copolymers (*Fig. 16B*). During H-bond recognition with complementary rigid P_sG-*b*-PNIPAM block, this flexibility allowed the polymer chains to aggregate which explained the dark points observed by TEM of the telophase structures. Overall, the rigidity of nucleobase-containing block is a crucial parameter that guide the H-bond based self-assembly to adopt a hindered morphology. Oppositely, a flexible nucleobase-containing block favors a facile co-assembly and thus access to a different morphology.

Otherwise, the non-covalent interactions established during the co-assembly of complementary nucleobase-containing copolymers are correlated to the flexibility of the polymer backbones. For example, Huang *et al.*[40] reported the formation of spherical micelles with a dot-type morphology (diameter lower than 200 nm) when mixing poly(carbazole-thymine) (PC-T) with adenine monofunctionalized poly(ethylene glycol) (PEG-A) in THF/water (*Fig. 17A and B*). The micelles had a hydrophobic core composed of PC-T covered by a PEG shell. In order to investigate the influence of hydrophobic PC-T and hydrophilic PEG in the formation of supramolecular complex, DSC experiments were performed. As the authors stated, the association of complementary H-bonds between T and A led to a decrease in the T_g from 145°C (for pure PC-T) to 119°C (for the supramolecular complex), while the T_g of PEG-A disappeared. The decrease in T_g was caused by changes in the system packing towards an increased flexibility induced by PEG-A chains. This work illustrated, as stated by the authors, that the hydrophilic behavior of co-assembled nucleobase-containing polymers can be improved by using flexible chain water-soluble polymers containing nucleobases.

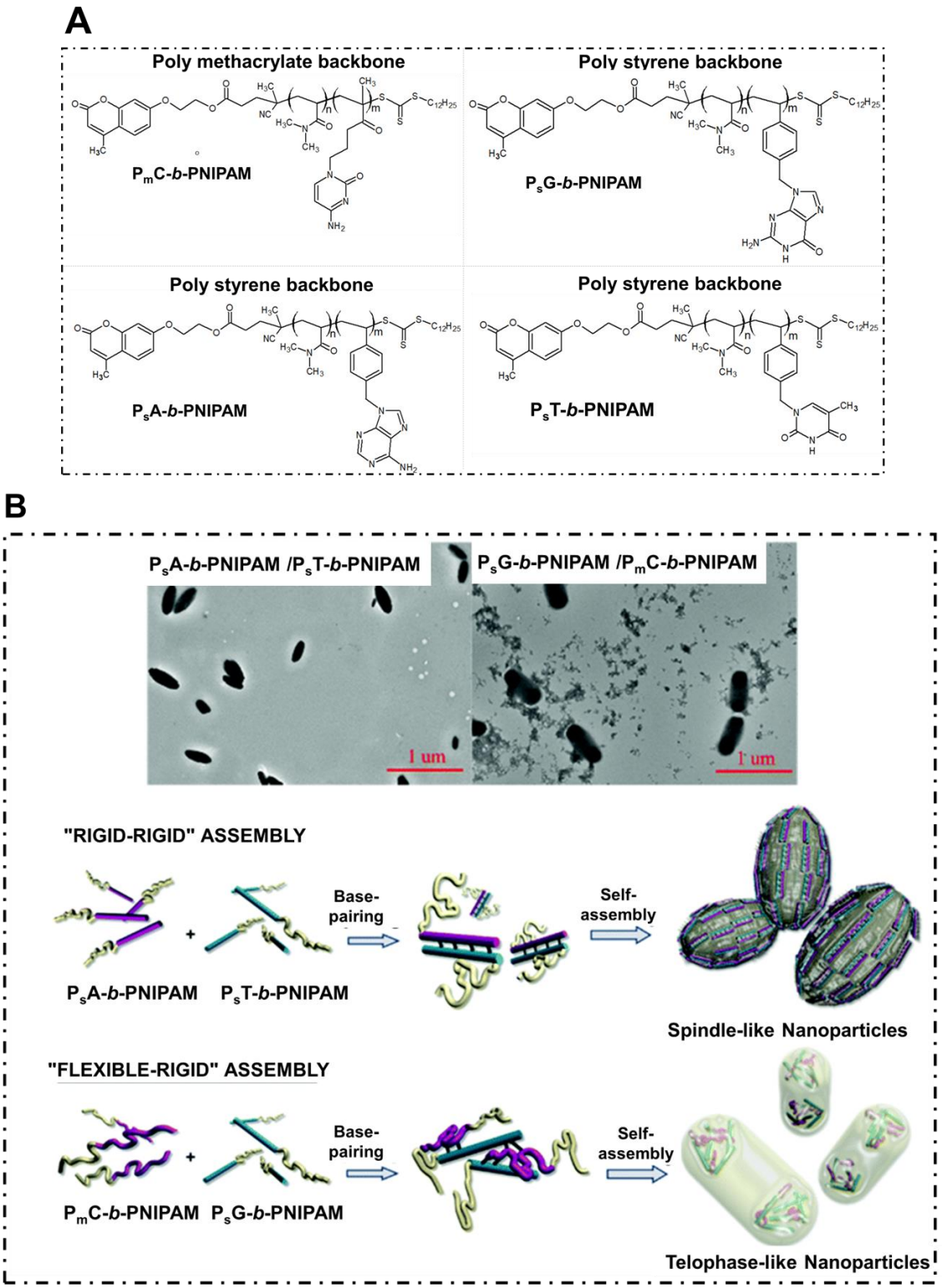

Fig. 16 (A) Structures of polymers containing nucleobases; (B) Morphologies obtained via the H-bond co-assembly of polymers containing nucleobases. Adapted from ref. 33 with permission from the Royal Society of Chemistry Copyright 2019.[33]

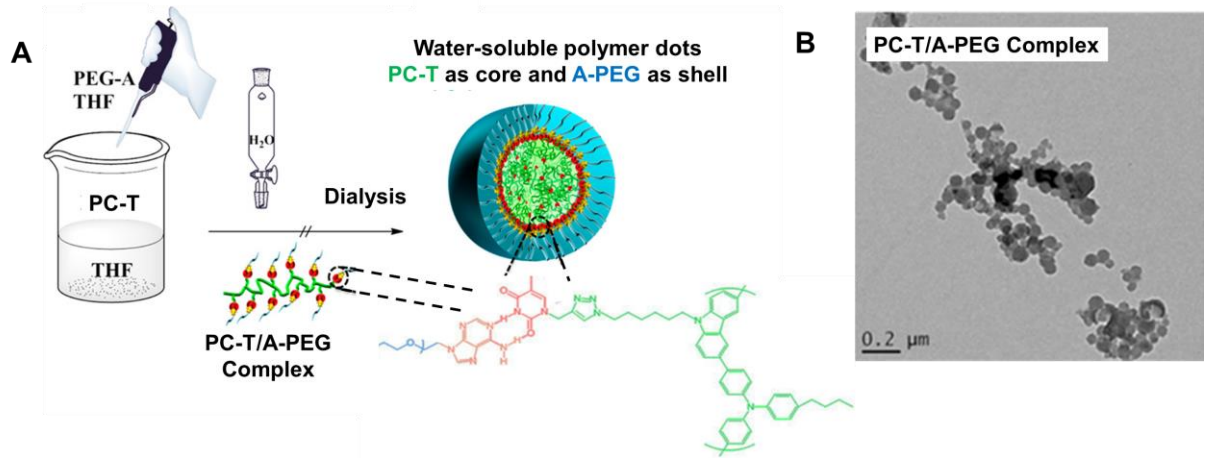

Fig. 17 (A) Poly(ethylene glycol)-Adenine (PEG-A) and poly(carbazoles-thymine) (PC-T) Micelles; (B) Morphology of PC-T/A-PEG complex micelles. Adapted with permission from ref. 40 Copyright (2017) American Chemical Society.[40]

- **Influence of the nucleobase position**

The position of the H-bond-promoting nucleobase at the extremity of the hydrophobic block or at the extremity of the hydrophilic block in the nucleobase-containing di-block copolymer structure significantly influenced the pairing ability with a complementary nucleobase, as shown by Wang *et al.*[36] In their work, the authors reported thymine-containing poly(n-butyl methacrylate) polymers T-PMBA, as well as poly(oligo(ethylene glycol) methacrylate)-*b*-poly (n-butyl methacrylate) (POEGMA-*b*-PMBA) block copolymers end-conjugated with adenine. In the case of adenine-containing copolymers, the adenine was attached either at the end of the hydrophilic block (P1, noted as A-POEGMA-*b*-PMBA, *Fig. 18A*) or at the end of the hydrophobic block (P2, noted as A-PMBA-*b*-POEGMA, *Fig. 18A*). To obtain the co-assemblies, adenine-containing copolymers were dissolved in DMSO, the solution being slowly dropped to phosphate buffer solution (PBS). Then, a solution of thymine-containing polymer (prepared in PBS) was added to the adenine-containing solution. In order to investigate the role of the adenine position in the copolymer and the ability of H-bond co-assembly with thymine-containing polymer, the authors performed NMR experiments (in DMSO-d_6/PBS solvent mixture), where the solution of thymine-containing polymer T-PMBA (40 mM) was mixed with solutions of adenine-containing polymer (P1, *Fig. 18, B-1* and P2, in *Fig. 18, B-2*) in different concentrations (1.1 mM, 3.5 mM, 6.4 mM and 10.6 mM). These NMR experiments showed, as stated by the authors, a shift of the protons of adenine in P1 upon interaction with the thymine polymer (*Fig. 18, B-1*), whereas in P2 this interaction was not detected (*Fig. 18, B-2*). As stated by the authors, the molecular recognition between complementary nucleobases

was influenced by their availability to be involved in H-bonding, which depended on the nucleobase position on the polymer backbone. In P2 the adenine at the hydrophobic end of the block copolymer located in the core of the micelles was inaccessible to thymine which cannot diffuse inside the micelle to bind adenine. In contrast, in P1 the adenine was on the hydrophilic block which form the shell of the micelle and thus is easily accessible for complementary recognition with thymine (*Fig. 18C*). However, these results were surprising, since a single adenine–thymine interaction is rather weak in DMSO/water medium. Nevertheless, the main conclusion according to Wang *et al.*[36] was that adenine– thymine binding was possible because the complementary nucleobases were accessible on the exterior of the micelles.[36]

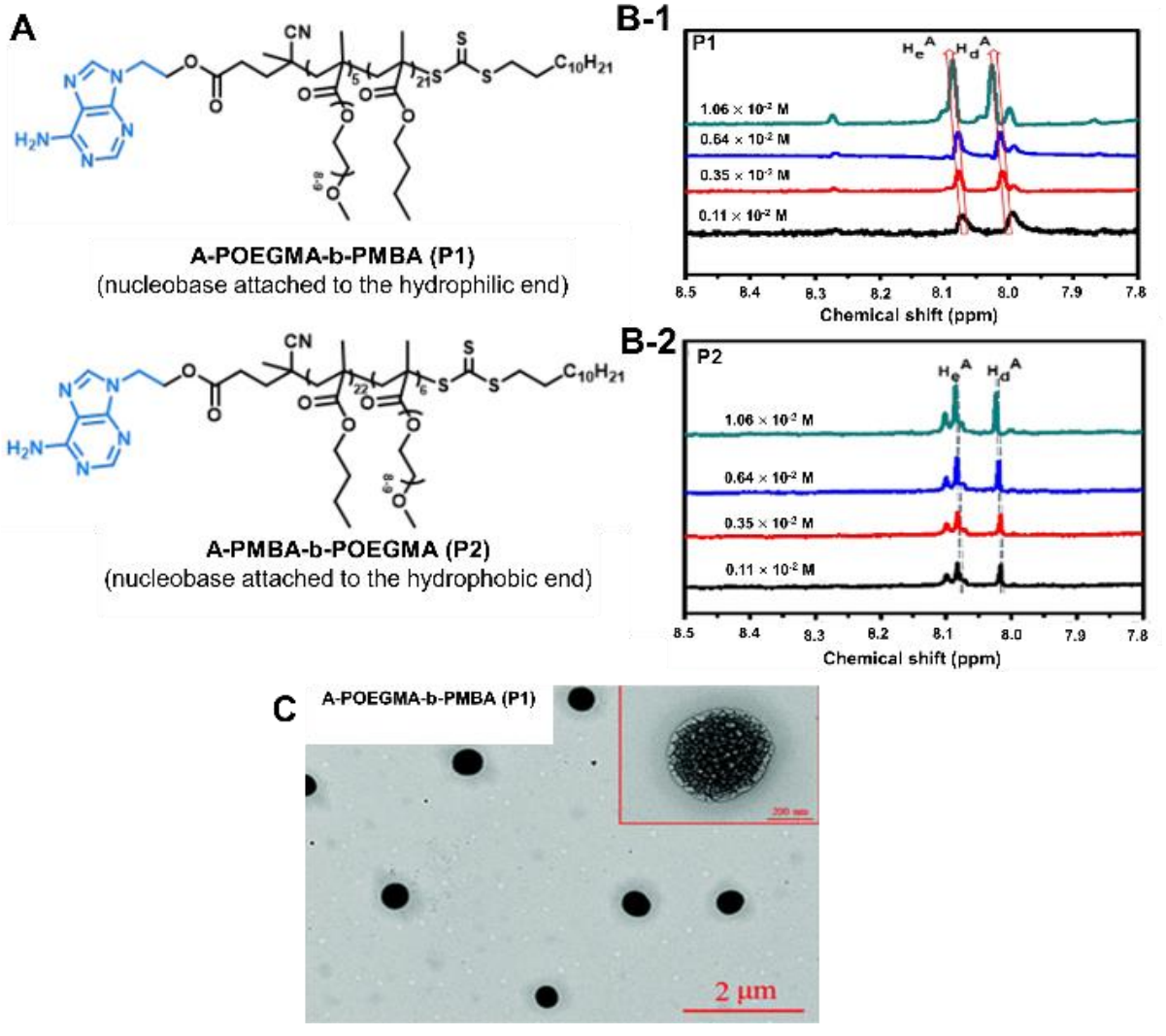

Fig. 18 (A) Representation of Adenine-poly(oligo(ethylene glycol) methacrylate)-poly(n-butyl methacrylate) (A-POEGMA–PMBA) systems; (B) NMR experiments (in DMSO-d6/PBS solvent mixture), where the solution of thymine-containing polymer T-PMBA (40 mM) was mixed with solutions of adenine-containing polymer (P1, Fig. B-1. and P2, in B-2.) in different

concentrations (1.1 mM, 3.5 mM, 6.4 mM and 10.6 mM). (C) Morphology of the co-assemblies of P1 with T-PMBA. Adapted from ref. 36 with permission from the Royal Society of Chemistry Copyright 2018.[36]

- **Influence of the pH**

The pH is another parameter which can influence the formation of different morphologies of self-assembled nucleobase-containing polymers. Nucleobases are sensitive to pH changes, especially to low pH. Indeed, in acidic conditions, the nitrogen atoms of the nucleobases which are involved in the H-bond recognition are protonated. As a consequence, the H-bond ability of the nucleobases is affected and the co-assembling properties (and morphologies) are modified. In 2016, Zhao *et al.*[44] developed amphiphilic conjugates able to co-assemble forming small-size (below 100 nm) nanoparticles (NPs), by mixing poly(ε-caprolactone)-*graft*-poly(2-hydroxyethylacrylate-adenine) (abbreviated as A-PCL) with poly(ethylene glycol)-*block*-poly(allyl glycidyl ether-β-mercapto-ethanol-thymine) (abbreviated as T-PEG), in DMSO/water. A-PCL and T-PEG functionalized polymers co-assembled via molecular recognition between complementary nucleobases (A and T) (*Fig. 19A*).

As stated by the authors, in neutral conditions (pH 7.4), the resulting NPs with a diameter of 45 nm were stable due to strong H-bonds linking the A and T moieties. Upon decrease of the pH to 6, the NPs diameter decreased to 25 nm due to the protonation of the nucleobases that partially disrupted the A-T H-bonds, provoking the shedding of the T-PEG corona (*Fig. 19B*). Interestingly, the variation of H-bond strength between nucleobases as a result of pH modification, was shown to have a high impact on the use of nucleobase-containing polymers co-assemblies in the field of drug delivery. Cheng *et al.* showed that the H-bonds stability of co-assembled nucleobase polymers used for doxorubicin (DOX, a drug used in anticancer therapy) release is influenced by the pH.

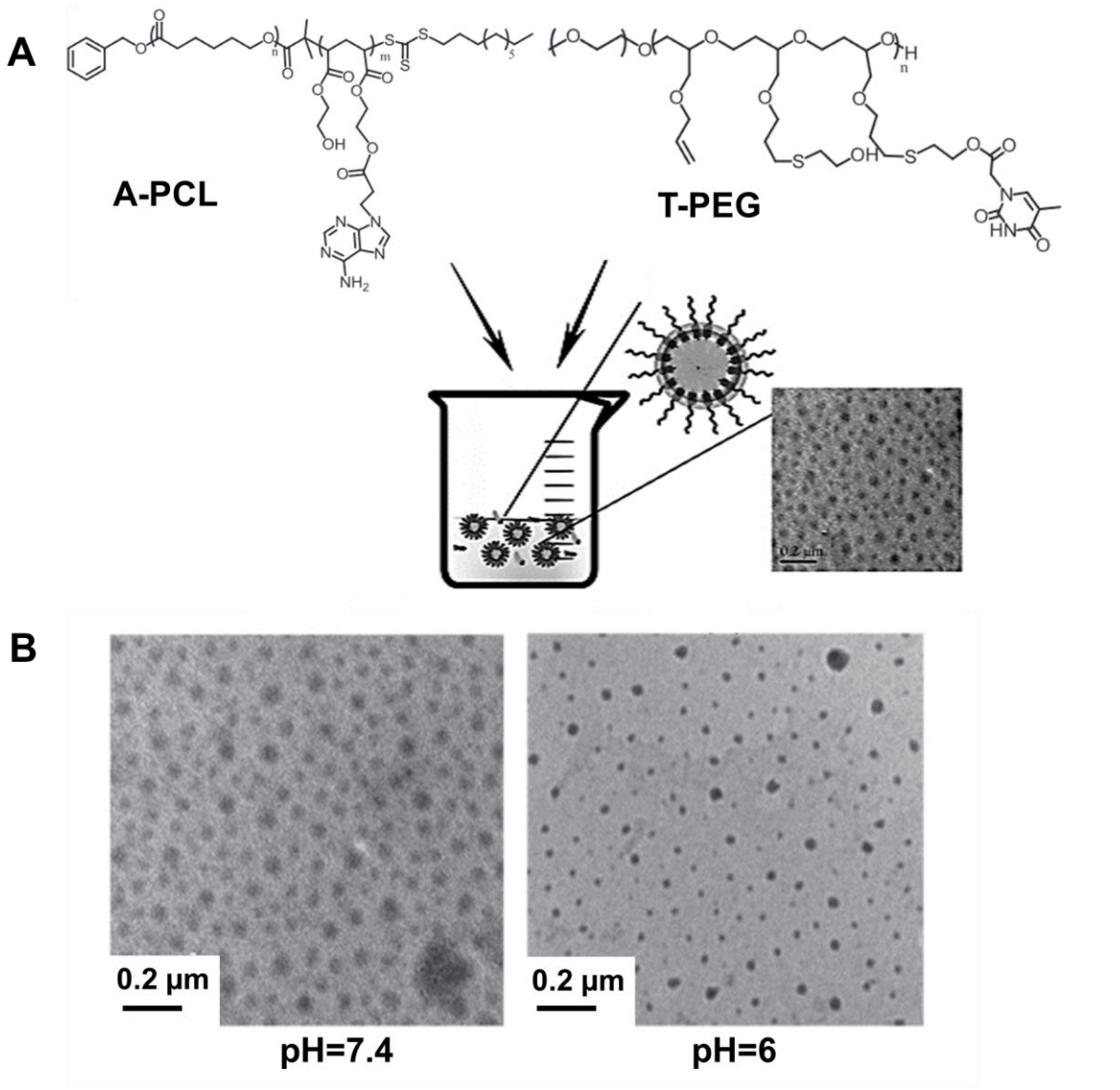

Fig. 19 (A) Poly(adenine)-poly(ε-caprolactone) (A-PCL) and poly (thymine)– poly(ethylene glycol) (T-PEG) micelles; (B) TEM images of A-PCL/T-PEG micelles at different pH. Note: a carbon in the structure of the repeating unit of A-PCL and the parenthesis of the repeating units of T-PEG are missing in the figure published. Reprinted with permission from ref. 44 Copyright (2016) Wiley.[44]

They prepared micelles *via* the co-assembly of uracil-containing poly(ε-caprolactone) (U-PCL) and telechelic poly(ethylene glycol) functionalized with two adenine groups (BA-PEG) (*Fig. 20*).[42] This system was tested for DOX release at acidic (pH 5) and neutral pH (pH 7.4). The micelles showed a faster release of DOX at pH 5 than at pH 7.4. According to the authors, these results were explained by the disassembly of the supramolecular U-A interactions in the micelles upon acidification. However, no information was given concerning the evolution of shape or dimension of the prepared micelles when pH was changed.

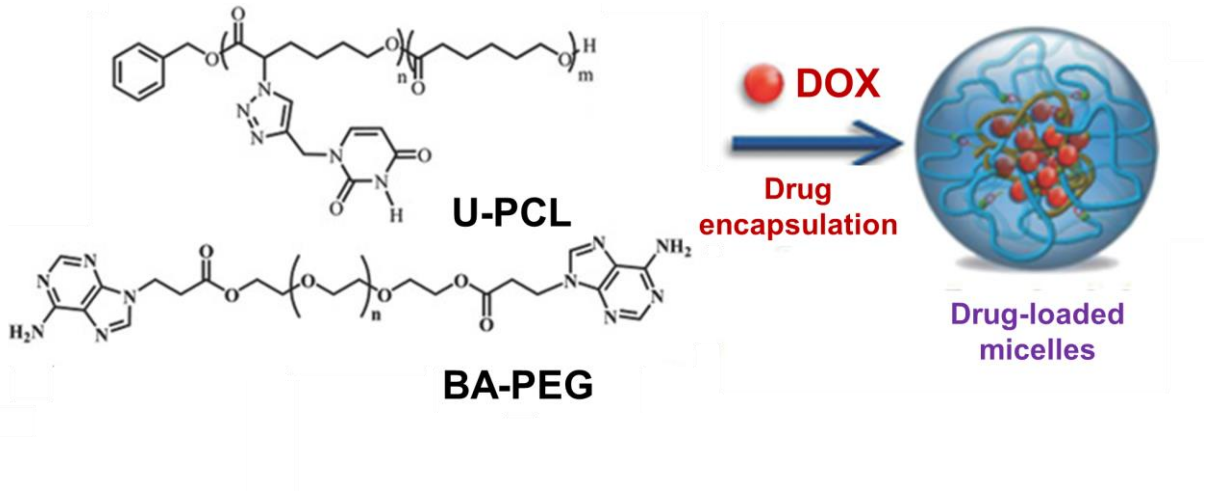

Fig. 20 Uracil-poly(ε-caprolactone) (U-PCL) and biadenine-poly(ethylene glycol) (BA-PEG) micelles entrapping DOX. Adapted with permission from ref. 42 Copyright (2016) Wiley.[42]

C. Self-assembled nucleobase-containing polymers prepared in water

- **Influence of the temperature**

Gebeyehu *et al.*[43] reported that self-assembled biuracil-poly(propylene glycol)-based micelles can change in size when the temperature is modulated. The nucleobase-containing polymer involved in the self-assembly was designed as follows: a bifunctional telechelic poly(propylene glycol) was end-capped with two uracil units (BU-PPG). BU-PPG polymers were able to self-assemble in water *via* H-bonds formed between uracil units into micelles with size between 148–370 nm and endowed with thermosensitive morphologies.

In the systems described by Gebeyehu *et al.*[43] the self-assembly took place as a result of H-bonds between the same nucleobase (uracil). Cheng *et al.*[46] investigated if the presence of a complementary nucleobase (*i.e.*, adenine) influences the strength of H-bonds and in consequence the behavior of co-assembled systems at various temperature, as well as the morphology. In this regard, they used adenine-methyl acrylate (A-MA) that co-assembled through complementary H-bonds with uracil fragments from BU-PPG (bi-uracil end-capped poly (propylene glycol)). As previously presented by the work of Gebeyehu *et al.*,[43] BU-PPG is a thermo-responsive polymer. Below the LCST (25 °C) the association of BU-PPG with A-MA (1:2 molar ratio) led to spherical micelles with diameters around 85 nm. For temperatures above LCST (45 °C), larger aggregates of about 240 nm were formed (*Fig. 21*). As stated by the authors, the complementary H-bonds between A and U promoted the formation of low-dimensional particles (for temperatures below LCST). For temperatures above the LCST, the

increase of the particle size was explained by the presence of hydrophobic effects induced by PPG chains that destroy the H-bonds and led to large aggregates.

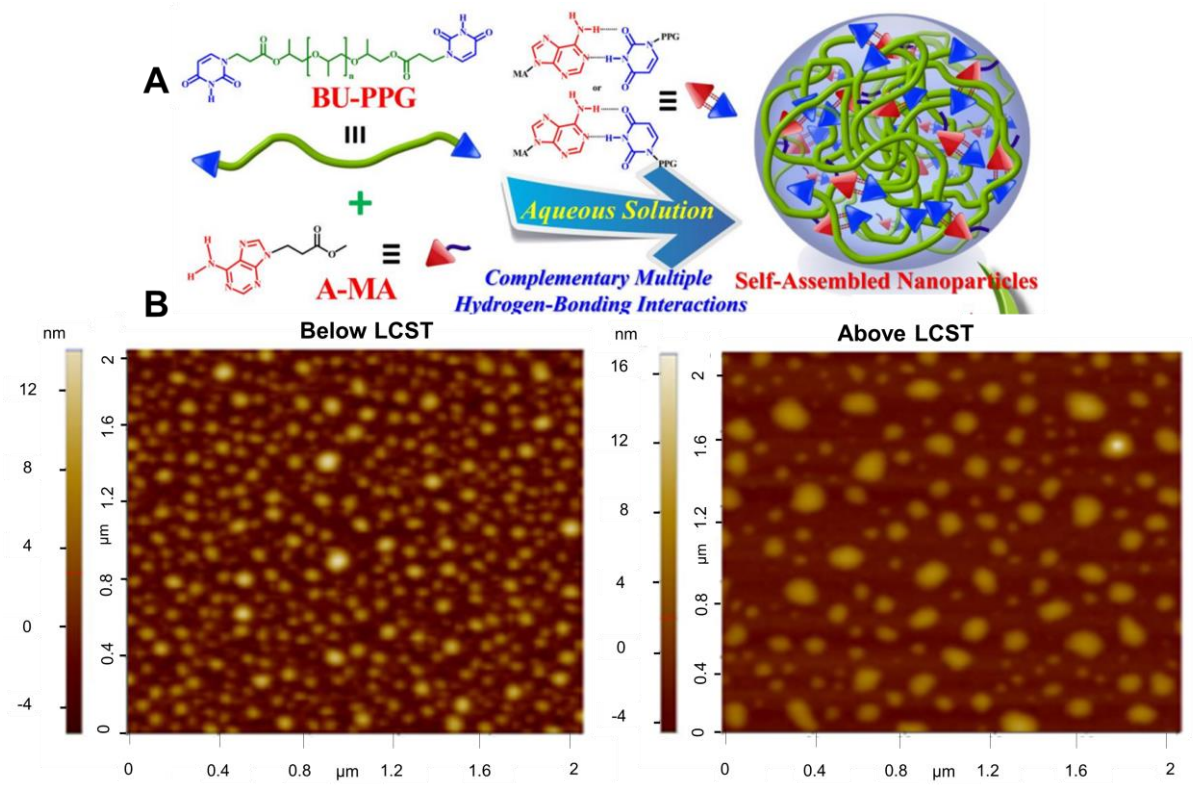

Fig. 21 (A) Development of micelles composed via co-assembly of biuracil-poly(propylene glycol) (BU-PPG) and adenine-methyl acrylate (A-MA); (B) AFM images of micelles below and above LCST. Adapted with permission from ref. 46 Copyright (2016) Elsevier.[46]

VI. Conclusions

This review aimed to emphasize the importance of different parameters such as polymer structure, pH, solvents and temperature in the formation of various morphologies of self-assembled nucleobase-containing copolymers.

First, this review summed up the main examples of nucleobase-derived monomers and the corresponding polymers resulting from these monomers. Few examples of monomers and polymers containing nucleobases were reported so far. The low number of synthetic macromolecules containing nucleobases reported until now might be a consequence of significant issues related to the synthesis of the starting monomers, especially during the purification steps.

However, nucleobase-containing copolymers have attracted a high interest in the field of bioinspired supramolecular self-assembly, since the nucleobases are functional moieties found

in the genetic material. The reported self-assemblies made from nucleobase-containing copolymers are formed *via* hydrophobic interactions, and *via* H-bonds established between complementary nucleobases. These interactions (and particularly the H-bonds) are sensitive to changes related to the polymer structure, pH, solvents or temperature.

These observations have already been stated by different research groups. However, not many papers illustrated how the morphology can be tailored by the above-mentioned parameters. For this reason, the second part of this review dealt with this aspect. Even if the papers presented in this review revealed interesting results in terms of morphology changes under a variety of conditions, the prediction of the obtained morphologies obtained under the influence of different parameters remains a difficult task. This subject is still under investigation and it is highly challenging because it aims to define the "rules" that direct the self-assemblies of nucleobase-containing copolymers into specific morphologies.

A preliminary step to get closer to this aim was to analyze how these parameters affected the self-assembled polymers and the obtained morphologies.

First, it was observed that the structural features (length of nucleobase-containing blocks, the number of nucleobase units, the position of nucleobases on the hydrophilic or hydrophobic block, or the flexibility of blocks) of nucleobase-containing polymers involved in the self-assembly can be largely modulated to achieve different morphologies. The most common morphology formed by self-assembly of nucleobase containing polymer was, without surprise, spherical micelle. However, important changes were observed concerning the size of the spherical micelles when the number of nucleobase units was varied, and were explained due to supplementary effects of hydrophobic interactions between nucleobases. In terms of shape, interesting elongated morphologies were developed when using flexible (alkyl chain containing-) or rigid (aromatic segments containing-) polymer architectures.

Secondly, pH variations induced important modifications to the nucleobase-containing copolymer self-assemblies. Most of the observed modifications concerned the size of the obtained spherical micelles that diminished when the pH decreased. However, the shape of the objects was not changed under pH variations. A possible explanation was that the presence of charges is a priori unfavorable to develop self-assembled architectures and in consequence the transition of the morphology.

The H-bonds are sensitive to temperature changes. Especially, the H-bonds between water molecules are completely disrupted at 100°C. However, the reported self-assembled

nucleobase-containing polymers did not show significant sensitivity to temperature. In addition, no morphological changes were reported as a result of temperature variations. Actually, the reported variations in size were mainly a result of LCST behavior of self-assembly induced by the presence of a temperature-sensitive polymer, without a clear impact of H-bonds between complementary nucleobases.

Lastly, the morphology (in terms of shapes and size) was highly adjusted by exploring different solvents. A possible explanation according to the reviewed papers was that the solvent could interfere with the hydrophilic or hydrophobic blocks and enable the blocks to self-assemble *via* the H-bonds in different shaped objects.

The overall conclusion stated by this review is that the morphology is highly dependent on the architecture of the nucleobase-containing copolymers which can perform self-assemblies with different shapes and sizes. Chemists are able to play with different parameters in order to tailor a variety of self-assembling morphologies, which could be further explored to obtain anisotropic shapes that started to receive a special interest in the field of drug delivery. The interest of an anisotropic shape of the self-assembly advocate for continuing the work to tune the architecture of the nucleobase-containing copolymers. In this context, the work of O'Reilly's group who developed an elegant architecture of nucleobase-containing copolymers, which is forming elongated morphologies, opens new perspectives.[47]

VII. References

1. J. Lehn, *PNAS*, 2002, **99(8)**, 4763-4768.
2. D. Lombardo, M. A. Kiselev, S. Magazù, P. Calandra, *Adv. Condens. Matter Phys.*, 2015, 1-22.
3. R. Nagarajan, *Langmuir* **2002**, *18*, 31–38.
4. Y. Mai, A. Eisenberg, *Chem. Soc. Rev.* **2012**, *41*, 5969–5985.
5. D. Chandler, *Nature* **2005**, *437*, 640–647.
6. T. Shimizu, M. Masuda, H. Minamikawa, *Chem. Rev.* **2005**, *105*, 1401–1443.
7. A. Sharma, K. Vaghasiya, R. K. Verma, A. B. Yadav, *Front. Bioeng. Biotechnol.*, 2018, **8**, 1-24.
8. G. B. Schuster, B. J. Cafferty, S. C. Karunakaran, N. Hud, *J. Am. Chem. Soc.*, 2021, **143**, 9279–9296.
9. M. Fathalla, C. M. Lawrence, N. Zhang, J. L. Sessler, J. Jayawickramajah, *Chem. Soc. Rev.*, 2009, **38**, 1608–1620.
10. S. Sivakova and S. J. Rowan, *Chem. Soc. Rev.*, 2005, **34**, 9–21.

11. J. S. Oh, Y. Wang, D. J. Pine, G. R. Yi, *Chem. Mater.* 2015, **27**, 8337–8344.

12. W. Wang, K. Zhang, D. Chen, *Langmuir* 2018, **34**, 15350–15359.

13. F. Jia, H. Li, R. Chen, K. Zhang, *Bioconjug. Chem.* 2019, **30**, 1880–1888.

14. X. Lu, E. Watts, F. Jia, X. Tan, K. Zhang, *J. Am. Chem. Soc.* 2014, **136**, 10214–10217.

15. H. Lu, J. Cai and K. Zhang, *Polym. Chem*., 2021, **12**, 2193– 2204.

16. A. Marsh, A. Khan, D. M. Haddleton, M. J. Hannon, *Macromolecules*, 1999, **32**, 8725–8731.

17. J. Li, Z. Wang, Z. Hua, C. Tang, *J. Mater. Chem. B*, 2020, **8**, 1576–1588.

18. H. J. Spijker, F. L. van Delft, J. C. M. van Hest, *Macromolecules*, 2007, **40(1)**, 12–18.

19. B. D. Mather, M. B. Baker, F. L. Beyer, M. A. G. Berg, M. D. Green, T. E. Long, *Macromolecules*, 2007, **40(19)**, 6834–6845.

20. S. Sivakova, J. Wu, C. J. Campo, P. T. Mather, S. J. Rowan, *Chem. – Eur. J.*, 2005, **12(2)**, 446–456.

21. J. Cortese, C. Soulié-Ziakovic, M. Cloitre, S. Tencé-Girault, L. Leibler, *J. Am. Chem. Soc*., 2011, **133(49)**, 19672– 19677.

22. W. H. Binder, M. J. Kunz, C. Kluger, G. Hayn, R. Saf, *Macromolecules*, 2004, **37**, 1749–1759.

23. A. del Prado, D. Gonzales-Rodriguez, Y.-L. Wu, *ChemistryOpen*, 2020, **9(4)**, 409–430.

24. R. McHale and R. K. O'Reilly, *Macromolecules*, 2012, **45(19)**, 7665–7675.

25. H. Yang and W. Xi, *Polymers*, 2017, **9(12)**, 666–690.

26. A. Sikder, C. Esen, R. K. O'Reilly, *Acc. Chem. Res*., 2022, **55(12)**, 1609–1619.

27. S. Chea, K. Schade, S. Reinicke, R. Bleul, R. R. Rosencrantz, *Polym. Chem.*, 2022, **13**, 5058–5067.

28. Y. Kang, A. Pitto-Barry, H. Willcock, W.-D. Quan, N. Kirby, A. M. Sanchez, R. K. O'Reilly, *Polym. Chem*., 2015, **6**, 106–117.

29. T. A. Hamlin, M. Swart, F. M. Bickelhaupt, *ChemPhysChem*, 2018, **19(11)**, 1315–1330.

30. Z. Hua, A. Pitto-Barry, Y. Kang, N. Kirby, T. R. Wilks, R. K. O'Reilly, *Polym. Chem.* 2016, **7**, 4254–4262.

31. K. Zhang, G. B. Fahs, M. Aiba, R. B. Moore, T. E. Long, *Chem. Commun.* 2014, **50**, 9145–9148.

32. Z. Hua, R. Keogh, Z. Li, T. R. Wilks, G. Chen, R. K. O'Reilly, *Macromolecules* 2017, **50**, 3662–3670.

33. M. Wang, B. Choi, Z. Sun, X. Wei, A. Feng, S. H. Thang, *Chem. Commun.* 2019, **55**, 1462–1465.

34. E. Kim, A. K. Mishra, C. Choi, M. Kim, S. Park, S. Y. Park, S. Ahn, J. K. Kim, *Macromolecules* 2018, **51**, 10223–10229.

35. K. Zhang, S. J. Talley, Y. P. Yu, R. B. Moore, M. Murayama, T. E. Long, *Chem. Commun.* 2016, **52**, 7564–7567.

36. M. Wang, B. Choi, X. Wei, A. Feng, S. H. Thang, *Polym. Chem.* 2018, **9**, 5086–5094.

37. E. Kim, H. Koo, *Chem. Sci.* 2019, **10**, 7835–7851.

38. P. Chakma and D. Konkolewicz, *Angew. Chem. Int. Ed*., 2019, 9682–9695.

39. D. Huang, Y. Liu, A. Qin, B. Z. Tang, *Polym. Chem*., 2018, **9**, 2853–2867.

40. C. W. Huang, W. Y. Ji, S. W. Kuo, *Macromolecules*, 2017, **50**, 7091–7101.

41. I. H. Lin, C. C. Cheng, C. W. Huang, M. C. Liang, J. K. Chen, F. H. Ko, C. W. Chu, C. F. Huang, F. C. Chang, *RSC Adv.*, 2013, **3**, 12598–12603.

42. C.-C. Cheng, I.-H. Lin, J.-K. Chen, Z.-S. Liao, J.-J. Huang, D.-J. Lee, Z. Xin, *Macromol. Biosci.*, 2016, **16(10)**, 1415– 1421.

43. B. T. Gebeyehu, S. Y. Huang, A. W. Lee, J. K. Chen, J. Y. Lai, D. J. Lee, C. C. Cheng, *Macromolecules*, 2018, **51**, 1189– 1197.

44. X. Zhao, H. Deng, H. Feng, J. Zhang, A. Dong, L. Deng, *Macromol. Chem. Phys*., 2016, **217**, 2611–2616.

45. Y. Kang, A. Pitto-Barry, A. Maitland, R. K. O'Reilly, *Polym. Chem.*, 2015, **6**, 4984–4992.

46. C. C. Cheng, B. T. Gebeyehu, S. Y. Huang, Y. Abebe Alemayehu, Y. T. Sun, Y. C. Lai, Y. H. Chang, J. Y. Lai, D. J. Lee, *J. Colloid Interface Sci.*, 2019, **552**, 166–178.

47. S. Varlas, Z. Hua, J. R. Jones, M. Thomas, C. Foster, R. K. O. Reilly, *Macromolecules*, 2020, **53**, 9747–9757.

Conclusion Chapitre I

Ce chapitre illustré sous la forme d'une revue vise à analyser l'influence de différents paramètres (la structure du polymère, le pH, les solvants et la température) sur la formation de morphologies distinctes obtenues lors de l'auto-assemblage des copolymères comportant des nucléobases. Ces paramètres induisent des modifications notables au niveau des interactions non-covalentes (liaisons hydrogène, interactions hydrophobes) qui sont responsables de l'auto-organisation des polymères de nucléobases dans une grande variété de morphologies spécifiques.

Les travaux pionniers menés par l'équipe du Dr. O'Reilly ont montré le grand potentiel des polymères de nucléobases à s'auto-assembler dans diverses morphologies remarquables. Ces systèmes peuvent trouver un jour des applications dans de nombreux domaines, tels que la biologie, la catalyse ou les matériaux intelligents. Toutefois, ces travaux ne mettent pas en évidence de corrélations générales entre les morphologies obtenues et les changements des paramètres structuraux (la structure des polymères), le type de nucléobase, les stimulus externes (pH, température) ou les solvants, qui sont responsables de leur apparition. Ainsi, les études de la littérature jusqu'à présent n'arrivent pas à distinguer quel est le type d'interaction supramoléculaire (liaisons hydrogène ou interactions hydrophobes) qui contribuent majoritairement à la formation de ces morphologies.

L'information majeure apportée par cette revue est que la morphologie dépend fortement de l'architecture des copolymères à bases nucléiques (dégrée de polymérisation, ratio entre les blocs polymère, balance hydrophobe/hydrophile) qui peuvent réaliser des auto-assemblages de différentes formes (micelles, vésicules, cylindres, ou worms) et tailles. De plus, les paramètres comme le pH ou la température changent surtout la taille des objets obtenus à l'échelle nanométrique, mais sans causer des transitions morphologiques des auto-assemblages obtenus. Cependant, le caractère anisotrope de certains de ces auto-assemblages suscite un fort intérêt pour développer des applications dans le domaine de la délivrance de substances actifs. D'autres études sur ce sujet sont certainement à prévoir dans un futur proche, même si cela reste clairement un défi important.

Chapitre II : Etat de l'art sur le développement des polymères hydrophiles dérivés de la morpholine et de la thiomorpholine pour des applications biologiques. Synthèse, caractérisation physico-chimique et propriétés biologiques des nouveaux polymères hydrophiles dérivées de thiomorpholine oxide.

Chapitre II : Etat de l'art sur le développement des polymères hydrophiles dérivés de la morpholine et de la thiomorpholine pour des applications biologiques. Synthèse, caractérisation physico-chimique et propriétés biologiques des nouveaux polymères hydrophiles dérivées de thiomorpholine oxide.

Introduction Chapitre II

Comme illustré dans la revue précédente, les copolymères à bases nucléiques sont insolubles dans l'eau. Ainsi, la plupart des autoassemblages formées à partir de ces copolymères sont réalisées dans des solvants organiques, ou dans des mélanges de solvants organiques/eau. Malgré la diversité morphologique apportée par ces architectures auto-assemblées, l'utilisation de solvant organique limite leur utilisation potentielle en interdisant en particulier les applications biologiques.

Comme annoncé dans l'introduction générale, l'un des objectifs majeurs de cette thèse a été de développer des polymères contenant des nucléobases qui sont solubles dans l'eau, en vue d'une future application en biologie. Dans ce but, la stratégie utilisée a été de synthétiser des copolymères statistiques avec une architecture contrôlée obtenus par copolymérisation RAFT entre un co-monomère contenant des nucléobases et un co-monomère hydrophile.

Pour ceci, un premier défi a été d'élaborer un co-monomère hydrophile avec une nouvelle structure qui n'induit pas des effets cytotoxiques. Après une recherche des co-monomères hydrophiles non-cytotoxiques utilisées dans la littérature pour des auto-assemblages, nous avons ciblé des structures contenant des hétérocycles dérivés de la morpholine. Leurs structures présentent des propriétés biologiques *in-vitro* similaires à celles du PEG. De plus, ces structures présentent un pK_a neutre à acide qui varie en fonction du type d'espaceur accroché à l'hétérocycle de morpholine, ce qui apporte un intérêt significatif pour leur utilisation dans le ciblage des protéines spécifiques.

Ce chapitre est divisé en deux parties. Une première partie présente une revue de la littérature réalisée sur les monomères et polymères contenant des hétérocycles dérivés de la morpholine,

en mettant en lumière la relation structure-propriétés biologiques de ces architectures. Une deuxième partie est illustrée sous la forme d'un article scientifique qui présente le développement d'un nouveau monomère hydrophile de type méthacrylate de thiomorpholine oxide, ainsi que les propriétés (température, pH, évaluation biologique *in-vitro*) des polymères obtenus à partir de ce monomère.

Introduction Chapitre II : Partie I

La morpholine et la thiomorpholine sont des hétérocycles multifonctionnels électrodonneurs, hydrosolubles, sensibles au pH due à la présence des groupes de type amine secondaire, avec des propriétés non cytotoxiques.

Les polymères contenant des fonctions morpholine ou thiomorpholine présentent un intérêt accru dans des applications biologiques. Ces polymères ont montré une hydrophilie et une biocompatibilité parfois meilleures que celles des dérivés du polyéthylène glycol (PEG). Notamment, le poly(*N*-acryloyl) morpholine c'est l'un des polymères contenant de la morpholine qui est le plus cité dans la litérature, avec des applications dans la délivrance de médicaments, systèmes de détection des molécules bioactives ou bien dans le dévéloppement des matériaux avec des propriétés anticoagulantes et hémocompatibles.

Cependant, il y a très peu d'exemples de polymères dérivés de la thiomorpholine. Ces composées sont moins hydrophiles que les polymères de morpholine, mais ils sont biocompatibles et ils présentent des propriétés antibactériennes et antifongiques. L'atome de soufre des polymères de thiomorpholine peut être oxydé en sulfoxide, ce qui augmente drastiquement l'hydrophilie de ces composés. Ainsi, des polymères de thiomorpholine oxydée ont été décrites mais uniquement les dérivés de type poly(acrylates) et de type poly(acrylamides), qui ont trouvé des applications dans la délivrance de médicaments anticancéreux.

Dans cette revue, nous mettons en évidence la corrélation entre les caractéristiques structurelles des polymères à base de (thio)morpholine et leur utilisation dans de nombreuses applications biologiques. Une bonne compréhension de la corrélation structure-propriétés est primordiale afin de savoir comment modifier chimiquement ces macromolécules pour ouvrir de nombreuses voies vers leur utilisation en biologie. Cette revue est en cours de préparation finale pour soumission dans le journal **Polymer Chemistry** (**IF : 5.582**).

Publication scientifique : Revue de littérature numéro 2

Morpholine and thiomorpholine derived polymers: multifunctional platforms for biological applications

Laura Vasilica Arsenie,[1] Patrick Lacroix-Desmazes,[1] Vincent Ladmiral,[1,*]Sylvain Catrouillet[1,*]

[1]ICGM, University of Montpellier, CNRS, ENSCM, Montpellier, France

I. Graphical abstract

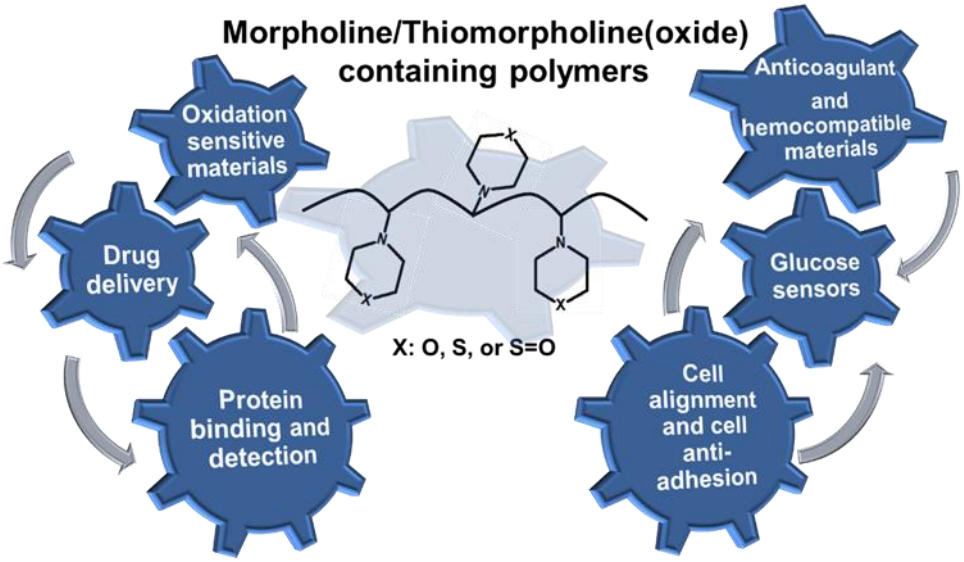

II. Introduction

Morpholine and thiomorpholine are multifunctional heterocycles with good water solubility,[1,2] pH sensitivity of secondary amino group,[3] electron-donor behavior [4] and non- cytotoxic properties.[5] These unique properties of the two heterocycles were exploited to generate various monomer structures, including (meth)acrylates [6] and (meth)acrylamides.[7,8,9,10] The variety of morpholine/thiomorpholine monomers is a result of the reactivity of the secondary amino group that can be involved in nucleophilic substitution for (meth)acrylate synthesis,[6] or direct amidation to obtain (meth)acrylamides.[10] In addition, the structure of these monomers can be tailored by changing the linker between the polymerizable synthon and the heterocycle. By this way, the hydrophobic/hydrophilic behaviour, the water solubility and pH responsiveness of the corresponding monomers can be tuned.

The tailored hydrophobic/hydrophilic behaviour of the morpholine monomers inspired the scientists to develop a series of homopolymers and amphiphilic copolymers.[11,12,13] Morpholine

derived polymers containing acrylate and acrylamide derived polymerizable functions present similar hydrophilicity as polyethylene glycol (PEG) derivatives, and were reported to be used in biological applications. Also, poly(acrylate)/poly(acrylamide) morpholine polymers showed a substantial improved biocompatibility and non-cytotoxicity than PEG, which makes them a new alternative to PEG analogs.[14] Furthermore, the hydrophilic poly(*N*-acryloyl)morpholine polymers were used in the fabrication of anticoagulant and hemocompatible membranes. Indeed, the hydrophilic behaviour of morpholine polymers provides a hydration layer which creates repulsion forces between the hydrophobic proteins (found in platelets) and the hydrophilic membrane.[15] Moreover, the tertiary amine of morpholine containing polymers can be protonated to a quaternary amine. The resulting cationic polymers has been used for DNA complexation in drug delivery and targeting. [16]

On the other hand, there are very few examples of thiomorpholine derived polymers. Thiomorpholine polymers are less hydrophilic than morpholine polymers, but they are highly biocompatible and show antibacterial and antifungal properties.[17] Compared to morpholine polymers, the thiomorpholine polymers show an interesting redox behavior due to the sulphur atom that can be oxidised to sulphur-oxide. However, only poly(acryloyl) and poly(acrylamide) thiomorpholine polymers were described in the literature. They were used as anticancer drug delivery systems sensitive to oxidative stimuli (specific for tumoral regions).[18]

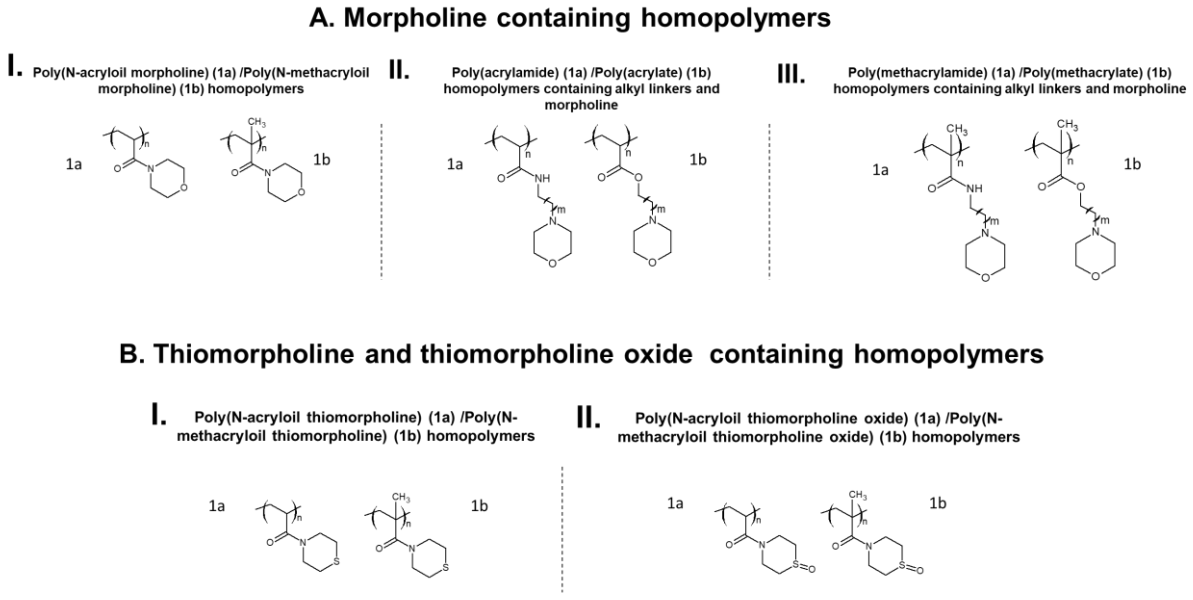

Fig. 1. (a) Morpholine containing polymers; (b) thiomorpholine and thiomorpholine-oxyde polymers

However, despite the use of these polymers in various biological applications attested by a considerable number of papers, only few studies presented the corelation between the structural and chemical properties of these polymers and their biological application. In consequence, in this review we will not focus on the chemistry used to modify the heterocycles with the polymerizable functions, nor the chemistry or mechanism of the type of polymerisation involved in their synthesis, since they were already discussed in organic and polymer chemistry related papers. Thus, in this review we will emphasize the correlation between the type of biological application in which these polymers are used and the structural polymer characteristics which make it possible. The first part of the review will highlight the structural features of individual heterocycles, and of their corresponding monomers and polymers. This section will focus on acrylate/methacrylate and acrylamide/methacrylamide polymers which are the only examples found in the literature to bear the morpholine/thiomorpholine heterocycles. The second and main part of the review will focus on the correlation between the chemical properties of morpholine/thiomorpholine polymers and their use in a specific biological application.

III. Structure and reactivity of morpholine, thiomorpholine and the derived polymers

Morpholine, thiomorpholine and their derived polymers have a multifunctional structure which presents a variety of reactive sites involved in the development of distinct properties. This section will briefly discuss the main structure-reactivity properties of the starting organic molecules (morpholine, thiomorpholine), the derived (meth)acrylate and (meth)acrylamide monomers, and some polymers (homo- and/or copolymers) containing these heterocycles (*Fig. 1.*).

Morpholine is hydrophilic due to the oxygen atoms which forms H-bonds with water molecules. In comparison, thiomorpholine is less hydrophilic since sulphur atom forms weaker H-bonds with water.[19] Both morpholine and thiomorpholine show good water solubility,[1] which make them ideal candidates in biological application. Besides their hydrophilicity, morpholine and thiomorpholine are biocompatible and non-cytotoxic.[20] Furthermore, both molecules can act as electron donor molecules (necessary in the formation of H-bonds for example) because of the oxygen or the sulphur heteroatoms which present non-bonding electron pairs.[21] Compared to the morpholine, the thiomorpholine contains a sulphur atom which led to supplementary biological properties such as antibacterial and antifungal action.[22] Some computational studies

reported that the sulphur atom of thiomorpholine was located inside the H-bond acceptor area of tested bacteria and thus blocked the bacteria inside the structure, thus allowing good antibacterial activity that was not observed in the case of morpholine.[1] Morpholine and thiomorpholine also present a secondary amine that can be protonated. The pK_a of morpholine is 8.33, while the pK_a of thiomorpholine is 9.13,[23] both molecules being intermediary bases in terms of basicity. These acido-basic characteristics were exploited in gene delivery systems, since the protonated morpholine or thiomorpholine cycles can complex with negatively charged DNA molecules and thus deliver DNA in the cell. [24]

The acrylamide/methacrylamide[25] monomers were prepared by direct amidation of the (thio)morpholine.[6] In contrast, acrylates/methacrylates[6] derived from morpholine/thiomorpholine are made by alkylation of the secondary cyclic amine leading to a tertiary cyclic amine. Another characteristic of morpholine/thiomorpholine monomers is that various structures can be obtained, by adding short or long alkyl chains between the (meth)acrylamide/(meth)acrylate backbone and the morpholine/thiomorpholine heterocycle. In consequence, the hydrophobic/ hydrophilic behaviour of these monomers could be tailored by changing the length of the linkers.

The morpholine/thiomorpholine monomers can copolymerise with a range of co-monomers (containing acrylate, methacrylate acrylamide, methacrylamide or styrene type polymerizable backbone, with different hydrophilic or hydrophobic behaviour).[28,29] The tailored hydrophilic/hydrophobic properties of morpholine/thiomorpholine containing copolymers are important in the development of micelles used for drug delivery systems, especially for drugs which have low water solubility.[30,31,32,33,34,35] In addition, the hydrophilic/hydrophobic behaviour is different for poly(meth)acrylamides and poly(meth)acrylates, for both homopolymers and copolymers. The poly(acrylates)/poly(acrylamides) are less hydrophobic than poly(methacrylates)/poly(methacrylamides), since the introduction of methyl group enables a steric hindrance and thus a higher hydrophobicity. Then, the poly(acrylamides)/poly(methacrylamide) are less hydrophobic than poly(acrylates)/poly(methacrylates) as a result of H-bond ability specific to amides. [36]

Thiomorpholine polymers present an interesting redox behavior, since the sulphur atom of thiomorpholine can be oxidized to its corresponding mono (S=O) or di- oxide (SO_2). The redox changes of the sulphur atom of these polymers influence their hydrophobic/hydrophilic properties, and transform hydrophobic thiomorpholine containing polymers in hydrophilic thiomorpholine oxide containing polymers. These polymers were used in anticancer therapy

since the hydrophobic thiomorpholine polymers should entrap hydrophobic anticancer drugs and, by oxidation of sulphur atom, release the drugs into the tumoral cell.[18] In other words, the oxidation of thiomorpholine rings result in a strong hydrophilic unit which is not compatible with the hydrophobic drug, expulsing it.

In summary, the properties of morpholine- and thiomorpholine-derived polymers can finely be tuned by playing with many parameters: hydrophobic/hydrophilic behaviour related to the type of heterocyclic moiety; nature of the polymerizable backbone; length of the aliphatic linker which relies the polymerizable backbone to the heterocycle; the protonation ability of nitrogen atom of the heterocycle and lastly, the oxidation ability of sulphur atom in the case of thiomorpholine. All these parameters, individually or associated, dictate the area of application of these polymers, as it will be described in the next section.

IV. Biological applications

Besides many applications of morpholine containing polymers reported so far in the literature, this section is focused on the biological properties of these macromolecules, since the biological area was the most studied in the case of these polymers.

As it was presented in the previous section, the hydrophilic behaviour of morpholine containing polymers is an important characteristic to be developed in biological field. In terms of biological applications, morpholine and thiomorpholine derived polymers were examined in: protein binding systems, drug delivery, glucose sensors, cell alignment and cell adhesion systems, oxidation sensitive materials, as well as hemocompatible and anticoagulant devices.

However, *N*-acryloil morpholine (NAM) is a commercial monomer, thus poly(*N*-acryloil morpholine) PNAM was the polymer the most cited in biological field. In addition, PNAM provides promising hydrophilic properties that recommended its use as alternative to poly(ethylene glycol) PEG. For this reason, most of the examples presented in this section are related to PNAM homopolymers as well as NAM-containing copolymers. Each of the biological properties will be further illustrated and the role of NAM-containing polymers will be underlined in accordance with each application.

IV.1. Protein binding and improvements in protein detection systems

In order to perform high quality *in-vivo* assays of polymers for biological applications, a high reactive interaction between the polymers and the proteins found in the cells is requested.[37] To reach reactivity towards specific proteins found in cells, common methods requests to

chemically modify the polymers (by covalent reactions) with biomacromolecules such as sugars, peptides, proteins, or enzymes. These biomacromolecules can recognize (*via* host-guest non-covalent interactions and/or coordinative interactions) the proteins founded in the cells. However, as described until now in the literature,[37] an efficient polymer-protein cell interaction in terms of reactivity remains a difficult task to be assessed despite the efforts done in the field of chemical modifications performed to link biomacromolecules to the polymer backbone, which represent a high obstacle to validate the *in-vivo* performance of the polymers.

In this section, these examples were divided depending on the type of biomacromolecule modified polymer- cell interaction, respectively host-guest type recognition (case A), or coordinative (electron donor-acceptor) (case B).

The case A (*i.e.*, non covalent host-guest type interaction) is related to sugar modified polymers which are promising protein binding systems. Herein, the traditional method consists to modify the polymer with a sugar which is a receptor of the targeted cell protein (so protein-sugar modified polymer interaction). The interaction between protein cells and sugar modified proteins follows the host-guest recognition mechanism found in biological systems (*Fig. 2. a*.). Nevertheless, this mechanism is elaborated and not completely presented here, since it is not the aim of this review.

Although, one of the main drawbacks of sugar modified polymers is the poor solubility in water which limits their potential for this application. Therefore, a classical method consists in the functionalisation of sugar moiety with PEG-derivatives.[38] However, some reports indicated that the copolymerisation of NAM (in a statistical or gradient manner) with the sugar modified reactive monomers improved the selectivity and reactivity towards some proteins.[39] This interesting observation was generally explained as a result of the disposition of NAM in the copolymer (in statistical/gradient way) which improved the solubility of sugar containing polymers and thus increased their efficacity in the recognition of proteins.[40]

In this context, an interesting example of sugar modified morpholine containing polymers used for the interaction with proteins was reported in 2017 by Prohl *et al.*[41] Their strategy was to create shell-core-shell polymeric micelles composed of a triblock terpolymer poly((n-butylacrylate)-*b*-(*N*-acryloylmorpholine)-*b*-(α-D-1-S-mannosyl)ethyl acrylate) (P(BA-*b*-NAM-*b*-ManEA)) able to interact with Concanavalin A (ConA)- a lectin co-receptor found on pathologic cell surfaces. The design of polymer micelles with size varying between 44 nm and 56 nm consisted of an inner core formed by hydrophobic n-butylacrylate (BA, used to

equilibrate the hydrophobic/hydrophilic balance) surrounded by a double hydrophilic shell designed by hydrophilic acryloyl morpholine (NAM) covered by mannosyl ethyl acrylate (EA) (*Fig. 2. b)*. Then, the micelles where mixed with ConA in order to determine the binding affinity between the mannose found in polymer micelles with the lectin. As reported by authors, the increase of the mannosyl polymer block density from 30% to 60% in the polymeric micelles resulted in a continuous increase of the binding constant with ConA (k_A, from 0.001 to 0.003 s^{-1}), while for less than 10% mannosyl block loading, no clustering effect was detectable, so the lectin binding could not be assessed. Authors concluded that highest density of mannosyl (60%) led to the best affinity with ConA with a binding constant around 0.003 s^{-1}, 30 times higher than the value reported in the literature.[42] This increase in the binding constant was explained by the improved accessibility of the mannosyl units in the polymer micelles for ConA due to the hydrophilicity induced by morpholine frameworks in the polymer. This result was coherent with previous reports in the literature which emphasised that the accessibility of mannosyl units is often restrained by highly hydrophobic micellar systems where the steric hindrance decreases the reactivity towards the lectin binding.

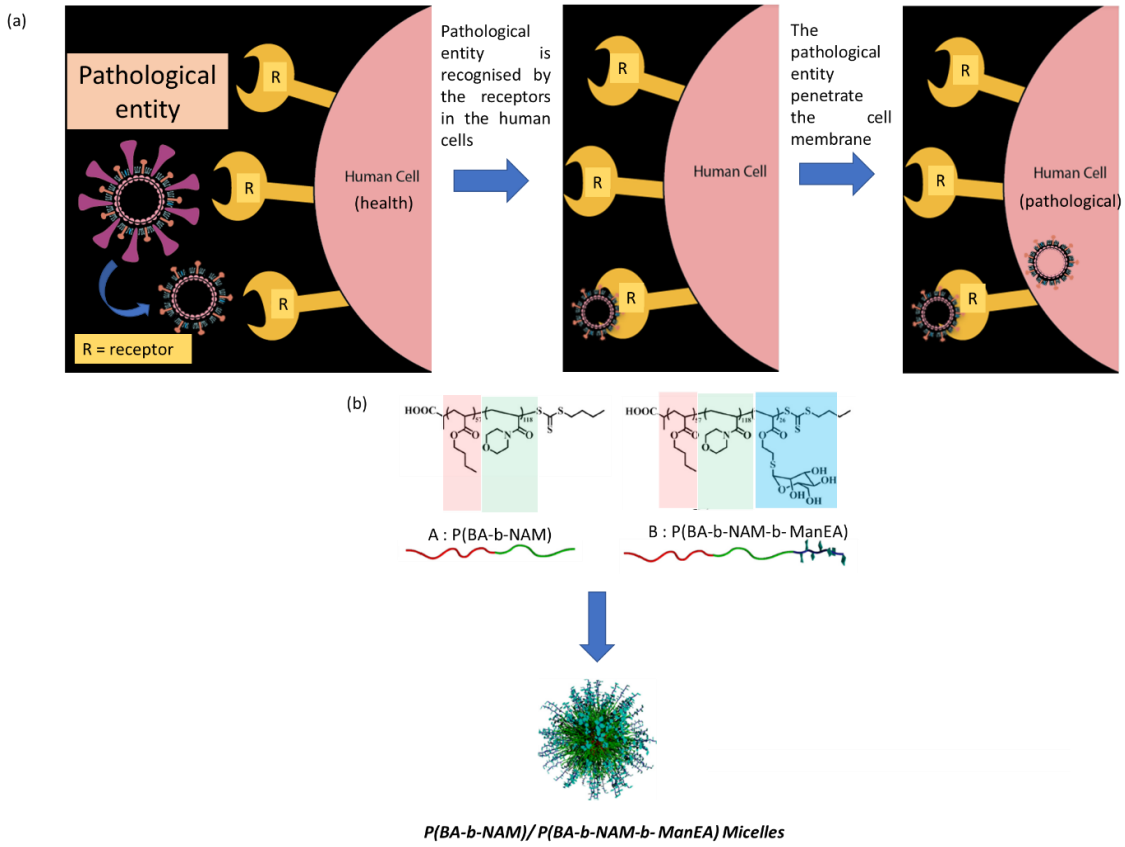

Fig. 2. (a) Interaction of cellular receptors and pathological entities.[44] *(b) Formation of P(BA-b-NAM)/ P(BA-b-NAM-b- ManEA) micelles.*[41]

Another interesting example which emphasizes the advantage of using morpholine derived polymers for protein recognition applications was presented by Leaver *et al.*[8] They reported the synthesis of telechelic poly (*N*-acryloil morpholine) PNAM polymers bearing galactopyranose chain ends which were used as inhibitors for cholera toxin (CT) (*Fig. 3)*. This toxin is a protein which binds preferentially the cellular receptors that contain galactose as terminal units.[45] PEG derivatives linkers were reported previously in the literature as inhibitors of CT, but their synthesis was considered to be very challenging because of repeated protecting/deprotecting steps and low solubilities of the synthetic intermediates in aqueous medium, which is an obstacle for the recognition process with the toxin.[46] To overcome the solubility issue, *N*-acryloil morpholine was used by the authors to design the polymer linker as it presents an enhanced hydrosolubility compared to PEG derivatives. The authors used a piperazine bifunctionalised chain transfer RAFT agent in order to obtain the telechelic bifunctional polymer by RAFT polymerisation of *N*-acryloil morpholine (*Fig. 3.*, **step a** and **step b**). Then, by including two galactose units by post-modification of the telechelic PNAM polymer linker (*Fig. 3.*, **step c**), they observed that the affinity of galactose to bind the toxin protein was increased and thus the inhibition of the toxin was more pronounced. A number of 130 acryloyl morpholine units led to the most efficient toxin inhibitor with an IC_{50} of 1.34 mM. The authors demonstrated that the degree of polymerisation of *N*-acryloil morpholine was balancing between an increased solubility which improved the efficiency and a decrease of the density of galactose which decreased the inhibition performance.

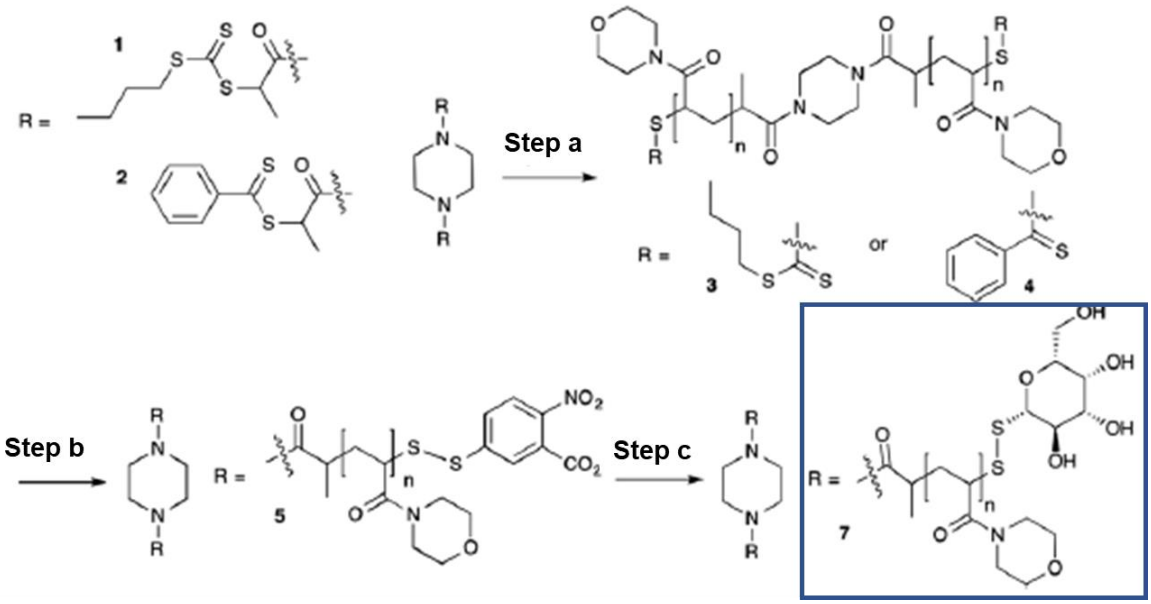

Fig. 3. Synthesis of galactose poly(N-acryloil morpholine) polymers (represented in the square): Step a (chain transfer RAFT agent -CTA- bifunctionalisation of piperazine); Step b

(RAFT polymerisation of N-acryloil morpholine NAM on the bifunctionalised CTA piperazine linker); Step c (Post-modification of PNAM with galactose) [8]

The previous applications[8,41] were based on sugar functionalised N-acryloil morpholine containing polymers non-covalently interacting with a cell protein. The potential of morpholine containing polymers was also investigated in the field of protein detection.

First examples in this field deals however with covalent reactions between modified NAM containing copolymers and targeted protein of the cells. Such example was reported by Tanaka *et al.*[47] who prepared hydrogels made of Poly(*N*-acryloyl morpholine-*co*-*N*-acryloxysuccinimide) P(NAM-*co*-NAS) (65:35 molar ratio, 86000 g/mol) used as microarrays in protein A screening (a specific protein of *Staphylococcus Aureus* and used to detect its infections). The 3D hydrogel network resulted in the reaction of NAS groups from P(NAM-*co*-NAS) copolymers with amino terminal groups of the protein A, being then dispersed on the chip surface (*Fig. 4.*). The particularity of this work was that this system provided a specific binding of protein A which was a real improvement of existent polymer arrays used in protein screening. This improvement was mainly due to NAM used in the polymer design, as stated in the article. According to the authors, the interest to use PNAM derived polymers instead of already reported PEG coatings or carboxymethyl dextran is that, additionally to the enhanced hydrophilic behaviour, PNAM polymers showed enhanced ability to suppress the undesired non-specific protein binding in physiological conditions.[48,49]

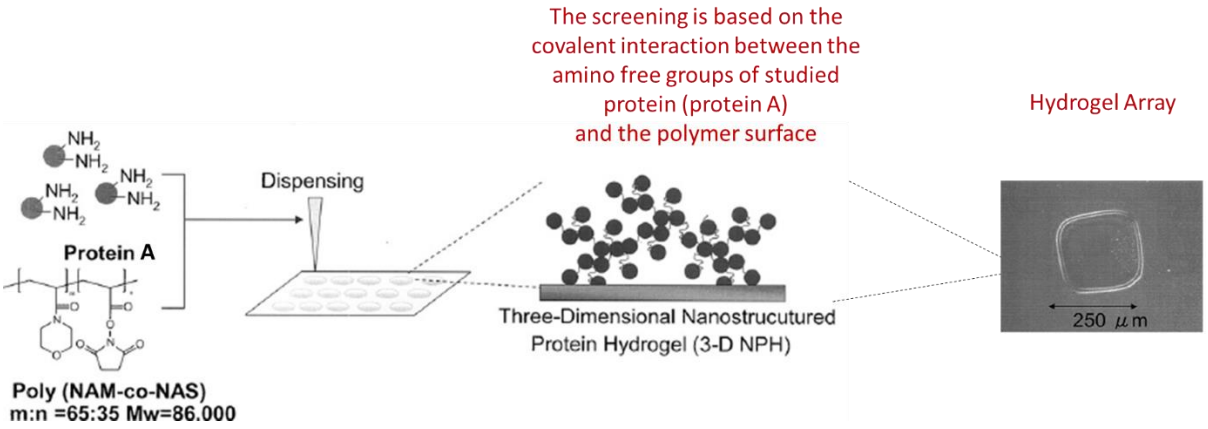

Fig. 4. Representation of SPR microarray technology involving P(NAM-co-NAS) polymers reacting covalently with amino terminal groups of the protein A. A microarray is a collection of mini spots arranged on a solid substrate which enables the simultaneous screening of proteins in a quick and efficient manner. The screening is based on the interactions between the studied proteins and host-proteins grafted on the microarray consisting of a polymer gel. [47]

Moreover, morpholine containing polymers were used for streptavidin-biotin screening applications, as described by Relogio and collaborators in 2013.[50] Compared to the systems reported by Tanaka *et al.*[47] (*i.e.*, where the interaction with target protein is covalent), these systems[50] used lucifer yellow (LY) dye labelled *N*-acryloil morpholine (NAM)-derived polymers covalently conjugated to biotin which were furthermore able to recognise the targeted streptavidin protein (by non-covalent host-guest interactions).[50] In order to introduce the LY in the polymer structure, the P(NAM-*co*-NAS) copolymers was reacted with amino functionalised LY dye. The NAS groups reacted with amino groups of LY, as in a similar strategy developed by Tanaka *et al.*[47] NAM was considered for its hydrophilicity and biocompatibility, which are important requirements in protein bio-sensing. NAS provided the reactivity to the copolymer with amino-functionalised LY dye. However, not all NAS segments were reacted: the remaining ones were either hydrolysed in acrylic acid, or were reacted with aminoethyl morpholine (AEM) resulting in AEM-capped acrylamide (*Fig. 5a.*). The final step consisted in the coupling of the thiol end copolymers previously described with polyethylene glycol (PEG) functionalised on one end with maleimide and on the other end with biotin (*Fig. 5b.*). Authors especially highlighted the reduced fluorescence self-quenching of the biotin NAM containing polymers, with 7- to 43-fold higher brightness than free LY dye. This result was explained according to the polymer chain conformation of poly(NAM-LY) in water. Even the water is a good solvent for poly(NAM-LY), the polymer chains were not fully extended and can adopt conformations in which the fluorophore molecules were protected from the solvent, reducing LY–water hydrogen-bonding and consequently, decreasing deactivation by excited-state proton transfer (ESPT), as previously observed for LY in water.[51]

These results are promising alternatives in fluorescent protein sensing detection, for example to recognise the streptavidin, a protein involved in cancer diagnosis.[52] In this context, the study reported complete complexation between streptavidin and polymer for a stoichiometry of 1:4 (streptavidin: polymer), evaluated by gel electrophoresis.

To summarize, this research emphasized the interest in using NAM to develop fluorescent water soluble polymers for protein detection, due to its advanced hydrophilic behaviour which improved the protein recognition process and the fluorescent properties of the copolymer.

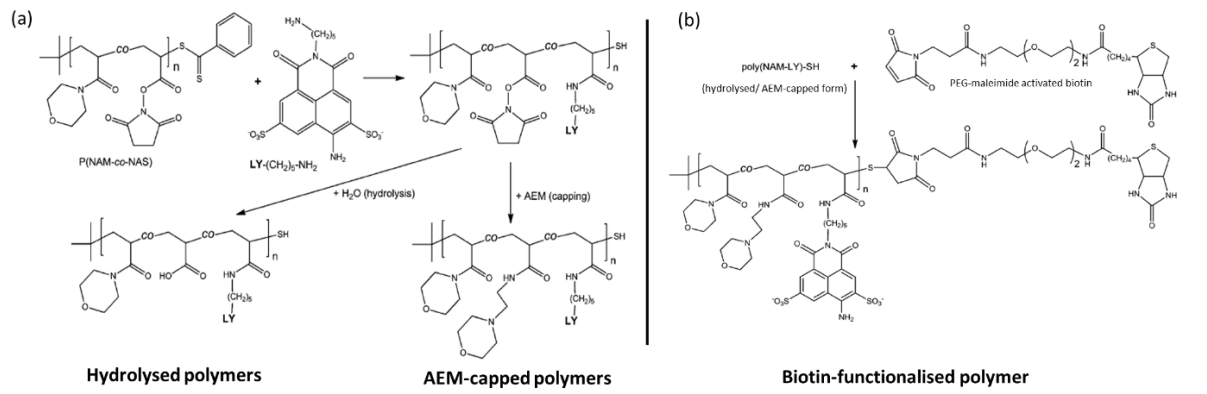

Fig. 5. (a) LY Dye functionalisation of P(NAM-co-NAS) polymers followed by hydrolysis and/or AEM-capping; (b) Conjugation of hydrolysed/AEM capped forms with PEO-activated biotin resulting in the formation of biotin-functionalised polymers. [50]

Another example that involved the use of poly(*N*-acryloyl morpholine)-*stat*-*N*-acryloxysuccinimide P(NAM-*stat*-NAS) copolymers for biotin- streptavidin protein recognition was shown in 2018 by Duret *et al.*[7] A previous example [50] showed that the biotin-streptavidin interaction could be performed by the non-covalent interaction of P(NAM-*stat*-NAS) covalently labelled with biotin and free streptavidin (*Fig. 6. a.*). In this work, the adduct between biotin-streptavidin proteins was achieved by the non-covalent interaction of streptavidin labelled P(NAM-*stat*-NAS) with biotin-PNAM homopolymer. In consequence, the *N*-acryloil morpholine is involved in both protein- containing macro frameworks. This design of polymer bearing protein labels was chosen, as stated by authors, due to the enhanced hydrophilic properties of PNAM which can improve both protein solubility and in consequence the protein-protein interaction.[53] However, the development of streptavidin labelled P(NAM-*stat*-NAS) copolymers was different by those used by Relogio and colaborators. [50] In this case, the P(NAM-*stat*-NAS) copolymers having a thiol -SH end group react first with amino free fluorescent dye (LY) and then the -SH free end group was involved in a thiol-ene reaction with a succinimide ester (*Fig. 6.b.*). The succinimide framework was then involved to the label of streptavidin on the polymer backbone (*Fig. 6. a.).* Which is important to retain, as stated in this study, is that by changing the way of how biotin and streptavidin interact (*i. e.*, by labelling the proteins to hydrophilic NAM containing polymer frameworks), a selective protein-protein interaction was achieved. Nevertheless, no comparison in terms of binding constant between biotin and streptavidin of the natural systems compared to the polymer systems was done. However, these works paved the way to continuous development of NAM containing polymers

in the field of protein sensing, since the hydrophilic nature of NAM solve the solubility issue found for other polymer candidates in this application.

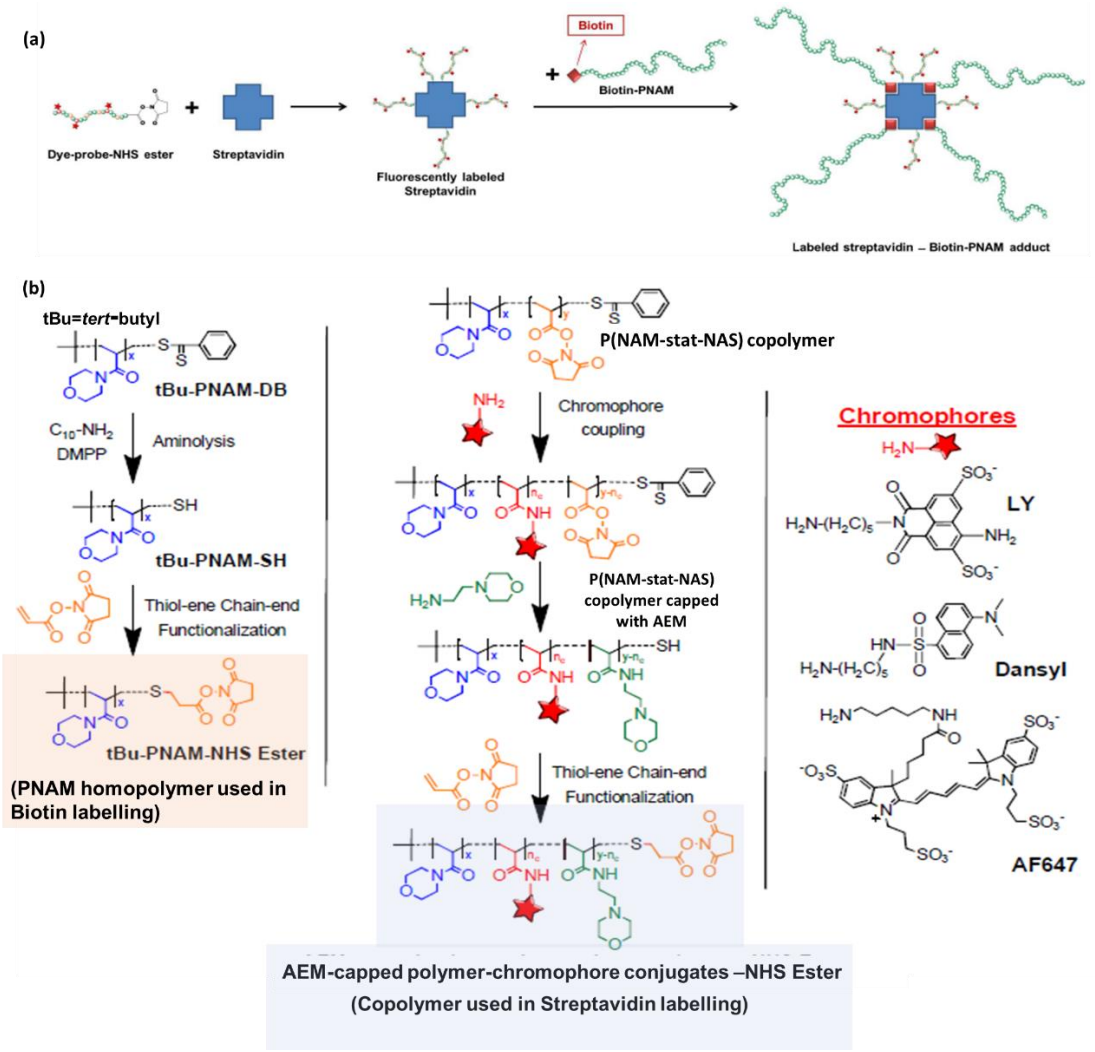

Fig. 6. (a) Formation of streptavidin-biotin adduct; (b) Structural representation of copolymers bearing organic chromophores [7]

In addition to the previous examples, poly(NAM-*co*-NAS) copolymers were reported by Duret *et al.* [25] as excellent candidates used to prepare new polymultivalent polymer-peptide ligands tested for integrin (the receptor of cRGD) expression. The main issue when polymultivalent polymer-peptide ligands were developed for this application, was that it is very difficult to perform the polymer-peptide conjugation in water, which limited the use of these polymultivalent ligands *in-vivo*. Because of the lack of the *in-vivo* efficiency, the authors opted for NAM in the preparation of the polymultivalent ligand, since it is recognised for good water solubility and can in consequence increase the water solubility of the peptide containing ligand. The design of polymultivalent ligands consisted of the four cyclic cRGD peptide ligands

covalently attached to poly(NAM-*co*-NAS) copolymers *via* the reaction between NAS moieties with free terminal amino groups of cRGD peptide ligand. This strategy (*Fig. 7.a.* and *Fig. 7.b.*) was already reported in the previous paragraphs [7, 27, 50] and presented the advantage of using highly reactive NAS units able to react *via* their ester bonds with terminal amino groups of the peptide in order to covalently conjugate the peptide on the polymer backbone *via* amide bonds. Then, the study reported that these ligands exhibited a high affinity for integrins which are actively involved in cell adhesion processes since they could efficiently bind the integrin by polymultivalent polymer-cRGD conjugate-integrin interaction (*i.e.*, integrins avoid cell adhesion). The interaction between polymultivalent polymer cRGD peptide with integrin resulted in a non-covalent complex. The authors reported that the best inhibition of cell adhesion (IC_{50}= 8 nM) was exclusively observed for the polymultivalent polymer peptide ligand/integrin complex, where the concentration in polymultivalent ligand was 4.2 % (% moles), while a decrease (at 1.5%) or an increase (at 5.9%) in the polymer conjugate concentration led to a less inhibitory effect. According to them, the correlation between polymer conjugate concentration and the inhibitory effect variation was a result of steric effects between the morpholine derived chains which supressed the lateral cRGD to recognise integrin, or supplementary crowding effects for high concentrations in polymer conjugate. However, which is particularly underlined is the role of NAM in the best inhibitory effect of polymultivalent ligand towards cell adhesion, at a concentration of 4.2%. This significant result was explained due to NAM ability to prevent non-specific bio-interaction,[35] by favouring specific binding of polymultivalent polymer cRGD peptide to the integrins located on the cell surface that prevented the cell adhesion.

Then, PNAM polymers showed particular interest in the conjugation of enzymes, as reported by Schiavon *et al.*[54] In their work,[54] they investigated the effect of PNAM on the enzymatic stability of uricase. This enzyme regulates the production of uric acid, by lowering the uric acid level in plasma. So, the development of polymers that contribute to the stabilisation of this enzyme in the organism is highly asked, since high levels of uric acid led to renal failure.[35] The authors discovered that the conjugation of PNAM (M_w= 6 kDa) on uricase led to a complex hybrid conjugate able to increase the proteolytic stability and blood resistance of uricase, thus decreasing the content in uric acid in organism.

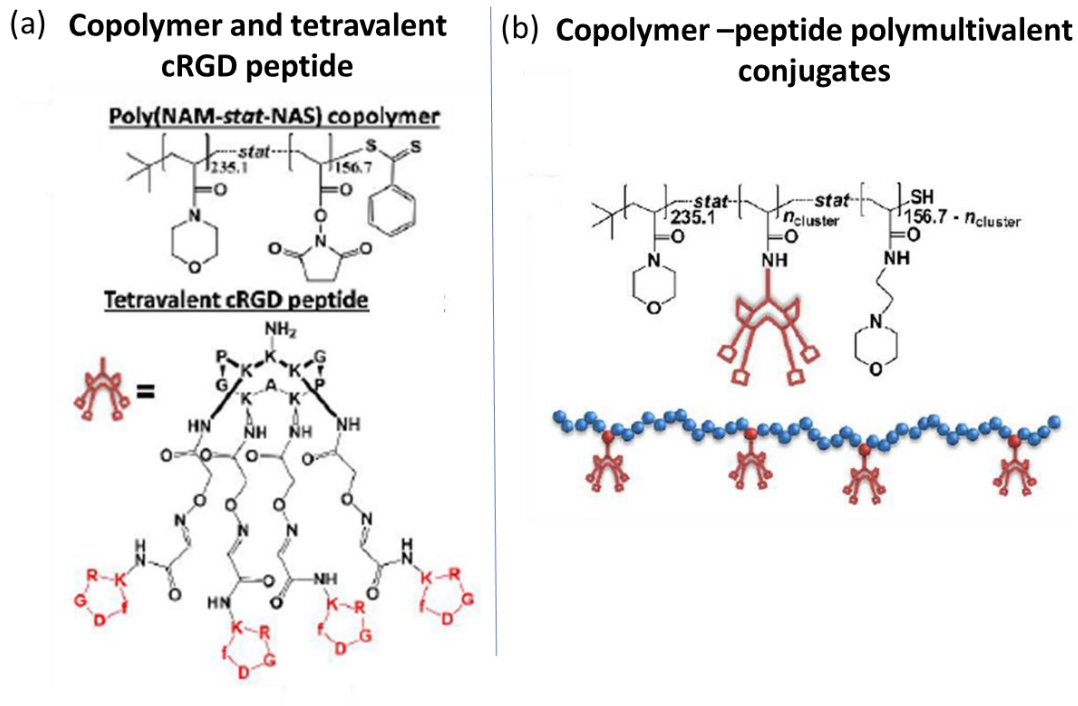

Fig. 7. (a) Structural representation of polyacryloil morpholine polymers and peptide ligand; (b) representation of copolymer-peptide multivalent conjugates [25]

The strategy used by Schiavon *et al.* was based on the reaction between PNAM having a -COOH terminal group and succinimide, followed by the reaction of succinimide-PNAM with the amino free group of enzyme. The uric acid inhibition and the blood residence time of the PNAM-uricase conjugate were respectively 100 times and 3 times higher than those of the native enzyme. According to the authors, these results were explained to be a consequence of PNAM that masked the enzyme surface due to adequate water solubility. In consequence, the residence time of the enzyme was increased which thus limited the long production of uric acid. The inhibitory action of PNAM against uricase is very promising and as authors stated this polymer could efficiently replace poly(ethylene glycol) (PEG) in enzyme inhibition applications.

However, the main obstacle when using enzymes such as the uricase to low the uric acid production in the plasma is that the individual enzyme could entail a severe risk of immunoresponse. In consequence, the conjugation of enzyme to a polymer was a strategy reported by some studies to allow the risks associated to non-desired immunoresponse, due to the ability of polymer to act as an antigen which will enable the organism to recognise the enzyme by producing anticorps.[35] However, there are few examples of polymers [55] with immunogenic properties since parameters such as water solubility, high molecular weight or

repetitive structure altered this property. Inspired by these considerations, Caliceti *et al.* [39] developed PNAM-uricase conjugates acting as artificial antigens that triggered the *in-vivo* immune response at uricase. The conjugation of PNAM with uricase proceeded as in the previous reported studies, [54] by NHS-ester activation. According to them, the immunogenic behaviour of PNAM-uricase conjugates was stronger compared to that of poly(*N*-vinylpyrrolidone) PVP or PEG, which are known in the literature for these applications. These results were explained in the relation with the improved hydrophilic nature of PNAM compared to PVP which increased the interaction of PNAM with the enzymes. Additionally, the polymer flexibility (*i.e.*, coiled or extended conformation) could affect the enzyme interaction and thus the immunogenic response. In consequence, the linear structure of PNAM was a real advantage in this regard since the linear polymer structure is more exposed to biological environment and to the enzyme, according to the authors. The PNAM performance compared to PEG was explained by steric hindrance effect of PEG in contact with proteins, which adopted a coiled conformation that restricted the interaction with the enzyme and limited the immunogenic effect. To sum up, this work highlighted the advantages of using PNAM for immunogenic enzyme-polymer conjugates.

Interactions between proteins and polymers can take place *via* coordination (case B). In such case, the conjugation was achieved by a ligand decorated-morpholine polymer and a metal-based protein. This concept was studied by Duret *et al.*[56] who prepared P(NAM- *stat*-NAS) copolymers labelled with a fluorescent Dansyl cadaverin dye moiety and terminated with a nitrilotriacetic (NTA) ligand (*Fig. 8a.*) used for site specific labelling of histidine end tagged streptavidin. As in the previous examples,[25] the P(NAM-*stat*-NAS) copolymer was chosen by the authors due to good hydrophilic properties which are highly requested to perform *in-vitro* protein labelling. The recognition and the selective binding between the copolymer backbone and the streptavidin protein was achieved by Ni^{2+} ions coordination of nitrilotriacetic ligand attached to the copolymer and the histidine units of the protein (*Fig. 8b.*). Then, the authors studied the copolymer selectivity towards three different HisTag-proteins as well as His-tagged streptavidin. The electrophoresis assay showed the selective binding of copolymer to His-tagged streptavidin. These results indicated a selective labelling and recognition of the copolymer for His Tag-proteins (and in particular His Tag streptavidin) as a result of coordination between His proteins, Ni^{2+} cations and nitriloacetic modified copolymer.

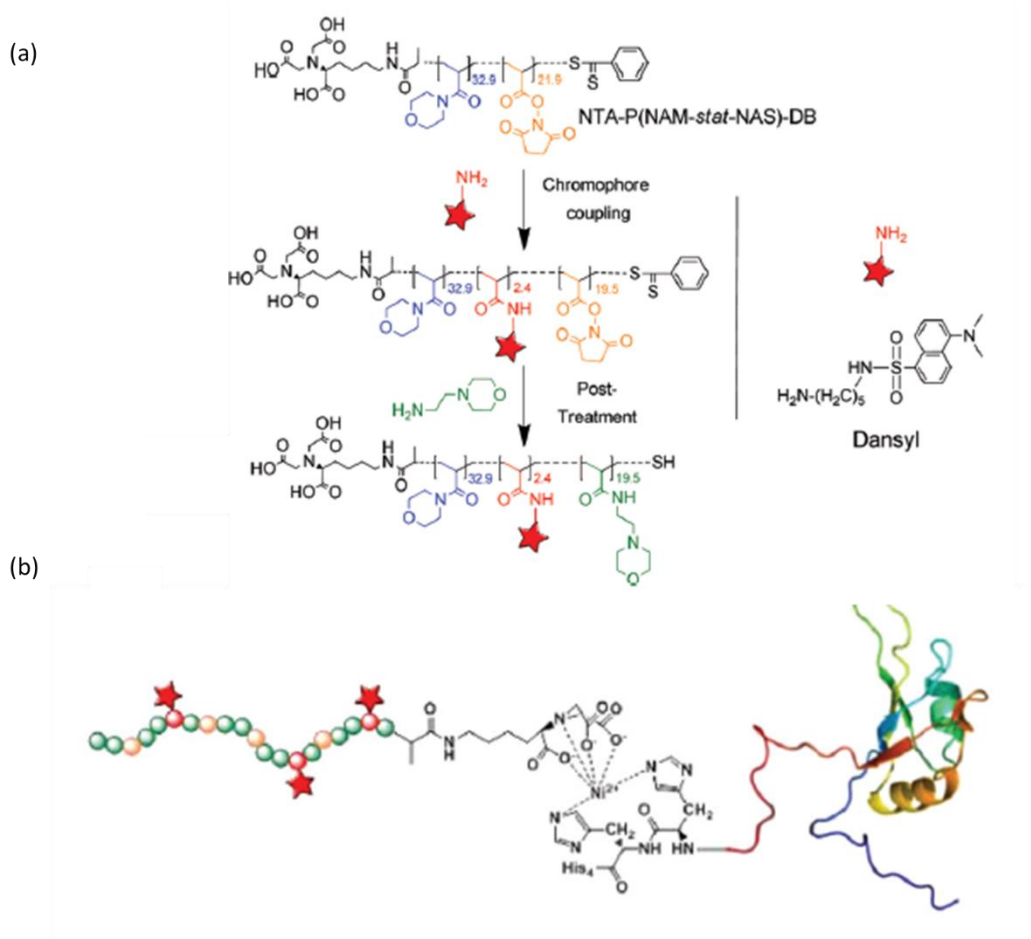

Fig. 8. (a) Structural representation of P(NAM-stat-NAS) polymers containing NTA ligand and organic chromophore(Dansyl) (b) Graphical representation of coordination process: the polymer-protein conjugate is formed by the coordination between NTA-polymer macroligand and His-containing protein by Ni^{2+} *ions* [56]

To conclude, poly(*N*-acryloyl morpholine) provided a high interest in the conjugation with various proteins in order to develop materials used in protein detection. While conjugated to sugar molecules, the PNAM polymers recognised concanavalin A protein simulating artificial models in antiviral therapy, as a result of high hydrophilic behaviour which increased the water solubility necessary for protein conjugation. The water solubility of PNAM was a high advantage which increased the aqueous solubility of proteins by conjugation, and performed in consequence new water soluble protein-polymer conjugates for *in-vitro* and *in-vivo* applications. This property was explored then by changing the type of sugar moiety to be conjugated with PNAM, these polymers enabling important results in the inhibition of cholera toxin protein. Also, PNAM polymers had, as a result of good biocompatibility and water solubility, significant contribution in the regulation of the enzymatic protein activity of uricase, *via* direct conjugation with the enzyme. In all mentioned reports, PNAM was used instead of

other polymers for protein conjugation due to advanced hydrophilic properties which are highly desired to perform the conjugation. However, any of the previous examples of the literature talked about the reactivity of PNAM polymers which is another condition in order to perform the covalent ligation with the proteins. For this reason, some interesting research showed the importance to use a high reactive *N*-acryloxysuccinimide (NAS) as co-monomer since it can bind to the amino-modified proteins via the NH-S reaction. In consequence, P(NAM-*co*-NAS) copolymers were very effective in the formation of responsive micelles simulating biotin-avidin protein interaction as a result of both NAS reactive properties and NAM hydrophilic behaviour. Lastly, the functionalisation of PNAM polymers and P(NAM-*co*-NAS) copolymers with ligands complexing Ni^{2+} enabled an efficient recognition with streptavidin protein *via* dative bonds between the histidine containing streptavidin and Ni^{2+} complex. These examples illustrated the high versatility of the PNAM in the field of protein recognition due to the hydrophilic structure and reactivity to be functionalised with responsive organic units necessary for biomolecule conjugation.

IV.2. Drug delivery systems

Interesting papers showed that morpholine-derived polymers were used in drug delivery of range of small molecules (anti-cancer or anti-viral drugs, antibiotics, anti-inflammatories, nitrogen monoxide NO) and biomacromolecules (hormones and DNA). For drug encapsulation, morpholine containing polymers were reported to be used as core-shell type micelles able to entrap and deliver the drug. The core-shell type micelles result in the self-assembly of morpholine containing amphiphilic copolymers formed by copolymerisation of hydrophilic morpholine monomers with hydrophobic monomers. As general strategy, [57] a hydrophobic drug will be entrapped in a hydrophobic core surrounded by a hydrophilic shell; in this case, the hydrophilic shell is composed by morpholine-derived blocks. Herein, the hydrophilicity of morpholine blocks will enable the transportation of drug in the organism and the penetration into cell membrane, producing the therapeutic effect. For hydrophilic drugs (or low hydrophobic), they are generally adsorbed on the hydrophilic morpholine chains surface (or the shell) and delivered then to the specific site. However, each drug present distinctive particularities that require a particular design of the polymer delivery system.

Morpholine derived polymers were used to deliver a range of anticancer drugs, particularly paclitaxel (PTX), doxorubicin (DOX), 4-hydroxy-2-nonenal (HNE), Everolimus, or anethole-dithiolethione (ADT-OH). Xu *et al.* reported in 2017 the preparation of H_2O_2-redox responsive core-shell micelles from $PNAM_{95}$-*b*-$PAEFC_{25}$ (Poly (*N*-acryloil morpholine)$_{95}$-*b*-(2-

acryloyloxyethyl ferrocene carboxylate)$_{25}$ block copolymers and 25 ferrocene functionalised hydroxyethyl acrylate (AEFC) units and their use for encapsulation and delivery of paclitaxel (PTX).[58] PNAM chains form the hydrophilic shell of micelle, while PAEFC is a redox sensitive and hydrophobic polymer which design the micelle's core (*Fig. 9.*). The micelles were responsive to H_2O_2 (due to oxidation sensitive ferrocene-containing PAEFC core-forming block) which concentration is higher in tumoral cells than in normal cells. As the authors stated, in the presence of H_2O_2 and in acidic medium (pH 5.8) specific to tumoral cells, these micelles released 38.2% of drug, while in neutral conditions (pH 7.4), the cumulative drug release amount was less than 12.2%. According to the authors, these results proved that the system was more responsive in acid medium (which is characteristic to cancer cells), performing enhanced drug encapsulation percentages as a result of balanced hydrophilic/hydrophobic balance *via* association of PNAM and PAEFC.

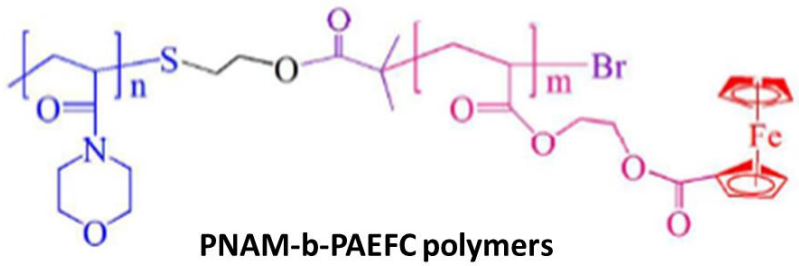

Fig. 9. General structure of PNAM-b-PAEFC block copolymers [58]

Another interesting example where PNAM were used in anticancer drug encapsulation was illustrated by Ramesh *et al.*[59] In their paper, the authors prepared doxorubicin DOX delivery systems based on AB_2 miktoarm star block copolymers designed by PLA (as A arm) and two poly(*N*-acryloil morpholine) (PNAM) as B arms (*Fig. 10. a.*). The synthesis consisted of ROP polymerisation of L-lactide of a mikto-initiator, resulting a PLLA macroinitiator, followed by RAFT polymerisation of NAM on the PLLA macroinitiator backbone. By using ROP-RAFT combined polymerisation, the authors prepared a range of star block copolymers containing 20 blocks of PLA and varied DP numbers of PNAM (13, 40 or 70 for one PNAM arm). Then, the self-assembly of prepared block copolymers resulted in micelles designed by PLA as core and PNAM as shell. According to the authors, by increasing the number of DP of PNAM arm (from 13, to 40 and 70), the DOX loading efficiency (*i.e.*, defined as [weight of loaded drug/weight in feed] x 100) in neutral pH increased from 55.6% to 66.8% and 78.7% respectively (*Fig. 10. b.*). As stated by authors, their results were reasonable with the fact that DOX was physically encapsulated in the hydrophobic PLA core of the copolymer micelles, a higher content in

hydrophilic PNAM changing the steric confinement of DOX inside the PLA (*i.e.*, by the decrease of hydrophobic interactions between PLA chains and favouring physical DOX entrapment in PLA core). Additionally, to study the ability of anticancer drug release in conditions specific to cancer affected cells, the authors studied the release profiles of DOX loaded micelles in slightly acidic conditions (pH 6.4). Essentially, all the three samples of the micelles exhibited a much higher cumulative drug release (between 42% and 67%) under these conditions than in neutral condition (between 31% and 50%) which means that the delivery system was more effective for tumoral environment. The higher amounts of DOX released in acidic conditions were explained by the protonation of the primary amine (pK_a=8.3) of DOX which increases its solubility in aqueous medium. This higher solubility facilitated the drug expulsion out of the polymer micelle by passing through the hydrophilic PNAM corona which enabled its delivery. These results highlighted the benefit of excellent hydrophilic PNAM behaviour in hydrophobic drug release in aqueous physiological medium. Underlined by the authors, their results were comparable to those obtained by using PEG as hydrophilic component instead of PNAM, that showed the high potential of PNAM for biological use. However, there was no direct evidence to explain why longer DP of PNAM can favour the release of DOX, this observation opening new perspectives to investigate the properties of PNAM for DOX-delivery systems.

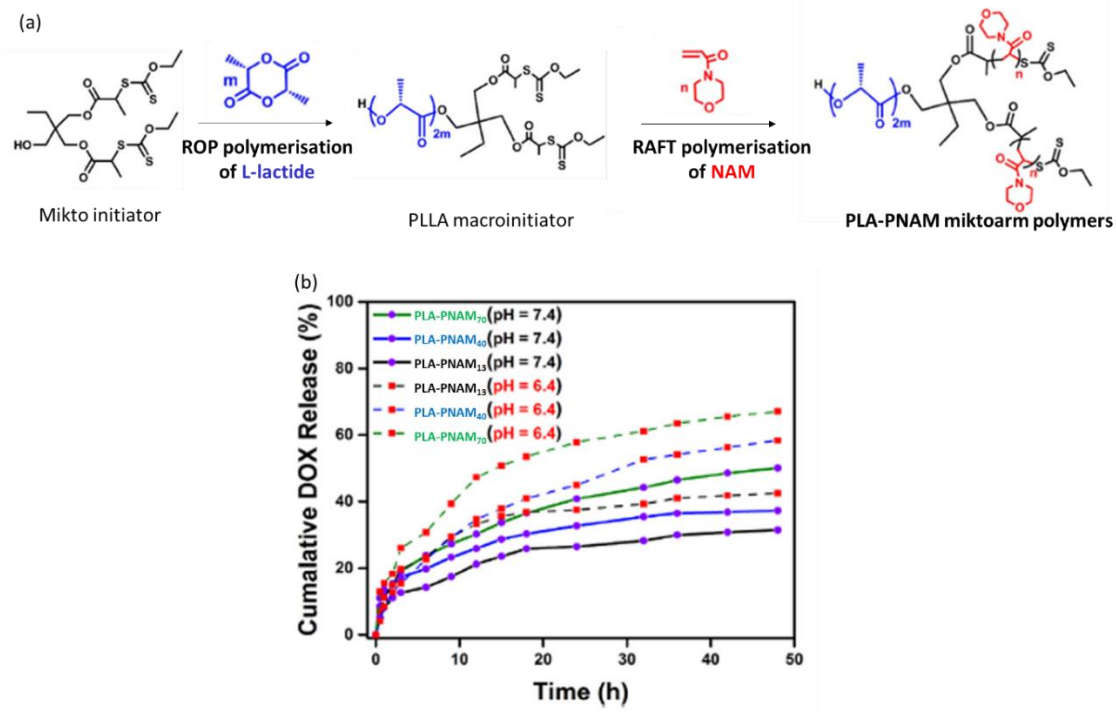

Fig. 10. (a) Structure of PLA-PNAM mikto-arm polymers; (b) Doxorubicin (DOX) cumulative release profiles in acid and neutral medium [59]

Nevertheless, despite of excellent properties showed *in-vitro*, any of previous PNAM derived polymers showed the same efficiency for *in-vivo* applications, which is an issue when developing polymers for biological applications. Pizzimenti *et al.* made a significant contribution to the field of polymer complexes containing PNAM for the *in-vivo* delivery of HNE (4-hydroxynenal, an anti-tumoral agent).[30] HNE is known for its preference to be internalised by melanoma cancer cells and for the strong antiproliferative effect. However, HNE presents poor water solubility which is a high obstacle for *in-vivo* applications. The authors demonstrated that an amphiphilic ßCD-PNAM conjugate led to a supramolecular complex able to entrap the HNE. The design of ßCD-PNAM conjugate consisted of a single ßCD moiety at one terminus and a lipophilic inner cavity able to entrap HNE. The hydrophilic outer surface of the conjugate was formed by the free hydroxyl groups of ßCD, and by the PNAM hydrophilic chain (*Fig. 11. a.*). According to the authors, the presence of PNAM improved the overall hydrophilic properties of ßCD-PNAM conjugate and thus enhanced the aqueous solubility of HNE, by enabling HNE encapsulation by non-covalent complexation, the encapsulation drug efficiency reaching values above 83.5%. Then, to show the importance of amphiphile complex in HNE entrapment, the *in-vitro* release results in PBS (pH 7.4) indicated a very slow-release rate for HNE (6% in 2h), demonstrating a stable host–guest complex based on noncovalent interactions. At the end, the *in-vivo* evaluation on melanoma cells showed that after 8 days in contact with the HNE/PNAM-βCD complex, the cells had smaller tumour nodules and remained closer to the epidermis with lower invasion of the dermal structures (*Fig. 11.b.*). This result was explained according to the addition of PNAM in the HNE-complex which acted as a protective hydrophilic shell by avoiding the degradation of HNE. In consequence, this study underlined that PNAM improved the hydrophilic properties of ßCD-PNAM conjugate (by polymerisation of hydrophilic NAM on hydrophobic modified ßCD) and thus promoted the internalisation of HNE within this conjugate, which enabled promising *in-vivo* results reported for the first time in the case of PNAM derived polymers. However, no clear precision was made about the correlation between the type of non-covalent interactions involved in the complexation of ßCD-PNAM conjugate with HNE, in other words if the non-covalent interactions were mainly van der Waals type (between hydrophobic ßCD inner core and HNE) or H-bond type (between terminal hydroxyl units of ßCD and PNAM and/or HNE). Nevertheless, the non-covalent association of hydrophilic and biocompatible PNAM polymers with hydrophobic cyclodextrin improved the entrapment and delivery of lipophilic HNE into the tumoral cells, by enhancing the anti-tumoral effect and decreasing the tumoral cells size.

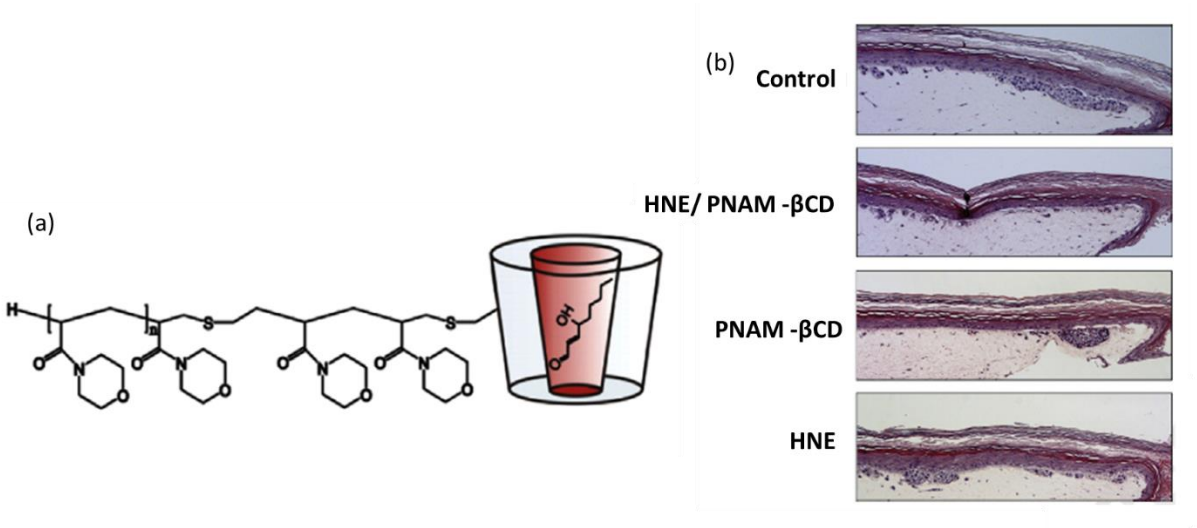

Fig. 11. (a) Structure of poly (N-acryloil morpholine)-cyclodextrin complex entrapping 4-hydroxynenal (HNE/PNAM –ßCD); (b) HNE/PNAM-βCD effect after 8 days on A375 melanoma invasion in a 3D tissue model. The top bright red layer represents the epidermis; the next layer of cells with dark blue nuclei represents the melanocyte layer; and the bottom largely unstained area represents the fibroblast-contracted collagen dermal substrate. [30]

In addition, the same PNAM-βCD previously reported polymer [30] was employed in the delivery of antiviral drugs. Bencini *et al.* [60] emphasised that the solubility of acyclovir (an antiviral) and a fast release rate was improved by linking acryloyl morpholine polymers to a cyclodextrin framework (*Fig. 12.*), 70% of drug being released in only 2h. The synthesis of PNAM-βCD conjugate was performed as described in the previous paragraph.[30] Herein, the hydrophilic character of morpholine blocks changed the cyclodextrin behaviour from highly hydrophobic to amphiphilic, the drug being able to be internalised and solubilised up to 13.3% in the cyclodextrin cavity.

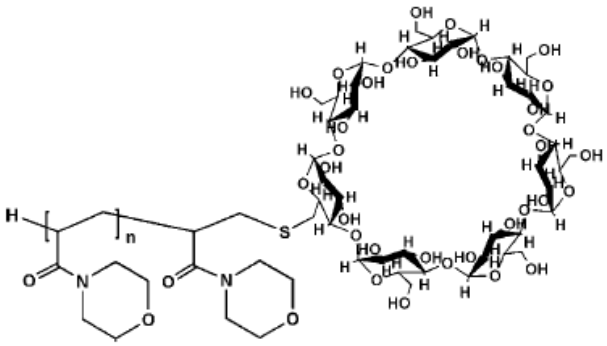

Fig. 12. The structure of β-cyclodextrin-PNAM [60]

Jo *et al.*, developed micelles formed *via* the self-assembly of poly(acryloyl morpholine-*co*-acryloyl azocane) copolymers (PNAM-*co*-PAH) (15% PNAM and 85% PAH, wt %) for the delivery of Everolimus, an anticancer hydrophobic drug also used for the treatment of cardiovascular diseases (*Fig. 13a.* and *Fig. 13b.*).[11] The system presented an encapsulation efficiency of 60%. This result was explained as a consequence of hydrophobic cavity of PAH which embedded the drug in the micelles matrix, while the hydrophilic PNAM assured a surface functionalisation of the micelle with the hydroxyl groups of the drug. Then, this polymeric system showed that in 3 weeks, 87% of Everolimus loaded was released. Herein, there was no evidence to explain the slow-release behaviour of the polymeric micelle. A hypothesis of the authors was that the non-covalent interactions between the PAH blocks of the copolymer and the cavity of drug contributed to maintain the drug in the polymer matrix. As summarizing, this study demonstrated that PNAM-PAH micelles could be suitable drug carriers for hydrophobic drugs encapsulation with a long-time span release profile.

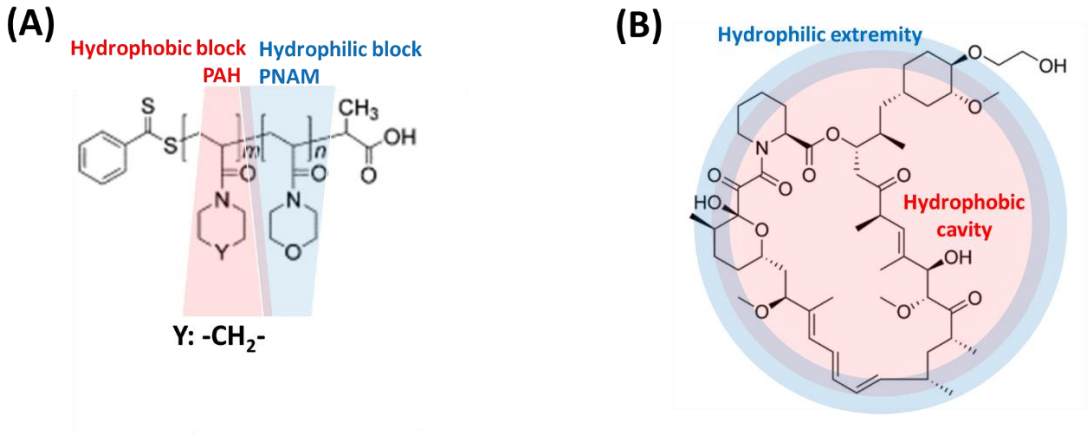

Fig. 13. (A)Structure of PNAM and PAH polymers; (B) Structure of Everolimus drug [11]

Supplementary contributions in anticancer drug delivery systems containing PNAM were reported in 2015 by Hasegawa *et al.*[33] Their study reported the formation of polymeric micelles *via* the self-assembly of amphiphilic block copolymers composed of hydrophilic PNAM blocks and poly(N-acrylamide) type hydrophobic blocks containing glycine (Gly) or isoleucine (Ile) and bearing ADT-OH units. In the hydrophobic block, ADT-OH was linked by ester bonds on the two different acrylamide derived linkers made of glycine (Gly) and isoleucine (Ile) (*Fig. 14.*). This system showed hydrolytic sensitivity which can be considered a suitable method to quantify the encapsulation and release of the drug from the polymer micelle matrix. By hydrolysis of ester bonds linking the ADT-OH to amino acid containing linkers, the ADT-OH was released from the micelles, whereas the use of amino acids as a linker helped to tailor the

hydrolysis rate of the drug-loaded micelles, thus controlling the drug release. As reported by authors, the ADT-OH *in-vitro* release studies showed that the drug was released faster from the PNAM-PGlyADT micelles (up to 80%) than from the PNAM-PIleADT micelles (only 10%). These differences in release percentage were attributed to the presence of sec-butyl hydrophobic group in Ile which slowed down the hydrolysis, without any contribution of PNAM. Then, cellular viability tests on three human cancer cell lines (Hep3B, MCF7 and HT29) showed that PNAM- PGlyADT micelles decreased the metabolic activity of cancer cells (*i.e.*, cellular viability below 60% which indicates cytotoxicity) as a result of fast ADT-OH release, whereas PNAM-PIleADT micelles did not show obvious toxicity up to 400mM due to slow release of ADT-OH from polymer matrix. Thus, the hydrolysis was necessary to release free ADT-OH from the micelles in order to enable cytotoxicity against cancer cells. Since the main parameter explaining the hydrolysis and drug release was the different stability of ester group which link the drug to Gly and Ile, the authors compared this result with that of some PEG-ADT conjugates where the ADT-OH was linked to PEG by ester bonds. According to them, the PNAM P(Gly/Ile)ADT performed better results than that of PEG-ADT, which could be due to hydrophilic PNAM that improved the swelling properties of micelles and drug release properties, opening the premises to be used as PEG alternative for drug-release systems.

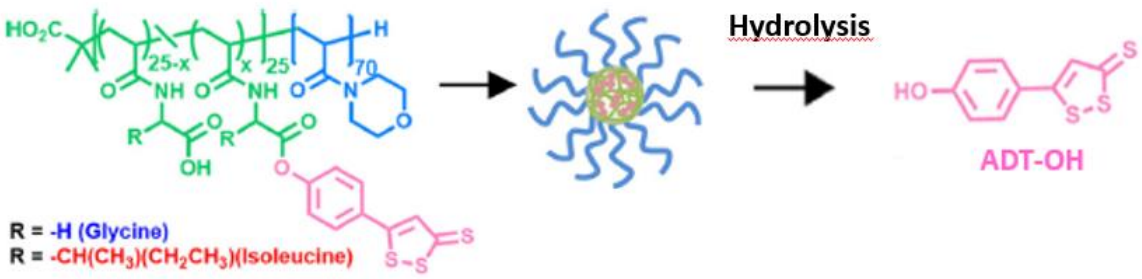

Fig. 14. Structure of polyacryloyl morpholine derived polymers containing Ile/Gly groups and ADT-OH and the mechanism of ADT-OH release [33]

Morpholine-containing polymers were also used to design a delivery system for ciprofloxacin (an antibiotic drug).[61] Efe and colaborators[61] reported the preparation of PNAM containing hydrogels (*Fig. 15.*) as matrix to deliver the ciprofloxacin. The hydrogels were obtained by UV curing technique by photopolymerization of NAM and HEMA (2-hydroxyethyl methacrylate) monomers with poly(ethylene glycol)-diacrylate PEG-DA as cross-linking agent, in order to obtain a cross-linked hydrogel network. As stated by authors, NAM played a significant role in the creation of hydrogels with porous interconnected morphology which was very suitable for ciprofloxacin delivery, since NAM exerted a steric hindrance against the polymer segments

orientation towards this morphology. Additionally, their study reported that an increase in hydrophilic NAM content (from 0 to 30 mol%) led to a higher drug release (from 73% to 98% after 7h) due to an increased swelling rate of NAM in water, by creating a channel like morphology appropriate for drug diffusion through the hydrogel. In consequence, their results showed that NAM should be a good candidate for the preparation of hydrogels for drug delivery as a result of appropriate water solubility which facilitate water penetration into the hydrogel network and thus ameliorate swelling and drug release properties.

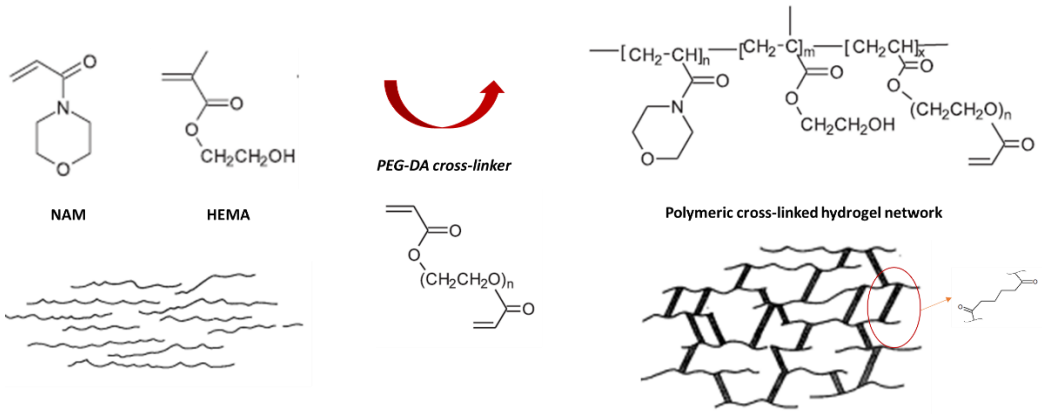

Fig. 15. Representation of PNAM containing hydrogels for ciprofloxacin delivery [61]

Moreover, P(*N*-ethylmorpholine methacrylamide) PNEMA homopolymers were used as hydrogels in the delivery of anti-inflammatory drugs such as ibuprofen, as reported by Velasco *et al.*[34] The hydrogels were prepared by bulk polymerisation of NEMA monomer in the presence of a trifunctional cross-linker 135-T in water/isopropanol solution (*Fig. 16.a.*). The authors reported that after 8h the cumulative release percentage of ibuprofen from the hydrogels increased from 18% to 23% and 26% when the pH increased from 2 to 5 and to 7.4. These results were explained, according to the authors that, in acidic medium, the carboxylic group of ibuprofen was protonated and thus the ibuprofen was in the ionized form. Also, the tertiary amine of PNEMA was protonated in acid conditions, thus the polymer was in an ionized state, as the ibuprofen. Therefore, the repulsive ionic interactions between PNEMA and ibuprofen were strong and the release of drug in acidic conditions was limited. Oppositely, at pH 7.4 the PNEMA was not ionized, while the ibuprofen was, thus the interactions were weaker, the release of ibuprofen being higher than for low pH (*Fig. 16. b)*. In addition, these results were reported by the authors to be highly improved than those obtained for Poly (N, N-dimethylacrylamide) PDMA, a largely explored polymer for ibuprofen delivery, which showed a drug cumulative release percentage below 10% for all pHs. The better results obtained for PNEMA were explained, in addition to tailorable ionisation properties, by good hydrophilic

behaviour which increased the swelling properties of hydrogel in accordance with the ionisation state at different pH (*i.e.*, swelling % decreased when pH increased). On the other side, even PDMA show good water solubility, the lack of ionic groups than in PNEMA decreased its swelling performance and drug release properties.

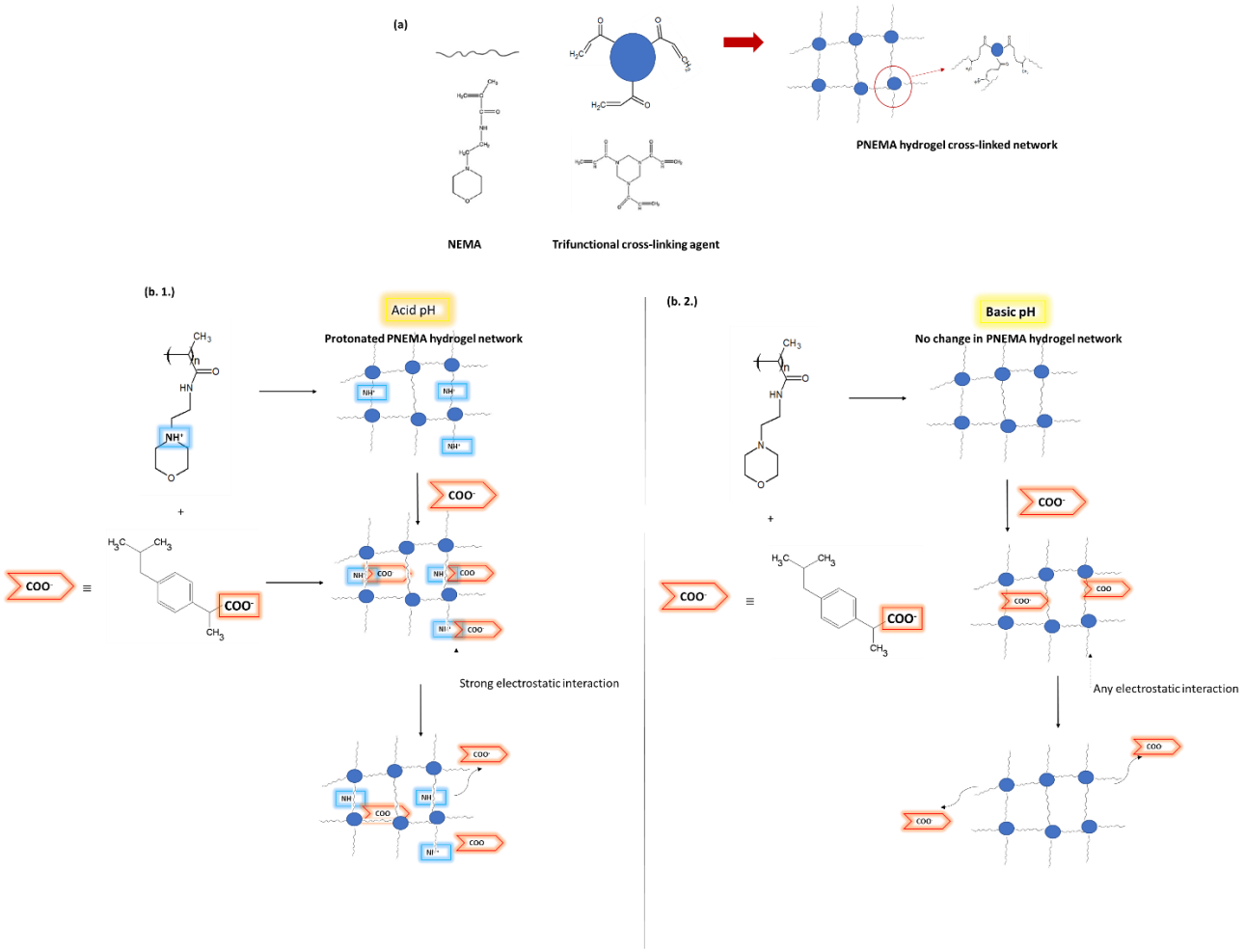

Fig. 16. (a) Representation of PNEMA homopolymers cross-linking resulting in hydrogel networks; (b) Entrapment and release of ibuprofen in PNEMA hydrogels studied in acid (b. 1.)and basic (b. 2.)pH [34]

In the same paper, the authors evidenced the importance of PNEMA-containing hydrogels in the prevention of crystallisation of ibuprofen during encapsulation in acidic medium. In pharmacology, a serious issue of ibuprofen is that it crystallizes in microdomains in stomach (where the pH is acidic) and the release profile is significantly altered, while the mucous stomach membrane is degraded. Velasco *et al.*, 2011 showed that at pH 7.4 PNEMA inhibited the crystallization of ibuprofen through specific polar with the methacrylamide groups.[34] By decreasing the pH to 5, again no crystalline ibuprofen was seen during this experiment, meaning

that the polymer was still able to prevent crystallization at this value. However, pH 2 was the point at which the polymer could no longer prevent the crystallization of the ibuprofen. As already stated by Velasco et al, at pH 2 the polymer was an ionized form and non-covalently interacted with the ionized carboxylic group of ibuprofen. Practically the ibuprofen was internalised in the hydrogel matrix. Globally, for moderate acid conditions, the use of PNEMA hydrogels prevented the ibuprofen crystallization.

In addition to the applications in drug delivery, morpholine-derived polymers were used in the development of nitric oxide (NO) release systems (*Fig. 17a.*) which were investigated by Seabra *et al.* [62] A lack or a disequilibrium in NO, a key modulator of the cardiovascular system, can lead to serious pathologic disfunctions such as hypertension or thrombosis. NO release polymers were intensively used to prevent the thrombus formation after cardiological stent implantation. The big challenges of NO releasing polymers are the short NO half-life (1.5s *in vivo*) and its sensitivity to oxidation. So, it is of a high interest to develop polymers able to protect NO from oxidative degradation and to release NO over a prolonged time. Poly(*N*-acryloylmorpholine)-*b*-poly(*N*-acryloyl-2,5-dimethylpiperazine) PNAM-*b*-PAZd block copolymers were synthesized and their self-assembly led to core-shell micelles with an average size of 50 nm used for NO release (*Fig. 17b.)*. The amphiphilic copolymers contained a hydrophilic PNAM block (as shell) and a PAZd hydrophobic block (as core). The reaction of hydrophobic PAZd block with NO resulted in a NONOate fragment that preserved the NO in the amphiphilic polymer system. The hydrophobic PAZd core of the micelles protected the NONOate from degradation, while the hydrophilic PNAM conferred adequate solubility in physiological medium. The micelles prolonged the NO release in aqueous solution (half-life of 7 days, NO release over 3 weeks in aqueous solution under physiological conditions). As stated by authors, these results were influenced by hydrophilic behaviour of PNAM shell that protected the hydrophobic core from quick degradation and release of NO, by avoiding the protons from physiological medium to penetrate and degrade the bulky hydrophobic core of micelle.

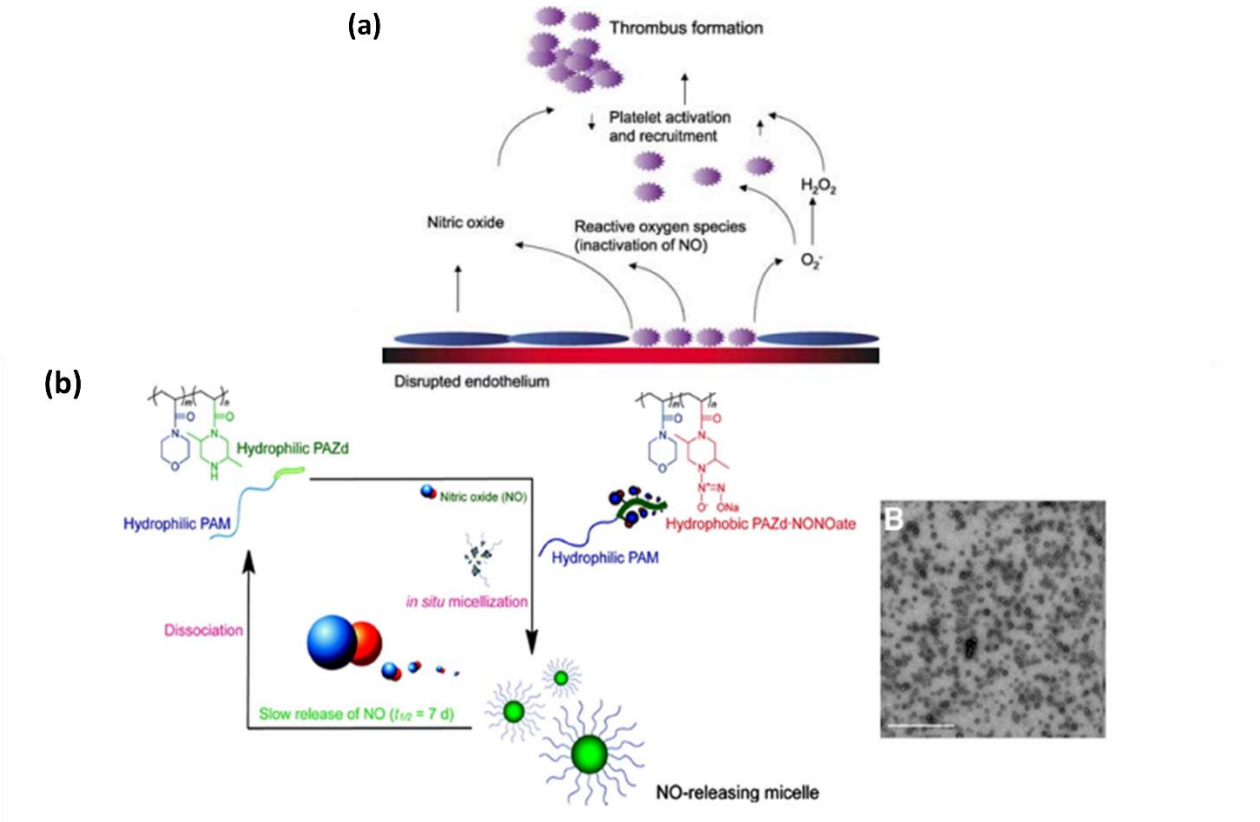

Fig. 17. (a) Importance of NO in preventing thrombus formation; (b) Representation of P(NAM-AZdNONOate) polymer micelles for NO release [62]

To sum up, the hydrophilic behaviour of morpholine containing polymers was important in improving the solubility and the passage of hydrophobic and amphiphilic drugs with multiple destinations (*i.e.*, anticancer therapy, antivirals, antibiotics, anti-inflammatory agents and NO-containing molecules). In the case of drug delivery, PNAM was mainly used in composition of polymer micelles, in combination with hydrophobic polymer blocks. The drug properties (*i.e.*, encapsulation, cumulative drug release, etc.) were reported to be comparable to those of PEG conjugates which were already developed for this application. Compared to PEG, PNAM presented the advantage to be synthesised in a various range of molar weights (which are crucial to develop specific applications), which is sometimes difficult for PEG when low molar weights are required. Moreover, PNAM was successfully involved to increase the release time of small bioactive inorganic molecules such as NO, used in the prevention of thrombus formation. The hydrophilic behaviour of PNAM protected the micellar core containing NO from degradation in contact with physiological medium and conferred a prolonged time release of NO. Furthermore, adding alkyl linkers between polymerizable synthons and morpholine heterocycles has resulted in PNEMA that showed good results as pH responsive drug delivery

system due to protonable tertiary amine group. For example, the protonation ability of PNEMA was very promising in the delivery of anti-inflammatory drugs which have to resist to certain pH of the body (*i.e.*, acid in the stomach, low acid in the intestine, etc.). Herein, PNEMA containing hydrogels were reported to avoid the crystallisation properties of drugs such as ibuprofen in different pHs, which led to undesired drug accumulation in organism. Overall, these preliminary results are very promising to find new alternatives to PEG derivatives. However, the most reported papers exploited only the *in-vitro* results, while *in-vivo* experiments were not completely investigated. In consequence, new fields of exploration are opened for morpholine containing polymers (and particularly PNAM) towards *in-vivo* drug delivery applications.

IV.3. Glucose sensors

Another area of biological applications of morpholine containing polymers is the development of glucose sensors. Boronic acid derivatives are involved in reversible reactions with diols, this property is used to identify and recognise sugar fragments (*via* reaction between two neighbouring hydroxyl units of sugar with the boronic acid fragment- *Fig. 18a*).[63] Zhang *et al*.[64] have developed an interesting biomimetic polymeric platform able to complete unfolding-folding cycles in the presence of glucose, acting as a sensor-like system. This artificial platform consisted in diblock copolymers described as poly(N-acryloyl morpholine)-*b*- poly(N-acryloyl-morpholine-*stat*-glycerol acrylate) PNAM-*b*-P(NAM-*stat*-GLA), containing one PNAM block and one statistical copolymer block composed by NAM and GLA. Then, the diblock copolymer was cross-linked with a phenyl diboronic acid framework (by covalent reaction between hydroxyl units of GLA with the hydroxyl units of diboronic acid) which acted as a linker. As a result of recognition between the boronic acid and glycerol moieties of the copolymers, the system self-assembled into a folded structure (*Fig. 18b.*). After the addition of glucose, the system unfolded, as a result of a transesterification competition reaction between glucose with boronic ester. Globally, this work proved the concept of molecular affinity for glucose by a templated boronic acid linker-sugar hydroxyl frameworks recognition by using hydrophilic morpholine containing polymers.

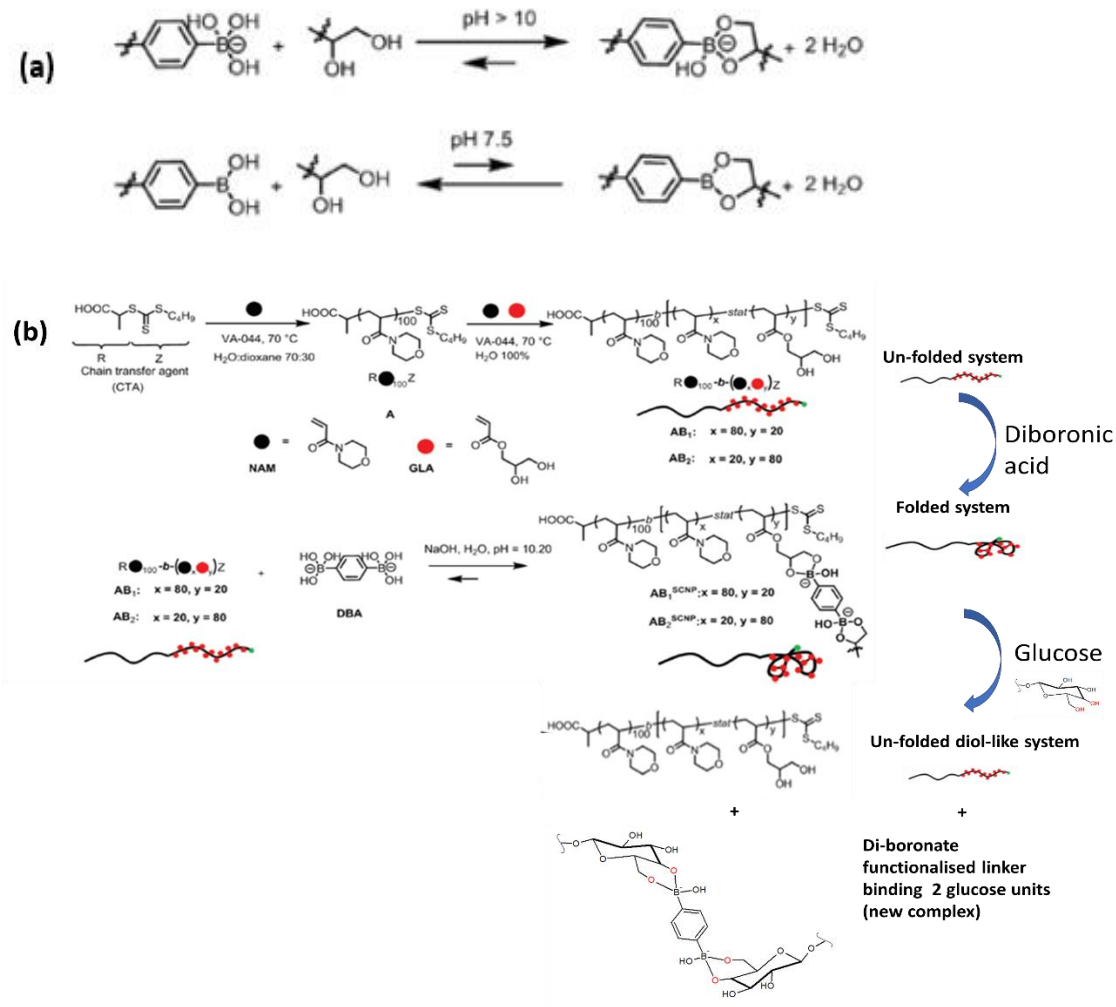

Fig. 18. (a) Reversible reaction of boronate esters with diol fragments (at pH 10) and reversible reaction of diboronic acid with diol fragments (at pH 7.5); (b) Representation of PNAM-b-P(NAM-co-GLA) diblock copolymers in reaction with diboronic acid and the influence of glucose in the polymer folding process. The folding takes place as a result of complexation between diboronic acid with diol units. After the addition of glucose, the bound between diboronic acid linker and diol framework is disrupted, the diboronic acid linker becoming free; the diol-like system becomes again un-folded, because there is any complex. Then, the free diboronic acid linker recognises glucose and complexation process with glucose occurs, resulting a new complex. All process takes place because the interaction between glucose - diboronic acid is stronger than diol-diboronic acid, thus the equilibrium is favourable to glucose binding, the polymer system acting as a glucose sensor. [64]

However, a serious issue in the development of boronic acid-based polymers for glucose recognition is that the glucose responsiveness takes place only for pH values higher than 9 because of high pK_a of boronic acid polymers, which is very limiting for *in-vivo* applications.

In this context, a strategy was to lower the pK_a of boronic acid polymers by adding electron-withdrawing groups such as carboxyl or amino that decreased the pK_a as a result of coordination between B atoms and O or N atoms.[55] For example, Wang *et al.* reported poly(ethylene glycol)-*b*-poly(acrylic acid-*co*-acrylamidophenylboronic acid), PEG-*b*-(PAA-*co*-PAAPBA) copolymers self-assembling in micelles able to recognise glucose at physiological pH (*i.e.*, 7.4). However, these micelles were efficient to recognise glucose only at concentrations above 20 mg/mL, which is quietly limited for biological applications. Inspired by this strategy, Gaballa & Theato [65] used acryloyl morpholine monomers since it contains N as electron-withdrawing atom. Their study reported poly[(N-acryloylmorpholine-*b*-(N-acryloylmorpholine-*co*-pentafluorophenyl acrylate)] copolymers, PNAM-*b*-(PNAM-*co*-PFPA), obtained by RAFT polymerisation of NAM and FPA monomers on a macromolecular PNAM chain transfer agent. Then, the reaction of PNAM-*b*-(PNAM-*co*-PFPA) with 3- amino phenyl boronic acid led to PNAM-*b*-(PNAM-*co*-PBA) block copolymers. The self-assembly of PNAM-*b*-(PNAM-*co*-PBA) led to core-shell micelles composed by a hydrophilic NAM shell and a hydrophobic PBA containing core (*Fig. 19.)*. According to the authors, the prepared micelles were sensitive to the glucose at concentrations above 1 g/L, which represented a significant improvement in terms of responsiveness compared to the PEG derived systems. This result should be assigned as authors stated due to a change in the swelling properties of the micelles as a result of a different hydrophilic behaviour of PNAM. In consequence, since the hydrophilicity of micelle was increased, the recognition of glucose will be effective including at low concentration, so the system is more sensitive. Another explanation stated by authors was correlated with the role of NAM as electron drawing group, that decreased the pK_a of the polymer through the formation of boronate ester bonding, which enhanced in consequence the glucose-responsiveness of the polymers in physiological medium.

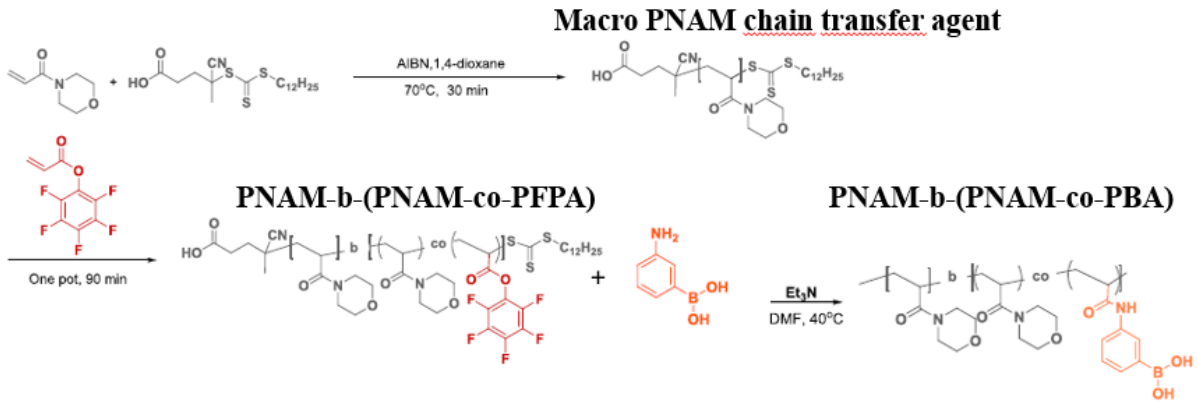

Fig. 19. Structure of PNAM-b-(PNAM-co-PBA) copolymers[65]

IV.4. Biomaterials for cell alignment and cell anti-adhesion

Another field of application of morpholine containing polymers is the development of biomaterials for cell alignment or cellular anti-adhesion devices. After a cardiovascular attack or a thrombosis, the arterial reconstruction demands materials able to promote the regeneration of tissue, a process which requires to avoid the adhesion of lipophilic substances. In addition, the materials used to prevent the adhesion of lipophilic compounds have to be efficient in physiological medium, so they have to perform a good hydrophilic behaviour at physiological pH. Some reports[66] showed that the hydrophilic nature of morpholine enhanced the adaptability in the aqueous physiological medium of the material used for arterial reconstruction. Another requirement of arterial reconstruction materials is that the material should perform a specific cell alignment in contact with cells, which is necessary to mimic the extracellular matrix (ECM). Takahashi *et al.*[67] synthesised by RAFT poly(acryloyl morpholine)-*b*-poly(*N*-isopropylacrylamide) PNAM-*b*-PNIPAM block copolymer brushes on a micropatterned surfaces where the cells were seeded and started to align as in the natural tissue (*Fig. 20a.*). The copolymer brushes where prepared by combining surface-initiated RAFT polymerization and photolithography technique for preparing micropatterned polymer brush surface. First, PIPAAm brush surfaces were prepared through the surface-initiated RAFT polymerization, by using an azoinitiator-imobilized glass surface. Then, PNAM was grafted as the "second block" from the termini of grafted PNIPAM chains, resulting in block copolymer brushes. The authors observed that compared to PNIPAM polymers alone or to the regions rich in PNIPAM (at 37°C, PNIPAM surface enabled hydrophobic and cell-adhesive properties because cell-adhesive proteins such as fibronectin from the physiological medium adhere to the hydrophobic PNIPAM surface [68]), the introduction of PNAM suppressed cell adhesion on the polymer surfaces in serum-containing culture media. They reported that in the presence of NHDF (normal human dermal fibroblasts), the patterned PNAM-*b*-PNIPAM regions enabled the cell to migrate and proliferate, but not to adhere (*Fig. 20b.*). After immunostaining the cell layers, the fluorescence microscopy showed the orientation of actin filaments and fibronectin which regulate the reformation of ECM. These results were explained by authors due to cell-repellent property of hydrophilic PNAM that allow the cells to migrate and proliferate, but not to adhere, which further led to a specific filament-like orientation as in the case of ECM. confirming that PNAM played a significant role in the development of PNAM-*b*-PNIPAM copolymer brushes used in reformation of the soft tissue skeleton (*Fig. 20c.*).

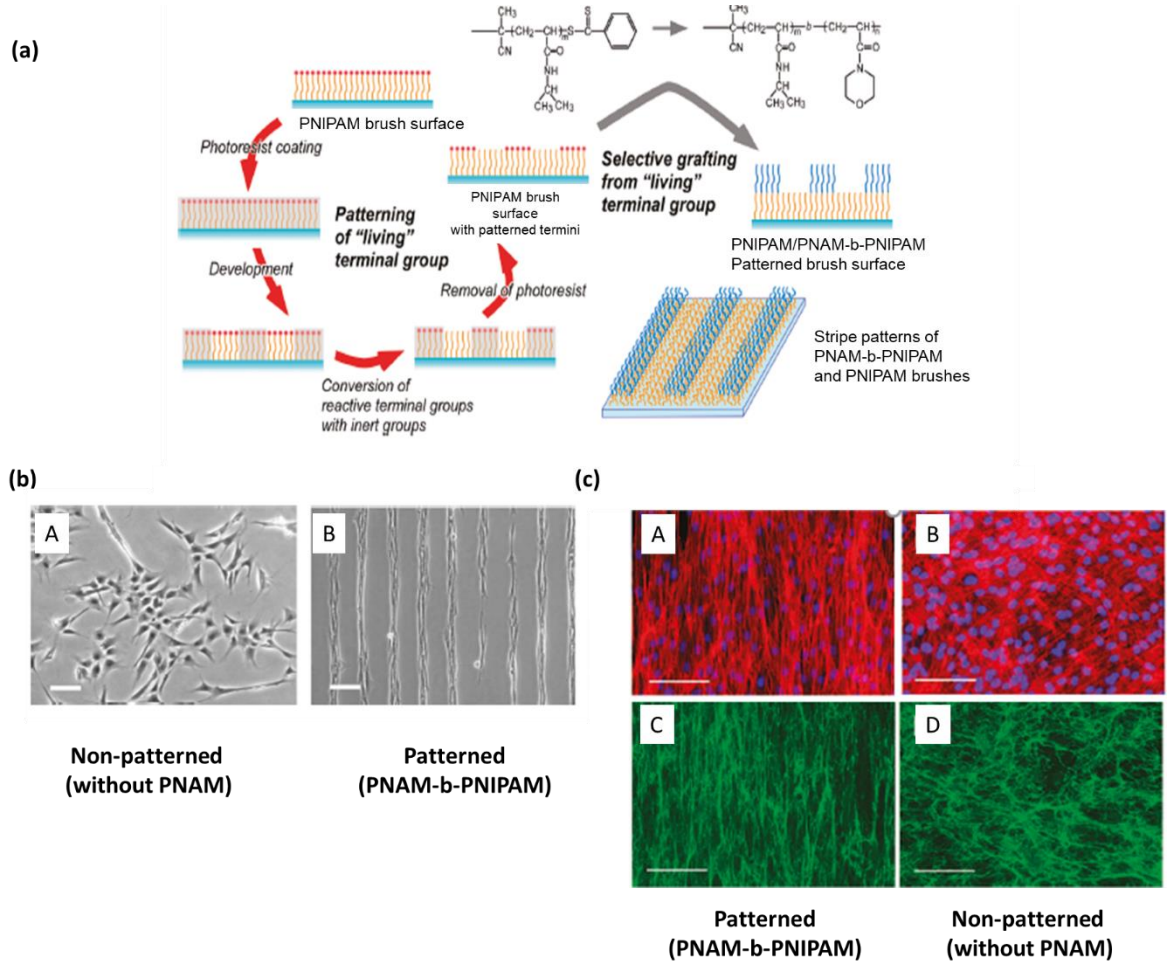

Fig. 20. (a) Representation of the process involved in the design of PNAM-b-PNIPAM brush polymers; (b) Behaviour of non-patterned (A) and patterned (B) polymer brushes for cell migration: for the non-patterned surfaces (without PNAM), the fibroblasts adhered but did not migrate; for patterned surfaces (containing PNAM-b-PNIPAM copolymer brushes, the fibroblasts did not adhere, but they migrated and proliferated;(c)The fluorescence images of adherent fibroblasts of patterned (A, C) and non-patterned (B, D) surfaces. The fibrolectin is aligned to reproduce ECM in the case of patterned surfaces (containing PNAM-b-PNIPAM copolymers brushes), while for non-patterned surfaces (without PNAM) the fibers are not aligned. Globally, the patterned surfaces using PNAM improved the cell migration and alignment to develop ECM biomimetic materials [67]

Other important contributions of PNAM-*b*-PNIPAM copolymers in this field were reported by Kobayashi & Okano.[69] Their work showed that additional grafting of short PNAM from the residual terminals of the PNIPAM polymer increased the hydrophilicity of polymer backbone and delayed the cellular attachment. Herein, they succeeded the alignment of myoblasts on the stripe micropatterns of the PNIPAM/PNIPAM-*b*-PNAM brush domains over a surface of 50/50

μm at 37 °C. At 20°C the aligned cells were detached from the copolymer brush domains as a contiguous sheet from the surface. This result was explained as a result of LCST properties of PNIPAM which become hydrophilic upon lowering the temperature to 20°C, but also a consequence of hydrophilic non LCST sensitive PNAM chains that are hydrophilic. To conclude, the reported PNAM-b-PNIPAM copolymers by Takanashi [67] and Kobayashi [69] showed that are able to modulate the direction of alignment within a cell sheet and to recover it only by changing the temperature. In both cases, PNAM has a significant contribution thanks to hydrophilic properties that delayed the cellular attachment and thus avoided non desired cellular adhesion effects that are the core of cardiovascular diseases.

Another study showing the anti-adhesion action of PNAM was shown by Gorman and collaborators. [70] Their paper presented the synthesis of PNAM containing physical hydrogels used as cell spatial barrier. The hydrogels were prepared in water and were formed as a result of non-covalent interactions such as H-bonds between hydrophilic PNAM chains and water molecules. As stated by the authors, the PNAM acted as a cell spatial barrier for 38 h, without cytoskeleton formation. After 80h, the cells occupied the hydrogel cavities and regenerated the natural tissue. This result was explained by the authors to be a consequence of quick dissolution of PNAM over short timeframes in water. Therefore, the polymer undergoes dissolution from water exposed cell surface to bulk, gradually decreasing in weight and surface area until a small quantity of polymer remains prior to full dissolution. In this study, the authors showed that PNAM is a non-adhesive material to cells, where deposited and dissolved at a predictable rate, it acted to delay cell adhesion over the covered area without affecting or harming cells adjacent to the boundary, proving no cytotoxicity. [70]

IV.5. Oxydation sensitive materials

H_2O_2-sensitive polymeric systems are of a high interest for cancer diagnosis and therapies because the tumoral regions are rich in hydrogen peroxide. Thus, the development of micelles sensitive to oxidative agents such as H_2O_2 is very promising. Moreover, oxidation sensitive polymeric micelles could destroy tumours when anticancer drugs are entrapped in the polymeric matrix cavity and then released under oxidation stimuli. Inspired by these properties of oxidation-sensitive materials, Sobotta *et al.*[18] designed poly(N-acryloyl morpholine)-*b*-poly(N-acryloyl thiomorpholine) PNAM-*b*-PNAT block copolymers. These polymers self-assembled in micelles containing a PNAT hydrophobic core covered by a hydrophilic PNAM shell. The PNAM-*b*-PNAT polymer micelles presented a good sensitivity towards low concentrations of hydrogen peroxide (10 mM) that provoked their disintegration (*Fig. 21.*). The micelles

degradation took place by the oxidation of thioether groups of PNAT hydrophobic block, resulting in thio-oxide containing PNATOx block that are hydrophilic due to oxidation process. As authors stated, the mechanism of oxidation was based on the diffusion of H_2O_2 molecules in the hydrophobic core of NAT which decreased the hydrophobicity of the system as a result of thiomorpholine oxidation. The micelle core become hydrophilic and thus the disintegration process was accelerated because of aqueous compatibility of micelles. This work evidenced the importance of using highly hydrophilic PNAM blocks in combination of tailorable PNAT block in terms of oxidation, when developing an oxidation sensitive self-assemble system with potential applications in biology.

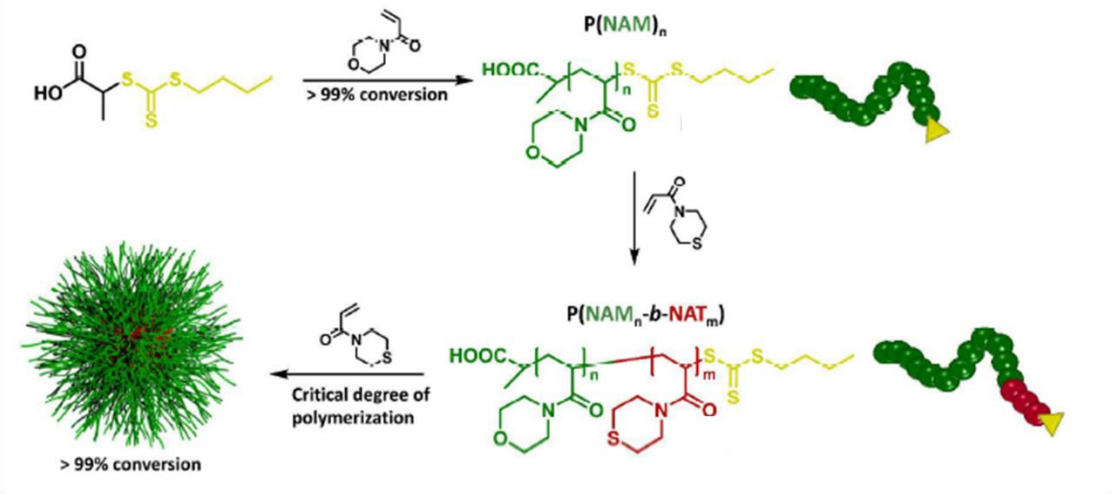

Fig. 21. Representation of P(NAM-b-NAT) copolymer oxidation sensitive micelles [18]

Other important contributions about oxidation responsive morpholine-based polymers and their use as anti-angiogenic compounds were showed by Hasegawa, Moriyama, *et al.* [71] The polymers providing an anti-oxidant behaviour (*i.e.*, that inhibit the oxidation process by scavenging the dangerous reactive oxidative radicals derived from H_2O_2) are known to be anti-angiogenic (*i.e.*, that prevent the angiogenesis process). Angiogenesis (*i.e.*, blood vessel growth) should become uncontrolled in the case of cancerous tissues and is described by the tube formation in the endothelial cells which is the result of non-desired oxidation of cells. Thus, in order to prevent the uncontrolled angiogenesis, the polymers used as anti-oxidants perform anti-angiogenic properties and thus act as inhibitory agents of the tube formation, by inactivating the reactive oxidative radicals that damage the cells and cause the uncontrolled appearance of tubes. The authors reported the synthesis of poly(N-acryloyl morpholine-*b*-

poly(glycyl modified catechol) copolymers (PNAM-*b*-PDA) by using RAFT polymerisation. To this, a macro-chain transfer agent containing Poly(N-acryloyl glycine tert-butyl ester) was prepared (1), and then the N-acryloyl morpholine was further polymerized to yield the PNAM-PAG block copolymers (2), as presented in the *Fig. 22.* After the removal of the chain transfer agent end group (3), the carboxyl group-bearing blocks (4) were modified with dopamine (DA) by DCC/NHS coupling to give PNAM-*b*-PDA_x (5) block copolymers (where "x" represented the degree of modification, respectively. the number of DA groups per polymer chain). The self-assembly of prepared PNAM-*b*-PDA_x block copolymers led to micelles with high stability against auto-oxidation (*i.e.*, high antioxidant effect), especially when increasing the length of PDA block (*Fig. 22.*). A micelle providing a high stability against auto-oxidation has the ability to scavenge low concentrations of H_2O_2. The study showed that, by increasing the number of hydrophobic DA units in the PDA block from 18 to 30 and to 38 respectively, the amount of scavenged concentration of H_2O_2 decreased from 5.5 to 3.5 µM. Since the scavenging mechanism consists of the inactivation of the reactive radical derived from H_2O_2 by accepting a hydrogen atom from a hydroxyl group of the DA,[72] it means that higher stable the micelle is, the slower mass transfer of H_2O_2 through the micelle core is.

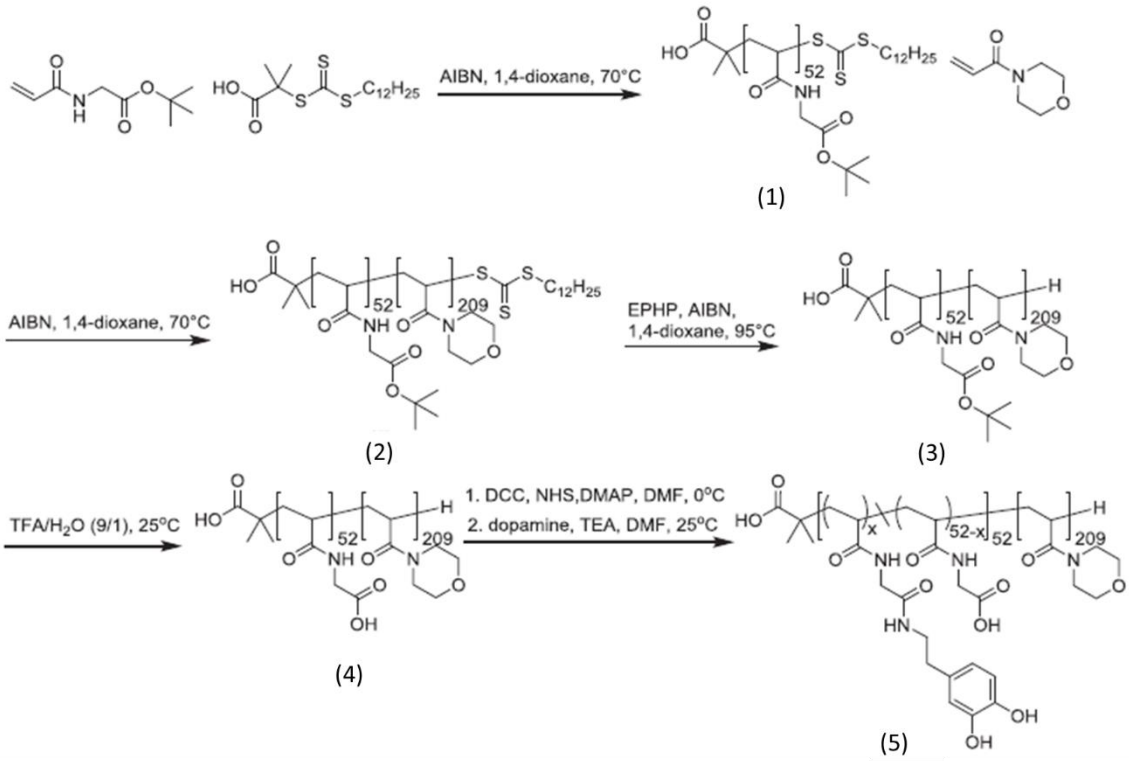

Fig. 22. Synthesis of PNAM-b-PDAx block copolymers

In addition, the authors reported that *in-vitro* endothelial cell tube formation assay showed that an increase in the DA units in the PDA block from 18 to 38 inhibited the tube formation. This

result was explained by the high oxidation stability of polymer micelles that depend on the number of DA units, but also by the hydrophilic PNAM corona that shield the DA units from uncontrolled oxidation, and thus prevented the tube formation on the cells.

IV.6. Anticoagulant and hemocompatible materials

A last section with biological applications of morpholine containing polymers is the development of anticoagulant and hemocompatible materials. Anticoagulants are of real importance for preventing or mitigating different diseases, such as thrombosis, haemophilia, or vitamin K deficiency.[73] Classical anticoagulant materials are generally hydrophobic polymer membranes that inhibit platelet aggregation during the coagulation process, interfering with the formation of fibrin and stable aggregated platelet products (*Fig. 23a.*).[74] Previous reports showed that the incorporation of hydrophilic polymers such as PEG improved the anticoagulant properties of such materials, since they reduced the interactions between membrane surface and blood protein, preventing the blood coagulation on the membrane. However, a disadvantage of the PEG modified anticoagulant membranes was that the hydrophilic behaviour of the membrane was reduced when the membrane was in contact with biological medium. This non-desired effect was the result of the oxidation of ether bonds in PEG to reactive aldehyde moieties which are toxic for the organism. To overcome the non-desired oxidation in contact with biological medium, Xu *et al*. (2016) [75] used PNAM in the development of anticoagulant polymeric membranes instead of PEG, since PNAM showed similar hydrophilic properties as PEG, but it not contains ether bonds susceptible to the oxidation. They prepared membranes composed of poly(vinylidene fluoride)-*g*- poly(acryloyl morpholine-acrylic acid-*g*-argatroban) PVDF-*g*-(PNAM – PAA-*g*-AG) copolymers. The membranes were obtained in two steps including the synthesis of grafted PVDF-*g*-(PNAM-PAA) copolymer followed by the grafting of AG (an anticoagulant) on the copolymer (*Fig. 23. b.*). First, PVDF was treated with KOH in order to produce -C=C- bonds necessary to perform the grafting process by free polymerisation of NAM and AA on the alkali modified PVDF, resulting PVDF-*g*-(PNAM-PAA) grafted copolymers. Secondly, AG was grafted on PVDF-*g*-(PNAM-PAA) copolymers *via* the reaction between amino group of AG with the carboxylic group of PAA in the presence of EDC/DMAP that lead to PVDF-*g*-(PNAM-PAA-*g*-AG) copolymers. The resulted polymeric membranes presented good hydrophilicity, high resistance to protein adsorption and decreased haemolysis ratio.

The authors reported that the hydrophilicity of membrane was mainly influenced by PNAM and not by AG, the PNAM introduction leading to a soft decrease of water contact angles from

90^0 (in the case of simple PVDF) to 80^0 for PVDF-*g*-(PNAM-PAA-*g*-AG), independently on the content of AG in the grafted copolymer. These results were then exploited to study the resistance of membranes to blood proteins, which is a requisite for anticoagulant materials production. According to their study, by increasing the AG % in PNAM-PVDF membranes from 1% to 3% (wt%), the amount of adsorbed BSA (bovin serum albumin) decreased from 75 µg/cm^2 to 50 µg/cm^2 which means that the resulted materials performed high resistance to protein adsorption. This result was explained by the authors due to the hydrophilic PNAM moieties that form a hydration layer after binding the water molecules, and thus avoid the direct contact between the membrane and proteins, and suppress the nonspecific protein adsorption. Finally, the authors evaluated the hemocompatibility of prepared membranes by the determination of hemolysis ratio which is obtained by detecting the erythrocyte damage caused by putting the material in contact with blood. Herein, the authors underlined a decrease the hemolysis ratio of polymer membranes from 2.11% to 1.81%, when the content in AG increased from 1% to 3% (wt%) (*Fig. 23c.*). These values confirmed the role of PNAM as hydrophilic polymer that improved the hemocompatibility of the membrane due to the protective hydration layer.

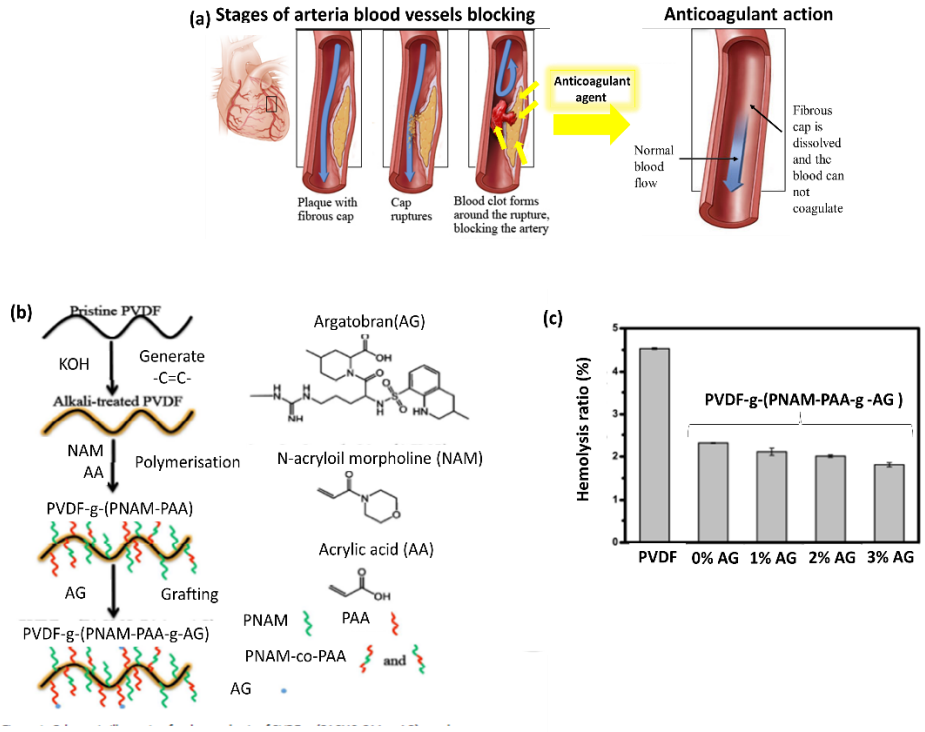

Fig. 23. (a) Anticoagulant drug action in the prevention of arteria blood vessels blockage; (b) The preparation of PVDF-g-(PNAM-PAA-g-AG) membranes; (c)Hemolysis ratio of anticoagulant blood membranes[75]

Other contributions in this field were done by X. Shen *et al.*[15] who designed poly(vinylidene fluoride – *g*- acryloil morpholine) PVDF-*g*-PNAM copolymers to develop membranes as hemocompatible materials to suppress protein adsorption and platelet adhesion (*Fig. 24a.*). The PVDF-*g*-PNAM copolymers were prepared by ATRP, the copolymer structure containing PVDF backbones and PNAM side chains. Three phenomena occur when the material surface is put in contact with blood: the protein adsorption, platelet adhesion and thrombus formation. BSA (bovine serum protein) and BFG (blood protein) were selected as model proteins to evaluate the protein adsorption resistance of the membranes. The authors reported that an increase of PNAM concentration in the membrane from 0.028 to 0.224 g/mL led to a consequent decrease of the protein adsorption from 119 µg/cm^2 to 30 µg/cm^2 respectively (*Fig. 24b.*). This decrease of protein adsorption was ascribed to the hydrophilic nature of PNAM which diminished the hydrophobic interactions between the protein and the hydrophobic PVDF. PNAM generated the formation of a hydration layer which disabled the adsorption of protein to the membrane surface, further suppressing the platelet adhesion. In addition, the study showed that the hydrophilicity of PNAM had a strong influence on the evolution of hemolysis rate which is important in the evaluation of hemocompatible materials. An increase in PNAM concentration led to a decrease of hemolysis rate from 4.8% (0 g/ mL PNAM) to 0.4% (0.224 g/mL PNAM) in PNAM-*g*-PVDF copolymer membrane. These results demonstrated that PNAM is a good candidate to improve the hemocompatibility of anticoagulant materials.

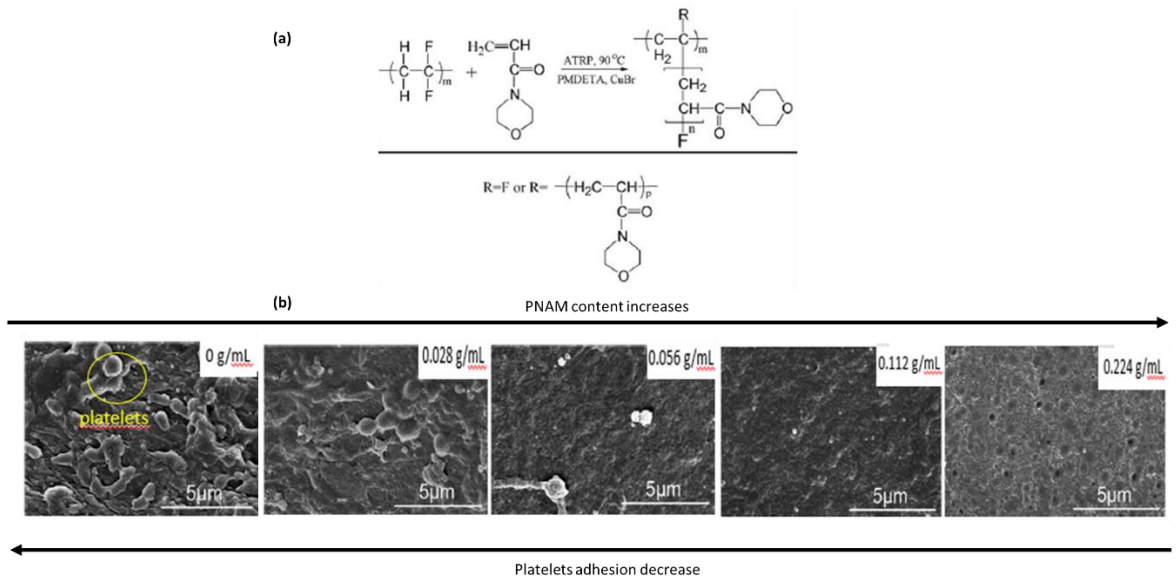

Fig. 24. (a) Structures of PNAM-g-PVDF copolymers; (b)SEM images of platelets adhesion for simple PVDF membranes and PNAM-g-PVDF membranes prepared with different contents of NAM [15]

Mochizuki *et al.*[76] studied the hemocompatibility performance of poly(acryloyl morpholine -*stat*-butyl methacrylate) P(NAM-*stat*-BMA) copolymers that were used as substrates spin-coated on the PET surfaces. The resulted P(NAM-*stat*-BMA) containing films exhibited an excellent blood platelet compatibility for NAM content ranging between 45-80% (mol %). This result was correlated with the fact that the platelets adhesion was lower for highly hydrophilic surfaces.

V. Conclusions

This review emphasises the correlation between the structural-chemical properties of morpholine and thiomorpholine derived polymers containing (meth)acrylate/(meth)acrylamide polymerizable motifs, and their use in biology. The high diversity in using these polymers was the result of structural tailoring of hydrophobic-hydrophilic balance by combining hydrophilic morpholine with hydrophobic (meth)acrylate or (meth)acrylamide synthons bearing supplementary alkyl chains. Differently from morpholine based polymers which are predominantly hydrophilic, the thiomorpholine derived polymers showed a global hydrophobic behaviour which can be easily tailored to hydrophilic materials through the oxidation of sulphur atom of thiomorpholine. In addition, the pH responsiveness of morpholine derived polymers due to protonable secondary amino group, non-cytotoxicity and biocompatibility were other significant properties to develop materials for biological applications.

As underlined by the most part of the papers, the main reasons to use poly(*N*-acryloil morpholine) based polymers in biology were the excellent hydrophilic properties and solubility in physiological conditions, comparable with that of PEG. Moreover, PNAM polymers showed a big advantage compared to high molar weight PEG derivatives that were reported to be less effective for *in-vivo* applications in the field of protein sensing. In addition, PNAM are favourable instead of high molar weight PEG analogs, since they could be easily synthesised by controlled polymerisation techniques. These advantages of PNAM were used to prepare peptide or protein-PNAM conjugates (*e.g.*, with cRGD peptide receptors, cholera toxin, biotin and streptavidin). The resulted polymeric micelles found their application as efficient markers for some therapeutically proteins responsible to the control of inflammation or immunological reactions, with results comparable to that of already tested PEG derivatives. Also, PNAM was reported in the conjugation with enzymes (*e.g.*, uricase) where the hydrophilic behaviour of PNAM was beneficial to improve the enzymatic activity compared to the simple enzyme since they improved the water solubility of the enzyme complex in the organism. Furthermore, the ability to easily change the hydrophilic-hydrophobic nature of morpholine derived polymers

was of a real use in the development of drug delivery systems with different polarities. Additionally, poly(*N*-acryloil/) poly(methacryloil) morpholine polymers were used as carriers for anticancer (*e.g.*, Paclitaxel, Doxorubicin, Everolimus, etc), anti-inflammatory (*e.g.*, Ibuprofen), or antiviral drugs (*e.g.*, Aciclovir), etc. Herein, the role of morpholine polymers was to create a hydrophilic capsule able to entrap the drug and to transport it through the cell. In addition, they were involved in the delivery of small instable molecules such as NO which are important in the prevention of blood platelet adhesion on the capillaries. Also, significant researches including PNAM derived polymers were done in the field of anticoagulant and hemocompatible membranes. In this case, PNAM was used as repellent due to the hydrophilic protective layer formed on the membrane that prevented the platelet adhesion.

While PNAM was highly explored for biological applications, the thiomorpholine polymers were less investigated. Even the thiomorpholine polymers are less hydrophilic than morpholine polymers, they present an interesting redox behaviour of the sulphur atom. Practically, this oxidation is the key to transform the less hydrophilic thiomorpholine polymers in highly hydrophilic thiomorpholine oxide polymers. The oxidative nature of the thiomorpholine-polyacrylate polymers to the corresponding sulfoxides was the key to explain their use as stimuli responsive systems in oxidative sensitive anticancer therapies. Herein, in contact with the tumoral regions (widely recognised for an enriched oxidised environment), thiomorpholine derived polymers loaded with an anticancer drug were loaded in the tumoral area *via* oxidation and released the therapeutic agent.

In summary, the morpholine and thiomorpholine related polymers represent intelligent artificial platforms with multiple uses in biology. Their particular structural features and versatile amphiphilic behaviour rests to be an interesting area of investigation in the development of intelligent materials with multiple functions.

VI. References

1. Y. Pourshojaei, A. Abiri, K. Eskandari, Z. Haghighijoo, *Sci. Rep.*, 2019, **9**, 1–19.
2. F. H. Sobotta, M. T. Kuchenbrod, C. Grune, D. Fischer, S. Hoeppener, J. C. Brendel, *Polym. Chem.*, 2021, **12**, 1668–1680.
3. M. S. Masoud, A. E. Ali, G. S. Elasala, R. E. Elwardany, *J. Mol. Struct.* 2019, **1175**, 648–662.
4. B. L. Rivas, A. Maureira, K. E. Geckeier, *J. Appl. Polym. Sci.*, 2006, **101**, 180–185.
5. Y. Gök, A. Akta, *J. Mol. Structure*, 2021, **1228**, 129462-129473.
6. B. H. Lessard, X. Savelyeva, M. Mari, *Polymer*, 2012, **53**, 5649–5656.

7. D. Duret, Z. Haftek-Terreau, M. Carretier, T. Berki, C. Ladavière, K. Monier, P. Bouvet, J. Marvel, Y. Leverrier, M. T. Charreyre, A. Favier, *Polym. Chem.*, 2018, **9**, 1857–1868.

8. D. J. Leaver, A. B. Hughes, R. M. Dawson, A. Postma, N. Malic, A. Polyzos, *RSC Adv.*, 2014, **4**, 14868–14871.

9. J. Bernal, L. Sanchez-Hernandez, C. Elvira, D. Velasco, E. Ibanez, A. Cifuentes, *J. Sep. Sci.*, 2009, **32**, 605–612.

10. M. Zhou, Y. He, Y. Chen, Y. Yang, H. Lin, S. Han, *Energy Fuels*, 2015, **29(9)**, 5618-5624.

11. Y. S. Jo, A. J. Van Der Vlies, J. Gantz, S. Antonijevic, D. Demurtas, D. Velluto, J. A. Hubbell, *Macromolecules*, 2008, **41**, 1140–1150.

12. F. A. Al-Sagheer, E. I. Ibrahim, K. D. Khalil, *Eur. Polym. J.*, 2014, **58**, 164–172.

13. Z. An, Y. Li, R. Xu, F. Dai, Y. Zhao, L. Chen, *Appl. Surf. Sci.*, 2018, **457**, 170–178.

14. V. P. Torchilin, V. S. Trubetskoy, *Adv. Drug Deliv. Rev.*, 1995, **16**, 141–155.

15. X. Shen, J. Liu, X. Feng, Y. Zhao, L. Chen, *J. Biomed. Mater. Res. - Part A*, 2015, **103**, 683–692.

16. S. Sharma, S. Mazumdar, K. S. Italiya, T. Date, R. I. Mahato, A. Mittal, D. Chitkara, *Mol. Pharm.*, 2018, **15**, 2391–2402.

17. M. Biava, G. C. Porretta, D. Deidda, R. Pompei, *Bioorg. Med. Chem.*, 2003, **11**, 515–520.

18. F. H. Sobotta, F. Hausig, D. O. Harz, S. Hoeppener, U. S. Schubert, J. C. Brendel, *Polym. Chem.*, 2018, **9**, 1593–1602.

19. P. Patil, R. Madhavachary, K. Kurpiewska, J. Kalinowska-Tłuścik, A. Dömling, *Org. Lett.*, 2017, **19**, 642–645.

20. A. Kumari, R. K. Singh, *Bioorg. Chem.*, 2020, **96**, 103578-103657.

21. V. Kaur, A. K. Malik, *Talanta*, 2007, **73**, 425–430.

22. K. S. Babu, V. Prabhakar, L. K. Ravindranath, J. Latha, *Int. J. Pharma Res. Rev.*, 2015, **4**, 23–33.

23. H. Fischer, I. Parrilla, F. Schuler, *J. Med. Chem.*, 2010, **53(8)**, 3227–3246.

24. L. Li, D. Zahner, Y. Su, C. Gruen, G. Davidson, P. A. Levkin, *Biomaterials*, 2012, **33**, 8160–8166.

25. D. Duret, A. Grassin, M. Henry, T. Jacquet, F. Thoreau, S. Denis-Quanquin, J. L. Coll, D. Boturyn, A. Favier, M. T. Charreyre, *Bioconjug. Chem.*, 2017, **28**, 2241–2245.

26. A. Frère, M. Kawalec, S. Tempelaar, P. Peixoto, E. Hendrick, O. Peulen, B. Evrard, P. Dubois, L. Mespouille, D. Mottet, G. Piel, *Biomacromolecules*, 2015, **16**, 769–779.

27. L. Peng, E. Wagner, *Biomacromolecules*, 2019, **20**, 3613–3626.

28. R. Chapman, A. J. Gormley, M. H. Stenzel, M. M. Stevens, *Angew. Chemie - Int. Ed.*, 2016, **55**, 4500–4503.

29. J. Zhao, H. Han, Q. Wang, C. Yan, D. Li, J. Yang, X. Feng, N. Yang, Y. Zhao, L. Chen, *React. Funct. Polym.*, 2019, **139**, 92–101.

30. S. Pizzimenti, E. Ciamporcero, P. Pettazzoni, S. Osella-Abate, M. Novelli, C. Toaldo, M. Husse, M. Daga, R. Minelli, A. Bisazza, P. Ferruti, E. Ranucci, M. Grazia Bernengo, C. Dianzani, F. Biasi, R. Cavalli, G. Barrera, *Free Radic. Biol. Med.*, 2013, **65**, 765–777.

31. K. Ramesh, D. S. B. Anugrah, K. T. Lim, *React. Funct. Polym.*, 2018, **131**, 12–21.

32. F. Xu, H. Li, Y. Luo, W. Tang, *ACS Appl. Mater. Interfaces*, 2017, **9(6)**, 5181-5192.

33. U. Hasegawa, N. Tateishi, H. Uyama, A. J. Van Der Vlies, *Macromol. Biosci.*, 2015, **15**, 1512–1522.

34. D. Velasco, C. B. Danoux, J. A. Redondo, C. Elvira, J. San Román, P. S. Wray, S. G. Kazarian, *J. Control. Release*, 2011, **149**, 140–145.

35. M. Bencini, E. Ranucci, P. Ferruti, A. Manfredi, F. Trotta, R. Cavalli, *J. of Pol. Sci., Part A: Pol. Chem.*, 2008, **46**, 1607–1617.

36. B. B. Sharma, C. Murli, S. M. Sharma, *J. Raman Spectrosc.*, 2013, **44**, 785–790.

37. A. Munasinghe, A. Mathavan, A. Mathavan, P. Lin, C. M. Colina, *J. Phys. Chem. B.*, 2019, **123**, 5196-5205.

38. G. Poovi, N. Damodharan, *Eur. J. of Appl. Sci.*, 2018, **10**, 1–14.

39. P. Caliceti, O. Schiavon, F. M. Veronese, *Bioconjug. Chem.*, 2001, **12**, 515–522.

40. F. Moncalvo, M. Isabel, M. Espinoza, F. Cellesi, *Front. Bioeng. Biotechnol.*, 2020, **8**, 1-22.

41. M. Pröhl, S. Seupel, P. Sungur, S. Höppener, M. Gottschaldt, J. C. Brendel, U. S. Schubert, *Polymer*, 2017, **133**, 205–212.

42. S. M. D. Addio, S. Baldassano, L. Shi, L. Cheung, D. H. Adamson, M. Bruzek, J. E. Anthony, D. L. Laskin, P. J. Sinko, R. K. Prud, *J. Control. Release*, 2013, **168**, 41–49.

43. H. Cabral, K. Miyata, K. Osada, K. Kataoka, *Chem. Rev.*, 2018, **118(14)**, 6844-6892.

44. F. S. Ielasi, M. Alioscha-perez, D. Donohue, S. Claes, H. Sahli, D. Schols, R. G. Willaert, *MBio*, 2016, **7**, 1–17.

45. J. C. Pickens, D. D. Mitchell, J. Liu, X. Tan, Z. Zhang, C. L. M. J. Verlinde, W. G. J. Hol, E. Fan, *Chem. Biol*., 2004, **11**, 1205–1215.

46. D. J. Leaver, R. M. Dawson, J. M. White, A. B. Hughes, *Org. Biomol. Chem.*, 2011, **9**, 8465–8474.

47. H. Tanaka, M. Hanasaki, T. Isojima, H. Takeuchi, T. Shiroya, H. Kawaguchi, *Colloids Surfaces B Biointerfaces*, 2009, **70**, 259–265.

48. X. Shen, J. Liu, X. Feng, Y. Zhao, L. Chen, *J. Biomed. Mater. Res. Part A*, 2014, **103**, 683–692.

49. A. Rodriguez-abetxuko, D. Sánchez-dealcázar, P. Muñumer, *Front Bioeng. Biotechnol.*, 2020, **8**, 1–27.

50. P. Relogio, M. Bathfield, Z. Haftek-Terreau, M. Beija, A. Favier, M. J. Giraud-Panis, F.

D'Agosto, B. Mandrand, J. P. S. Farinha, M. T. Charreyre, J. M. G. Martinho, *Polym. Chem.*, 2013, **4**, 2968–2981.

51. F. Alexandre, E. Vauthey, *Photochem. phobiol. sci.*, 2005, **4(3)**, 260–267.
52. VP. Hytonen, *C. C. Biology*, 2017, **24(8)**, 921–922.
53. A. Favier, Y. Leverrier, et al. *Polym. Chem.*, 2013, **4**, 61-67.
54. O. Schiavon, P. Caliceti, P. Ferruti, F. M. Veronese, *Farmaco*, 2000, **55**, 264–269.
55. J. Tsuji, K. Hirose, *Int. J. Immunopharmac.*, 1985, **7**, 725–730.
56. D. Duret, Z. Haftek-Terreau, M. Carretier, C. Ladavière, M. T. Charreyre, A. Favier, *Polym. Chem.*, 2017, **8**, 1611–1615.
57. S. Chen, S. X. Cheng, R. X. Zhuo, *Macromol. Biosci.*, 2011, **11**, 576–589.
58. F. Xu, H. Li, Y. L. Luo, W. Tang, *ACS Appl. Mater. Interfaces*, 2017, **9**, 5181–5192.
59. K. Ramesh, B. Thangagiri, A. K. Mishra, B. H. Ahn, Y. S. Gal, K. T. Lim, *React. Funct. Polym.*, 2018, **132**, 112–119.
60. E. D. Gmbh, C. Technologies, *Polymer*, 2010, **48**, 1973–1978.
61. H. Efe, M. Bicen, M. V. Kahraman, N. Kayaman-Apohan, *J. Braz. Chem. Soc.*, 2013, **24**, 814–820.
62. A. B. Seabra, G. Z. Justo, P. S. Haddad, *Biotechnol. Adv.*, 2015, **33**, 1370–1379.
63. G. F. Whyte, R. Vilar, R. Woscholski, *J. Chem. Biol.*, 2013, **6**, 161–174.
64. J. Zhang, J. Tanaka, P. Gurnani, P. Wilson, M. Hartlieb, S. Perrier, *Polym. Chem.*, 2017, **8**, 4079–4087.
65. H. Gaballa, P. Theato, *Biomacromolecules*, 2019, **20**, 871–881.
66. L. Chen, C. Yan, Z. Zheng, *Mater. Today*, 2018, **21**, 38–59.
67. H. Takahashi, M. Nakayama, K. Itoga, M. Yamato, T. Okano, *Biomacromolecules*, 2011, **12**, 1414–1418.
68. H. Takahashi, T. Shimizu, M. Nakayama, M. Yamato, T. Okano, *Biomaterials*, 2013, **34**, 7372–7380.
69. J. Kobayashi, T. Okano, *Bull. Chem. Soc. Jpn.*, 2019, **92**, 817–824.
70. M. Gorman, Y. H. Chim, A. Hart, M. O. Riehle, A. J. Urquhart, *J. Biomed. Mater. Res. - Part A*, 2014, **102**, 1809–1815.
71. U. Hasegawa, M. Moriyama, H. Uyama, A. J. Van Der Vlies, *Polymer*, 2015, **66**, 1–7.
72. B. C. Dickinson, C. J. Chang, *Nat. Chem. Biol.*, 2011, **7**, 504–511.
73. R. De Caterina, S. Husted, L. Wallentin, G. Agnelli, F. Bachmann, C. Baigent, J. Jespersen, S. D. Kristensen, G. Montalescot, A. Siegbahn, F. W. A. Verheugt, J. Weitz, *Eur. Heart J.*, 2007, **28**, 880–913.
74. B. Dahlbäck, *Lancet*, 2000, **355**, 1627–1632.
75. A. G. B. Wanna, J. H. Noble, M. L. Carlson, H. Gifford, M. S. Dietrich, D. S. Haynes,

B. M. Dawant, *Laryngoscope*, 2014, 2–31.

76. A. Mochizuki, M. Kimura, A. Ina, Y. Tomono, M. Tanaka, *J. Biomater. Sci. Polym. Ed.*, 2010, **21**, 1895–1910.

Conclusion Chapitre II : Partie I

Cette revue a présenté la corrélation entre les propriétés structurales et chimiques des polymères dérivés de la morpholine et de la thiomorpholine contenant des motifs polymérisables (méth)acrylate/(méth)acrylamide, et leur vaste utilisation en biologie.

Comme le souligne la plupart des articles, l'avantage majeur des polymères à base de la morpholine est lié à une très bonne solubilité dans des conditions physiologiques, ainsi qu'une non-cytotoxicité et une biocompatibilité qui sont comparables et parfois meilleures à celles du PEG.

Néanmoins, très peu des recherches ont été citées dans la littérature concernant les polymères à base de la thiomorpholine. Ces polymères présentent des atomes de soufre qui peuvent être oxydés en groupements sulfoxides. Cette propriété d'oxydation est unique et caractéristique aux polymères contenant de la thiomorpholine, mais elle n'est pas retrouvée dans le cas des polymères ''classiques'' à base de morpholine. Comme certains travaux précédents l'ont évoqué, cette oxydation transforme les polymères de thiomorpholine moins hydrophiles en polymères d'oxyde de thiomorpholine hautement hydrophiles. Donc, en modulant la capacité d'oxydation d'un seul synthon hétérocyclique, des matériaux avec des propriétés hydrophiles modulables peuvent être développés. Cet avantage a été utilisé dans le cas des polyacrylates contenant des fonctions thiomorpholine qui, par oxydation, ont été transformés dans des dérivées sulfoxides qui ont ainsi été utilisés dans des thérapies anticancéreuses.

Pour conclure, cette revue valorise les polymères dérivés de la morpholine et de la thiomorpholine comme des alternatives intelligentes pour la conception de matériaux hydrophiles aux multiples usages en biologie. Le caractère hydrophile modulable des polymères à base de thiomorpholine, ainsi que le nombre assez restreint d'articles sur ces matériaux avec des applications biomédicales, nous a conduit à élaborer nous-même des nouvelles structures de monomères et de polymères contenant cet hétérocycle, comme illustré dans la 2eme partie de ce chapitre.

Introduction Chapitre II : Partie II

Comme illustré dans la partie précédente de ce chapitre, les polymères contenant de la thiomorpholine ou bien thiomorpholine oxide ont été très rarement explorées dans la litérature, jusqu'à présent.

Dans la litérature, il n'y a que le poly(*N*-acryloil thiomorpholine oxide) qui a été étudié dans les sciences biologiques, notamment dans les thérapies anti-cancéreuses. Cependant, aucune étude n'a pas été cité sur la synthèse, les propriétés physico-chimiques ainsi que les propriétes biologiques des polymétacrylates contenant de la thiomorpholine oxide. Or, un changement de l'unité polymérisable (acrylate, métacrylate, acrylamide, etc.) ou bien du linker aliphatique qui rélie l'unité polymérisable à l'héterocycle peut influencer les propriétés physico-chimiques et biologiques de ces polymères.

Notre objectif a donc été de développer un nouveau polymère appartenant à la classe des polymères à base de thiomorpholine oxide, dans le but d'élargir le spectre d'utilisation de ces polymères qui sont uniques dans la littérature et de les valoriser en biologie.

L'article scientifique présenté dans ce chapitre décrit de nouveaux polymères de type polymétacrylate contenant de la thiomorpholine oxide qui sont hydrosolubles à température ambiante, présentant une double sensibilité (LCST et pH) ainsi que des propriétés biocompatibles et hémocompatibles.

Une nouvelle classe de polymères : poly(éthylthiomorpholine oxyde méthacrylate) PTHOXMA, a été synthétisée par polymérisation RAFT. Ces polymères présentent une fonction amine tertiaire protonable qui est sensible aux variations du pH. De plus, des copolymérisations ont été développées avec HEMA (dont la LCST est connue dans la littérature) afin de moduler la LCST des copolymères résultants et de trouver les LCST des nouveaux homopolymères pures PTHOXMA, aux différents pHs (4, 7.4 et 10). Enfin, des tests de cytotoxicité, d'hémolyse et de taux d'agrégation cellulaire ont été réalisés pour évaluer le potentiel des polymères développés pour une utilisation biologique. Ces travaux ont fait l'objet d'un article de recherche qui a été publié dans le journal **Molecules** (**IF : 4.927**), réalisé en collaboration avec le Dr. Johannes Brendel (laboratoire IOMC, Iéna, Allemagne) en particulier pour l'évaluation des propriétés biologiques.

Publication scientifique : Article de recherche numéro 1

Stimuli-responsive thiomorpholine oxide derived polymers with tailored hydrophilicity and hemocompatible properties

Laura Vasilica Arsenie,[1] Franziska Hausig,[2] Carolin Kellner,[2] Johannes Brendel,[2,3] Patrick Lacroix-Desmazes,[1] Vincent Ladmiral,[1,*] Sylvain Catrouillet[1,*]

[1]ICGM, University of Montpellier, CNRS, ENSCM, Montpellier, France

[2]Laboratory of Organic and Macromolecular Chemistry (IOMC), Friedrich Schiller University Jena, Jena, Germany

[3]Jena Center for Soft Matter (JCSM), Friedrich Schiller University Jena, Philosophenweg 7, 07743 Jena, Germany

I. Abstract

Thermo-responsive hydrophilic polymers, including those showing tunable lower critical solution temperature (LCST), represent a continuous subject of exploration for a variety of applications, but particularly in nanomedicine. Since biological pH changes can inform the organism about the presence of disequilibrium or diseases, the development of dual LCST/pH-responsive hydrophilic polymers with biological potential is an attractive subject in polymer science. Here, we present a novel polymer featuring LCST/pH double responsiveness. The monomer ethylthiomorpholine oxide methacrylate (*THOXMA*) can be polymerised *via* the RAFT process to obtain well-defined polymers. Copolymers with hydroxyethyl methacrylate (*HEMA*) were prepared, which allowed the tuning of the LCST behaviour of the polymers. Both, the LCST behaviour and pH responsiveness of hydrophilic *PTHOXMA* were tested by following the evolution of particle size by dynamic light scattering (DLS). In weak and strong alkaline conditions, cloud points ranged between 40–60 °C, while in acidic medium no LCST was found due to the protonation of the amine of the *THOX* moieties. Additional cytotoxicity assays confirmed a high biocompatibility of *PTHOXMA* and haemolysis and aggregation assays proved that the thiomorpholine oxide-derived polymers did not cause aggregation or lysis of red blood cells. These preliminary results bode well for the use of *PTHOXMA* as smart material in biological applications.

II. Graphical Abstract

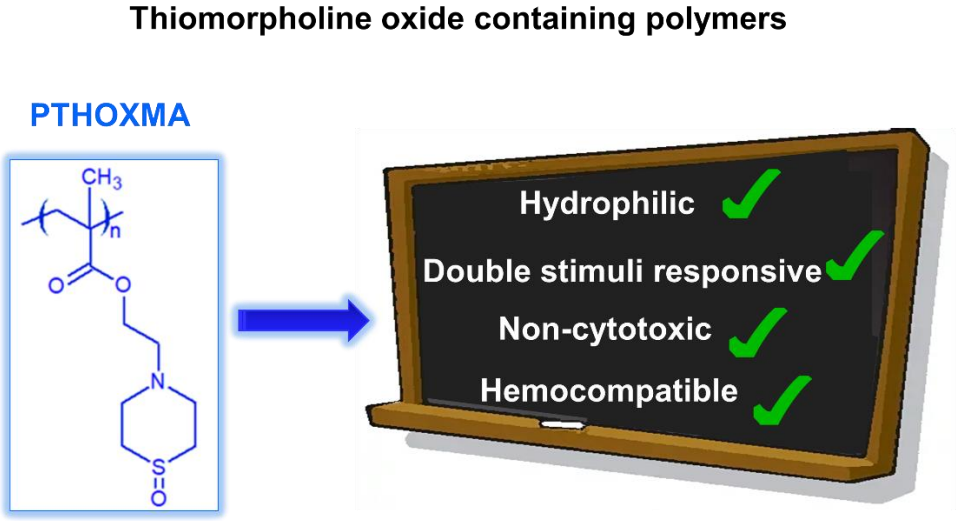

III. Introduction

Smart polymers which react upon external stimuli are attractive materials in bio-medical applications and promise for example the selective release of encapsulated drugs only under specific conditions or in targeted tissue or cells.[1] LCST behaviour is one unique feature polymers may demonstrate, which can be exploited in this regard.[2] Lower critical solution temperature (LCST) in water is an important property for polymers destined to biological applications. Below the LCST, the polymer is soluble due to the H-bonds formed with water molecules.[3] Above the LCST, these H-bonds are disrupted and polymer chain aggregation takes place as a result of non-covalent interactions between hydrophobic moieties of polymer.[4] In addition, above the cloud point, the entropy is a dominating factor which results in the release of water molecules and turns into the collapse and coagulation of the polymer chains. [4]

Biocompatible homopolymers exhibiting an LCST in the physiological relevant range (30–40°C),[5] such as POEGMA (poly(oligoethylene glycol methacrylate)), polyoxazolines or PNIPAM (poly(N-isopropyl acrylamide)) have been thoroughly investigated and tested in biomedical applications.[6–8] In the case of OEGMA, increase in EG units decreases the LCST. For oxazolines, long alkyl chains led to low LCST values. In addition, HEMA is a co-monomer that could be used to tune the LCST of responsive polymers. For example, Zhang *et al.* reported that an increase in the HEMA molar fraction from 1% to 7% in poly(N-isopropyl acrylamide-co-acrylamide–co-hydroxyethyl methacrylate) P(NIPAM-*co*-AM-*co*-HEMA) terpolymers led to an LCST decrease from 68.2 °C to 44.7 °C.[9,10] Similar observations were reported by

Kasprow and collaborators for poly (hydroxyethyl methacrylate-*co*-oligoethylene glycol methacrylate) P(HEMA-*co*-OEGMA) co-polymers.[11] Their research demonstrated that HEMA decreased the LCST of copolymers (from 61.5 °C to 21.5 °C) *via* intermolecular H-bonds, while hydrophilic OEGMA controlled the hydrophilic/hydrophobic balance and increased LCST. Poly (2-(N-(dimethylamino) ethyl methacrylate) (PDMAEMA) is a biocompatible homopolymer which shows dual pH- and thermo-responsivity, which is advantageous in tailoring LCST.[8]

Another important parameter in the development of stimuli-responsive polymers for biomedical applications is the pH. The physiological pH value of blood (for human or animal cells) is 7.4. Changes in this physiological pH are often symptomatic of the presence of infections or cancer.[12] Morpholine-derived polymers contain tertiary amino groups which are protonated in acidic pH (pK_a of morpholine ~ 8.3).[13,14] This property can be used to tailor the behaviour of the polymer in different biological environments. [13,14] Moreover, poly(*N*-acryloylmorpholine) (PNAM) and copolymers of NAM present a high water solubility and biocompatibility and are thus particularly interesting for bio-logical applications.[15] Furthermore, pH-responsive materials with pK_a values ranging between 5 and 7.4 are further interesting candidates for entering the cells and facilitating a pH-induced endosomal escape. [13,16]

Previous studies showed that poly (morpholine ethyl methacrylate) (PMEMA) possesses a pK_a of 4.9 and displays molar mass-dependent LCST at pH 7 and higher.[17,18] PMEMA and PTHOXMA are interesting pH-responsive platforms since their pK_a is below 7.4 and they thus remain neutral at physiological conditions.[8] This property is important since these polymers are possible alternatives to cationic polymers which are currently used in the field of cellular transfection. Indeed, cationic polymers are intrinsically toxic and they have no stealth features since they strongly interact with any cell surface.[19]

Replacing morpholine motif with thiomorpholine could result in new polymer platforms with huge potential as responsive materials. However, the thiomorpholine-containing polymers show a relative low water solubility.[20] Sobotta *et al.* reported that the oxidation of the sulphur atom of thiomorpholine in poly [(*N*-acryloylmorpholine)-*b*-(*N*-acryloylthiomorpholine)] resulted into poly[(*N*-acryloylmorpholine)-*b*-(*N*-acryloylthiomorpholine oxide)] with high water solubility and no cytotoxicity.[20]

To the best of our knowledge, few examples of thiomorpholine oxide-containing polymers have been reported so far, and the dual pH/temperature sensitivities of these polymers have never been explored yet. In this work, a new class of polymers containing thiomorpholine oxide units, named poly (ethylthiomorpholine oxide methacrylate) *PTHOXMA*, was synthesised by

reversible addition−fragmentation chain-transfer (RAFT) polymerisation. This polymer presents protonable tertiary amine functions which are sensitive to pH and sulfoxide groups which confer a strong hydrophilic character. To gain deeper insight into the double LCST/pH responsivity of this new polymer class, the present study also explores how copolymerisation of *THOXMA* with HEMA can be used to modulate the LCST of the resulting copolymers. HEMA was chosen since it is a common co-monomer used to modify the LCST behaviour and because it could easily statistically copolymerise with *THOXMA*. The double LCST/pH responsivity was monitored by DLS at different pHs (4, 7.4 and 10). Cytotoxicity, haemolysis tests and cell aggregation rate assays were performed to evaluate the biocompatibility of *PTHOXMA*.

IV. Experimental section

Materials

Methacryloyl chloride (97% purity) was purchased from Fluka (France) and distilled at 50°C, 400 mbar before use. Hydrochloric acid solution (37% wt), sodium bicarbonate ($NaHCO_3$) and magnesium sulphate ($MgSO_4$) were obtained from Fluka (France). 2-bromoethanol (95% purity) was purchased from Alfa Aesar. Thiomorpholine (98% purity) was acquired from Fluorochem and hydrogen peroxide (H_2O_2) solution (30% wt%) from Carlo Erba. Hydroxyethylmethacrylate (95% purity, HEMA), 4-dimethylaminopyridine (99% purity, DMAP), triethylamine (99% purity, TEA), 2-cyano-2-propyl benzodithioate (CPDB), 2,2′-azobis(2-methylpropionitrile) (AIBN) (recrystallised from methanol at 65°C before use in the polymer synthesis), potassium carbonate (K_2CO_3), disodiumphosphate basic dodecahydrate ($Na_2HPO_4{\cdot}12H_2O$) and deuterated solvents ($CDCl_3$ and DMSO-d_6) were provided by Sigma Aldrich. Sodium chloride (NaCl) and citric acid monohydrate ($C_6H_8O_7{\cdot}H_2O$) were obtained from VWR Chemical. Dimethyl sulfoxide (98% purity, DMSO) was obtained from Acros Organics. Dry solvents (dichloromethane, 95% purity, CH_2Cl_2, and acetonitrile, 99% purity, CH_3CN) were dried on a solvent purification system PureSolv Micro (Sigma Aldrich). The dialysis membranes used for purification of polymers (Spectra/Por 7 Preteated RC Dialysis Tubing, MWCO= 1kDa, diameter 24mm, 4.6 mL/cm) were bought from Krackeler Scientific, USA. 2 mM L-glutamine 100 U/mL penicillin, and 100 µg/mL streptomycin solutions were achieved from Biochrom. 10% fetal calf serum was bought from FCS, Capricorn Scientific. The PrestoBlue solution was obtained from Thermo Fisher, Germany. Sheep blood was provided by the Institute for Experimental Animal Science and Animal Welfare, Jena

University Hospital. Branched poly(ethylene imine) (bPEI) solution was purchased from Polysciences Inc.

Instrumentation

^{1}H-NMR spectra were recorded on NMR Bruker Avance 400-MHz or III HD -400 MHz spectrometers using $CDCl_3$ or DMSO-d_6 as deuterated solvent. The chemical shifts of protons were relative to tetramethylsilane (TMS) at $\delta = 0$.

Size exclusion chromatography (SEC) data were obtained in DMF containing 0.1 wt. % LiCl, with a flow rate of 0.8 mL/ min at 40°C. Sample were filtered using TE36 Whatman PTFE-supported membrane filter paper (0.45 µm, 47 mm diameter) before the injection. The data were calibrated using poly(methyl methacrylate) (PMMA) narrow standards.

Fourier Transform Infrared spectroscopy (FTIR) analysis was achieved with a Perkin Elmer Spectrum 100 spectrometer. The spectral data were acquired in the 3500 -500 cm^{-1} range.

Dynamic light scattering (DLS) analyses were performed on a Malvern Zetasizer NanoZS instrument at a detection angle of 173° (back scattering), in the 10 °C-60 °C temperature range.

The cells incubation for the cytotoxicity tests was performed in a 96 well plate from VWR, Germany. The fluorescence measurements used to determine the cell viability were assessed using an Infinite M200 PRO microplate reader from Tecan, Germany. The haemoglobin release measurements and the cell aggregation rate were performed using a plate reader from Tecan, Männedorf, Switzerland.

Synthesis of 2-bromoethyl methacrylate

2-bromoethyl methacrylate was prepared according to a published procedure.[20] Briefly, to a solution of 4-(dimethylamino)pyridine (DMAP) (103.4 mg, 0.846 mmol, 0.05 eq.) in CH_2Cl_2 (100 mL), 2-bromoethanol (1.2 mL, 17 mmol, 1 eq.) and triethylamine (TEA) (4.7 mL, 34 mmol, 2 eq.) were added under continuous stirring. Then, methacryloyl chloride (1.66 mL, 17 mmol, 1 eq.) was added dropwise in an ice bath and under inert (N_2) atmosphere. The reaction mixture was kept at room temperature and under inert atmosphere overnight. The resulting mixture was washed twice with a saturated $NaHCO_3$ aqueous solution (2 x 100 mL) and then with distilled water (100 mL). The organic layer was collected, dried with $MgSO_4$, filtered and concentrated under vacuum to give a brown oil (3g, yield: 89%).

Synthesis of ethylthiomorpholine methacrylate (THMA)

Anhydrous K_2CO_3 (2.14 g, 15.5 mmol, 1 eq.) was dissolved in dry acetonitrile (100 mL) under stirring for 30 min. Then, thiomorpholine (1.56 mL, 15.5 mmol, 1 eq.) was added and the reaction mixture was stirred for another 30 min. Subsequently, freshly prepared 2-bromoethyl methacrylate (3g, 15.5 mmol, 1 eq.) was added and the reaction mixture was kept under inert atmosphere for 6 days at 40°C using an oil bath. The solvent was then evaporated using a rotary evaporator. Then, dichloromethane was added to the resulting oil and the mixture was washed 6 times with distilled water (6 x 100 mL). The organic phase was collected, dried with $MgSO_4$, filtered and concentrated under vacuum to give a viscous liquid (*THMA*, 2.77 g, yield: 83%). ^{1}H NMR for *ethylthiomorpholine methacrylate* (400 MHz, $CDCl_3$, *Fig. S1*) δ (ppm) = 6.01 (d, C**H**$_2$, noted as **a**); 5.58 (d, C**H**$_2$, noted as **a'**); 1.87 (s, C**H**$_3$, noted as **b**); 4.18 (t, C**H**$_2$CH$_2$**,** noted as **c**); 2.66 (t, C**H**$_2$CH$_2$, noted as **d**); 2.72 (t, C**H**$_2$CH$_2$, cyclic thiomorpholine, noted as **e**); 2.58 (t, C**H**$_2$C**H**$_2$, cyclic thiomorpholine, noted as **f**).

Synthesis of ethylthiomorpholine oxyde methacrylate (THOXMA)

2-thiomorpholine ethyl methacrylate (2.77 g, 12.8 mmol, 1 eq.) was put in a single neck round-bottom flask sealed with a rubber stopper. The flask containing the product was kept in an ice bath and purged with N_2 for 15 min, then a 30% wt% hydrogen peroxide solution (1.44 mL, 14.1 mmol, 1.1 eq.) was slowly added and the reaction mixture was stirred for 24 h. The reaction was then diluted with 50 mL of deionized water. The aqueous solution was washed 3 times with 100 mL of dichloromethane. The organic phase was collected, dried over $MgSO_4$ and then dried under vacuum, resulting in an orange liquid (*THOXMA*, 2.37g, yield: 80%).^{1}H NMR for *ethylthiomorpholine oxide methacrylate* (400 MHz, $CDCl_3$, *Fig. S1*) δ (ppm) = 6.01 (d, C**H**$_2$, noted as **a**); 5.58 (d, C**H**$_2$, noted as **a'**); 1.87 (s, C**H**$_3$, noted as **b**); 4.18 (t, C**H**$_2$CH$_2$, noted as **c**); 3.2 (t, C**H**$_2$CH$_2$, noted as **d**); 2.85 (t, C**H**$_2$CH$_2$, cyclic thiomorpholine, noted as **e**); 2.85 (t, C**H**$_2$CH$_2$, cyclic thiomorpholine, noted as **e**); 2.93 (t, C**H**$_2$CH$_2$, cyclic thiomorpholine, noted as **f**); 2.93 (t, C**H**$_2$CH$_2$, cyclic thiomorpholine, noted as **f**).

Synthesis of poly(ehylthiomorpholine oxide methacrylate) P(THOXMA)$_{100}$ homopolymer and statistical copolymers poly(ethylthiomorpholine oxide methacrylate-stat-hydroxyethylmethacrylate) P(THOXMA$_n$-stat-HEMA$_m$) by RAFT

The general procedure used to prepare *P(THOXMA)$_{100}$* homopolymer was as follows. A 10 mL ampoule was charged with *THOXMA* (2g, 8.65 mmol, 100 eq.), CPDB (19 mg, 0.085 mmol, 1eq.) and AIBN (0.35 mg, 0.002 mmol, 0.25 eq.) and then dissolved in 1.5 mL DMSO. The

mixture was degassed *via* three freeze pump thaw cycles. The ampoule was then filled with nitrogen and immersed in an oil bath at 75°C. Every hour, an aliquot was taken and analysed by ^{1}H NMR and SEC. After 6h (conversion 99.3%) the reaction was stopped by exposure to air. The mixture was dialysed against water (with a 1kDa MWCO membrane) for 2 days, followed by lyophilisation during 1 day. The resulting pink powder (yield: 80%) was analysed by ^{1}H NMR and SEC. ^{1}H NMR (400 MHz, DMSO-d_6, *Fig. 2*) δ (ppm) = 0.94-1,5 (m, C**H**$_3$, polymer backbone, noted as **a**); 1.8 (br s, C**H**$_2$, polymer backbone, noted as **b**); 2.63 (br s, C**H**$_2$-S, noted as **f**); 2.88 (br s, C**H**$_2$-N, noted as **d**); 2.97 (br s, C**H**$_2$-N in the thiomorpholine cycle, noted as **e**); 3.99 (br s, C**H**$_2$-O, noted as **c**).

Following the previous protocol, a range of statistical copolymers of 2-thiomorpholine oxide ethyl methacrylate (*THOXMA*) and 2-hydroxyethyl methacrylate (HEMA) *P(THOXMA$_n$-stat-HEMA$_m$)* were prepared. For example, *P(THOXMA$_{50}$-stat-HEMA$_{50}$)* was prepared as follows. *THOXMA* (2g, 8.65 mmol, 50 eq.), *HEMA* (1.12g, 8.65 mmol, 50 eq.), CPDB (38 mg, 1 eq.), AIBN (7 mg, 0.25 eq.) and 1.5 mL of DMSO were mixed in a 10 mL ampoule. The mixture was degassed *via* three freeze pump thaw cycles, the ampoule was filled with nitrogen and then immersed in an oil bath at 75°C. An aliquot was taken every hour for ^{1}H-NMR and SEC-HPLC analyses. After 4h (conversion above 99 % for both monomers) the reaction was quenched by exposure of the mixture to the air. At the end, the mixture was dialysed against water (with a 1kDa MWCO membrane) for 2 days, followed by lyophilisation during 1 day. The pink polymer (yield: 78%) was analysed by ^{1}H NMR and SEC-HPLC. ^{1}H NMR (400 MHz, DMSO-d_6, *Fig. S5*) δ (ppm) = 0.97-1.6, (m, C**H**$_3$, polymer backbone, noted as **g**); 1.77 (br s, C**H**$_2$, polymer backbone, noted as **h**); 2.6-2.8 (br m, C**H**$_2$-N, noted as **c** and **e**); 2.97 (CH$_2$C**H**$_2$-S, noted as **f**); 3.57 (br s, C**H**$_2$-O, HEMA, noted as **b**); 3.86 (br s, C**H**$_2$-OH, noted as a); 4.01 (br s, C**H**$_2$-O, THOXMA, noted as **d**); 4.85 (br s, -O**H**, noted as **j**); 7.4- 7.9 (m, aromatic protons of CPDB, noted as **i**, **k** and **m**).

The conversions of co-monomers were calculated by ^{1}H NMR (Eq. 1.), *via* the comparison of signal integrals of the CPDB (7.4-7.9 ppm) and of the protons of -C=C- double bond of *THOXMA* (6.06-5.68 ppm) and/or HEMA (6.02-5.74 ppm).

$$\text{Conversion (\%)} = \frac{(I_{0,vinyl\ function}/I_{0,CTA}) - (I_{t,vinyl\ function}/I_{t,CTA})}{(I_{0,vinyl\ function}/I_{0,CTA})} \times 100 \quad \text{(Eq. 1.)}$$

Where $I_{0,CTA}$ and $I_{t,CTA}$ are the values of the integrals of the signal of the aromatic protons of the chain transfer agent CTA (between 7.4 ppm and 7.9 ppm) at t=0 and t respectively;

$I_{0,vinyl\ function}$ and $I_{t,vinyl\ function}$ are the value of the integral of the signal of one of the protons of the vinyl group of methacrylate (5.68 ppm and 6.06 ppm for *THOXMA*, 5.74 ppm and 6.02 ppm for HEMA), at t=0 and t respectively.

The DPs of the polymers were determined by ^{1}H-NMR (Eq. 2.), by comparing the integrals of the signals from the polymethacrylate backbone (δ = 0.51-2.1 ppm) with those of the CPDB (δ = 7.4-7.9 ppm).

$$DP=\frac{\left(I_{polymethacrylate\ backbone}/_5\right)}{\left(I_{CTA}/_5\right)} \quad \text{(Eq. 2.)}$$

Where $I_{polymethacrylate\ backbone}$ is the value of the integral of the signal of the polymethacrylate backbone (between 0.51 ppm and 2.1 ppm), and I_{CTA} is the value of the integral of the signal of the aromatic protons of the chain transfer agent (between 7.4 ppm and 7.9 ppm).

Molecular weight by ^{1}H-NMR (M_n) was calculated by the Equation 3 (Eq. 3.):

$$M_n = \left(DP \times Conv.HEMA \times M_{n,HEMA}\right) + \left(DP \times Conv.THOXMA \times M_{n,THOXMA}\right) + M_{n,chain\ transfer\ agent} \quad \text{(Eq. 3.)}$$

Where $M_{n,chain\ transfer\ agent}$= 221.34 g/mol, $M_{n,HEMA}$ = 130.14 g/mol, $M_{n,THOXMA}$= 231 g/mol. DP (the degree of polymerisation) was calculated by ^{1}H-NMR according to the Equation 2 (Eq. 2.). The conversion of HEMA and *THOXMA* co-monomers (Conv. HEMA, Conv. THOXMA) was calculated by ^{1}H-NMR according to the Equation 1 (Eq. 1.).

Determination of the pK$_a$ of the monomers and polymers

The pK$_a$ of the monomers and corresponding polymers were evaluated by titration with a solution of HCl. Aqueous solutions of *THOXMA* (0.1M) and *PTHOXMA* (0.1M) were titrated with a solution of HCl 0.1M. Each measurement of the pH (at different volumes of HCl added) was carried out in triplicate. The pK$_a$ values were derived from the values of pK$_b$ which were measured at the midpoint of the titration curves. The pK$_a$ was calculated according to the equation (Eq. 4.).

$$pK_a = 14 - pK_b \quad \text{(Eq. 4.)}$$

Additional experiments were performed in an NaCl aqueous solution (0.9% wt%) in order to evaluate the acido-basic properties of PTHOXMA in conditions similar with those of physiological medium.

Evaluation of the LCST of P(THOXMA$_{100}$) and P(THOXMA$_n$-stat-HEMA$_m$) statistical copolymers

DLS measurements were performed at different temperatures ranging between 10°C and 60°C. The temperature corresponding to a sharp increase in the particle size was associated to the LCST of the statistical *P(THOXMA$_n$-stat-HEMA$_m$)* copolymers. The LCST of *P(THOXMA)$_{100}$* was determined by extrapolation (to % HEMA=0) on the plot of the evolution of the LCST value as a function m. For each measurement, solutions of 1 g/L of the corresponding copolymers in three distinct buffers (pH 4, 7.4 and 10) were analysed by DLS. The measurements were done in triplicate.

Cytotoxicity assays

Cytotoxicity studies were performed using the mouse fibroblast cell line L929 (400620, CLS), as recommended by ISO10993-5. L929 cells were routinely cultured in Dulbecco's modified eagle's medium with 2 mM L-glutamine supplemented with 10% fetal calf serum, 100 U/mL penicillin, and 100 μg/mL streptomycin at 37 °C under a humidified 5% (v/v) CO_2 atmosphere. In detail, cells were seeded at 10^3 cells/mL (10^4 cells per well) in a 96 well plate and incubated for 24 h. No cells were seeded in the outer wells. The medium was changed to fresh cell culture medium 1 h prior to treatment. Afterward, the cold polymer solution in 20 mM HEPES (4-(2-hydroxyethyl)-1-piperazineethanesulfonic acid) were added to the cells at the indicated concentrations (from 5 to 700 μg/mL), and the plates were incubated for 24 h. The control cells were incubated with fresh culture medium containing the same amount of HEPES as the treated cells. Subsequently, the medium was replaced by a mixture of a fresh culture medium and the resazurin-based solution PrestoBlue (prepared according to the manufacturer's instructions). After further incubation for 45 min at 37 °C under a humidified 5% (v/v) CO_2 atmosphere, the fluorescence was measured at λ_{ex} = 560 nm/λ_{em} = 590 nm with gain set to optimal, with untreated cells on the same well plate serving as negative controls. The negative control was standardized as 0% of metabolism inhibition and referred to as 100% viability. Cell viability below 70% was considered to be indicative of cytotoxicity. Experiments were conducted in three technical replicates. All experiments were conducted including blanks and negative controls.

Hemolysis tests

The membrane damaging properties of the polymer were quantified by analysing the release of hemoglobin from erythrocytes. Sheep blood was provided by the Institute for Experimental Animal Science and Animal Welfare, Jena University Hospital. Briefly, sheep blood was centrifuged at 4 500g for 5 min. The pellet was washed three times with PBS (pH 7.4) by centrifugation at 4 500g for 5 min. Erythrocytes were suspended in PBS at pH 7.4 to resemble physiological conditions in blood/cytoplasm or in PBS at pH 6 to mimic the slightly acidic environment in the early endosome. The polymer was dissolved in cold 20 mM HEPES (4-(2-hydroxyethyl)-1-piperazineethanesulfonic acid) at a concentration of 7 mg/mL and diluted to 1 mg/mL. Cold polymer solutions of different concentrations in PBS with the respective pH were mixed 1:1 with cold erythrocyte suspensions and were incubated at 37°C for 1 h. Erythrocyte suspensions were centrifuged at 2 400g for 5 min. The release of hemoglobin in the supernatant was determined at 544 nm. The absorbance was measured using a plate reader. Concurrently, determinations were conducted with washed erythrocytes either lysed with 1% Triton X-100 or suspended in PBS at the respective pH as a reference. The hemolytic activity of the polymer was calculated as follows (Eq. 5.):

$$Hemolysis\ \% = \frac{\mathrm{A(sample)-A(PBS)}}{\mathrm{A(Triton\ X-100)}} \qquad \text{(Eq. 5.)}$$

Here, $A_{(sample)}$, $A_{(PBS)}$, and $A_{(Triton\ X\text{-}100)}$ are the absorbance of erythrocytes incubated with a respective sample, suspended in PBS, and erythrocytes lysed with Triton X-100, respectively. The analysis was repeated with blood from three different animals.

Erythrocyte aggregation

To investigate the behaviour of the pH-sensitive polymer towards cellular membranes at different pH values, red blood cells were treated with the polymer under physiological conditions in human blood (pH 7.4) and in slightly acidic environment representing the pH of the early endosome (pH 6). Erythrocyte suspensions in PBS at different pH values were prepared and mixed 1:1 with polymer solutions as described above. After incubation at 37 °C for 2 h, erythrocyte aggregation was measured at 645 nm. As positive and negative assay controls erythrocytes were treated with 50 µg/mL25 kDa branched poly(ethylene imine) (bPEI) solution or PBS buffer at respective pH. The aggregation activity of the polymer at different concentrations is given as an aggregation rate calculated as follows (Eq. 6.):

$$Aggregation\ rate = \frac{1}{\mathrm{A(sample)}} \qquad \text{(Eq. 6.)}$$

Here, $A_{(sample)}$ is the mean absorbance of a given sample.

V. Results and Discussion

V.1. Synthesis of monomers and hydrophobic/hydrophilic polymers

Two new methacrylates derived from thiomorpholine (named *THMA*) or thiomorpholine-oxide (named *THOXMA*) were prepared as presented in the *Fig. 1*. *THMA* was prepared by nucleophilic substitution of 2-bromoethylmethacrylate with thiomorpholine in the presence of K_2CO_3. The one step-reaction afforded *THMA* with a yield of 75% (*Fig. 1.*). The mild oxidation of *THMA* with H_2O_2 (aq., 30%) produced *THOXMA* with a yield of 80% (*Fig. 1.*). Monomers were obtained in sufficient purity without need for elaborate purification methods such as distillation or column chromatography. ^{1}H-NMR analysis confirmed the formation of both pure monomers (*Fig. S1.*). FTIR spectroscopy confirmed the presence of sulfoxide group (S=O) in *THOXMA* and the success of the oxidation reaction (*Fig. S2.*).

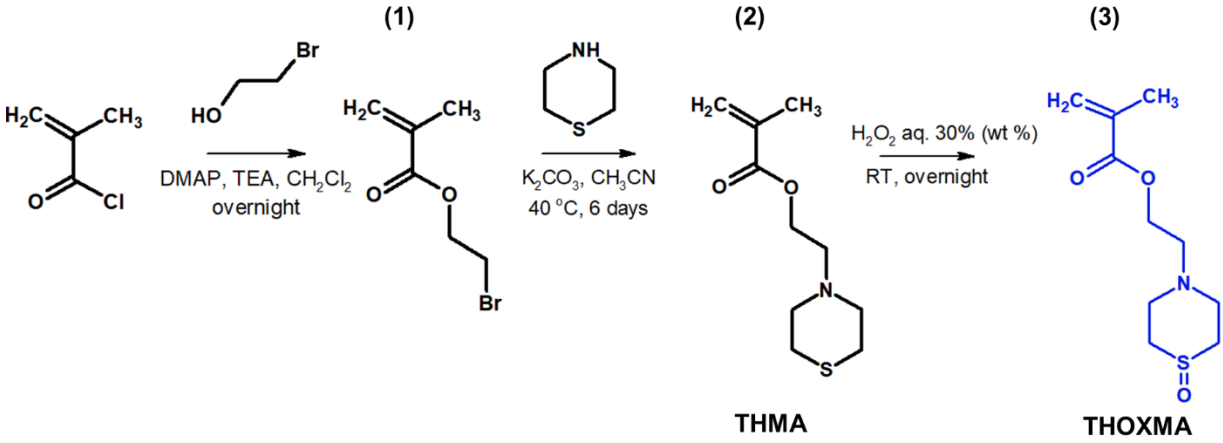

Fig. 1. Synthesis of 2-bromoethylmethacrylate intermediary product (1), the synthesis of ethyl thiomorpholine methacrylate monomer THMA (2) and its oxidation to ethyl thiomorpholine oxide methacrylate monomer THOXMA (3)

Since *THOXMA* is hydrophilic, one of the goals of this work was to study the homo- and co-polymerisation of this monomer, in order to develop new hydrophilic polymers. The RAFT process was used to prepare *P(THOXMA)$_{100}$* homopolymer (*Fig. 2.*), as well as a series of *P(THOXMA$_n$-stat-HEMA$_m$)* statistical copolymers (*Fig. 3.*). All polymerisations were performed in DMSO using CPDB as chain transfer agent, while the pH was maintained at 4 to prevent CPDB degradation *via* hydrolysis. The molar ratios of Monomer(s): CPDB: AIBN was kept at 100: 1: 0.25 in all polymerizations (*Table S1*).

The ^{1}H NMR spectrum of *P(THOXMA)$_{100}$*, a new hydrophilic homopolymer, is shown in *Fig. 2.* High conversion (*i.e.*, 99.3%, by ^{1}H-NMR) of *THOXMA* monomer was achieved after 6h (*Table 1*, *Fig. S3.*). The linear increase of M_n over time (*Fig. 2B.*), the linear 1st order kinetic plot (*Fig. S3.*), as well as the low dispersity (~1.2) indicate that the homopolymerisation was well controlled.

THOXMA was then copolymerised with HEMA by RAFT. The structure and the characterization results of all the (co)polymers are presented in *Fig. 3.* and *Table 1* respectively. Overall, the DPs of the resulting polymers (evaluated by ^{1}H NMR, *Fig. S5.*) were above 80 and were close to the targeted DPs. High conversions (≥ 95% after 4h, *Table 1*, *Fig. S4.*), determined by ^{1}H NMR, were attained for all (co)polymerizations. Again, the linear evolution of $\ln(M_0/M)$ with time (*Fig. S4.*), as well as the low dispersity (remaining relatively constant around 1.2) (*Table 1*) suggested that the polymerisations were controlled.

Table 1: Characterisation data of homopolymers and statistical copolymers prepared by RAFT

Entry	**Conversion of monomers (%)[a]**		**Experimental DP[b]**	**DP_{Target}[c]**	**M_n (g/mol)[d]**	**M_n (g/mol)[e]**	**Dispersity (Đ)[e]**
	THOXMA	**HEMA**					
P(THOXMA$_{100}$)	99.3	-	111	100	25,640	21,570	1.21
P(THOXMA$_{80}$-*stat*-HEMA$_{20}$)	95.6	98.1	80	100	16,900	14,100	1.19
P(THOXMA$_{50}$- *stat*-HEMA$_{50}$)	98	99	82	100	14,970	18,200	1.24
P(THOXMA$_{40}$- *stat*-HEMA$_{60}$)	97	99.5	81	100	14,600	16,100	1.22
P(THOXMA$_{35}$-*stat*-HEMA$_{65}$)	98.5	99.3	80	100	13,000	17,900	1.19
P(THOXMA$_{30}$-*stat*-HEMA$_{70}$)	99	99.2	82	100	13,100	19,110	1.2

[a]Calculated by ^{1}H NMR using Equation 1. [b]Calculated by ^{1}H NMR using Equation 2. [c]Calculated using the following equation DP_{target} = (([HEMA]/[CPDB]) x $Conv_{HEMA}$) + (([THOXMA]/[CPDB]) x $Conv_{THOXMA}$) [d]Calculated by ^{1}H NMR using Equation 3. [e]SEC analysis performed in DMF containing 0.1% LiCl and by using PMMA standards.

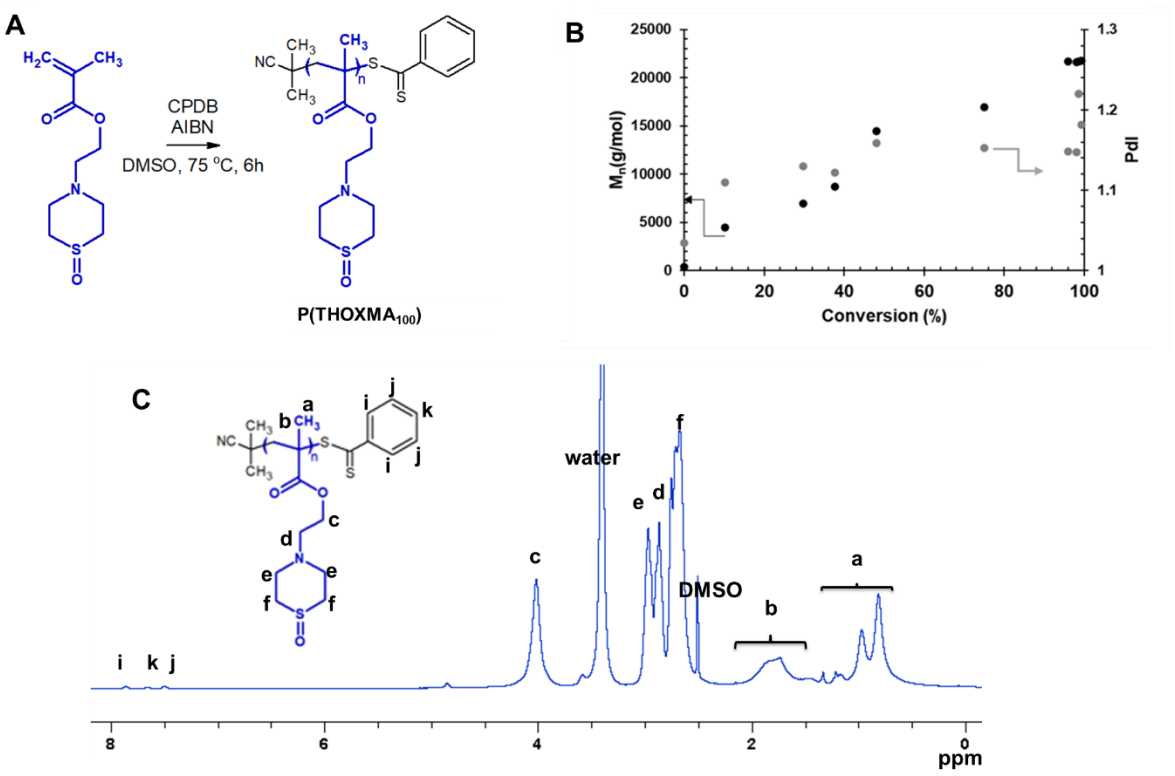

Fig. 2. Synthesis of P(THOXMA$_{100}$)(A);evolution of M_n and dispersity with conversion during the polymerisation of THOXMA (entry 1, Table 1) evaluated by SEC (B); ^{1}H-NMR spectrum of P(THOXMA$_{100}$)in DMSO d6(C).

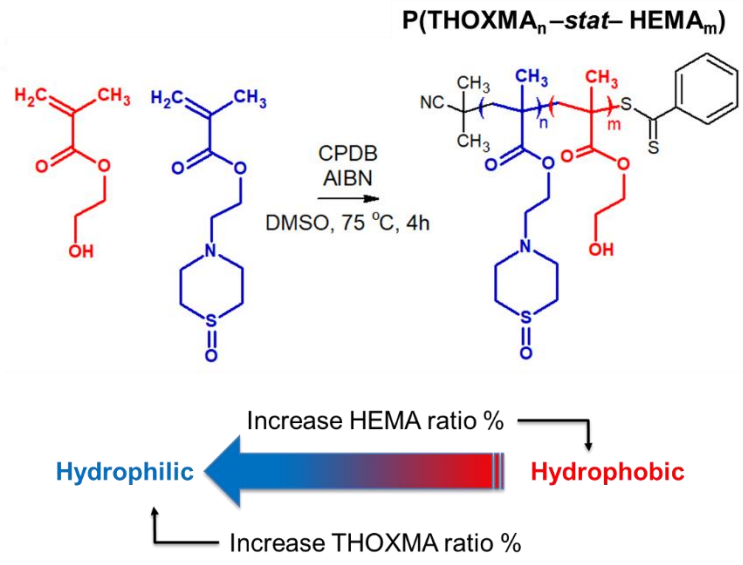

Fig. 3. Structure of statistical copolymers of HEMA and THOXMA

V.2.Acido-basic properties of the THOXMA monomer and PTHOXMA polymer

The acido-basic properties of the monomer and polymer are summarised in *Table S3* and shown in *Fig. S6*. *THOXMA* displayed a pK_a value around 5.42 (*Table S3*). This value corresponds to a slightly acidic character. The pK_a of *PTHOXMA* is around 5.57 (*Table S3*). However, this value is lower than that of polymers presenting a tertiary amine function, such as poly (2-(dimethyl amino)ethyl methacrylate PDMAEMA (pK_a ~ 7.5)[22] and could be explained due to the steric hindrance of the heterocycle which renders the tertiary amine less accessible to protonation by the acid.[23] Hausig *et al.*[13] reported low pK_a values (between 6 and 7.1) for polymers comporting *N*-alkyl-piperazine units. Low pK_a values were also observed for poly(2-methyl-acrylic acid 2-[(2- (dimethylamino)-ethyl)-methyl-amino]-ethyl ester),[24] a polymer used in cellular transfection. The tertiary amine situated in the beta position of the ester function presented a pK_a around 5.[24] In addition, low pK_a values (around 4.9) were reported by Butun *et al.* for poly(morpholine ethyl methacrylate) (PMEMA).[18] According to their study,[18] these unexpectedly low values of pK_a were a consequence of intra-molecular cyclisation (between the amino group of cyclic morpholine and the carbonyl groups of side chains) which decreased the overall basicity of the polymers. The same ring structure likely also explains the low pK_a of *PTHOXMA*. The presence, in *THOXMA*, of a sulfonyl group which is less electron withdrawing than an oxygen atom may explain the higher pK_a of *PTHOXMA* compared to PMEMA.

When the acido-basic properties of *PTHOXMA* were tested in a solution of NaCl (0.9%wt), at a concentration specific to physiological serum, the pK_a values shifted slightly from 5.57 to 5.65 (*Table S3*). This slight increase in the pK_a values in NaCl solution is related to the shielding effect of the salt that minimised the charge repulsion between the protonated amino groups. This result was consistent with previous works reported by Douglas et al.[25] It is important to underline that the pK_a value of *PTHOXMA* around 5.6 is interesting for a potential use in biological applications such as cellular transfection.[26]

V.3.Determination of LCST

LCST was determined using DLS. The cloud point for *PTHOXMA* was barely visible as the upper temperature limit was 60 °C. Therefore, the cloud point temperature of the copolymers with variable composition was used and the LCST was estimated *via* extrapolation to pure *PTHOXMA*. HEMA was chosen because it provides a structural ethyl-methacrylate pattern similar to *THOXMA* and because it is hydrophilic and biocompatible. The statistical *P(THOXMA$_n$-stat-HEMA$_m$)* copolymers were dissolved in a range of aqueous buffers (at pH 4,

7.4 and 10) and the particle size evolution *vs.* temperature was investigated at each pH, in order to determine the LCST of the various copolymers.

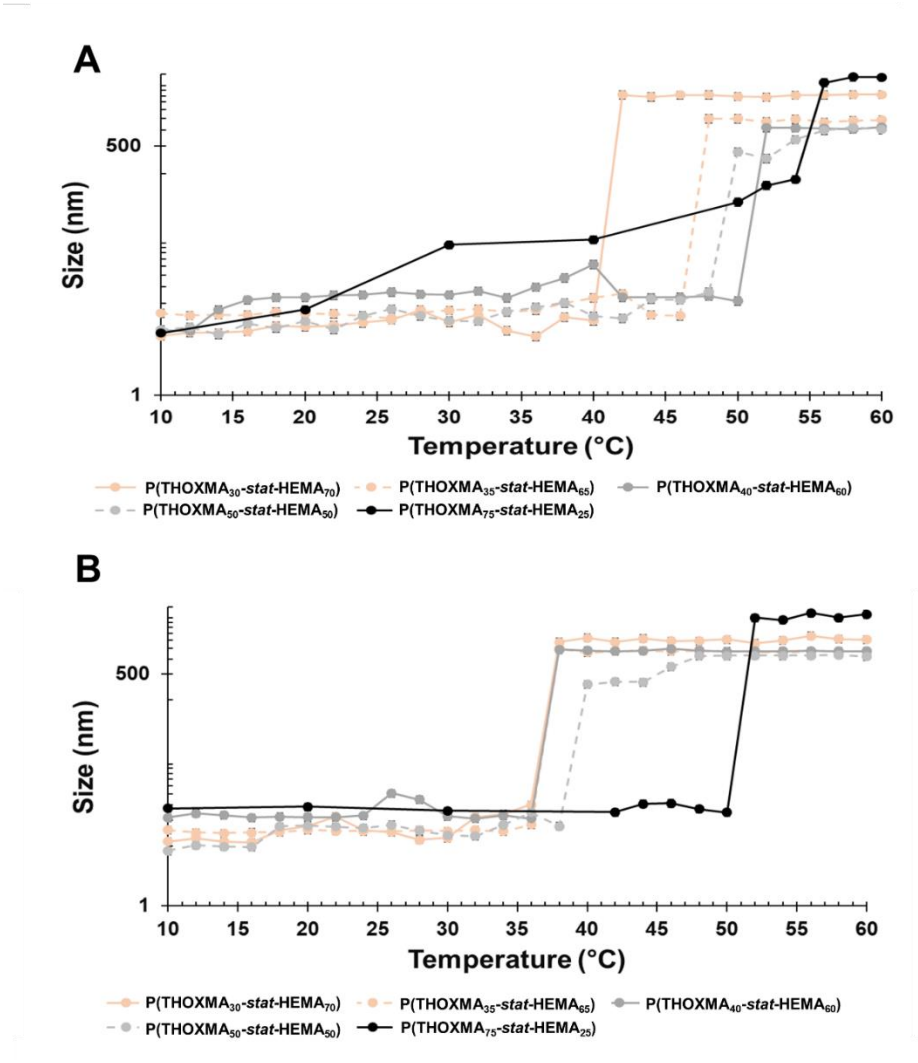

Fig. 4. Particle size variation with the temperature of copolymer formulations (1 g/L) at physiological pH (pH 7.4) (A) and alkaline pH (pH 10) (B)

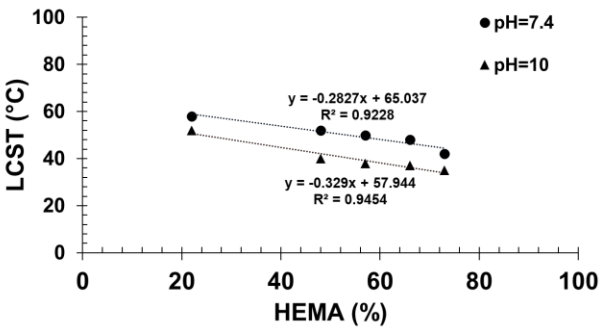

Fig. 5. Determination of the LCST of PTHOXMA at pH 7.4 and pH 10

The particle size variation over temperature at physiological pH (pH 7.4) is presented in *Fig. 4A*. All copolymers showed a sharp increase in the particle size in the temperature range examined (10–60 °C), which was considered the cloud point temperature. As expected, the decrease in the *THOXMA* molar fraction (from 75% to 20%) shifted down the cloud point temperature from 56 °C to 42 °C. The decrease in the cloud point temperature could be explained by the intermolecular H-bonds induced by HEMA.

At pH 10, the polymers had a behaviour close to that of pH 7.4 (*Fig. 4B.*). The polymer cloud point varied from 52 °C (for a content of 75% in *THOXMA*) to 36 °C (for 20% *THOXMA*).

Then, by extrapolation of the cloud point temperatures measured at different contents in HEMA to 0% HEMA, the apparent cloud point temperature of *PTHOXMA* was determined in both physiological and alkaline environments (*Fig. 5.*). At pH 7.4, the cloud point temperature was 65°C, and at pH 10 the cloud point temperature was 57.9 °C.

In comparison, PMEMA of similar DP (around 100) and at a similar concentration (1 w/v %) displayed cloud points around 36 °C at pH 7 and at lower temperatures at higher pH (8 and 10).[18] The differences between *PTHOXMA* and PMEMA are thus subtle. *PTHOXMA* is more water soluble and shows higher cloud points than PMEMA at different pHs. This is likely a consequence of the slightly higher pK_a of *PTHOXMA*.

In contrast, at pH 4, no cloud point was observed for *PTHOXMA* (or for PMEMA). In acid medium the particle size was constant (around 7 nm) over the complete range of temperatures scanned (10–60 °C) and for all copolymer compositions (*Fig. S7.*). This result is a consequence of the complete protonation of polymer chains at such acidic pH, leading to hydrosoluble polymers which were not sensitive to temperature.

V.4. Biocompatibility of PTHOXMA

In biological applications such as cellular transfection, the polymer that complex the genetic material must survive to the endosomal passage (where the pH is ∼5–6) and thus prevent the degradation of the genes. Cationic polymers are currently used for this purpose, but they are toxic and damage the cell surface.[19] Thus, polymers acting as a proton-sponge system are highly required to overcome the endosomal barrier. Proton-sponge polymers are neutral at physiological pH (so before entering the endosome) but become charged in an acid environment (specific to the endosome). As it was presented before, *PTHOXMA* is neutral at physiological conditions, but become charged at a pH around 5.6, so it could emphasise an emerging potential for this application. Herein, the biocompatibility of *PTHOXMA* was assessed, by evaluating *in*

vitro the cytotoxicity and hemocompatibility of this polymer. Copolymers of *THOXMA* and HEMA were not assessed since PHEMA is known to be biocompatible.[27] If both PHEMA and *PTHOXMA* are biocompatible, copolymers of HEMA and *THOXMA* will very likely be biocompatible too.

Firstly, the cytotoxicity of the *PTHOXMA* was studied on the mouse fibroblast cell line L929 using PrestoBlue assay, at pH 7.4 (*Fig. 6A.*). This assay works as a cell health indicator which uses the reducing ability of living cells in order to measure the cellular viability.[28] A cellular viability below 0.7 (or 70%) indicates cytotoxic behaviour.[29] These assays showed that *PTHOXMA* presented no cytotoxicity on L929 cells for concentrations below 400 µg/mL, while the cellular viability was above 0.9 (90%). These promising results further proved the interest to investigate *PTHOXMA* for blood compatibility.

Then, further investigations were conducted to study the red blood cell aggregation activity of *PTHOXMA* in sheep blood (*i.e.*, pH 7.4) and in a slightly acidic environment representing the pH of the early endosome (*i.e.*, pH 6). The results are summarised in *Fig. 6B.*, where the aggregation activity was expressed by the aggregation rate and compared to a polycationic commercial polymer (*i.e.*, polyethyleneimine PEI) which is known for its high aggregation rate.[30] For both pH values tested and all *PTHOXMA* concentrations, an aggregation rate below 1 was observed. These results confirm that *PTHOXMA* did not cause the undesired cell aggregation.

Since *PTHOXMA* did not provoke the aggregation of red blood cells, further attempts were developed in order to investigate if the thiomorpholine oxide-containing homopolymer could damage the red blood cell membrane. To this regard, the release of haemoglobin from the erythrocytes was measured.[29] As evidenced in *Fig. 6C.*, the haemoglobin release was studied in two selected media: at pH 7.4 (to mimic the physiological conditions) and at pH 6 (specific for endosomal escape process which is a reference step in cellular transfection applications). At physiological pH (*i.e.*, pH 7.4.), haemoglobin was released in low amounts (below 1%), without significant influence of the polymer concentration in the blood medium. Haemoglobin release value below 2% is correlated with a non-haemolytic activity,[31] this result thus suggested that the *PTHOXMA* is blood compatible at pH 7.4 for concentrations between 10–100 µg/mL and that it did not damage the plasma membrane of the erythrocytes. In slightly acidic conditions (*i.e.*, pH 6), a concentration-dependent haemoglobin release profile was observed. Particularly, an increase in *PTHOXMA* concentration from 10 µg/mL to 100 µg/mL led to an increase in the haemoglobin percentage from 0.8% to 6%, which indicates a variable haemolytic activity. For

example, at the middle concentration of 50 µg/mL, a haemoglobin release slightly above 2% was detected. At this concentration, *PTHOXMA* was slightly haemolytic, so the blood cells were not significantly damaged. On the contrary, at 100 µg/mL, the *PTHOXMA* is highly haemolytic and it interacts with the cell membrane. Compared to the results obtained at physiological pH, the different hemocompatibility observed at pH 6 is likely a result of partial protonation of the thiomorpholine oxide heterocycles, since this pH is close to the pK_a of *PTHOXMA* (around 5.6). Despite this slight haemolytic activity at high concentrations, the results at pH 6 are very promising for a prospective use of *PTHOXMA* in cellular transfection application, which requires a polymer that promotes the release of active substances from the endosome. Statistical and block copolymers of DMAEMA and MEMA were also shown to be biocompatible and showed interesting results as transfection agents.[17,32] Given its *in-vitro* non-cytotoxicity and hemocompatibility, *PTHOXMA* is also potentially suitable for drug delivery and transfection strategies. Its higher pK_a compared to PMEMA could also be advantageous for drug release approaches. These applications are under investigation in our laboratories and will be reported in due course.

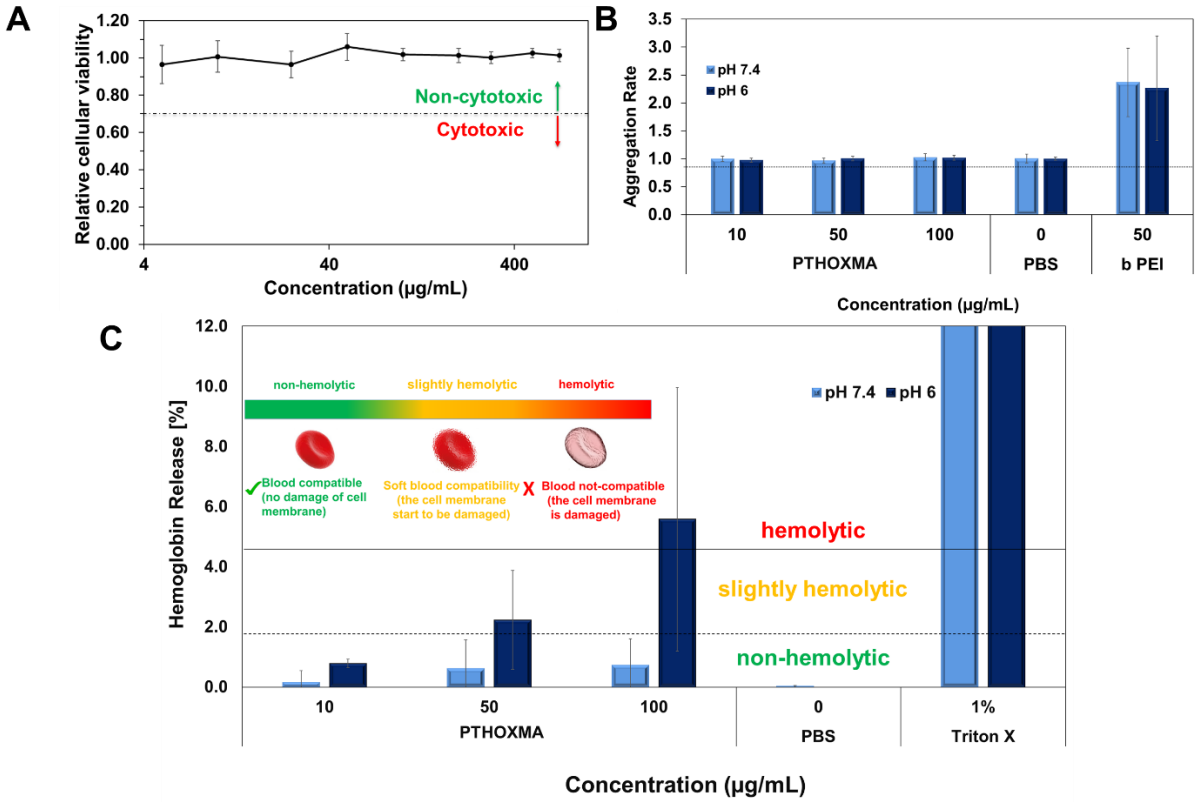

Fig. 6. A: Cellular viability results of PTHOXMA on fibroblast cell line L929 (at pH=7.4); B : Aggregation activity of PTHOXMA polymer ; C: Hemolytic activity of PTHOXMA evaluated by the release of hemoglobin from sheep blood erythrocytes.

VI. Conclusions

New thiomorpholine oxide-containing polymers with tailored LCST at different pHs were developed in order to design stimuli-responsive materials for biological applications. Hydrophilic poly(thiomorpholine oxide ethyl methacrylate) polymers possessed a pK_a around 5.6 which denotes a weak acid character which could be exploited in biological applications such as cellular transfection. Interesting results were obtained concerning the behaviour of hydrosoluble *PTHOXMA* in environments with different pHs. At physiological and alkaline pHs, LCSTs around 65 °C and 56 °C were reported, while in acid conditions the polymer remained hydrophilic. In acid medium, the protonation of the *PTHOXMA* amino groups increased the solubility of the polymer and no aggregation occurred at any temperature. The high LCST values (65 °C in physiological conditions and 56 °C in alkaline conditions) open the gates to explore a large area of applications, such as thermal therapy in biomedicine (or thermal tumour ablation which requires temperatures above 50 °C).[33] Lastly, *PTHOXMA* showed no-cytotoxicity and no haemolytic behaviour, without any cellular aggregation, which proved promising biocompatibility. To conclude, this study highlights the development of non-cytotoxic, blood compatible, pH- and temperature-responsive polymers based on thiomorpholine oxide ethyl methacrylate with tailored LCST, which may find applications in biosciences.

VII. References

1. R. Duncan, M.J. Vicent, *Adv. Drug Deliv. Rev.*, 2013, **65**, 60–70.

2. J. Kost, R. Langer, *Adv. Drug Deliv. Rev.*, 2012, **64**, 327–341.

3. Q. Zhang, C. Weber, U. S. Schubert, R. Hoogenboom, *Materials Horizons*., 2017, **4**, 109–116.

4. G. Pasparakis, C. Tsitsilianis, *Polymers*, 2020, **211**, 123146-123206.

5. M. A. Ward, T. K. Georgiou, *Polymers*, 2011, **3(3)**, 1215–1242.

6. K. Nagase, M. Yamato, H. Kanazawa, T. Okano, *Biomaterials*, 2018, **153**, 27–48.

7. L. Hou, P. Wu, *Soft Matter*, 2014, **10**, 3578–3586.

8. M. T. Cook, P. Haddow, S. B. Kirton, W. J. Mcauley, *Adv. Funct. Mater.*, 2021, **31**, 2008123-2008148.

9. T. M. Quynh, M. Yoneyamab, Y. Maki, T. Dobashi, *J. Appl. Pol. Sci.*, **2011**, *123*, 2368–2376.

10. X. Zhang, L. Zhou, X. Zhang, H. Dai, *J. Appl. Pol. Sci.*, 2009, **116(2)**, 1099-1105.

11. M. Kasprow, *RSC Advances*., 2019, **9**, 40966–40974.

12. G. Hao, Z. P. Xu, Z.P. Li, *RSC Adv.*, 2018, **8**, 22182–22192.
13. F. Hausig, F. H. Sobotta, F. Richter, D. Harz, A.Traeger, J. C.Brendel, *ACS Appl. Mater. Interfaces*, 2021, **13**, 35233–35247.
14. V. Butun, G. Kocak, C. Tuncer, *Polym. Chem.*, 2016, **8**, 144–176.
15. F. Xu, H. Li, Y. L. Luo, W.Tang, *ACS Appl. Mater. Interfaces*, 2017, **9**, 5181–5192.
16. M. Wei, Y. Gao, X. Li, M. J. Serpe, *Polym. Chem.*, 2017, **8**, 127–143.
17. N. Van Overstraeten-Schlogel, Y. H. Shim, V. Tevel, G. Piel, J. Piette, P. Dubois, M. Raes, *Drug Deliv.*, 2012, **19**, 112–122.
18. V. Butun, S. P. Armes, N. C. Billingham, *Polymers*, 2001, **42**, 5993–6008.
19. S. Taranejoo, J. Liu, P. Verma, K. Hourigan, *J. Appl. Polym. Sci.*, 2015, *42096*, 2–9.
20. F. H. Sobotta, F. Hausig, D. O. Harz, S. Hoeppener, U. Schubert, J. C. Brendel, *Polym. Chem.*, 2018, **9**, 1593–1602.
21. Y. Kang, A. Pitto-Barry, M. Rolph, Z. Hua, I. Hands-Portman, N. Kirby, R. O'Reilly, *Polym. Chem.*, 2016, **7**, 2836–2846.
22. O. Samsonova, C. Pfeiffer, M. Hellmund, O. M. Merkel, T. Kissel, *Polymers*, 2011, **3**, 693–718.
23. J. Hu, G. Zhang, Z. Ge, S. Liu, *Prog. Polym. Sci.*, 2014, **39**, 1096–1143.
24. A. M. Funhoff, C. Van Nostrum, G. A. Koning, N. Schuurmans-Nieuwenbroek, D. Crommelin, W. Hennik, *Biomacromol.*, 2004, **5**, 32–39.
25. A. Chremos, J. F. Douglas, *J. Chem. Phys.*, 2018, **149**, 163305–163311.
26. H. Chang, O. Samsonova, S. Kang, Y. Han, *Biomaterials*, 2012, **33**, 1651–1662.
27. M. Zare, A. Bigham, H. Luo, E. R. Ghomi, S. Ramakrishna, *Int. J. Mol. Sci.*, 2021, **22**, 6376–6394.
28. C. E. Vasey, R. Cavanagh, V. Taresco, C. Moloney, S. Smith, R. Rahman, C. Alexander, *Pharmaceutics*, 2021, **13**, 208–225.
29. I. Greco, N. Molchanova, E. Holmedal, H. Jenssen, *Sci. Rep.*, 2020, **10**, 1–13.
30. I. Gonzales-Dominguez, I. Grimaldi, L. Cervera, N. Ventosa, F. Godia, *New Biotechnol.*, 2014, **49**, 88–97.
31. L. Isaacs, D. N. Chin, N. Bowden, Y. Xia, G. M. Whitesides, *Supramol. Mater. Technol.*, 2007, **4**, 1–46.
32. S. Eggers, B. Fischer, V. Abetz, *Macromol. Chem. Phys.*, 2016, **217**, 735–747.
33. A. Reschner, Y-H. Shim, P. Dubois, P. Delvenne, B. Evrard, L. Marcelis, C. Moucheron, A. Kirsch-De Mesmaeker, E. Defrancq, M. Raes, et al. *J. Biomed. Nanotech.*, 2013, **9**, 1432–1440.

VIII. Acknowledgements

This research was funded by DAAD (German Academic Exchange Service) Research Grants-Short Term Grants 2022 (Funding program number: 57588366) as well as by the French Ministry of higher education and research.

IX. Supplementary Information

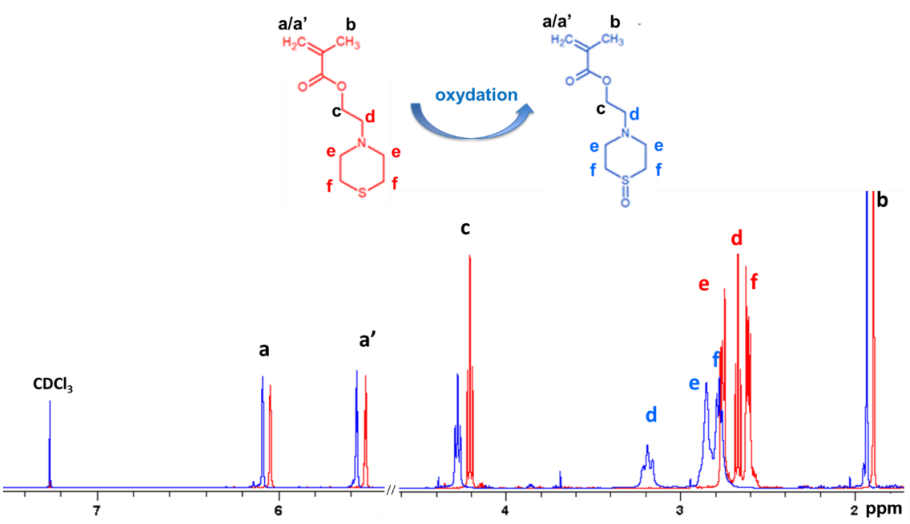

Fig. S1. ^{1}H-NMR spectra in $CDCl_3$ of THMA (red traces) and THOXMA (blue traces)

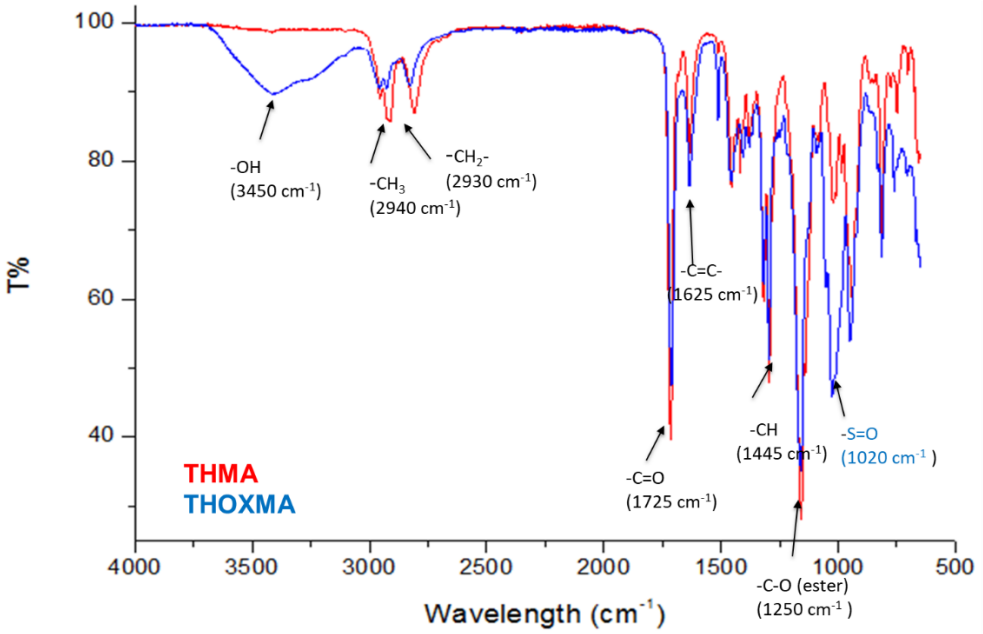

Fig. S2. FTIR characterization of THMA (red traces) and THOXMA (blue traces)

Table S1: Experimental conditions for the synthesis of P(THOXMA)$_{100}$ homopolymer and statistical P(THOXMA$_n$-*stat*-HEMA$_m$) copolymers by RAFT polymerization

Entry	Theoretical degree of polymerization (DP)	Theoretical molar fraction of monomers (%)		Experimental degree of polymerization (DP), determined by ^{1}H-NMR	Experimental molar fraction of monomers (%), determined by ^{1}H-NMR		Reaction yield (%)	[Monomer(s)]/ [CPDB]/[AIBN]	Reaction time (h)
		THOXMA	HEMA		THOXMA	HEMA			
P(THOXMA$_{100}$)	100	100	-	111	100	-	80	100/1/0.25	6
P(THOXMA$_{80}$-*stat*-HEMA$_{20}$)	100	80	20	80	78	22	80	100/1/0.25	4
P(THOXMA$_{50}$-*stat*-HEMA$_{50}$)	100	50	50	82	52	48	78	100/1/0.25	4
P(THOXMA$_{40}$-*stat*-HEMA$_{60}$)	100	40	60	81	43	57	82	100/1/0.25	4
P(THOXMA$_{35}$-*stat*-HEMA$_{65}$)	100	35	65	80	33	66	75	100/1/0.25	4
P(THOXMA$_{30}$-*stat*-HEMA$_{70}$)	100	30	70	82	27	73	83	100/1/0.25	4

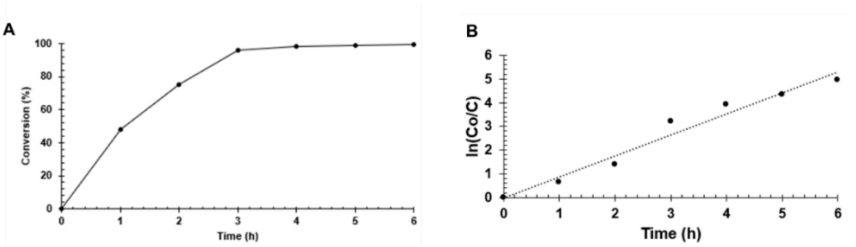

Fig. S3. Evolution of conversion of THOXMA over time for P(THOXMA)$_{100}$ (A), 1st order monomer kinetic plot (B) of RAFT homopolymerization of THOXMA

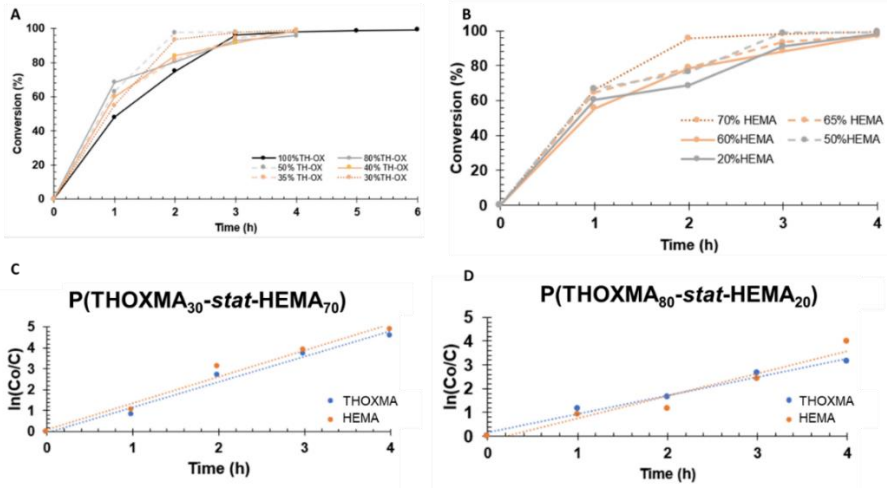

Fig. S4. Conversion of THOXMA (A) and HEMA (B) co-monomers used to prepare P(THOXMA$_n$-stat-HEMA$_m$) copolymers; First order monomers kinetic plot for RAFT statistical copolymerizations of THOXMA and HEMA (C, D).

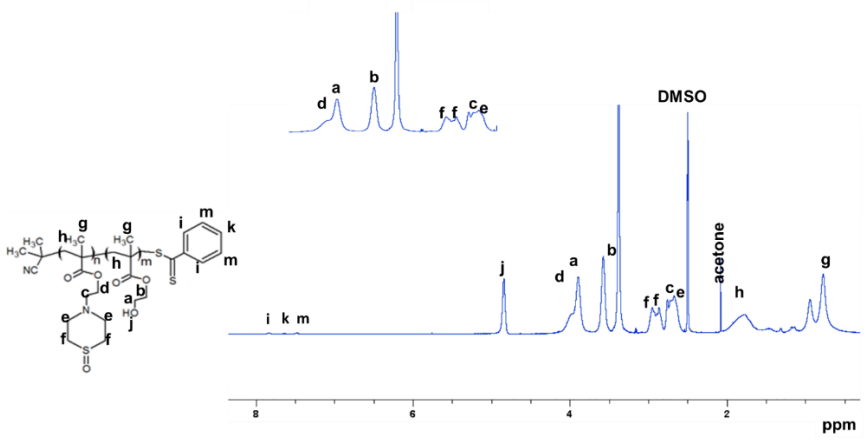

Fig. S5. ^{1}H-NMR spectrum in DMSO-d6 of P(THOXMA$_{70}$-stat-HEMA$_{30}$) copolymer prepared by RAFT polymerization

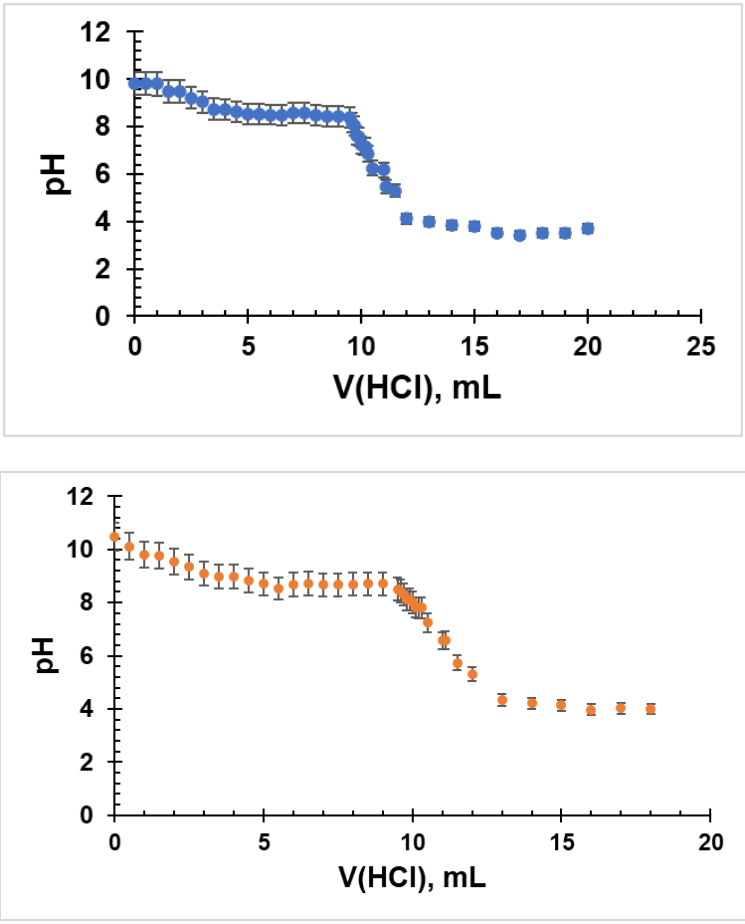

Fig. S6. Titration curve of PTHOXMA (blue) and THOXMA (orange).

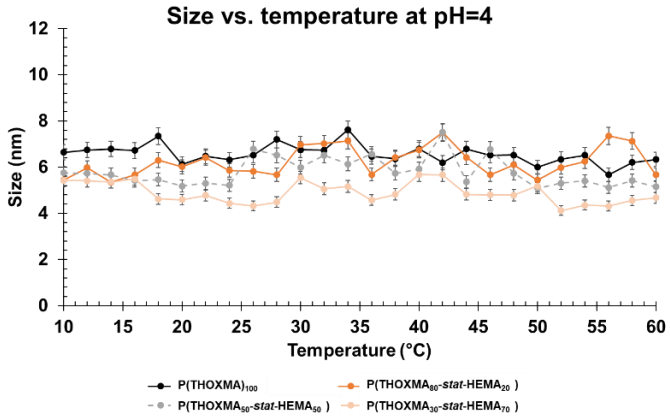

Fig. S7. Size evolution vs. temperature at pH 4, determined by dynamic light scattering.

Table S2: LCST values of THOXMA containing copolymers evaluated at pH 7.4 and pH 10

Entry	LCST (°C, at pH 7.4)	LCST (°C, at pH 10)
P(THOXMA$_{30}$-*stat*-HEMA$_{70}$)	42.0	36.0
P(THOXMA$_{35}$-*stat*-HEMA$_{65}$)	47.1	37.0
P(THOXMA$_{40}$-*stat*-HEMA$_{60}$)	49.5	37.2
P(THOXMA$_{50}$-*stat*-HEMA$_{50}$)	52.0	39.5
P(THOXMA$_{75}$-*stat*-HEMA$_{35}$)	56.0	52.0

Table S3. pK_a values of monomer and corresponding polymer in water and 0.9% (wt%) NaCl solution

Entry	pK_a
THOXMA	5.42
PTHOXMA	5.57
PTHOXMA in NaCl	5.65

Conclusion Chapitre II : Partie II

Dans cette partie, de nouveaux polymères de type polyméthacrylates contenant des fonctions thiomorpholine oxydé ont été développés. Ils représentent une alternative originale pour obtenir des matériaux hydrophiles, biocompatibles et hémocompatibles.

Les polymères de type poly(thiomorpholine oxide éthyl méthacrylate) *PTHOXMA* ont un pK_a autour de 5.6 qui dénote un caractère d'acide faible qui pourrait être exploité dans des applications biologiques telles que la transfection cellulaire. Les dérivés *PTHOXMA* présentent une LCST modulable en fonction du pH, qui varie entre 65°C (à pH 7.4) et 56°C (à pH 10). A l'inverse, à pH 4, la protonation des groupes amine du *PTHOXMA* a augmenté la solubilité du polymère et l'agrégation des chaines polymères n'a pas eu lieu, donc aucune LCST n'a pu être déterminé. Ces valeurs de LCST supérieures à 50°C sont favorables car ils signifient qu'à pH et température physiologique le polymère ne forme pas d'agrégats, phénomène qui peut empêcher certaines applications biomédicales.

Enfin, l'évaluation *in-vitro* de PTHOXMA a montré des résultats très prometteurs. Les essais réalisés sur des cellules L929 ont révélé que ce polymère est non-cytotoxique, tandis que les tests réalisés sur des échantillons de sang d'origine animale ont conclus que *PTHOXMA* est hémocompatible et n'endommage pas la membrane des globules rouges à pH physiologique.

Globalement, ces résultats nous ont conduit à choisir d'incorporer le monomère hydrophile de type méthacrylate-thiomorpholine oxide dans le développement de copolymères contenant des bases nucléiques, dans le but d'obtenir des macromolécules solubles dans l'eau et à pH physiologique. C'est le sujet du chapitre suivant.

Chapitre III : Développement de co-assemblages à pH physiologique à partir de copolymères hydrosolubles contenant des nucléobases : propriétes physico-chimiques et application biologique

Chapitre III : Développement de co-assemblages à pH physiologique à partir de copolymères hydrosolubles contenant des nucléobases : propriétes physico-chimiques et application biologique

Introduction Chapitre III

Les exemples de copolymères comportant des bases nucléiques sont assez rares. Une partie de ces polymères ont été synthétisées par post-fonctionnalisation de polymères commerciaux avec des nucléobases. Cependant, cette méthode a conduit à un faible taux de fonctionnalisation. Au contraire, la polymérisation RAFT de monomères de nucléobases a apporté de nombreux avantages car elle permet de synthétiser, de manière contrôlée, des polymères incorporant une haute densité de nucléobases capables de former des architectures auto-assemblées bien définies. Différentes architectures auto-assemblées avec des morphologies différentes (sphères, vésicules, cylindres) ont été observées lors des travaux pionniers du groupe du Professeur O'Reilly.

Néanmoins, un inconvénient des polymères contenant des nucléobases est qu'ils sont insolubles dans l'eau. La majorité des autoassemblages formées par ces polymères sont préparées en solvants organiques (DMF, DMSO). Il existe cependant quelques exemples (dans le cas de structures de type polyacrylamide) qui sont obtenues dans des mélanges solvant organique/eau. Ces architectures sont globalement dirigées par les interactions hydrophobes. De plus, l'influence des liaisons d'hydrogène entre les nucléobases complémentaires sur la formation des autoassemblage n'a pas été étudiée.

Dans ce chapitre, notre objectif est de répondre aux problématiques des copolymères de nucléobases et de leurs autoassemblages : l'insolubilité dans l'eau, le peu d'information sur l'influence des liaisons hydrogène dans le processus d'autoassemblages, ainsi que leur biocompatibilité (notamment la cytotoxicité et l'hémocompatibilité).

Pour ceci, nous avons développé des copolymères solubles à pH physiologique, dans l'intérêt d'ouvrir un grand nombre d'applications biologiques pour ces polymères à bases azotées. L'approche utilisée pour atteindre ces objectifs a été donc de copolymériser par RAFT des co-monomères hydrophobes contenant des nucléobases (adénine ou uracile) avec des co-

monomères hydrophiles contenant des fonctions thiomorpholine-oxide, qui ont été présentés dans le chapitre précédent.

Notre étude s'est ensuite concentrée sur la caractérisation des co-assemblages (par SLS, DLS, TEM) formées à pH physiologique à partir de ces copolymères. Différents paramètres ont été étudiés : la longueur de chaine, le ratio des co-monomères, le type et le nombre des fonctions nucléobases, le ratio entre les nucléobases complémentaires. De plus, le rôle primordial des liaisons hydrogène sur la formation des autoassemblages a été mis en évidence par l'ajout de molécules compétitrices des liaisons hydrogène (suivies par SLS/DLS). Enfin, ce chapitre ouvre des perspectives encourageantes pour une future application biologique de ces polymères, en étudiant leur cytotoxicité et leur hémocompatibilité *in-vitro*.

Les résultats inclus dans ce chapitre ont fait l'objet d'un second article de recherche réalisé en collaboration avec le laboratoire IOMC (Iéna, Allemagne), pour l'élaboration des essais biologiques. Cet article a été publié dans le journal **Polymer Chemistry** (**IF : 5.582**).

Publication scientifique : Article de recherche numéro 2

Supramolecular co-assembly of water soluble nucleobase-containing copolymers: bioinspired synthetic platforms towards new biomimetic materials

Laura Vasilica Arsenie,[1] Mona Semsarilar,[2] Johannes C. Brendel, [3] Patrick Lacroix-Desmazes,[1] Vincent Ladmiral,[1] and Sylvain Catrouillet [1]

[1]ICGM, University of Montpellier, CNRS, ENSCM, Montpellier, France

[2]IEM, University of Montpellier, CNRS, ENSCM, Montpellier, France

[3]IOMC, Friedrich-Schiller University of Jena, 07743 Jena, Germany

I. Graphical abstract

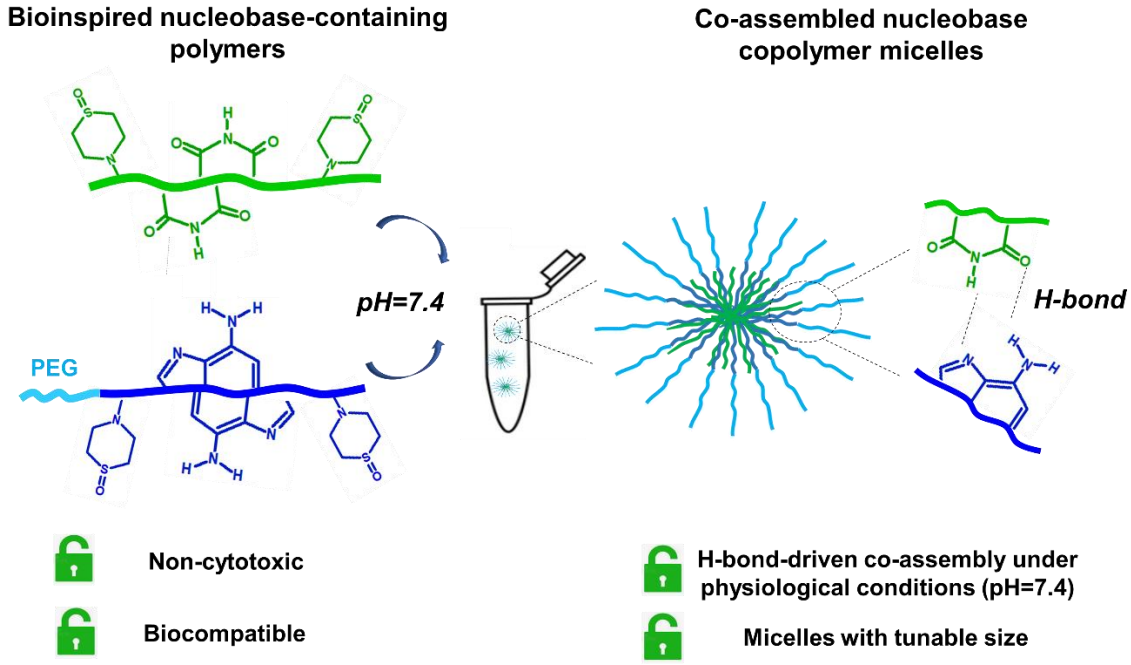

II. Abstract

This study presents the development of co-assembled copolymer architectures at physiological pH (pH 7.4) formed *via* H-bonds between complementary nucleobase-containing copolymers. Well-defined hydrophilic copolymers were synthesised by RAFT polymerisation: statistical uracil- and thiomorpholine oxide-containing copolymers P(UrMA$_n$-*stat*-THOXMA$_m$) as well as diblock copolymers PEG$_{112}$-*b*-P(AdMA$_n$-*stat*-THOXMA$_m$) composed of a PEG block and a second block of a copolymer of adenine- and thiomorpholine oxide-derived methacrylates. Binary mixtures of the resulting copolymers formed co-assembled nanoobjects in aqueous

solution as a result of the H-bonds established between nucleobases. The influences of the polymer architecture (degree of polymerisation, co-monomer composition, length of the nucleobase-containing block), the ratio between complementary nucleobases, and the impact of H-bond competitors on the self-assembly properties were investigated. Light scattering techniques (SLS, DLS) and transmission electron microscopy (TEM) were used to characterise the co-assembled objects. This study demonstrates that the size of the resulting co-assemblies was mainly governed by the type and content of nucleobases, and by the length of the nucleobase block. Moreover, the *in-vitro* evaluation of the nucleobase-containing polymers revealed that they were non-cytotoxic and hemocompatible. This study increases the understanding of nucleobase pairing in artificial copolymer architectures which are potential platforms for further use in biosciences.

III. Introduction

The structures of deoxyribonucleic acid (DNA) and ribonucleic acid (RNA) originate from self-assembly *via* H-bonds between complementary nucleobases such as adenine–thymine (in DNA) or adenine–uracil (in RNA).[1] In the case of DNA, the complementary nucleobases match perfectly to pack in a double helix structure.[1] RNA only has one strand, but could sometimes form secondary double helix structures as well.[1] While the self-assembly *via* nucleobase pairing is well known in the cases of DNA and RNA, it has been barely explored in the case of synthetic copolymers containing nucleobases. Interesting attempts in this context were reported in the field of peptide nucleic acids (PNAs).[2] The structure of PNAs consists of peptide-like backbones derived from 2-aminoethylglycine containing sequences of nucleobases able to form various supramolecular architectures with helicoidal morphologies mimicking the DNA. Numerous nucleobase-containing polymers reported so far were prepared by post-functionalisation of synthetic polymers such as PEG (polyethylene glycol), PCL (polyε −caprolactone) or PPG (polypropylene glycol).[3–5] However, reaching high degrees of functionalization which would induce enhanced cooperativity by multiple H-bonds remains challenging. A solution is to polymerize vinyl monomers bearing nucleobases. This strategy was implemented to prepare nucleobase-containing copolymers by Ring-Opening Metathesis Polymerisation (ROMP)[6,7] or Atom Transfer Radical Polymerisation (ATRP).[8] Reversible addition fragmentation chain transfer (RAFT) polymerisation is arguably one of the most versatile polymerization techniques and it has been applied advantageously to prepare polymers incorporating a high density of nucleobases able to form well-defined self-assembled

architectures.[9–14] The use of RAFT allows the preparation of polymers with controlled molar masses, contents of nucleobases, architectures and chain-end functionality.[15] Interactions between complementary nucleobase-containing polymers made by RAFT polymerisation led to a variety of self-assembled architectures with tailored morphologies (spheres, vesicles, cylinders).[9–14,16] Nevertheless, the hydrophobicity of the nucleobase moiety required the use of an organic solvent (DMF, DMSO, dioxane or chloroform) for the formation of self-assembled objects.[9–14,16,17] For example, Kang *et al.* (2015)[9] studied the self-assembly of poly(2-(2-(thymine-1-yl)acetoxyl)ethyl methacrylate)-*b*-poly(methyl methacrylate) diblock copolymers in different mixtures of $CHCl_3$/dioxane and reported various morphological transitions, from long flexible cylinders (at 50% vol. $CHCl_3$) to short worm-like structures (at 12.5% vol. $CHCl_3$). A few studies have reported the formation of self-assembled objects based on nucleobase polymers in an organic solvent/ water mixture, using the solvent switch method.[10,14,16,17] Representative examples by Hua *et al.* illustrated various morphological shapes such as spheres or cylinders obtained in DMF/water, by using block copolymers consisting of a hydrophilic poly(4-acryloyl morpholine) (PNAM) block and a hydrophobic poly(adenine propyl acrylamide) (PAAm) block.[10] Therein, the self-assembly was mainly driven (in terms of size and morphologies) by hydrophobic interactions caused by the adenine heterocycle. Only a few examples of systems that form stacks of multiple supramolecular units (such as urea-containing toluidine heterocycles, peptides and nucleobases) are suitable to self-assemble in water. Their self-assembly is driven by both hydrogen bonds and hydrophobic interactions and is therefore rarely at the thermodynamic equilibrium in water.[18–20] The hydrophobic interactions introduce a new parameter influencing the self-assembly that was poorly studied experimentally due to the synthetic difficulty of modulating the self-assembling moiety.[21] The present study targets this problem and deals with hydrophilic nucleobase-containing copolymers able to co-assemble under physiological conditions. Polymethacrylate copolymers containing nucleobase (adenine or uracil) and hydrophilic thiomorpholine oxide were synthesized using the RAFT process. Various macromolecular structures were finely tailored in terms of degrees of polymerisation and contents of nucleobases. A binary mixture of uracil- and adenine-containing copolymers led to a wide range of co-assembled structures in water at physiological pH (pH 7.4). In contrast to previously described systems, H-bonds between complementary nucleobases rather than hydrophobic interactions were the main driving force of the assemblies. The influences of the number of nucleobases, the ratios between complementary nucleobases and the polymer architecture on the co-assembly were studied by SLS, DLS and TEM. In addition, *in vitro*

investigations (cytotoxicity and compatibility assays on red blood cells) were carried out to test the potential of these nucleobase-containing copolymers for future biological applications.

IV. Experimental

Materials

Methacryloyl chloride (97% purity) was acquired from Fluka (Switzerland) and distilled (50°C, 400 mbar) before use. 2-bromoethanol (95% purity), adenine (Ad, 99% purity) and uracil (Ur, 98% purity) were purchased from Alfa Aesar (Germany). Thiomorpholine (98% purity) and 3-bromo-1-propanol (97% purity) were bought from Fluorochem (UK). Hydrogen peroxide (H_2O_2) solution (30 wt%) was received from Carlo Erba (France). 4-dimethylaminopyridine (DMAP, 96% purity), triethylamine (TEA, 99% purity), 2-cyano-2-propyl benzodithioate (CTA, 97% purity), poly(ethylene glycol) methyl ether (4-cyano-4-pentanoate dodecyl trithiocarbonate) (macro-CTA), disodiumphosphate basic dodecahydrate ($Na_2HPO_4 \cdot 12H_2O$, 95% purity), potassium carbonate (K_2CO_3, 99.9% purity), sodium hydride (NaH, 90% purity) and deuterated solvents (deuterated chloroform, $CDCl_3$, and hexadeuterodimethyl sulfoxide, DMSO-d_6) were provided by Sigma Aldrich. 2,2′-azobis(2-methylpropionitrile) (AIBN, 98% purity) was acquired from Sigma Aldrich (Germany) and recrystallised from methanol at 65°C before use. Sodium chloride (NaCl) and citric acid monohydrate ($C_6H_8O_7$ H_2O, 99% purity) were obtained from VWR Chemical. Sodium bicarbonate ($NaHCO_3$, 95% purity) was purchased from Fluka (France). Dimethylformamide (DMF, 99.8% purity) was acquired from Fisher Scientific (Belgium). HEPES (4-(2-hydroxyethyl)-1-piperazineethanesulfonic acid) buffered saline solution (30 mM) was acquired from PromoCell (Germany). Dry solvents (dichloromethane, CH_2Cl_2, and acetonitrile, CH_3CN) were purified using a PureSolv Micro solvent purification system purchased from Sigma Aldrich (USA). The dialysis membranes used for purification of polymers (Spectra/Por 7 Pretreated RC Dialysis Tubing, MWCO= 1kDa, diameter 24mm, 4.6 mL/cm) were bought from Krackeler Scientific, USA. 2 mM L-glutamine 100 U/mL penicillin, and 100 µg/mL streptomycin solutions were acquired from Biochrom. 10% fetal calf serum was obtained from FCS, Capricorn Scientific. PrestoBlue solution was acquired from Thermo Fisher, Germany. Human blood was provided by the Department of Transfusion Medicine from Jena University Hospital (Germany). Branched poly(ethylene imine) (bPEI) solution was purchased from Polysciences Inc.

Instrumentation

^{1}H NMR spectra were recorded on NMR Bruker Avance 400-MHz or RMN Bruker Avance III HD -400 MHz spectrometer using $CDCl_3$ or DMSO-d_6 as deuterated solvent. The chemical shifts of protons were relative to tetramethylsilane (TMS) at $\delta = 0$.

Size exclusion chromatography (SEC) was performed in DMF containing 0.1 wt. % LiCl, with a flow rate of 0.8 mL min^{-1} at 40°C. Sample were filtered using TE36 Whatman PTFE-supported membrane filter paper (0.45 µm, 47 mm diameter) before the injection. The data were calibrated using polymethyl methacrylate (PMMA) standards.

Dn/dc values in water were determined using a differential refractometer and were estimated from the integrated refractive index (RI)-signal knowing the polymer concentration. The light scattering measurements were performed using a LS spectrometer (from LS Instruments, Switzerland) incorporating a goniometer based multi-angle static light scattering (SLS) and dynamic light scattering (DLS) instrument. Transmission electron microscopy (TEM) assays were conducted on JEOL 1200 EXII-120 kV instrument.

L929 cells used for cytotoxicity tests were incubated by using 96 well plate from VWR, Germany. The fluorescence measurements used to determine the cell viability were assessed using an Infinite M200 PRO microplate reader from Tecan, Germany. The haemoglobin release measurements and the cell aggregation rate were performed using a plate reader from Tecan, Männedorf, Switzerland.

Methods

Synthesis of 3-bromopropyl methacrylate and 2-bromoethyl methacrylate

To a solution of 4-(dimethylamino)pyridine (DMAP) (162.4 mg, 0.05 eq., 16.8 mmol) in CH_2Cl_2 (100 mL), 3-bromopropanol (2.4 mL, 1 eq., 26.54 mmol) and triethylamine (TEA) (7.4 mL, 2 eq., 53.2 mmol) were added under continuous stirring. Then, methacryloyl chloride (2.6 mL, 1 eq., 26.54 mmol) was added dropwise in an ice bath and under inert (N_2) atmosphere. The reaction mixture was kept at room temperature and under inert atmosphere for 5h. The resulting mixture was washed twice with a saturated $NaHCO_3$ aqueous solution (2 x 100 mL) and then with distilled water (100 mL). The organic layer was collected, dried over magnesium sulfate and concentrated under vacuum to give a yellow oil (5 g, yield: 91%). 2-bromoethyl methacrylate was obtained by a similar procedure as 3-bromopropyl methacrylate, following a published protocol.[22]

Synthesis of 2-ethyl thiomorpholine oxide methacrylate (THOXMA)

2-ethyl thiomorpholine oxide methacrylate was synthesized by oxydation of 2-ethyl thiomorpholine methacrylate, following a previously published procedure.[23]

Synthesis of 3-(adenin-9-yl)propyl methacrylate (AdMA)

Adenine (1.5g, 1 eq., 11.1 mmol) was dissolved in anhydrous DMF (100 mL) in a two-neck round-bottom flask and stirred for 1h under inert atmosphere at room temperature. Then, NaH (0.296g, 1 eq., 11.1 mmol) was gently added and the mixture was kept under continuous stirring at room temperature for 30 min. Subsequently, the freshly obtained 3-bromopropyl methacrylate (2.29g, 1 eq., 11.1 mmol) was added and the flask containing the reaction mixture was immersed in an oil bath at 40°C for 10 days. Then, the inorganic salts resulting from the reaction were removed by filtration. The resulting yellow filtrate was cryo-distilled to evaporate the organic solvent. A viscous yellow residue was formed after the cryo-distillation. Anhydrous dichloromethane (100 mL) was added to the residue, and the resulting mixture was vigorously stirred for 30 min. Then, the mixture was filtrated under vacuum and the filtrate was collected, dried with anhydrous magnesium sulphate and concentrated under vacuum to give a viscous yellow liquid (2g, global yield: 68%). ^{1}H NMR, *Fig. S1* (400 MHz, DMSO-d_6) δ (ppm) = 5.9 (d, C**H**$_2$, noted as **a**); 5.58 (d, C**H**$_2$, noted as **a'**); 1.87 (s, C**H**$_3$, noted as **b**); 4.27 (t, OC**H**$_2$CH$_2$, noted as **c**); 2.20 (m, CH$_2$C**H**$_2$CH$_2$, noted as **d**); 4.10 (t, NC**H**$_2$CH$_2$, noted as **e**); 7.26 (s, N**H**$_2$, adenine heterocycle, noted as **g**); 8.15 (s, N=C**H**-N, adenine heterocycle, noted as **h**); 8.13 (s, N=C**H**-N, adenine heterocycle, noted as **i**).

Synthesis of 3-(uracil-1-yl)propyl methacrylate (UrMA)

Uracil (1.5g, 1 eq., 13.38 mmol) and anhydrous potassium carbonate (1.84g, 1 eq., 13.38 mmol) was dissolved in anhydrous DMF (100 mL) in a two-neck round-bottom flask and stirred for 1h under inert atmosphere at room temperature. Then, 3-bromopropyl methacrylate (2.77g, 1 eq., 13.38 mmol) was gently added using a syringe and the mixture was gently stirred at room temperature for 10 days. The mixture was filtrated under vacuum and the filtrate was cryo-distilled to remove the organic solvent. After this step, dichloromethane (100 mL) was added and the resulting reaction mixture was stirred for another 15 min. Then, the mixture was filtrated under vacuum to remove the inorganic salts. The filtrate was dried with anhydrous magnesium sulphate and then concentrated under vacuum, leading to a viscous pale yellow liquid (2g, global yield: 63%).^{1}H NMR, *Fig. S2* (400 MHz, DMSO-d_6) δ (ppm) = 6.01 (d, C**H**$_2$, noted as **a**); 5.58 (d, C**H**$_2$, noted as **a'**); 1.87 (s, C**H**$_3$, noted as **b**); 4.11 (t, C**H**$_2$CH$_2$, noted as **e**); 1.96 (m,

$CH_2C\mathbf{H}_2CH_2$, noted as **d**); 3.79 (t, $C\mathbf{H}_2CH_2$, noted as **c**); 7.62 (d, C**H**=CH, uracil heterocycle, noted as **g**); 5.53 (d, CH=C**H**, uracil heterocycle, noted as **f**); 11.5 (s, N**H**, uracil heterocycle, noted as **h**).

Synthesis of Poly((3-(uracil-1-yl) propyl methacrylate) -stat-(2-ethyl thiomorpholine oxide methacrylate)) P(UrMA$_n$ -stat-THOXMA$_m$) by RAFT polymerisation

In a typical protocol, 2-cyano-2-propyl benzodithioate (CTA, 1 eq.), AIBN (0.25 eq.), uracil methacrylate (UrMA) (x eq.) and thiomorpholine oxide methacrylate THOXMA ((y-x) eq.) were dissolved in a mixture of DMF/ aqueous phosphate buffer (pH 4, C_M = 4 M), in a volume ratio (DMF/buffer) of 2:1. The mixture was thoroughly degassed *via* 3 freeze–pump–thaw cycles, filled with nitrogen and immersed into an oil bath at 80 °C. At different time, an aliquot of the reaction mixture was taken and analysed by ^{1}H NMR and SEC. After 7h, the reaction was stopped by exposure to air. The mixture was then dialysed against water (with a 1kDa MWCO membrane) for 3 days, followed by lyophilisation during 2 days. The resulting pink polymer powder was analysed by ^{1}H NMR in DMSO-d_6 and DMF SEC. For example, to obtain P(UrMA$_8$-stat-THOXMA$_{34}$), the quantities of reagents used were: CTA (1eq., 8 mg, 0.036 mmol), AIBN (0.25 eq., 1.5 mg, 0.009 mmol), uracil methacrylate UrMA (10 eq., 82 mg, 0.36 mmol), thiomorpholine oxide methacrylate THOXMA (40 eq., 332 mg, 1.44 mmol), dissolved in DMF (2 mL)/ aqueous buffer (pH=4, C_M =4 M, 60 eq., 0.54 mL). ^{1}H NMR, *Fig. S3* (400 MHz, DMSO-d_6) δ (ppm) = 1.8 (s, C$\mathbf{H}_2$, polymerizable synthon, noted as $\mathbf{I_b}$); 1.8 (m, C$\mathbf{H}_2$, UrMA aliphatic linker, noted as $\mathbf{II_b}$); 3.43 (d, C$\mathbf{H}_2$, UrMA aliphatic linker, noted as $\mathbf{II_a}$ and $\mathbf{II_c}$); 3.43 (d, C$\mathbf{H}_2$, THOXMA aliphatic linker, noted as $\mathbf{II_d}$ and $\mathbf{II_e}$); 2.62 (t, $C\mathbf{H}_2CH_2$, thiomorpholine oxide cycle, noted as $\mathbf{III_b}$); 3.87 (t, $C\mathbf{H}_2CH_2$, thiomorpholine oxide cycle, noted as $\mathbf{III_a}$); 0.87, 0.97, 1.1 (s, C$\mathbf{H}_3$, noted as $\mathbf{I_a}$); 7.57 (d, CH=C**H**, uracil heterocycle, noted as **i**); 5.87 (d, C**H**=CH, uracil heterocycle, noted as **h**); 11.5 (s, N**H**, uracil heterocycle, noted as **g**).

Synthesis of Poly(ethylene glycol)-b-Poly((3-(adenine-9-yl) propyl methacrylate) -stat-(2-ethyl thiomorpholine oxide methacrylate)) PEG$_{112}$-b-P(AdMA$_n$ -stat-THOXMA$_m$) by RAFT polymerisation

PEG-macro chain transfer agent (macro CTA PEG, 1 eq.), adenine methacrylate AdMA (x eq.) and thiomorpholine oxide methacrylate THOXMA ((y-x) eq.) and AIBN (0.25 eq.) were dissolved in a mixture of DMF / aqueous phosphate buffer (pH 4, C_M =4 M), in a volume ratio (DMF/buffer) of 2:1. The mixture was degassed *via* 3 freeze–pump–thaw cycles, back filled with nitrogen and then immersed into an oil bath at 80 °C for 7 hours. The conversion of the

reaction was monitored each hour by ^{1}H NMR. The reaction was then quenched by immersion in a liquid nitrogen bath and exposure to air. The final mixture was dialysed against water (with a 1kDa MWCO membrane) for 3 days, followed by lyophilisation during 2 days. The resulting pale yellow powder was analysed by ^{1}H NMR spectroscopy in DMSO-d_6 and DMF SEC. For exemplification in the case of PEG_{112}-b-P($AdMA_{30}$-stat-$THOXMA_{70}$), the quantities of reagents used were: macro CTA PEG (1eq., 20 mg, 0.0036 mmol), AIBN (0.25 eq., 0.15 mg, $9 \cdot 10^{-4}$ mmol), adenine methacrylate AdMA (30 eq., 28.2 mg, 0.11 mmol), thiomorpholine oxide methacrylate THOXMA (70 eq., 58.2 mg, 0.25 mmol), dissolved in DMF (1 mL)/ aqueous buffer (pH 4, C_M =4 M, 130 eq., 0.12 mL). ^{1}H NMR, *Fig. S4* (400 MHz, DMSO-d_6) δ (ppm) = 1.35 (s, C**H**$_2$, polymerizable synthon, noted as **I$_b$**); 1.35 (m, C**H**$_2$, Ad aliphatic linker, noted as **II$_b$**); 3.47 (m, C**H**$_2$, PEG, noted as **IV**); 3.96 (d, C**H**$_2$, AdMA aliphatic linker, noted as **II$_a$** and **II$_c$**); 3.96 (d, C**H**$_2$, THOXMA aliphatic linker, noted as **II$_d$** and **II$_e$**); 4.44 (t, C**H**$_2$CH$_2$, thiomorpholine oxide cycle, noted as **III$_a$** and **III$_b$**); 0.9 (s, C**H**$_3$, noted as **I$_a$**); 8.56 (s, N**H**$_2$, adenine heterocycle, noted as **g**); 8.97 (s, N=C**H**-N, adenine heterocycle, noted as **h**); 9.6 (s, N=C**H**-N, adenine heterocycle, noted as **i**).

Preparation of starting polymer solutions and of self-assembled formulations

The starting polymer solutions (noted as P1, P3 -uracil polymer solutions and P2, P4- adenine polymer solutions see *Table 2*, *Table S1*) were prepared in HEPES buffer (pH 7.4) at a concentration of 5 g/L and stirred overnight at room temperature. Then, the self-assembled formulations (*Scheme 3*) were obtained by slowly adding the uracil solution to the adenine solution, the resulting mixture was then stirred for 2 days. For example, to prepare the Formulation A (P1+P2, 1 mL), P1 solution (0.55 mL from a solution at concentration of 5 g/L, in HEPES buffer, calculated as stated by Eq. S15.) was gently added by using a micropipette (15 min, 200 rpm) to P2 solution (0.46 mL from a solution at a concentration of 5 g/L, in HEPES buffer, calculated according to Eq. S16.). Then, the solution mixture was stirred for 2 days (200 rpm, at room temperature). The solutions of starting polymers (P1, P2, P3, P4) were filtered through 0.2 μm pore size Waters filters (USA) prior to perform SLS, DLS and TEM characterizations. The absence of the concentration variation due to filtration was checked. Dilutions were made by adding the filtered solvent (through 0.2 μm filters) and then stirring the solution for 5 min.

Static light scattering

Static light scattering (SLS) measurements were performed using an LS spectrometer operating with a vertically polarized laser with wavelength λ = 660 nm. All measurements (including dilutions) were done at room temperature (25 °C), collected from 30° to 90° with an interval of 5°, from 90° to 110° with an interval of 10°, and up to 150° with an interval of 20°. Prior to measurements, filtered toluene and filtered buffer (through 0.2 μm pore size Waters filter membrane) were measured as reference and solvent respectively.

The Rayleigh ratio (R_θ) of the solution was determined following the Eq. 1. [19,20]

$$R_\theta = \frac{I_{solution}(\theta) - I_{solvent}(\theta)}{I_{toluene}(\theta)} \times \left(\frac{n_{solvent}}{n_{toluene}}\right)^2 \times R_{toluene} \quad \text{(Eq.1)}$$

where $I_{solution}$, $I_{solvent}$, and $I_{toluene}$ are the average intensities scattered by the solution, the solvent, and the reference (toluene) respectively, and $n_{solvent}$ = 1.333 (water) and $n_{toluene}$ = 1.496, and $R_{toluene} = 1.33 \times 10^{-5}$ cm^{-1} is the Rayleigh ratio of toluene for a wavelength λ = 660 nm.

At a given concentration C, R_θ is related to the apparent weight average molar mass of the scatterers (or apparent molecular weight), M_a, and to the structure factor, S(q), which depends on the scattering wave vector, as shown by Eq. 2.[19,20] It is important to underline that M_a corresponds to the true molar mass (M_w) only in very dilute solutions, where the interactions between the scatterers can be neglected.[21,20] At high concentrations, interactions cause M_a to differ strongly from M_w. For this reason, in order to accurately evaluate the true M_a of the self-assemblies, SLS measurements were performed for concentrations ranging between 5 g/L and 1 g/L. Consequently, the curve representing each M_a corresponding to each tested concentration was fitted, in order to determine the real M_w of the self-assembled objects as the intercept.

$$R_\theta = K \times C \times M_a \times S(q) \quad \text{(Eq. 2.)}$$

with C the polymer concentration in g/L and K a constant:

$$K = \frac{4\pi^2 n_{solvent}^2}{\lambda^4 N_a}\left(\frac{\partial n}{\partial C}\right)^2 \quad \text{(Eq. 3.)}$$

where N_a is Avogadro's number.

The aggregation number (N_{agg}) was expressed according to the Eq. 4. [19,20] :

$$N_{agg} = \frac{M_w}{M_u} \quad \text{(Eq. 4.)}$$

where N_{agg} is the aggregation number of particles, M_w is the average molar mass, and M_u is the molar mass of the unimer. M_u values were determined by multiplying their M_n (determined by ^{1}H-NMR spectroscopy) by the corresponding M_w/M_n values determined by SEC. In the case of self-assembled structures, the aggregation number was evaluated by using the same equation, with an exception concerning the calculation of M_u. For self-assembled structures, the M_u was expressed as a sum between the weight ratio of each polymer multiplied by the $M_{polymer}$, according to the Eq. 5. $M_{polymer}$ was calculated by multiplying the M_n (determined by ^{1}H NMR spectroscopy) by the corresponding M_w/M_n values determined by SEC.

$$M_u = w_{polymer1} \times M_{polymer1} + w_{polymer2} \times M_{polymer2} \text{ (Eq. 5.)}$$

Dynamic Light Scattering

Particle size (Z_{ave}) of co-assembled polymers were determined by dynamic light scattering (DLS). The DLS instrumentation consisted of the same LS spectrometer used for SLS experiments. DLS measurements were performed at 25 °C with a He–Ne 630 nm laser module, at a detection angle of 150°.

Transmission Electron Microscopy

TEM assays were analysed by using a JEOL 1400+ instrument equipped with a numerical camera, operating with a 120 kV acceleration voltage at 25 °C. TEM samples were prepared by placing a drop (10.0 μL) of self-assembled polymers solution onto a carbon coated copper grid for 20 s, blotted with filter paper and then dried under ambient conditions.

Cytotoxicity assays

Cytotoxic evaluation of nucleobase containing copolymers was assessed by using the mouse fibroblast cell line L929 (400620, CLS), as recommended by ISO10993-5. L929 cells were cultured in Dulbecco's modified eagle's medium with 2 mM L-glutamine supplemented with 10% fetal calf serum, 100 U/mL penicillin, and 100 μg/mL streptomycin at 37 °C under a humidified 5% (v/v) CO_2 atmosphere. To this, the L929 cells were firstly seeded at 10^3 cells/mL (10^4 cells per well) in a 96 well plate and then incubated for 24 h. No cells were seeded in the outer wells. The medium was changed to fresh cell culture medium 1 h prior to treatment. Cold nucleobase containing polymer solutions prepared in 20 mM HEPES (4-(2-hydroxyethyl)-1-piperazineethanesulfonic acid) were added to the cells in various concentrations (from 5 to 700 μg/mL), and then the plates were incubated for 24 h. The control cells were incubated with fresh culture medium containing the same amount of HEPES as the treated cells. Moreover, the

medium was replaced by a mixture of a fresh culture medium and the resazurin-based solution PrestoBlue. After incubation for another 45 min at 37 °C under a humidified 5% (v/v) CO_2 atmosphere, the fluorescence was measured at λ_{ex} = 560 nm/λ_{em} = 590 nm with gain set to optimal, with untreated cells on the same well plate serving as negative controls. The negative control was standardized as 0% of metabolism inhibition and referred to as 100% viability. Cell viability below 70% was considered to be an indication of a cytotoxic behaviour. All experiments were performed in triplicate.

Erythrocyte aggregation

Red blood cells from human blood were treated with the nucleobase containing polymers under physiological pH (pH 7.4). Human blood was provided by the Department of Transfusion Medicine from Jena University Hospital. Erythrocyte suspensions in PBS were prepared and mixed 1:1 (volume ratio) with polymer solutions as described above. After incubation at 37 °C for 2 h, the erythrocyte aggregation was measured at 645 nm. As positive and negative controls, erythrocytes were treated with 50 µg/mL of 25 kDa branched poly(ethylene imine) (bPEI) solution or PBS buffer at pH 7.4. The aggregation activity of the polymer samples was expressed as the aggregation rate (Eq. 6.):

$$Aggregation\ rate = \frac{1}{\mathrm{A(sample)}} \qquad \text{(Eq. 6.)}$$

where, $A_{(sample)}$ is the mean absorbance of a given sample.

Hemolytic activity

The release of the haemoglobin from the erythrocytes was assessed in order to evaluate the damaging properties of red blood cells membrane in the presence of nucleobase-containing copolymers. The blood was centrifuged at 4 500g for 5 min. Subsequently, the pellets were washed three times with PBS (pH 7.4) by centrifugation at 4 500g for 5 min. Furthermore, the erythrocytes were suspended in PBS at pH 7.4 to mimic the physiological conditions of blood/cytoplasm. Cold nucleobase containing polymer solutions were made in 20 mM HEPES (4-(2-hydroxyethyl)-1-piperazineethanesulfonic acid) at a stock concentration of 1 mg/mL. Then the solutions were mixed 1:1 (volume ratio) with cold erythrocyte suspensions and were incubated at 37°C for 1 h. Erythrocyte suspensions were centrifuged at 2 400g for 5 min. The release of hemoglobin in the supernatant was determined at 544 nm. The absorbance was measured using a plate reader. Additionally, determinations were conducted with washed erythrocytes either lysed with 1% Triton X-100 or suspended in PBS at the pH 7.4 as a

reference. The hemolytic activity of the polymers was calculated according to the following equation (Eq. 7.):

$$\text{Hemolysis (\%)} = \left(\frac{A_{(sample)} - A_{(PBS)}}{A_{(Triton\ X-100)}} \right) \times 100 \qquad \text{(Eq. 7.)}$$

where, $A_{(sample)}$, $A_{(PBS)}$, and $A_{(Triton\ X\text{-}100)}$ are the absorbance of erythrocytes incubated with the polymer sample, suspended in PBS, and erythrocytes lysed with Triton X-100, respectively. This study was performed in line with the principles of the Declaration of Helsinki. All experiments were performed and approved by the ethics committee at the Friedrich Schiller University Jena (2021-2266-Material). Informed consent was obtained from human participants of this study.

V. Results and discussion

V.1. Nucleobase-containing methacrylates

The synthesis of adenine- and thymine-containing methacrylates has already been reported by Kang *et al.*[13,22,27] In this work, we adapted the previously reported synthetic routes to improve the yield and to reduce the synthetic efforts. *Scheme 1* illustrates the synthesis of nucleobase-containing methacrylates used in the present study, called adenine methacrylate (AdMA) and uracil methacrylate (UrMA), which afforded the final monomer products with relatively high yields (above 63%) by straightforward techniques of organic chemistry.

These adenine- and uracil-methacrylates were insoluble in water. Our previous study reported the synthesis and characterisation of a new hydrosoluble thiomorpholine oxide methacrylate. Using RAFT polymerisation, hydrophilic polymers with no cytotoxicity and high blood compatibility were synthesized.[23] Ethyl-thiomorpholine oxide methacrylate (THOXMA) was thus used as a hydrophilic comonomer for the synthesis of nucleobase-containing copolymers to modulate their hydrophobicity.

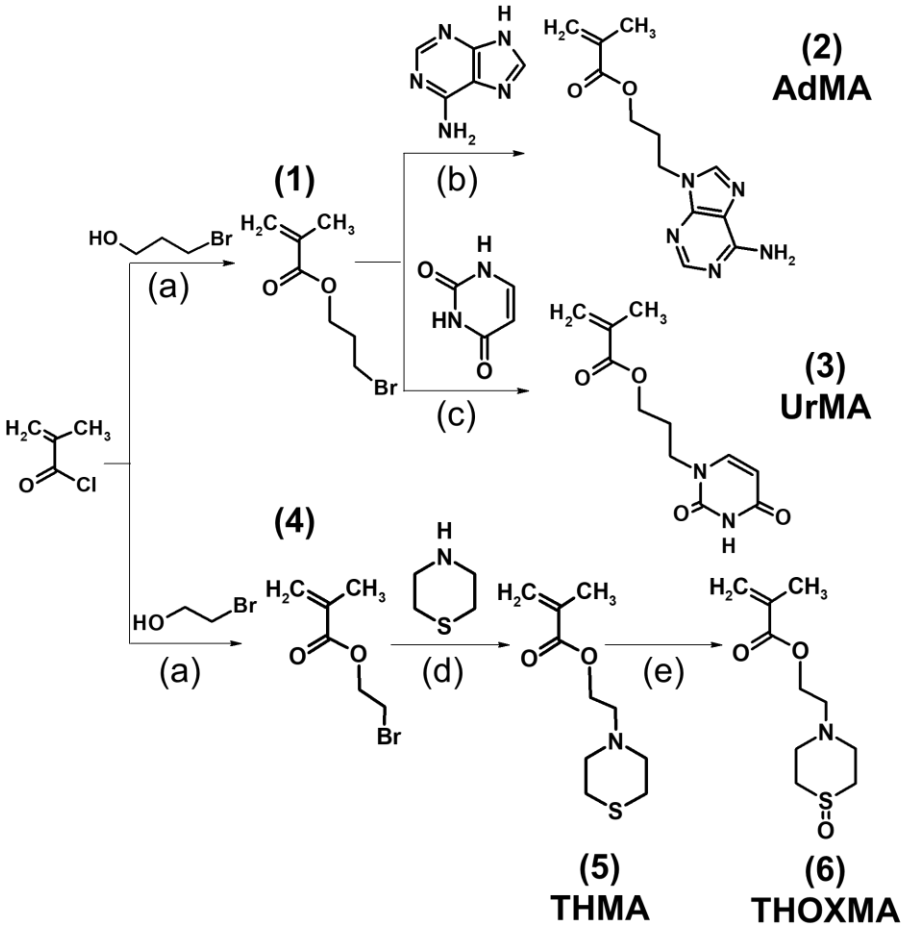

Scheme 1 Syntheses of an adenine containing monomer (AdMA) (2), uracil methacrylate (UrMA) (3), thiomorpholine methacrylate (THMA) (5), and thiomorpholine oxide methacrylate (THOXMA) (6). (a): DMAP, TEA, CH_2Cl_2, RT, under N_2, overnight; (b): NaH, DMF, 40 °C, 10 days; (c): K_2CO_3, DMF, RT, 10 days; (d) K_2CO_3, CH_3CN, under N_2, 40 °C, 6 days; (e): H_2O_2, under N_2, RT, overnight.

These adenine- and uracil-methacrylates were insoluble in water. Our previous study reported the synthesis and characterisation of a new hydrosoluble thiomorpholine oxide methacrylate. Using RAFT polymerisation, hydrophilic polymers with no cytotoxicity and high blood compatibility were synthesized.[18] Ethyl-thiomorpholine oxide methacrylate *(THOXMA)* was thus used as hydrophilic comonomer for the synthesis of nucleobase-containing copolymers to modulate their hydrophobicity.

V. 2. Synthesis of nucleobase copolymers

Two families of nucleobase-containing copolymers were synthesised by RAFT polymerisation, as shown in *Scheme 2.*: A) Diblock copolymers (*PEG_{112}-b-P($AdMA_n$-stat-$THOXMA_m$)*)

composed of a hydrophilic block of PEG (with a constant DP=112) and a second block driving the self-assembly prepared by copolymerization of *AdMA* and *THOXMA*; B) Statistical copolymers of *UrMA* and *THOXMA*, noted as *P(UrMA$_n$-stat-THOXMA$_m$)*. In all structures, the nucleobases (adenine, uracil) are H-bond promoters. In the case of adenine-containing block copolymer, *PEG$_{112}$-b-P(AdMA$_n$-stat-THOXMA$_m$)*, PEG was selected for its high hydrosolubility and for the steric stabilisation it can provide to self-assembled structures in water,[28] while THOXMA was introduced in the self-assembling moiety to modulate its hydrophobicity.

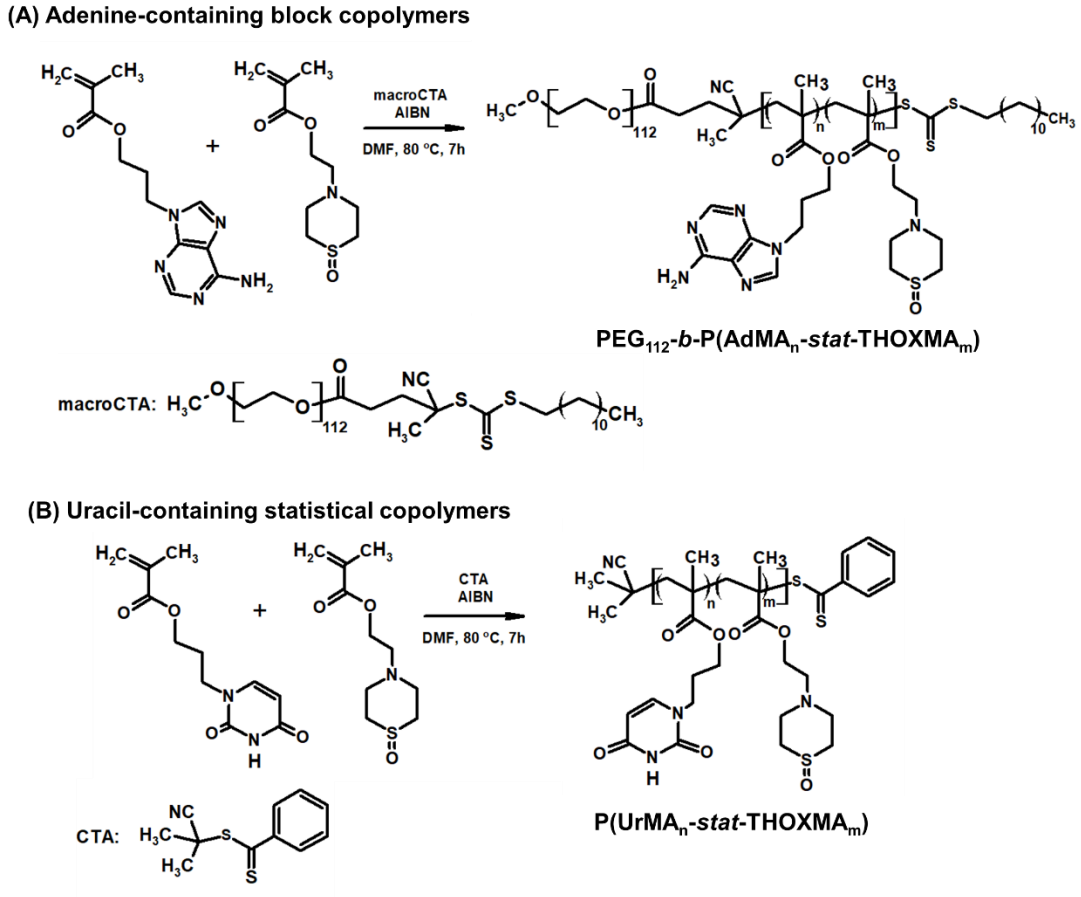

Scheme 2. Syntheses of the nucleobase-containing copolymers: A) PEG$_{112}$-b-P(AdMA$_n$-stat-THOXMA$_m$) diblock copolymers (P2, P4); B) P(UrMA$_n$-stat-THOXMA$_m$) statistical copolymers (P1, P3).

Both nucleobase copolymer families were synthesized by RAFT polymerization in a mixture of DMF/ aqueous phosphate buffer (pH 4). The acidic buffer was used to prevent undesired aminolysis/hydrolysis of the dithioester and trithiocarbonate moieties of the chain transfer agents. The characterization data of these copolymers are summarized in *Table 1*. A good correlation between theoretical and experimental molar masses calculated by ^{1}H NMR, and

comonomer ratios were observed (*Table 1*). In addition, SEC analysis revealed a narrow molecular weight distribution (*Đ* ranging between 1.1 and 1.3, *see Table 1*) for all the copolymers, while the evolution of molar mass with conversion was linear, thus confirming that the polymerisation was controlled (*Fig. S5.*, *Fig. S6.*). These results indicate that the RAFT polymerisation led to the formation of well-defined nucleobase-containing copolymers with controlled molar masses and desired compositions.

Table 1. Characterisation of nucleobase-containing copolymers

	Polymer name	Experimental DP[a]	Experimental molar composition (%)[b]		Co-monomer conversion (%), by ^{1}H-NMR[c]		M_n (g/mol), by ^{1}H-NMR[d]	M_n (g/mol), by SEC[e]	Dispersity (Đ)[e]	Average number of nucleobases per polymer chain	M_{th} (g/mol)	Theoretical target DP[f]
			Nucleobase	THOXMA	Nucleobase	THOXMA						
P1	P($UrMA_8$-*stat*-$THOXMA_{34}$)	42	20	80	85	92	10,000	10,430	1.21	8	11,840	50
P2	PEG_{112}-*b*-P($AdMA_{30}$-*stat*-$THOXMA_{70}$)	104	30	70	72	88	30,200	32,100	1.32	30	29,400	100
P3	P($UrMA_{22}$-*stat*-$THOXMA_{19}$)	41	53	47	81	90	10,500	11,200	1.1	22	11,950	50
P4	PEG_{112}-*b*-P($AdMA_5$-*stat*-$THOXMA_5$)	10	50	50	70	87	7,900	9,000	1.11	5	7,700	15

[a] Calculated by ^{1}H-NMR performed in DMSO-d6, according to the Eq. S4. and Eq. S9.; [b] Calculated by ^{1}H-NMR performed in DMSO-d6, according to the Eq. S5., Eq. S6., Eq. S12., Eq. S13.; [c] Calculated by ^{1}H-NMR performed in DMSO-d6, according to the Eq. S1. and Eq. S8.; [d] Calculated by ^{1}H-NMR performed in DMSO-d6, according to the Eq. S7. and Eq. S14.; [e] SEC analysis performed in DMF containing 0.1% LiCl and by using PMMA standards. [f]Calculated using the following equation DP_{target} = (([THOXMA]/[chain transfer agent]) x $Conv_{THOXMA}$) + (([AdMA or UrMA]/[chain transfer agent]) x $Conv_{AdMA\ or\ UrM}$

V. 3. Formation of co-assembled nucleobase polymer architectures at physiological pH

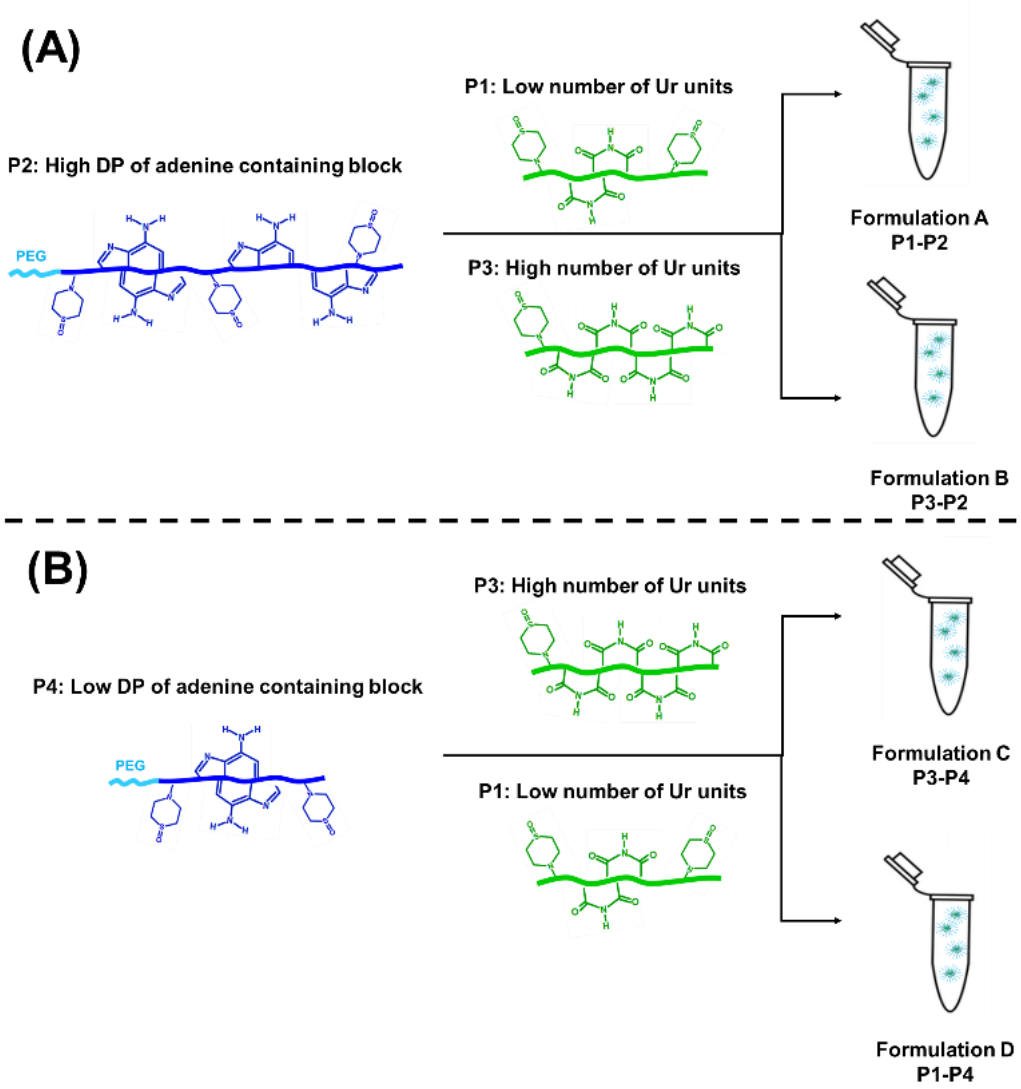

Scheme 3. (A) Schematic representation of the composition of Formulation A, made by adding the solution of P1 (with a low number of uracil units) to the solution of P2 (long DP of adenine-containing block) and of the composition of Formulation B, made by adding the solution of P3 (with a high number of uracil units) to the solution of P2 (long DP of adenine-containing block); (B) Composition of Formulation D, prepared by adding the solution of P1 (with a low number of uracil units) to the solution of P4 (short DP of adenine-containing block) and of the composition of Formulation C, formed by adding the solution of P3 (with a high number of uracil units) to the solution of P4 (short DP of adenine-containing block).

Table 2. Characterisation of co-assembled nucleobase-containing copolymer formulations

Formulation	Description	Ur/Ad molar ratio	Aggregation number (N_{agg})[a]	Particle hydrodynamic diameter (D_H)[b]
A	P1+P2	1:1	315	130
B	P3+P2	1:1	194	101
C	P3+P4	1:1	9.95	40
D	P1+P4	1:1	7.8	35
Polymer solution	P1	-	1.6	11
Polymer solution	P2	-	7.5	20
Polymer solution	P3	-	3.3	13.2
Polymer solution	P4	-	11.4	10.8

[a]Evaluated by SLS; [b]Evaluated by DLS; formulations A, B, C, and D were prepared with a Ur/Ad molar ratio of 1/1.

The obtained nucleobase copolymers were then dissolved in HEPES buffer (pH 7.4) and the properties of the resulting solutions were analysed (*Scheme 2, A*). First, starting filtered solutions of P1 and P2 were investigated by light scattering (SLS and DLS). The results are presented in *Fig. 1* and *Table 2*. Low apparent molar mass (~ 20 000 g/mol) and N_{agg} (~1.6) were observed for the uracil-containing copolymer (P1) (*Table S2*). This slight aggregation did not result in typical micellar structures observed in the case of previously reported nucleobase blocks. The analysis of the adenine-containing copolymer (P2) showed slightly higher aggregation number N_{agg} (~7.5) and apparent molar mass (*Table S2*). Solutions of P3 and P4 showed similar behaviour but slightly higher aggregation numbers (3.3 and 11.4, respectively) likely caused by their higher molar contents in hydrophobic nucleobases (*Table 2* and *Table S2*). This slight aggregation is likely caused by hydrophobic interactions. Indeed, the light scattering signatures of solutions of P1 or P2 were not affected by the addition of urea (*Fig. 2*). Overall, in contrast to pure hydrophobic nucleobase-containing polymers reported thus so far, these results show that uracil- (P1) and adenine-containing (P2) copolymers have no tendency to form large aggregates (N_{agg} <8 by SLS; particle hydrodynamic diameter D_H < 20 nm, by DLS *Table 2*).

Previous studies on DNA[29] indicated that the co-association between complementary nucleobases is stronger than uracil-uracil association or adenine-adenine association. Thus, it is expected that the co-assembly between uracil- and adenine-containing copolymers led to self-assembled objects with high N_{agg} and particle size, if the complementary H-bond interactions are strong enough to overcome the competition with water molecules. For this reason, the next

step consisted in the investigation of the co-assembly of P1 and P2 in aqueous solution at physiological pH. Compared to individual P1 or P2 solutions, Formulation A (P1 + P2, Ur/Ad ratio of 1/1) featured a high increase of apparent molar mass M_a (~ 10^7 g/mol) by SLS (*Fig. 1. A.*). This result proves the co-assembly of the complementary nucleobases-containing copolymers into aggregates with high N_{agg} (~315). The formation of co-assembled micelles was confirmed by DLS (*Fig. 1. B.*). Compared to P1 and P2 which showed low D_H (below 20 nm), Formulation A led to D_H 6.5 times higher (130 nm) than the starting polymers. These results suggest that the co-assembly originate from strong interactions between complementary nucleobases.

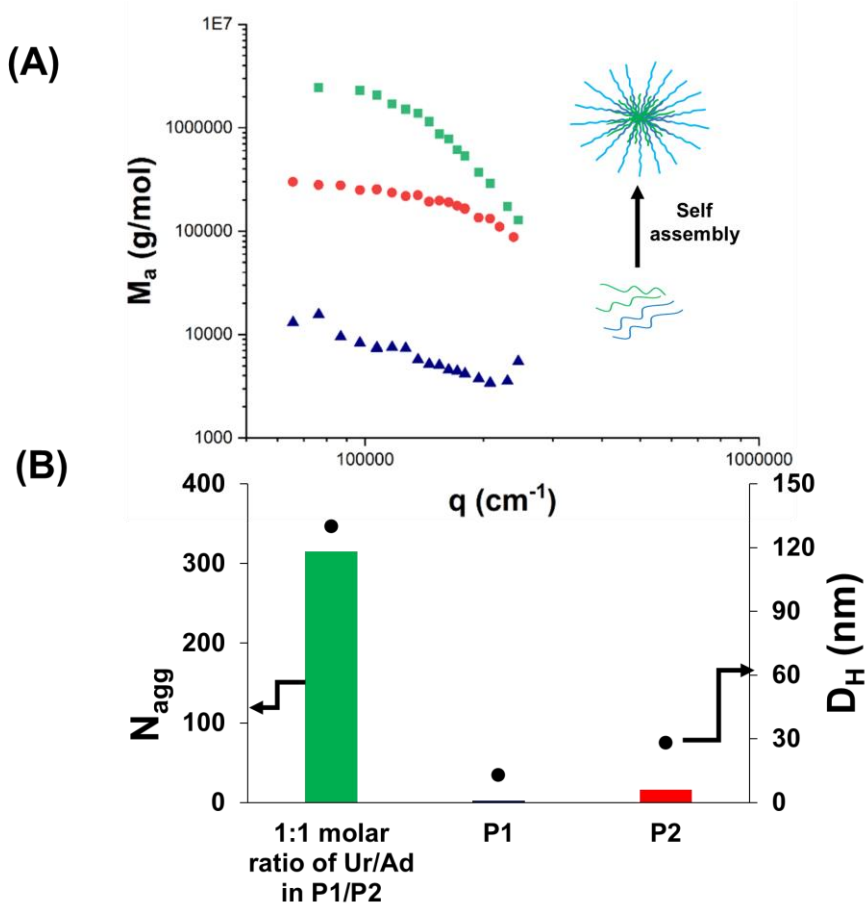

Fig. 1 Co-assembly of P1 and P2 (formulation A): (A) apparent molar mass M_a evolution for individual polymer solutions (P1, P2) and formulation A, measured by SLS at a concentration of 5 g L^{-1}; (B) N_{agg} (evaluated by SLS) and D_H (evaluated by DLS) of individual polymer solutions and formulation A measured between 1 g L^{-1} and 5 g L^{-1}.

V.4. Co-assembly in the presence of a H-bond competitor

Most of the self-assembled systems in water are driven by hydrophobic interactions. In order to prove unequivocally that the resulting co-assembly was mainly guided by H-bonds between

complementary nucleobases instead of hydrophobic interactions, the effect of urea on the co-assembly was investigated. Urea is known as a strong competitor for H-bonds.[25, 26,27,28] A diluted solution of urea (0.01 M) was added to Formulation A (P1 + P2, Ur/Ad ratio of 1/1), the mixture was stirred for 1h and then examined by SLS and DLS. As presented in *Fig. 2*, significant decrease of the aggregation number was observed after the addition of urea. Small particles with an average hydrodynamic diameter of 15 nm (measured by DLS) were formed. The size and the N_{agg} were close to that of individual P1 and P2 copolymers (*Fig. 1*, *Fig. 2*, *Table 2*). Urea cleaves the H-bonds between complementary nucleobase between P1 and P2 thus preventing the formation of the co-assemblies, and leading to the release of P1- and P2-urea structures.[25] The dramatic effect of urea on Formulation A(P1 + P2, Ur/Ad ratio of 1/1) confirms that H-bonds between complementary nucleobases are responsible for the co-assembly between P1 and P2.

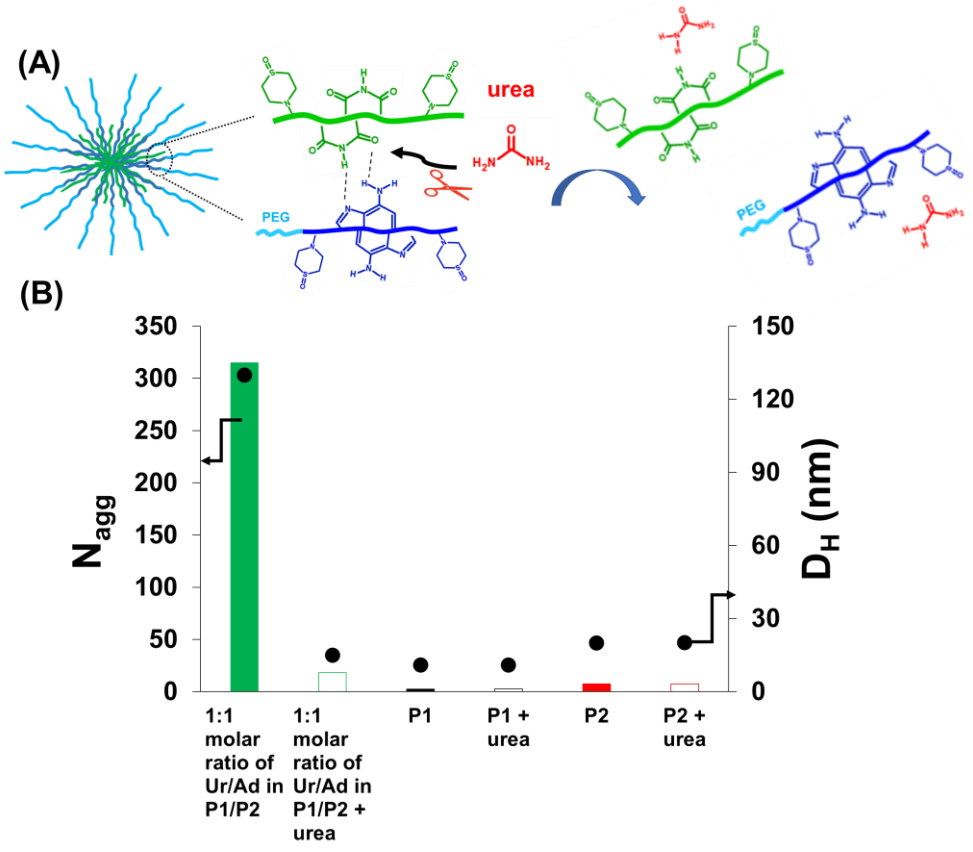

Fig. 2. Disassembly of co-assembled nucleobase-containing copolymers P1 + P2 in HEPES buffer (pH 7.4) in the presence of urea: (A) schematic representation of disassembly under urea influence; (B) N_{agg} (determined by SLS) and D_H (measured by DLS) of formulation A, P1 and P2 before vs. after the addition of urea measured between 1 g L^{-1} and 5 g L^{-1}.

V.5. Impact of adenine and uracil nucleobases

The effect of the length of the adenine-containing block on the co-assembly was investigated. Four formulations (Formulation A, B, C and D) were compared (*Table 2*, *Fig. 3.*).

Formulation A and B were prepared using the same high length adenine-containing block copolymers (P2: PEG_{112}-*b*-P($AdMA_{30}$-*stat*-$THOXMA_{70}$), DP ~ 100, 30 units of adenine) and two different uracil containing copolymers (P1, P3) with the same degree of polymerisation (DP~ 42) but different number of uracil units (P1: 8 units of Ur and P3: 22 units of Ur).

SLS and DLS data of formulations A and B displayed in *Fig.3.*, show that micelles with high N_{agg} (above 200) and particle size (above 100 nm) were formed when long adenine-containing block (DP~ 100) were used (*Table 2*, *Fig. 3.*).

However, significant differences were noted depending on the uracil copolymer (P1 or P3) used in the co-assembled formulations A and B. Formulation A (P1+P2) prepared with P1 that contains only 8 uracil units per chains, led to objects with high N_{agg} (~ 315, by SLS). In contrast, Formulation B (P2+P3), in which P3 has 22 uracil units per chains, produced smaller co-assemblies with an N_{agg} ~ 194 (by SLS, *Fig. 3.*). DLS measurements revealed a similar trend for the hydrodynamic particle diameters (D_H) which reached 130 nm and 101 nm for Formulation A and Formulation B respectively. Thus, increasing the number of uracil units per chain in the uracil-containing copolymer (from 8 to 22) led to smaller self-assembled objects. This might be because a smaller number of chains of the copolymer containing a higher density of uracil units (P3) is required to bind the complementary adenine containing copolymer (P2). This translates into lower N_{agg} and particle hydrodynamic diameter for Formulation B than for Formulation A. Spherical morphologies were observed by TEM in formulations A (~ 150 nm) and B (~ 100 nm) (*Fig. 4.*), and their sizes were in agreement with the previous data obtained by DLS.

Formulation C and D were made using a shorter adenine containing block copolymer (P4: PEG_{112}-*b*-P($AdMA_5$-*stat*-$THOXMA_5$), DP~ 10, 5 units of adenine) and the same uracil containing copolymers (P1, P3).

Low N_{agg} and hydrodynamic diameters were determined when short length adenine blocks (Formulation C and D) were used. For formulation C (using P3, DP = 42, 22 units of uracil), very low N_{agg} (~ 10, by SLS) and particle size (~ 40 nm, by DLS) were observed. In addition, TEM analysis (*Fig. 4.*) showed small spherical particles with size of ca. 35 nm (Formulation C, *Fig. 3.*), in agreement with the DLS data. For formulation D (using P1, DP=42, 8 units of Ur), N_{agg} (~ 8) was calculated by SLS (*Fig. 3.*). This low N_{agg} (~ 8) obtained for Formulation D in

comparison to the results observed for Formulation A shows that the use of polymers containing only small amounts and low density of adenine diminished the co-assembly ability to form large aggregates, likely because the H-bond cannot be formed in sufficiently high numbers.

Further investigation of the co-assembly in the presence of urea revealed a decrease of the particle hydrodynamic diameter in all formulations, the urea treatment leading to particles as small as 30 nm (*Fig. S7.*). This confirmed that the co-assemblies formed in the different formulations studied are driven by H-bonds between complementary nucleobases units rather than from hydrophobic interactions.

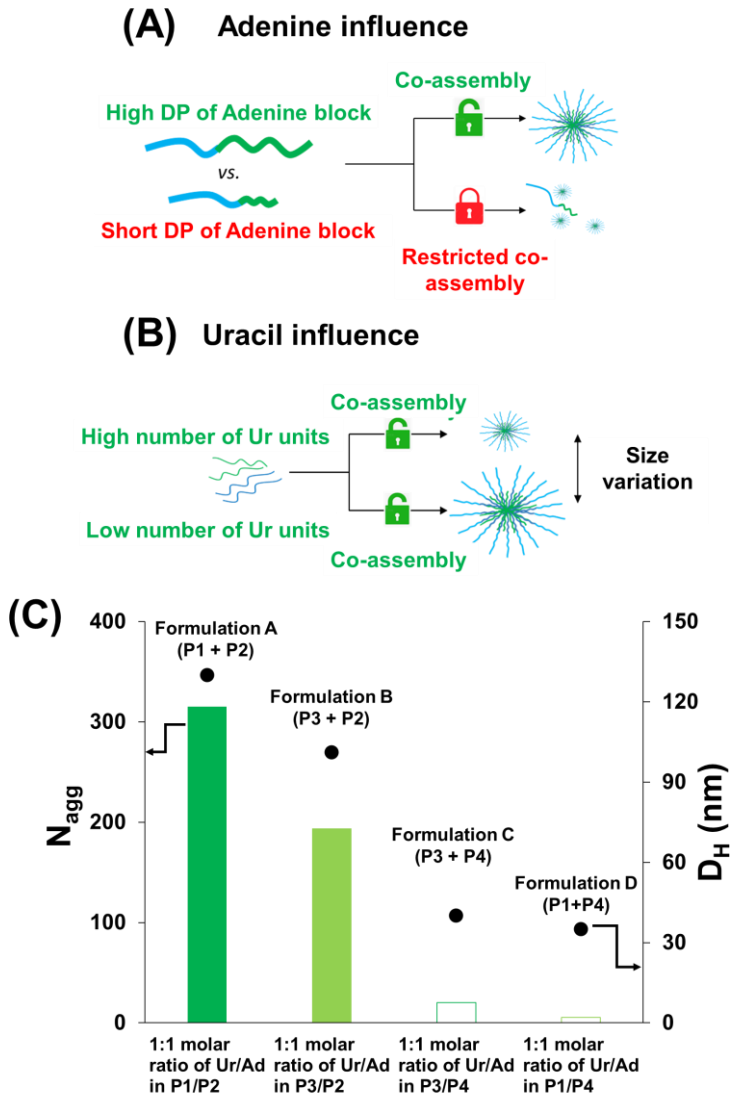

Fig. 3 Impact of adenine (A) and uracil (B) nucleobases on the properties of co-assembled structures; (C) variation of N_{agg} by SLS and particle size (D_H) by DLS of formulations A, B, C and D. The experiments were performed at concentrations between 1 g L^{-1} and 5 g L^{-1}.

V.6. Influence of the molar ratios between Ur/Ad

Then, lower ratios of uracil and adenine equivalents (0.1/1 molar ratio of Ur/Ad) were studied on four formulations (formulation E, F, G, H), as presented in *Table S1*. Co-assembled micelles (*Table S1, Fig. S8. A.*) with average hydrodynamic diameter and particle size of around 50 nm were formed. These results suggest that at such low stoichiometries, the amount of uracil was likely too low to completely complex (by H-bonds) with adenine.

Moreover, high ratios between uracil and adenine equivalents (10/1 molar ratio of Ur/Ad) were investigated by preparing additional formulations (formulations I, J, K, L, *Table S1, Fig. S8. B.).* Co-assembled formulations with moderate N_{agg} (~100) and nanometric particle size (~ 80 nm) were observed when long adenine-containing blocks (formulation I and J) were used, while low N_{agg} (below 40) and particle size (~30 nm) were observed for the formulations based on short adenine-containing blocks (formulation K and L). These values were higher than those obtained for low ratios of Ur/Ad (*i. e.*, Ur/Ad = 0.1/1), which is coherent since the increase of the amount of complementary nucleobases increases the number of H-bonds which translates into the increase of N_{agg} and D_H.

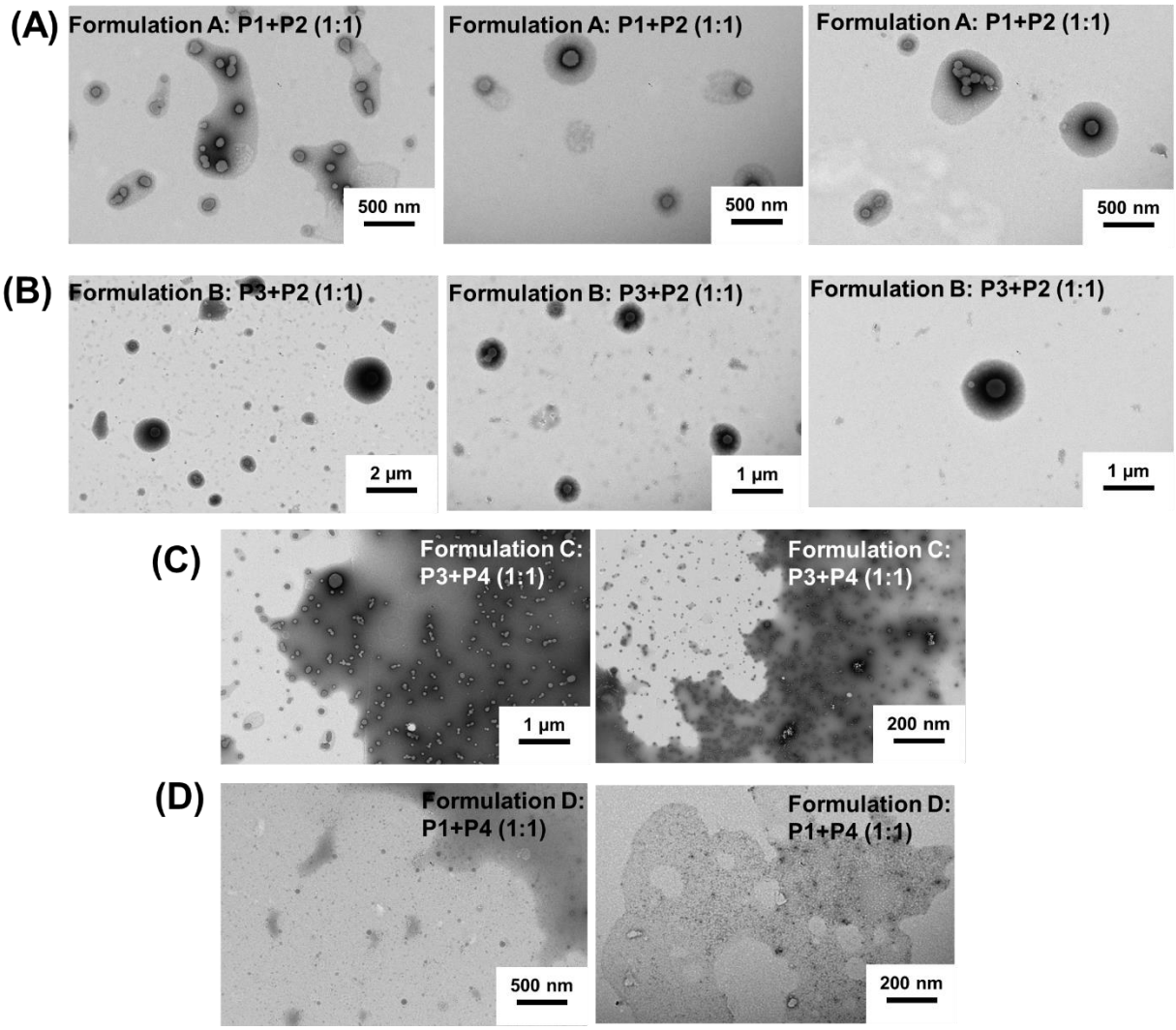

Fig. 4. TEM characterisation of co-assemblies (A) formulation A: P1 + P2 mixture (1 : 1); (B) formulation B: P3 + P2 mixture (1 : 1); (C) formulation C: P3 + P4 mixture (1 : 1); (D) formulation D: P1 + P4 mixture (1 : 1). The co-assemblies were prepared at an initial concentration of 1 g L^{-1}*. TEM experiments were performed at a concentration of 0.1% w/w.*

However, compared to the 1/1 stoichiometry (*Fig. 3.*), the increase of the stoichiometry to 10/1 led to an overall decrease of N_{agg} and D_H. This behaviour was previously reported by Hua *et al.*[10] who explained this phenomenon to be a consequence of a low energy barrier for chain exchange which occurs at high stoichiometry, since the system is oversaturated in complementary nucleobase copolymers. Smaller spherical micelles were, therefore, formed to reduce the increased corona-chain repulsion introduced through the insertion of the complementary hydrophobic copolymer.[10] Applied to our system, the increase of the

stoichiometry ratio increases the hydrophobicity of the system (by adding high amounts of the uracil containing copolymer) which led to more compact and smaller particles.
Globally, these results emphasize that structural parameters such as the copolymer architecture (DP, nucleobase number per polymer chain), the type of nucleobase, and the ratio between complementary nucleobases are important to control the size of the resulting micelles co-assembled by H-bonds.

V.7. Biocompatibility of nucleobase copolymers

Since the obtained nucleobase-containing copolymers were soluble at physiological pH and might be interesting for further biomedical applications, their *in-vitro* biocompatibility was evaluated. Cytotoxicity, blood aggregation rate, as well as hemolytic activity evaluation are summarized in *Fig. 5*.

The cytotoxicity was assessed at pH 7.4 on mouse fibroblast L929 cell line, by using the PrestoBlue assay (*Fig. 5. A*).[34] This test works as a cell health indicator which uses the reducing ability of living cells to finally measure the cellular viability. [34] A cellular viability below 0.7 (or 70%) indicates a cytotoxic behavior. [34] As shown in *Fig. 5.A.*, the nucleobase containing copolymers showed a cellular viability above 95% up to concentrations of 0.7 mg/mL. Indeed, a slightly increased cell growth is observed for higher concentrations. A more detailed investigation of this phenomenon was however beyond the scope of this study.

These promising results led us to further evaluate the nucleobase containing copolymers towards blood compatibility, in terms of red blood cell aggregation activity (*Fig. 5. B.*) and hemoglobin release (*Fig. 5.C.*). The aggregation activity was expressed by the aggregation rate and compared to a polycationic commercial polymer *(i.e.*, polyethyleneimine PEI) which is known for its high aggregation rate (around 2.5).[35] All the tested copolymers showed an aggregation rate below 1.2 that underlines that they do not provoke undesired cell aggregation. This result could be explained by the neutral character of the nucleobase copolymers at physiological pH which avoided the cellular aggregation, a frequent phenomenon observed for cationic polymers. Moreover, we investigated the interaction of nucleobase copolymers with the red blood cell membrane. In this regard, the release of hemoglobin at physiological pH (pH 7.4) from the erythrocytes was measured. As presented in *Fig. 5.C.*, the hemoglobin was released in low amounts (below 1%), which is consistent with a non-hemolytic activity.[36] Overall, these results emphasize a promising potential for the neutral and hydrosoluble

nucleobase-containing copolymers as alternatives to cationic polymers in biological applications.

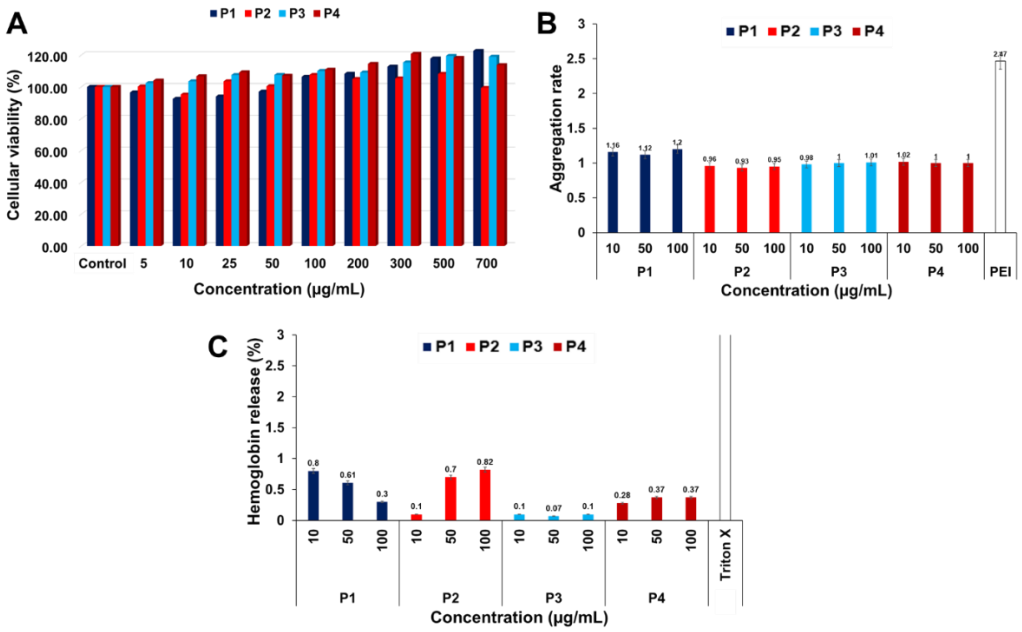

Fig. 5. Cytotoxicity of nucleobase containing copolymers evaluated on L929 mouse cell line, pH 7.4, by using as control non-treated cells (A); blood aggregation rate of copolymers evaluated at pH 7.4, on human blood (B); hemoglobin release of nucleobase copolymers tested at pH 7.4, on human blood (C).

VI. Conclusion

A set of adenine- and uracil-containing statistical and block polymethacrylate copolymers have been successfully synthesized by RAFT polymerization. The resulting macromolecular structures were different from those previously reported in the literature, as a result of their hydrophilic behaviour. The novelty of the developed co-assembled systems was that their preparation occurred exclusively in aqueous buffer. The co-assembly was mainly driven by H-bond between complementary adenine and uracil nucleobases, like in DNA. This approach is original compared to previously reported nucleobase polymethacrylate that self-assembled in organic solvents,[5] because of their insolubility in water. A range of structural parameters (number of nucleobase units per polymer, length of blocks and ratio between complementary nucleobases) were investigated to show their influence on the co-assembly behaviour and on the physico-chemical properties (aggregation number, particle size) of the resulting nano-objects. Overall, spherical co-assembled morphologies were observed by TEM. However,

significant modifications were observed (by SLS, DLS) due to the variations in the length of the nucleobase-containing block as well as in the content of complementary nucleobases. High DP of adenine blocks led to self-assembled architectures with high N_{agg}, while low DP of adenine blocks enabled the formation of small-sized spherical co-assembled objects. The uracil block had a significant contribution to the regulation of the size of the co-assemblies. Low contents in uracil groups led to co-assembled objects with high aggregation number and particle size, whereas higher contents of uracil resulted in smaller particles. Structural parameters (such as the number of the nucleobases/per polymer, the length of the nucleobase block) could thus lead to different co-assembly behaviour. We proposed that these results are a consequence of possible dynamic H-bond interchanges between the nucleobases present in the copolymers. Furthermore, individual uracil or adenine polymers showed no ability to self-assemble. This observation emphasized that complementary adenine-uracil H-bond interactions were at the core of co-assembly formation. The co-assembly by H-bonds was proven by the competition assays with urea which led to a significant decrease of N_{agg} and particle size of the co-assembled objects. Evaluation of the *in-vitro* biological properties of the nucleobase copolymers showed that they are not cytotoxic and are blood compatible. This work emphasized the huge potential to use nature inspired H-bond interactions between complementary nucleobases to develop novel co-assembled architectures which may find future application in biological systems.

VII. References

1. F. Crick, and J. Watson, © 1953 Nature Publishing Group. (1953).
2. C. Suparpprom and T. Vilaivan, *RSC Chem. Biol*., 2022, **3**, 648–697.
3. C. W. Huang, W.Ji, and S. W. Kuo, *Macromolecules*, 2017, **50(18)**, 7091–7101.
4. I. Hong-Lin, C-C. Cheng, C-W. Huang, M-C Liang, J-K. Chen, F-H Ko, C-W. Chu, C-F. Huang and F-C. Chang, *RSC Adv.*, 2013, **3**, 12598–12603.
5. C-C. Cheng, I-H.Lin, J-K. Chen, Z-S. Liao, J-J. Huang, D-J. Lee and Z. Xin, *Macromol. Biosci.*, 2016, **16(3)**, 1415–1421.
6. H. S. Bazzi and H. F. Sleiman, *Macromolecules*, 2002, **35(26)**, 9617–9620.
7 . H. Lu, J. Cai, K. Zhang, *Polym. Chem.*, 2021, **12**, 2193–2204.
8. M. Garcia, K. Kempe, D. M. Haddleton, A. Khan, A. Marsh, *Polym. Chem.*, 2015, **6**, 1944–1951.
9. Y. Kang, A. Pitto-Barry, H. Willcock, W-D. Quan, N. Kirby, A. M. Sanchez and R. K. O'Reilly, *Polym. Chem.*, 2015, **6**, 106–117.
10. Z. Hua, A. Pitto-Barry, Y. Kang, N. Kirby, T. R. Wilks and R. K. O'Reilly, *Polym.*

Chem., 2016, **7**, 4254–4262.

11. Z. Hua, R. Keogh, Z. Li, T. R. Wilks, G. Chen and R. K. O'Reilly, *Macromolecules*, 2017, **50 (9)**, 3662–3670.
12. Z. Hua, T. R. Wilks, R. Keogh, G. Herwig, V. G. Stavros, R. K. O'Reilly, *Chem. Mater.*, 2018, **30(4)**, 1408–1416.
13. Y. Kang, A. Lu, A. Ellington, M.C. Jewett and R. K. O'Reilly, *ACS Macro Lett*., 2013, **2(7)**, 581-586.
14. Y. Kang, A. Pitto-Barry, M. S. Rolph, Z. Hua, I. Hands-Portman, N. Kirby and R. K. O'Reilly, *Polym. Chem.*, 2016, **7**, 2836–2846.
15. H. Yang, and W. Xi, *Polymers*, 2017, **9(12)**, 666-690.
16. S.Varlas, Z. Hua, J. R. Jones, M. Thomas, J. C. Foster and R. K. O'Reilly, *Macromolecules*, 2020, **53(22)**, 9747-9757.
17. G. B. Schuster, B. J. Cafferty, S. C. Karunakaran, and N. V. Hud, *J. Am. Chem. Soc.*, 2021, **143(25)**, 9279-9296.
18. S. C. Larnaudie, J. C. Brendel, I. Romero-Canélon, C. Sanchez-Cano, S. Catrouillet, J. Sanchis, J. P. C. Coverdale, J-I. Song, A. Habtemariam, P. J. Sadler, K. A. Jolliffe and S. Perrier, *Biomacromolecules*, 2018, **19(1)**, 239-247.
19. E. Obert, M. Bellot, L. Bouteiller, F. Andrioletti, C. Lehen Ferrenbach, F. Boué, *J. Am. Chem. Soc.*, 2007, **129**, 15601–15605.
20. S. Han, E. Nicol, F. Niepceron, O. Colombani, S. Pensec, L. Bouteiller, *Macromol. Rapid Commun.*, 2018, 1800698–180070316.
21. D. Bochicchio, M. Salvalaglio and G. M. Pavan, *Nat. Commun.*, 2017, **147(8)**,1–11.
22. Y. Kang, A. Pitto-Barry, M. S. Rolph, Z. Hua, I. Hands-Portman, N. Kirby and R. K. O'Reilly, *Polym. Chem.*, 2016, **7**, 2836–2846.
23. L. V. Arsenie, F. Hausig, C. Kellner, J. C. Brendel, P. Lacroix-Desmazes, V. Ladmiral and S. Catrouillet, *Molecules*, 2022, **27**, 4233-4288.
24. K. E. B. Doncom, A. Pitto-Barry, H. Willcock, A. Lu, B. E. McKenzie, N. Kirby and R. K. O'Reilly, *Soft Matter*, 2015, **11**, 3666–3676.
25. J. P. Patterson, M. P. Robin, C. Chassenieux, O. Colombani, and R. K. O'Reilly, *Chem Soc Rev.*, 2014, **43**, 2412-2425.
26. R. Xu, *Particuology* , 2015, **18**, 11-21.
27. H. A. Spijker, F. L. van Delft and J. C. M. van Hest, *Macromolecules*, 2007, **40 (1)**, 12–18.
28. J. Thevenot, A-L.Troutier, L. David, T. Delair, and C. Ladavière, *Biomacromolecules*, 2007, **8(11)**, 3651–3660.
29. S. Scott, C. Shaheen, B. McGuinness, K. Metera, F. Kouzine, D. Levens, C. J. Benham and S. Leslie, *Nucleic Acids Res.*, 2019, **47(12)**, 6360-6368.
30. W. Zhang, M. Liu, C. Lee, B. J. Salena, and Y. Li, *Sci. Rep.* 2018, **8**, 3–10.

31. W. K. Lim, J. Rosgen and S. Walter Englander, *PNAS*, 2009, **106(8)**, 2595-2600.

32. A. Bende, *Theor Chem Acc*, 2010, **125**, 253–268.

33. F. Jia, H. Li, R. Chen, and K. Zhang, *Bioconjug. Chem.*, 2019, **30(7)**, 1880–1888.

34. M. Xu, D. J. McCanna, and J. G. Sivak, *J. Pharmacol. Toxicol. Methods*, 2015, **71**, 1–7.

35. A. Frère, M. Kawalec, S. Tempelaar, P. Peixoto, E. Hendrick, O. Peulen, B. Evrard, P. Dubois, L. Mespouille, D. Mottet and G. Piel, *Biomacromolecules*, 2015, **16(3)**, 769–779.

36. I. Greco, N. Molchanova, E. Holmedal, H. Jenssen, B. D. Hummel, J. L. Watts, J. Hakansson, P. R. Hansen and J. Svenson, *Sci. Rep.*, 2020, **10**, 1–13.

VIII. Acknowledgements

The authors kindly thank to Philippe Gonzales (IBMM, Montpellier, France) who performed dn/dc measurements, as well as to Carolin Kellner (IOMC, Jena, Germany) who performed the biological investigations. This research was funded by DAAD (German Academic Exchange Service) Research Grants- Short Term Grants 2022 (Funding program number: 57588366) as well as by the French Ministry of higher education and research and the PHC Procope program (Project-ID: 48137ZE). JCB further thank the German Science Foundation (DFG) for generous funding within the Emmy-Noether Programme (Project-ID: 358263073).

IX. Supplementary Information

Table of contents

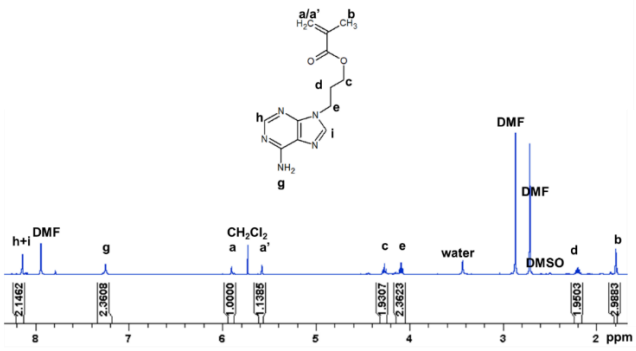

Fig. S1 ^{1}H-NMR spectrum of 3-(adenin-9-yl)propyl methacrylate (AdMA)

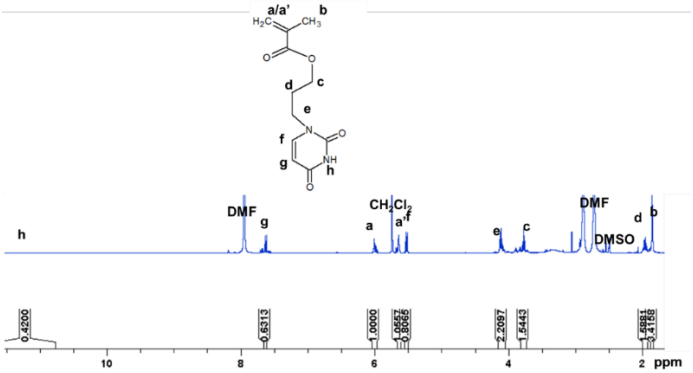

Fig. S2 ^{1}H-NMR spectrum of 3-(uracil-1-yl)propyl methacrylate (UrMA)

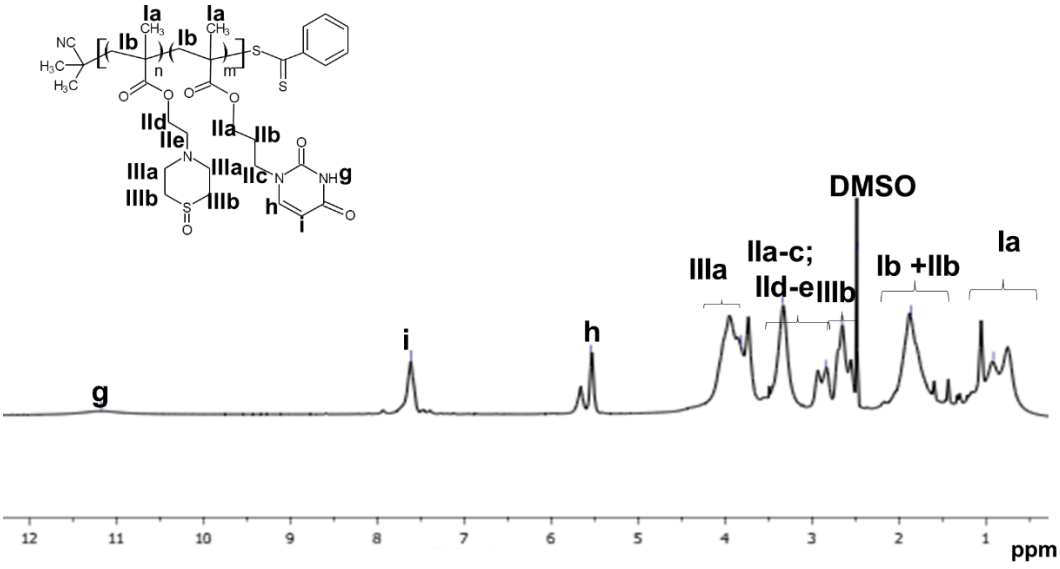

Fig. S3 ^{1}H-NMR spectrum of Poly((3-(uracil-1-yl) propyl methacrylate) -*stat*-(2-ethyl thiomorpholine oxide methacrylate)) P(UrMA$_n$ -*stat*-THOXMA$_m$)

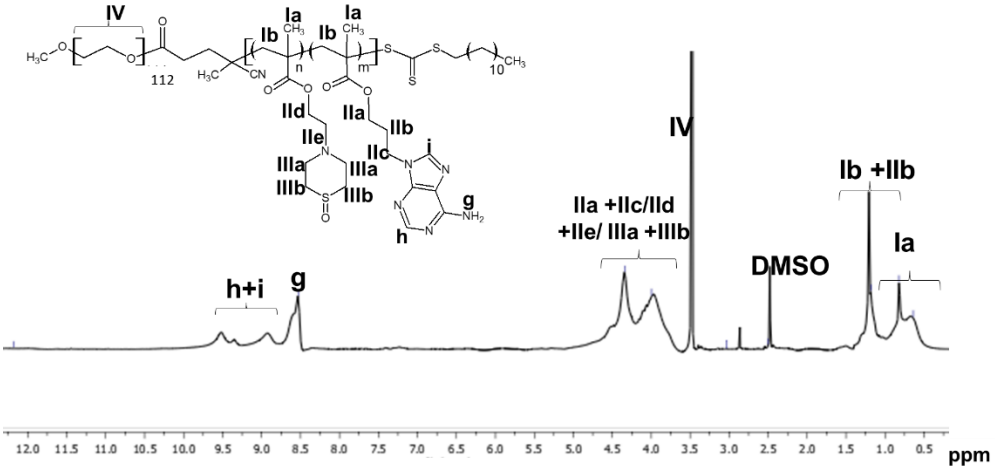

Fig. S4 ^{1}H-NMR spectrum of Poly(ethylene glycol)-*b*-Poly((3-(adenine-9-yl) propyl methacrylate) -*stat*-(2-ethyl thiomorpholine oxide methacrylate)) PEG$_{112}$-*b*-P(AdMA$_n$ -*stat*-THOXMA$_m$)

Table S1 Properties of developed co-assembled formulations

Code	Co-assembly formulation	Molar ratio between Ur/Ad units	Aggregation number (N_{agg})[a]	Particle size (D_H)[b]
A	P1+P2	1:1	315	130
B	P3+P2	1:1	194	101
C	P3+P4	1:1	9.95	40
D	P1+P4	1:1	7.8	35
E	P1+P2	0.1:1	44	58
F	P3+P2	0.1:1	47.6	52
G	P3+P4	0.1:1	12	28.5
H	P1+P4	0.1:1	5.2	31
I	P1+P2	10:1	101	81
J	P3+P2	10:1	92	75
K	P3+P4	10:1	33	21
L	P1+P4	10:1	21	29

[a]Evaluated by SLS: for 0.1:1 and 1:1 stoechiometries the measurements were performed at different concentrations (ranging from 1 g/L to 5 g/L), according to the protocol presented in Materials and Methods section; for 10:1 stoechiometry, the measurements were performed at a mass concentration of 5 g/L; [b]Evaluated by DLS, at a concentration of 5 g/L.

Table S2 Molar mass of individual unimers (M_u) vs. apparent molar mass and aggregation number N_{agg} of objects in the starting polymer solutions (evaluated by SLS)

Polymer entry	Molar mass of unimers (M_u, g/mol)*	Apparent molar mass (g/mol, by SLS)	Aggregation number (N_{agg})
P1	12100	20000	1.6
P2	39864	300000	7.5
P3	11550	38000	3.3
P4	8769	100000	11.4

*** M_u determined by multiplying the M_n (determined by end-group analysis from ^{1}H-NMR spectroscopy) by the corresponding M_w/M_n values determined by SEC**

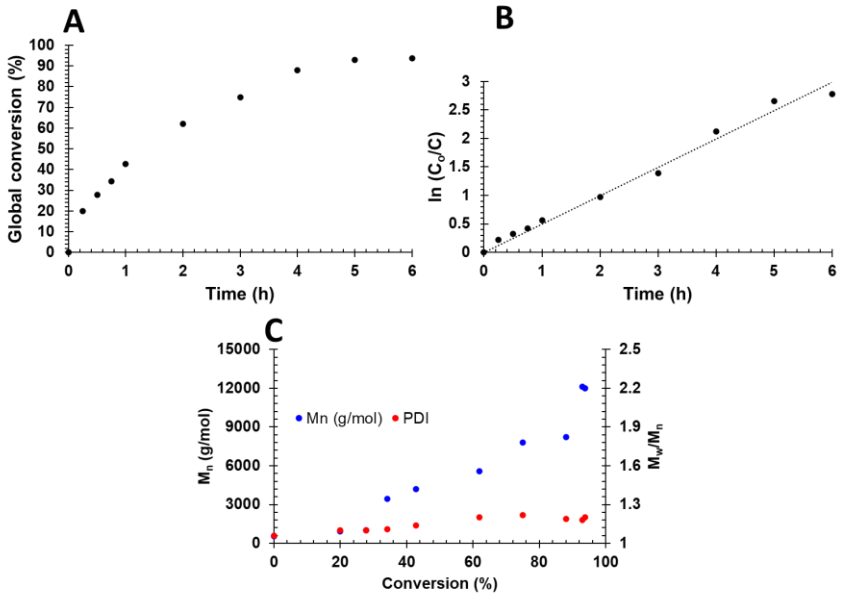

Fig. S5 (A) Overall conversion evaluated by ^{1}H-NMR; (B) Representation of ln(C_o/C) versus time for statistical copolymers prepared by RAFT; (C) Evolution of number-average molecular weight M_n and dispersity (Đ) versus global monomer conversion monitored by SEC. Experiments performed for P(UrMA$_n$ -*stat*-THOXMA$_m$)

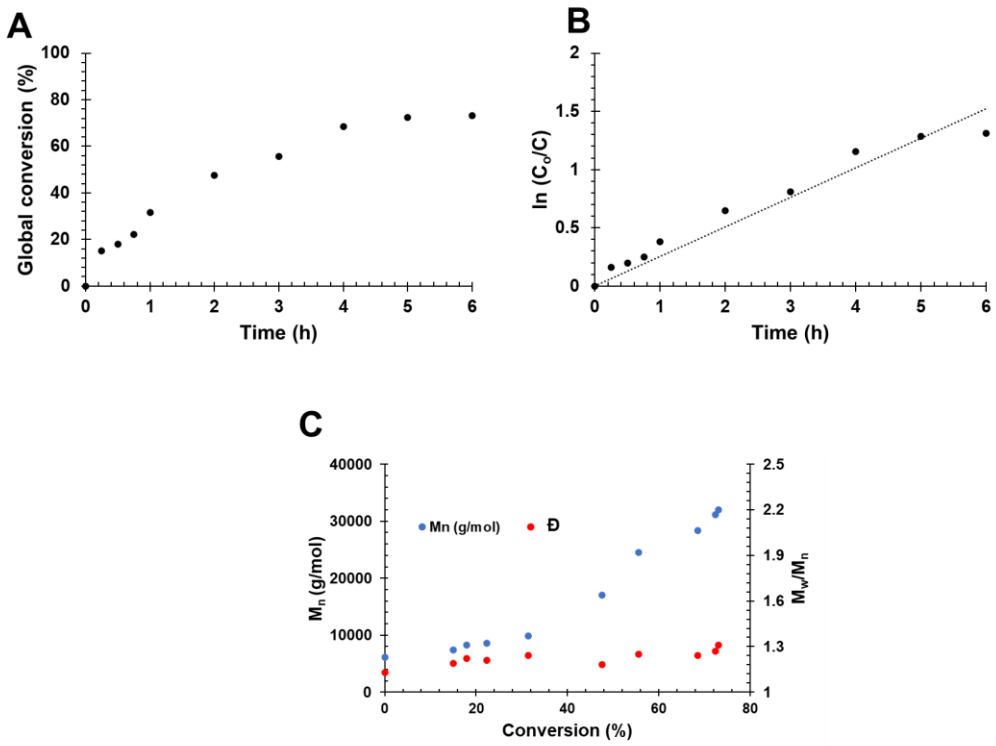

Fig. S6 (A) Overall conversion evaluated by ^{1}H-NMR; (B) Representation of ln(C_0/C) versus time for statistical copolymers prepared by RAFT; (C) Evolution of number-average molecular weight M_n and dispersity (Đ) versus global monomer conversion monitored by SEC. Experiments performed for PEG$_{112}$-*b*-P(AdMA$_n$ -*stat*-THOXMA$_m$)

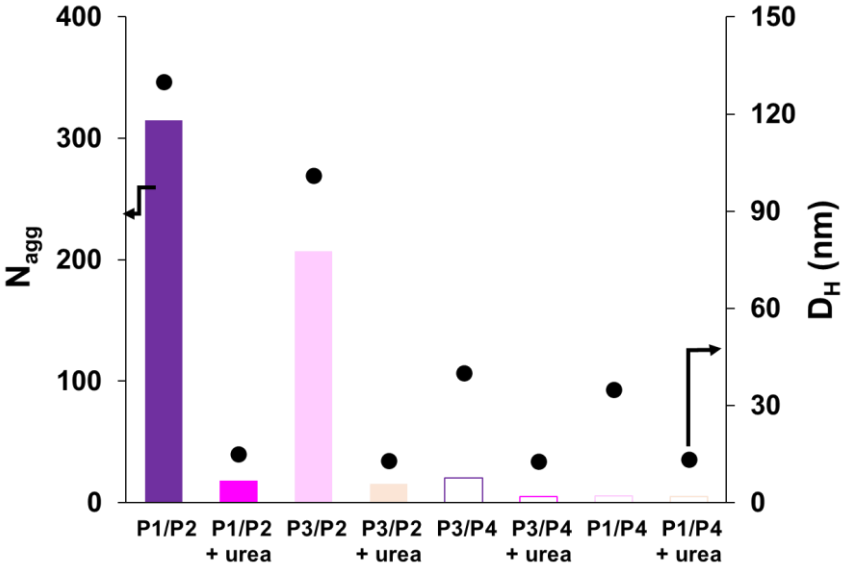

Fig. S7 Urea effect on the co-assembled structures: N_{agg} and D_H evolution data

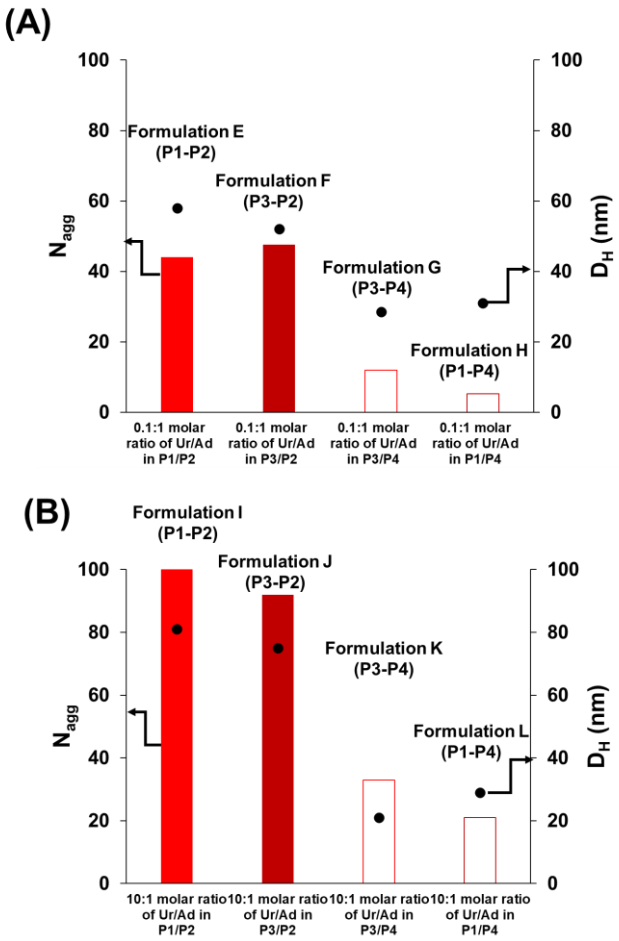

Fig. S8 N_{agg} (determined by SLS) and D_H (determined by DLS) for the co-assembled nucleobase copolymer compositions for a ratio 0.1/1 of Ur/Ad (A) and 10/1 of Ur/Ad (B).

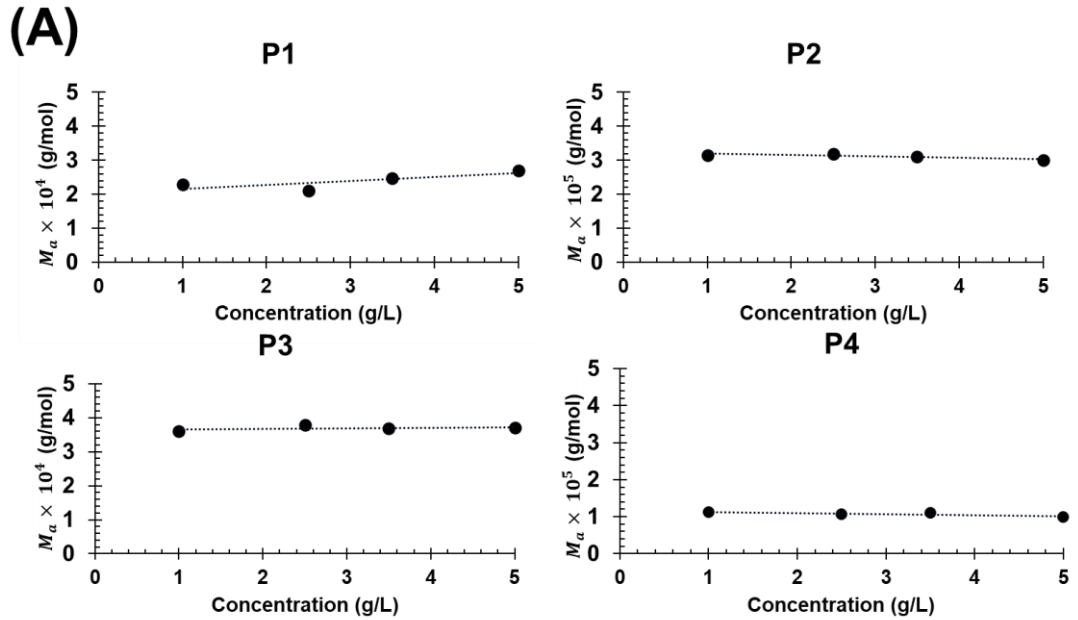
(A)
P1
P2
P3
P4
$M_a \times 10^4$ (g/mol)
$M_a \times 10^5$ (g/mol)
Concentration (g/L)

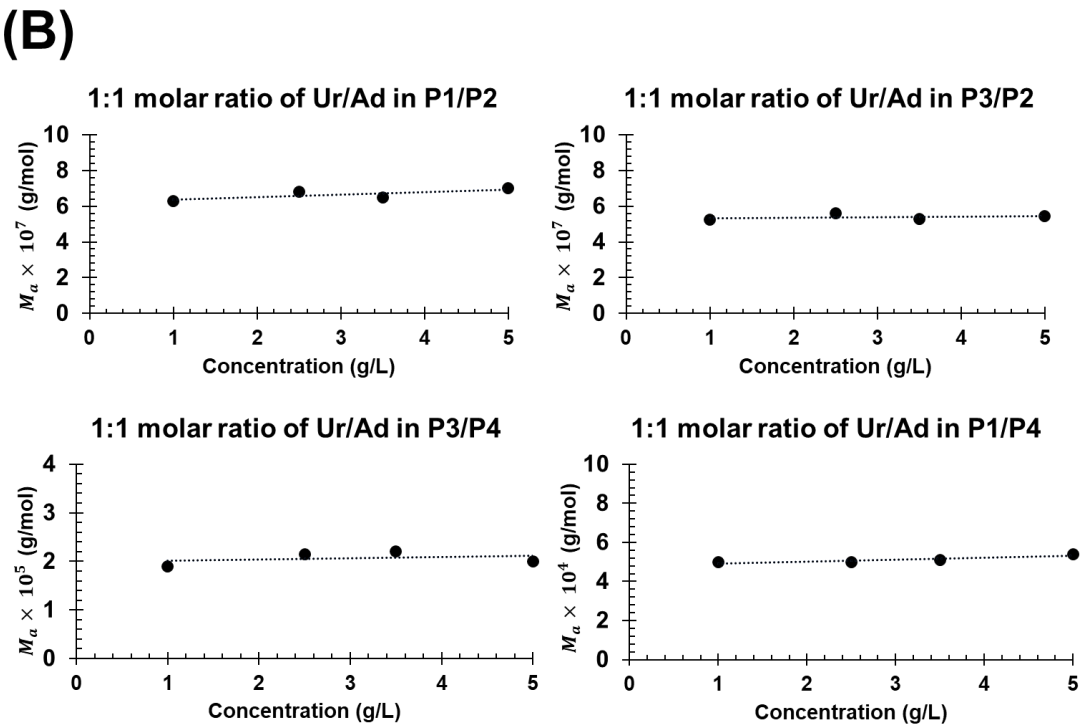
(B)
1:1 molar ratio of Ur/Ad in P1/P2
1:1 molar ratio of Ur/Ad in P3/P2
1:1 molar ratio of Ur/Ad in P3/P4
1:1 molar ratio of Ur/Ad in P1/P4
$M_a \times 10^7$ (g/mol)
$M_a \times 10^5$ (g/mol)
$M_a \times 10^4$ (g/mol)
Concentration (g/L)

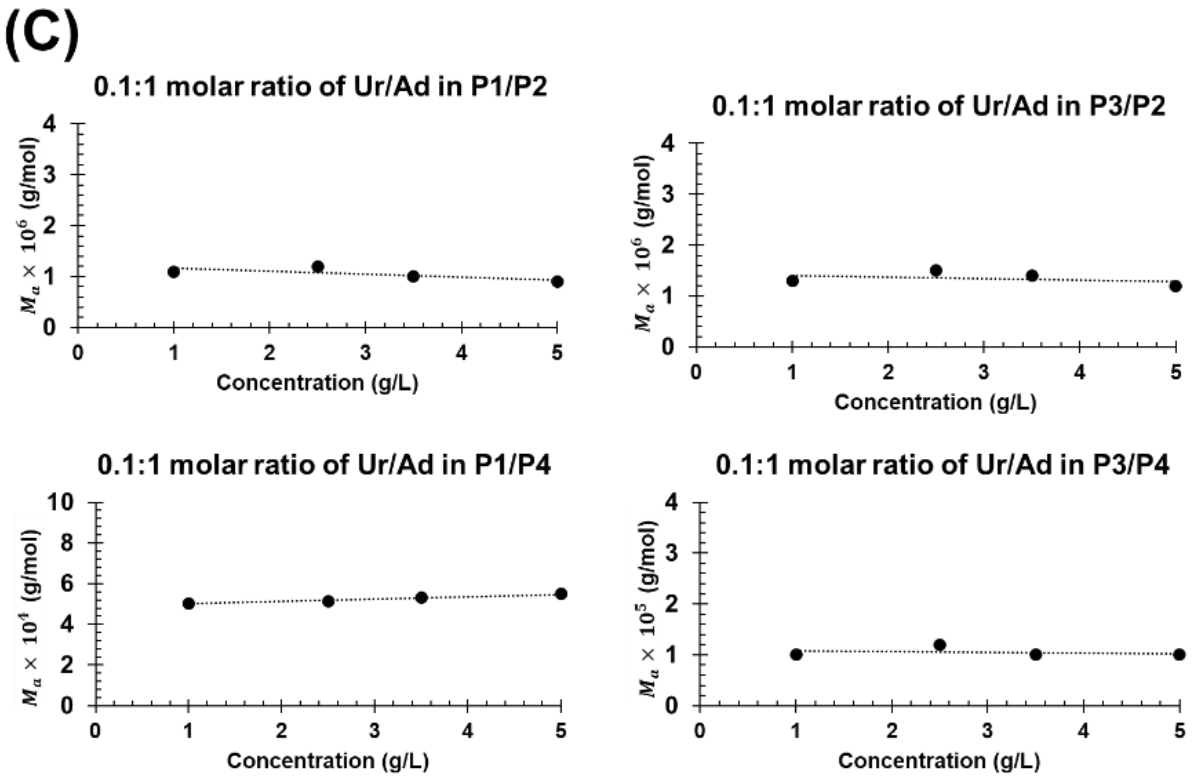

Fig. S9 Evolution of apparent molecular weight (M_a) at different concentrations (g/L) for different formulations (A) individual polymer solutions; (B) formulations using 1:1 molar ratio between uracil and adenine nucleobases; (C) formulations using 0.1:1 molar ratio between uracil and adenine nucleobases

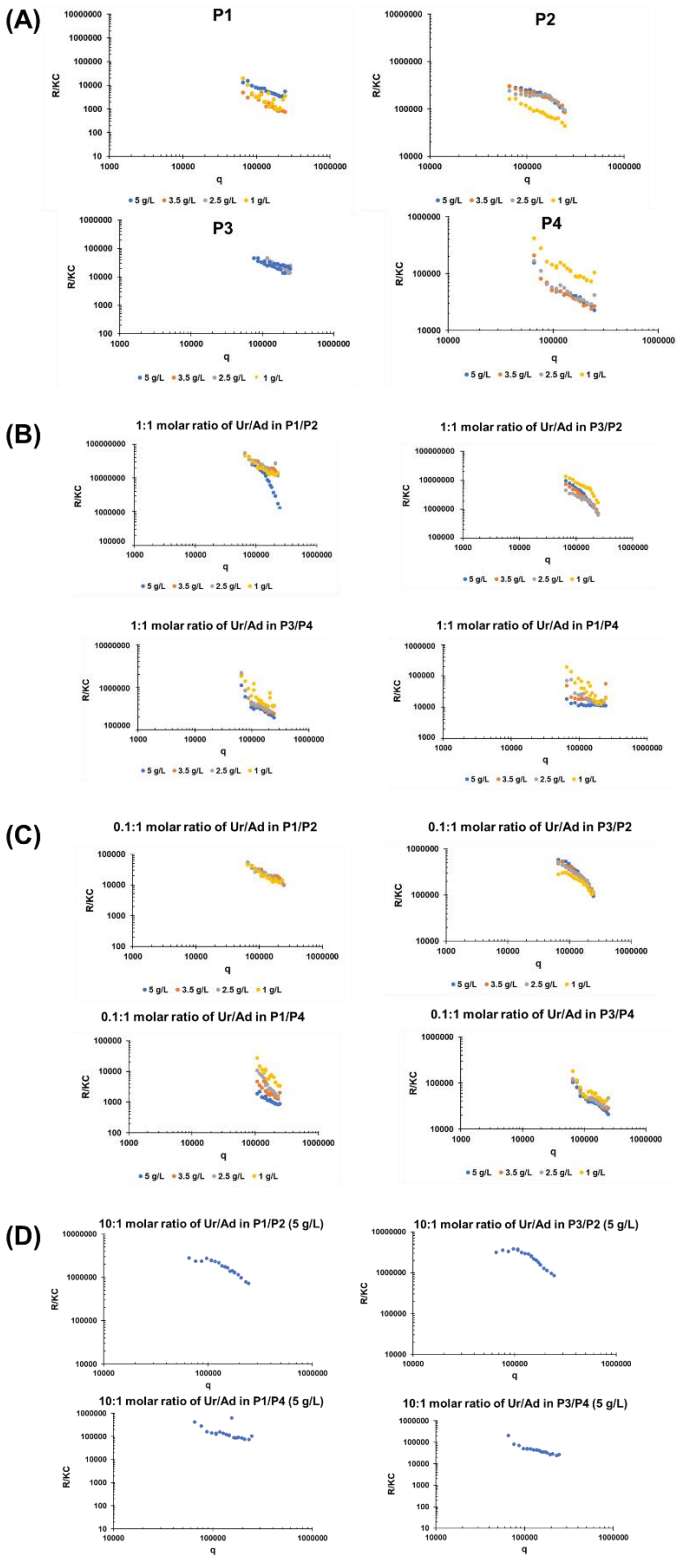

Fig. S10 Evolution of R/KC over q for different formulations (A) individual polymer solutions; (B) formulations using 1:1 molar ratio between uracil and adenine nucleobases; (C) formulations using 0.1:1 molar ratio between uracil and adenine nucleobases; (D) formulations using 10:1 molar ratio between uracil and adenine nucleobases.

Equations used for polymer characterisation

A. Characterisation of P(UrMA$_n$ -stat-THOXMA$_m$) copolymers

- *Conversion of co-monomers*

The conversions of co-monomers were calculated by ^{1}H NMR (Eq. S1.), *via* the comparison of signal integrals of the CPDB (7.4-7.9 ppm) and of the protons of -C=C- double bond of *THOXMA* (6.06-5.68 ppm) and/or *UrMA* (5.99-5.73 ppm).

$$\text{Conversion (\%)} = \frac{(I_{0,vinyl\ function}/I_{0,CTA}) - (I_{t,vinyl\ function}/I_{t,CTA})}{(I_{0,vinyl\ function}/I_{0,CTA})} \times 100 \quad \text{(Eq. S1.)}$$

Where $I_{0,CTA}$ and $I_{t,CTA}$ are the values of the integrals of the signal of the aromatic protons of the chain transfer agent (between 7.4 ppm and 7.9 ppm) at t=0 and t respectively; $I_{0,vinyl\ function}$ and $I_{t,vinyl\ function}$ are the value of the integral of the signal of one of the protons of the vinyl group of methacrylate (5.68 ppm and 6.06 ppm for *THOXMA*, 5.73 ppm and 5.99 ppm for *UrMA*), at t=0 and t respectively.

- *Degree of polymerisation*

DP$_{\text{uracil copolymer}}$ was calculated as a sum between the number of *UrMA* (noted as DP$_{\text{UrMA synthons}}$) and *THOXMA* (noted as DP$_{\text{THOXMA}}$).

The number of *UrMA* was calculated considering the integral values at 5.56-5.58 ppm and 7.64 ppm that correspond to -C=C- double bond protons of uracil, compared to the two of the protons of CPBD (between 7.88 ppm and 7.9 ppm) as it follows (Eq. S2.):

$$\text{DP}_{\text{UrMA}} = \left(\frac{(I_1+I_2)/2}{I_{CTA}/2}\right) \quad \text{(Eq. S2.)}$$

Where I_1 is the value of the integral of the signal of the proton of double bond of uracil heterocycle (between 7.6 ppm and 7.83 ppm (H_i)), I_2 is the value of the integral of the other signal of the proton of double bond of uracil heterocycle (between 5.31 ppm and 5.71 ppm (H_h)), and I_{CTA} is the value of the integral of the signal of two of the aromatic protons of the chain transfer agent (between 7.88 ppm and 7.9 ppm).

The number of *THOXMA* were calculated according to Eq. S3.:

$$\text{DP}_{\text{THOXMA}} = \left(\frac{(I_3+I_4+I_5-2(I_1+I_2))/12}{I_{CTA}/2}\right) \text{(Eq. S3.)}$$

The I_3 and I_4 are the values of the integrals of the proton signals in the field of 3.5 ppm-4.5 ppm and 2.52 ppm- 2.82 ppm respectively that correspond to the protons of thiomorpholine oxide cycle (**III$_a$ and III$_b$**). I_5 is the value of the integral of the protons of *UrMA* aliphatic linker

(**II_a and II_c)**, and the protons of *THOXMA* aliphatic linker (**II_d and II_e)** in the field of 2.82 ppm-3.48 ppm. To calculate the DP of *THOXMA*, the sum of integrals corresponding to these signals was assessed. Because this sum includes the integral of the protons of *UrMA* aliphatic linker, these values (I_1 and I_2) were subtracted in order to correctly evaluate the DP of *THOXMA*. However, it was impossible to determine exactly the region where the protons of *UrMA* aliphatic linker were situated, due to signal interferences. Since in *UrMA*, 4 protons of aliphatic linker are present in the field of 2.52 ppm- 4.55 ppm, the sum of integrals of uracil double bond protons (that correspond to 2 protons in *UrMA*) was multiplied by 2, to calculate the integral value of *UrMA* aliphatic linker protons. Then, this multiplied value (corresponding with the *UrMA* aliphatic linker) was subtracted and the result was divided by 12 (that correspond to the total of protons of thiomorpholine oxide cycle and *THOXMA* aliphatic linker).
Then, $DP_{uracil\ copolymer}$ was calculated (Eq. S4.):

$$DP_{uracil\ copolymer} = DP_{UrMA} + DP_{THOXMA} \text{ (Eq. S4.)}$$

- *Experimental molar percentage of co-monomers*

The molar percentage of *UrMA* and *THOXMA* were calculated according to the equations:

$$\%\text{ (molar) of } UrMA = (DP_{UrMA} \times 100) / DP_{uracil\ copolymer} \text{ (Eq. S5.)}$$

$$\%\text{ (molar) of } THOXMA = (DP_{THOXMA} \times 100) / DP_{uracil\ copolymer} \text{ (Eq. S6.)}$$

- *Experimental M_n*

The experimental M_n of P($UrMA_n$-*stat*-$THOXMA_m$) copolymer was calculated as:

$$M_n = (\%\text{ (molar) of UrMA} \times DP_{uracil\ copolymer} \times M_{th\ of\ UrMA}) + (\%\text{ (molar) of THOXMA} \times DP_{uracil\ copolymer} \times M_{th\ of\ THOXMA}) + M_{th,CTA} \text{ (Eq. S7.)}$$

Where % (molar) of UrMA was calculated by Eq. S5., % (molar) of THOXMA was calculated by Eq. S6., $DP_{uracil\ copolymer}$ was calculated by Eq. S4. $M_{th,CTA}$ = 221.34 g/mol, $M_{th\ of\ THOXMA}$ = 231 g/mol, $M_{th\ of\ UrMA}$ = 238 g/mol.

B. Characterisation of PEG-*b*-P(AdMA$_n$ -stat-THOXMA$_m$) copolymers

- *Conversion of co-monomers*

The conversions of co-monomers were calculated by ^{1}H NMR (Eq. S8.), *via* the comparison of signal integrals of the PEG region (noted as region IV) of the macro-CTA agent (3.48-3.58 ppm) and of the protons of -C=C- double bond of *THOXMA* (6.06-5.68 ppm) and/or *AdMA* (5.95-5.72 ppm).

$$\text{Conversion (\%)} = \frac{(I_{0,vinyl\ function}/I_{0,macroCTA}) - (I_{t,vinyl\ function}/I_{t,macro\ CTA})}{(I_{0,vinyl\ function}/I_{0,macro\ CTA})} \times 100 \quad \text{(Eq. S8.)}$$

Where $I_{0,macro\ CTA}$ and $I_{t,macroCTA}$ are the values of the integrals of the signal of the methylene protons of the PEG region of the macro-chain transfer agent (between 3.48 ppm and 3.58 ppm) at t=0 and t respectively; $I_{0,vinyl\ function}$ and $I_{t,vinyl\ function}$ are the value of the integral of the signal of one of the protons of the vinyl group of methacrylate (5.68 ppm and 6.06 ppm for *THOXMA*, 5.72 ppm and 5.95 ppm for *AdMA*), at t=0 and t respectively.

- *Degree of polymerisation of the adenine containing block*

DP$_{\text{adenine containing block}}$ was calculated as a sum between the number of *AdMA* (noted as DP$_{\text{AdMA}}$) and *THOXMA* (noted as DP$_{\text{THOXMA}}$).

The number of *AdMA* was calculated considering the integral values at 8.7-9.3 ppm and 9.48-9.56 ppm that correspond to the heterocycle protons of adenine (noted with h and i), compared to the methylene protons of the PEG region (region IV) of the macro-CTA (between 3.48 ppm and 3.58ppm) as it follows (Eq. S9.). The DP of the macro-CTA is equal to 112, so it is assigned to 112 ethylene glycol units. Since 1 unit of ethylene glycol contains 4 protons, in the PEG region (with 112 ethylene glycol units) of macro-CTA we have 4x 112= 448 protons.

$$\text{DP}_{\text{AdMA}} = \left(\frac{(I_1+I_2)/2}{I_{macroCTA}/448}\right) \quad \text{(Eq. S9.)}$$

Where I_1 is the value of the integral of the signal of the first proton of adenine heterocycle (between 8.7 ppm and 9.3 ppm (H_h)), I_2 is the value of the integral of the other signal of the proton of double bond of uracil heterocycle (between 9.48 ppm and 9.56 ppm (H_i)), and $I_{macroCTA}$ is the value of the integral of the proton signals of PEG region the macro-chain transfer agent (between 3.48 ppm and 3.58 ppm).

The number of *THOXMA* were calculated according to Eq. S10.:

$$\text{DP}_{\text{THOXMA}} = \left(\frac{(I_3+I_4-2(I_1+I_2))/12}{I_{macroCTA}/448}\right) \quad \text{(Eq. S10.)}$$

The I_3 and I_4 are the values of the integrals of the proton signals in the field of 3.7 ppm-4.3 ppm and 4.31 ppm- 4.8 ppm respectively that correspond to the protons of thiomorpholine oxide cycle (**III_a and III_b**), the protons of *AdMA* aliphatic linker (**II_a and II_c)**, and the protons of *THOXMA* aliphatic linker (**II_d and II_e)**. To calculate the DP of *THOXMA*, the sum of integrals corresponding to these signals was assessed. Because this sum includes the integral of the protons of *AdMA* aliphatic linker, these values were subtracted in order to correctly evaluate the DP of *THOXMA*. However, it was impossible to determine exactly the region where the protons of *AdMA* aliphatic linker were situated, due to signal interferences. Since in *AdMA* 4 protons of aliphatic linker are present in the field of 3.7 ppm- 4.8 ppm, the sum of integrals of the protons of adenine heterocycle (that correspond to 2 protons in *AdMA* monomer) was multiplied by 2, to calculate the integral value of *AdMA* aliphatic linker protons. Then, this multiplied value (corresponding with the *AdMA* aliphatic linker) was subtracted and the result was divided by 12 (that correspond to the total of protons of thiomorpholine oxide cycle and *THOXMA* aliphatic linker).

Then, $DP_{\text{adenine containing block}}$ was calculated (Eq. S11.):

$$DP_{\text{adenine containing block}} = DP_{\text{AdMA}} + DP_{\text{THOXMA}} \text{ (Eq. S11.)}$$

- *Experimental molar percentage of co-monomers*

The molar percentage of *AdMA* and *THOXMA* were calculated according to the equations:

$$\%\text{ (molar) of } AdMA = (DP_{AdMA} \times 100) / DP_{adenine\ containing\ block} \text{ (Eq. S12.)}$$

$$\%\text{ (molar) of } THOXMA = (DP_{THOXMA} \times 100) / DP_{adenine\ containing\ block} \text{ (Eq. S13.)}$$

- *Experimental M_n*

The experimental M_n of PEG-*b*-P($AdMA_n$ -stat-$THOXMA_m$) was calculated as:

M_n = (% (molar) of AdMA $\times DP_{\text{adenine containing block}} \times M_{\text{th of AdMA}}$) + (% (molar) of THOXMA $\times DP_{\text{adenine containing block}} \times M_{\text{th of THOXMA}}$) + $M_{\text{n (macro CTA)}}$ (Eq.S14.)

Where % (molar) of AdMA was calculated by Eq. S12., % (molar) of THOXMA was calculated by Eq. S13., $DP_{\text{adenine containing block}}$ was calculated by Eq. S11. $M_{\text{th,CTA}}$ = 5400 g/mol, $M_{\text{th of THOXMA}}$ = 231 g/mol, $M_{\text{th of AdMA}}$ = 261 g/mol.

Equation used for the preparation of co-assembled formulations

The volumes of uracil-containing copolymer solution (noted as V_1) and of adenine-containing copolymer solution (noted as V_2) were calculated according to the following equations (Eq. S15. And Eq. S16):

$$V_1 = \frac{R \times c_2 \times Number_{Ad} \times M_{Ur\ polymer}}{c_1 \times Number_{Ur} \times M_{Ad\ polymer} + R \times c_2 \times Number_{Ad} \times M_{Ur\ polymer}}$$ (Eq. S15.)

Where:

V_1 is the volume (in mL) of the uracil-containing copolymer solution; R is the molar ratio between the molar equivalents of the number of uracil groups and the number of adenine groups; $Number_{Ad}$ is the number of adenine groups in the copolymer; $Number_{Ur}$ is the number of uracil groups in the copolymer; c_1 is the concentration of uracil containing copolymer (in mg/mL); c_2 is the concentration of adenine containing copolymer (in mg/mL); $M_{Ur\ polymer}$ is the molecular weight of uracil containing copolymer (calculated by ^{1}H-NMR, according to the Eq. S7.) and $M_{Ad\ polymer}$ is the molecular weight of adenine containing copolymer (calculated by ^{1}H-NMR, according to the Eq. S14.).

$$V_2 = V_{total} - V_1$$ (Eq. S16.)

Where: V_2 is the volume (in mL) of the adenine-containing copolymer solution and V_{total} is the total volume (in mL) of the formulation prepared by using uracil-containing and adenine-containing copolymers.

Conclusion Chapitre III

Dans cette partie, des copolymères statistiques de type polymétacrylate contenant de l'adénine et de l'uracile ont été synthétisés avec succès par polymérisation RAFT. Leur originalité est leur solubilité dans l'eau, ce qui n'avait pas été obtenu auparavant dans le cas de copolymères dérivés de nucléobases. Le caractère hydrophile de ces polymères a été apporté par des co-monomères méthacrylate d'oxyde de thiomorpholine ainsi que des macromonomères dérivés du PEG.

L'étude des solutions de polymères d'uracile et d'adénine individuelles (par SLS et DLS) ont relevées des nombres d'agrégations très proches de ceux des unimères. Tandis que leurs mélanges ont conduit à des nombres d'agrégation drastiquement plus élevés que ceux des unimères de départ. Ces résultats montrent que le co-assemblage de ces systèmes développés à pH physiologique présente la particularité d'être principalement dirigé par les liaisons hydrogène entre des nucléobases complémentaires (adénine-uracile). Cette hypothèse a été vérifiée par des suivis de l'évolution du nombre d'agrégation (par SLS) et de la taille des particules (par DLS) en présence d'urée (qui est une molécule compétitrice des liaisons hydrogène), qui ont montré une diminution significative du nombre d'agrégation et de la dimension des nano-objets après l'ajout de l'urée.

Différents paramètres (nombre d'unités nucléobase/par polymère, longueur des blocs polymères et rapport entre les nucléobases complémentaires) et leur effet sur la formation de co-assemblage ont ensuite été étudiés. Il est à noter que tous les systèmes observés ont mené à des morphologies sphériques. Cependant, ces paramètres ont conduit à des différences significatives par des techniques de diffusion de la lumière (SLS, DLS). Globalement, ces travaux ont montré que des DP élevés du bloc d'adénine sont propices à la formation des co-assemblages avec des N_{agg} élevés, tandis que pour l'uracile ce sont les DP faibles qui sont favorables pour obtenir des N_{agg} élevés et des tailles d'objets grandes. Nous avons proposé que ces résultats sont la conséquence d'échanges dynamiques de liaisons hydrogène entre les bases nucléiques présentes dans les polymères préparés, mais qui sont guidées par la nature de l'architecture des polymères de départ.

Enfin, les essais *in-vitro* n'ont montré aucune cytotoxicité (même à concentration élevée en polymère), ainsi qu'une bonne hémocompatibilité sur des échantillons de sang humain. Ces résultats sont meilleurs que ceux obtenus par le standard que représente le PEG. Ces travaux ouvrent de nouvelles portes vers l'utilisation des co-assemblages à partir des copolymères

comportant des nucléobases dans le domaine des sciences de la vie, comme par exemple la délivrance du matériel génétique.

Chapitre IV : Co-assemblages obtenues à partir de copolymères contenant des nucléobases : nouvelles plateformes présentant des morphologies modulables sous l'action des stimuli

Chapitre IV : Co-assemblages obtenues à partir de copolymères contenant des nucléobases : nouvelles plateformes présentant des morphologies modulables sous l'action des stimuli

Introduction Chapitre IV

Dans la nature, l'organisation hélicoïdale de l'ADN est la conséquence d'échanges dynamiques de liaisons hydrogène entre les nucléobases complémentaires, tandis que les interactions hydrophobes (c'est-à-dire l'empilement entre les régions aromatiques des nucléobases) sont impliquées dans la stabilisation de l'hélice d'ADN.

Cependant, dans le cas des systèmes artificiels, il y a très peu d'exemples dans la litérature portant sur des auto-assemblages dont la morphologie est dirigée par les liaisons hydrogène. Les deux principaux exemples sont les travaux dirigés par Dr. Rieger et par Dr. Perrier. Les recherches ménées par le groupe de Dr. Rieger ont montré que c'est possible, grâce à PISA, d'induire une morphologie cylindrique à partir des polymères amphiphiles décorés avec des fonctions urées présentant initialement une morphologie sphérique. Les travaux de l'équipe du Dr. Perrier ont aussi permis une transition des morphologies sphériques à des morphologies cylindriques, en décorant des copolymères amphiphiles par des peptides cycliques. Dans ce cas, la corrélation entre les morphologies obtenues et la dynamique du système a été mise en évidence par des expériences d'ITC et de FRET. Selon les résultats obtenus, les morphologies cylindriques sont causées par des liaisons hydrogène dynamiques qui diminuent favorablement l'énergie libre du système.

Dans le chapitre précédent, il a été mis en évidence que les morphologies des auto-assemblages réalisées à partir des copolymères de bases nucléiques sont conditionnées majoritairement par des liaisons hydrogène formés entre nucléobases complémentaires.

Cependant, il y a très peu de recherches sur ces polymères qui ont exploré l'influence de la cinétique or de la dynamique d'auto-assemblage sur les morphologies obtenues en milieu aqueux. Un article du groupe de Prof. O 'Reilly a mis en évidence une influence des échanges de liaisons hydrogène entre les copolymères contenant des nucléobases, sur les transitions

morphologiques qui se produisent lors de l'auto-assemblage de ces copolymères dans des solvants organiques.

Dans ce chapitre, nous étudions les co-assemblages de copolymères de nucléobases présentant des cinétiques d'association ainsi que des morphologies variables en fonction du pH. Ces co-assemblages ont été caractérisées par la diffusion de la lumière (SLS/DLS), microscopie éléctronique en transmission (TEM), ainsi que par titrage calorimétrique isotherme (ITC). Les essais ITC ont été menés en collaboration avec le Dr. Bénédicte Prélot et avec le l'ingénieur d'étude Amine Geneste (ICGM, Montpellier), tandis que les clichés TEM ont été réalisés en collaboration avec Dr. Mona Semsarilar (IEM, Montpellier). Les résultats inclus dans ce chapitre ont fait l'objet d'un troisième article de recherche qui est en cours de préparation pour soumission dans le journal **Macromolecules** (**IF : 6.057**).

Publication scientifique : Article de recherche numéro 3

Switchable pH-responsive morphologies of co-assembled nucleobase copolymers

Laura Vasilica Arsenie,[1] Mona Semsarilar,[2] Amine Geneste,[1] Phillippe Gonzales,[3] Benedicte Prélot,[1] Patrick Lacroix-Desmazes,[1] Sylvain Catrouillet[1,] and Vincent Ladmiral,[1,*]*

[1]*ICGM, University of Montpellier, CNRS, ENSCM, 34095 Montpellier, France*

[2]*IEM, University of Montpellier, CNRS, ENSCM, 34095 Montpellier, France*

[3]*IBMM, University of Montpellier, CNRS, ENSCM, 34095 Montpellier, France*

I. Graphical Abstract

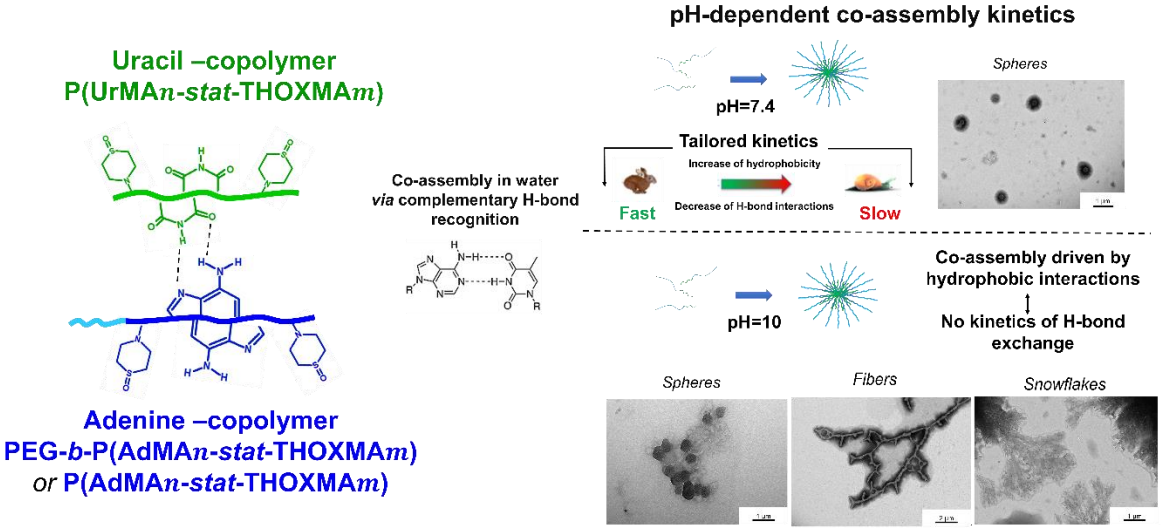

II. Abstract

This work presents supramolecular co-assembled nucleobase copolymers with transitional morphological changes induced by distinct supramolecular driving forces (H-bonds and hydrophobic interactions) at physiological pH (pH 7.4) and under alkaline conditions (pH 10). Uracil and adenine containing copolymers were prepared by RAFT, which allowed to finely tailor the polymerisation degree and the composition of the developed macromolecules. The co-assembled formulations prepared in aqueous buffer at two distinct pH (7.4 and 10) were analysed by light scattering (SLS, DLS), transmission electron microscopy (TEM), and isothermal titration calorimetry (ITC). While spherical morphologies were observed at physiological pH, the increase of the pH induced the apparition of various large anisotropic supramolecular architectures: giant spheres with a fiber like texture, dendritic morphologies and snowflake like shapes. These morphologies were a consequence of molecular recognition

via H-bonds between complementary nucleobases, as well as secondary hydrophobic interactions, since the individual uracil and adenine copolymers showed a low tendency to self-assemble. ITC revealed that the co-assembly which occurred in the systems analysed at pH 7.4 was mainly guided by H-bonds between complementary nucleobases, while the experiments conducted at pH 10 showed that the systems were mainly driven by hydrophobic interactions. These results highlighted that the type of supramolecular main driving force (H-bonds or hydrophobic interactions) impacted the morphology of nucleobase containing co-assemblies when switching the pH, which may open further perspectives in the field of anisotropic biomaterials.

III. Introduction

DNA originates from the molecular recognition by H-bonds between complementary nucleobases, as well as by hydrophobic interactions such as non-covalent van der Waals interactions, $\pi - \pi$ stacking, etc.[1] These supramolecular interactions are at the genesis of the formation of distinct helicoidal architectures of the DNA.[2]

Inspired by the genetic material, nucleobase containing polymers have therefore recently been the subject of growing interest.[3] The nucleobase motifs of these polymers act as H-bond promoters and self-assemble in supramolecular architectures with various morphologies (spheres, vesicles, cylinders, etc.)[4,5,6,7,8,9,10] Such morphologies were accessed through changes in the hydrophobic/hydrophilic balance of nucleobase containing polymers, as well as a consequence of H-bond molecular recognition between complementary nucleobases.[4,5,6,7,8,9,10]

Recent works reported the formation of complex rigid morphologies (fibers, miktostars) resulting from the self-assembly of nucleolipids,[11,12,13] and were related to hydrophobic interactions between lipid chains.[11,12] Furthermore, interesting large morphologies (dendrites, fibers, snowflakes) resulted from the self-assembly of peptide containing synthetic polymers and originated from $\pi - \pi$ transitional stacking of aromatic rings of phenyl alanine derived peptides.[14,15] Nevertheless, little is known about the true origin of the various morphologies of self-assembled nucleobase polymers, specifically if they resulted from the complementary H-bonds between nucleobases or if they were a consequence of non-covalent hydrophobic interactions.

Previous reports[16,17,18,19] on the oligonucleotides showed that the helicoidal like organisation of the DNA could be a consequence of dynamic H-bond interchanges between complementary

nucleobases, while the hydrophobic interactions (*i.e.*, stacking between aromatic regions of nucleobases) were involved in the stabilisation of the DNA helix.

In the case of artificial supramolecular assemblies made of synthetic polymers, representative examples were illustrated on the urea containing poly(isobutylene) and polystyrene polymers assembling as cylinders or micelles.[20,21] In this case, the process driving the self-assembly was described thanks to isothermal titration calorimetry (ITC) and molecular modelling experiments. The competition between the favorable decrease of the free energy of the system (produced by dynamically attractive H-bond interactions) led to cylinder type morphologies, while a nonfavorable increase of the free energy (caused by the loss of translational entropy) influenced the organisation of unimers in micelles morphologies.[20,21] Similar observations have been additionally observed for cyclic oligopeptides.[22] Moreover, recent reports in the field of urea containing polymers,[23] showed that the pH changes led to distinct morphologies which were correlated to different dynamic models of self-assembly.[23]

To the best of our knowledge, the correlation between the type of supramolecular driving force of the self-assembly and the morphological transitions resulted in aqueous medium was barely explored so far in the field of co-assemblies made of nucleobase containing polymers. A previous paper of Prof. O'Reilly's group[24] highlighted an influence of H-bond interchanges between nucleobases on the morphological transitions that occurred in the co-assembly of nucleobase copolymers in organic solvents.

In a previous paper (ref. article 2), we described for the first time the co-assembly of hydrophilic nucleobase containing polymers at physiological pH (pH 7.4). The resulted spherical micelles were supposed to be a consequence of the H-bonds between complementary nucleobases, since no co-assembly was observed for the individual uracil and adenine polymers in solution.

Starting from these preliminary results, in this paper we present pH-responsive co-assembled nucleobase copolymers with a tailorable morphology in water which is dependent on the type of main supramolecular interaction driving the co-assembly (H-bonds and/or hydrophobic interactions). RAFT copolymerisation of nucleobase containing methacrylate (adenine and uracil), and hydrophilic thiomorpholine oxide-based methacrylate led to polymers with various degree of polymerisation, block length and content of nucleobases. A range of co-assembled formulations made of uracil- and adenine-containing polymers were assessed in physiological (pH 7.4) and alkaline (pH 10) conditions. The light scattering (SLS/DLS) and TEM characterisation revealed nano-sized spherical objects at pH 7.4, while the increase of the pH

(pH 10) led to large anisotropic architectures with transitional morphologies (from textured spheres, to dendrites and snowflakes). These morphological transitions were supposed to originate from changes in the type of supramolecular main driving force (H-bonds or hydrophobic interactions), as illustrated by ITC experiments. Overall, the use of bio-inspired complementary uracil-adenine interactions enabled us to obtain supramolecular organisations with various morphologies and to get a deeper insight into the kinetics of co-assembly of pH-responsive nucleobase containing copolymers as potential biomimetic systems.

IV. Experimental section

Materials

Methacryloyl chloride (97% purity) was purchased from Fluka (Switzerland) and distilled (50°C, 400 mbar) before use. 2-bromoethanol (95% purity), adenine (Ad, 99% purity) and uracil (Ur, 98% purity) were acquired from Alfa Aesar (Germany). Thiomorpholine (98% purity) and 3-bromo-1-propanol (97% purity) were obtained from Fluorochem (UK). Hydrogen peroxide (H_2O_2) solution (30 wt%) was bought from Carlo Erba (France). 4-dimethylaminopyridine (DMAP, 96% purity), triethylamine (TEA, 99% purity), 2-cyano-2-propyl benzodithioate (CTA, 97% purity), poly(ethylene glycol) methyl ether (4-cyano-4-pentanoate dodecyl trithiocarbonate) (macro-CTA), disodiumphosphate basic dodecahydrate ($Na_2HPO_4 \cdot 12H_2O$, 95% purity), potassium carbonate (K_2CO_3, 99.9% purity), sodium hydride (NaH, 90% purity) and deuterated solvents (deuterated chloroform, $CDCl_3$, and hexadeuterodimethyl sulfoxide, DMSO-d_6) were provided by Sigma Aldrich. 2,2′-azobis(2-methylpropionitrile) (AIBN, 98% purity) was acquired from Sigma Aldrich (Germany) and recrystallised from methanol at 65°C before use. Sodium chloride (NaCl) and citric acid monohydrate ($C_6H_8O_7$ H_2O, 99% purity) were bought from VWR Chemical. Sodium bicarbonate ($NaHCO_3$, 95% purity) was purchased from Fluka (France). Dimethylformamide (DMF, 99.8% purity) was acquired from Fisher Scientific (Belgium). HEPES (4-(2-hydroxyethyl)-1-piperazineethanesulfonic acid) buffered saline solution (30 mM) was acquired from PromoCell (Germany). Dry solvents (dichloromethane, CH_2Cl_2, and acetonitrile, CH_3CN) were purified using a PureSolv Micro solvent purification system purchased from Sigma Aldrich (USA). The dialysis membranes used for purification of polymers (Spectra/Por 7 Pretreated RC Dialysis Tubing, MWCO= 1kDa, diameter 24mm, 4.6 mL/cm) were bought from Krackeler Scientific, USA.

Instrumentation

^{1}H NMR spectra were recorded on NMR Bruker Avance 400-MHz or NMR Bruker Avance III HD -400 MHz spectrometer using $CDCl_3$ or DMSO-d_6 as deuterated solvent. The chemical shifts of protons were relative to tetramethylsilane (TMS) at $\delta = 0$.

Size exclusion chromatography (SEC) was performed in DMF containing 0.1 wt. % LiCl, with a flow rate of 0.8 mL min^{-1} at 40°C. Sample were filtered using TE36 Whatman PTFE-supported membrane filter paper (0.45 µm, 47 mm diameter) before the injection. The data were calibrated using polymethyl methacrylate (PMMA) standards.

Dn/dc values in water were determined using a differential refractometer and were estimated from the integrated refractive index (RI)-signal knowing the polymer concentration. The light scattering measurements were performed using a LS spectrometer (from LS Instruments, Switzerland) incorporating a goniometer based multi-angle static light scattering (SLS) and dynamic light scattering (DLS) instrument.

Transmission electron microscopy (TEM) assays were conducted on JEOL 1200 EXII-120 kV instrument.

Isothermal Titration Calorimetry (ITC) measurements were performed by using a TAM III Thermostat.

Methods

Synthesis of 2-ethyl thiomorpholine oxide methacrylate (THOXMA)

2-ethyl thiomorpholine oxide methacrylate was synthesized by oxydation of 2-ethyl thiomorpholine methacrylate, following a previously published procedure by our team (*Scheme S1*). [25]

Synthesis of 3-(adenin-9-yl)propyl methacrylate (AdMA) and 3-(uracil-1-yl)propyl methacrylate (UrMA)

3-(adenin-9-yl)propyl methacrylate (*AdMA, Scheme S1*) and 3-(uracil-1-yl)propyl methacrylate *(UrMA, Scheme S1)* were prepared according to a previous protocol published by our group. (ref. article 2) ^{1}H NMR for *AdMA*, *Fig. S1 a* (400 MHz, DMSO-d_6) δ (ppm) = 5.9 (d, C**H**$_2$, noted as **a**); 5.58 (d, C**H**$_2$, noted as **a'**); 1.87 (s, C**H**$_3$, noted as **b**); 4.27 (t, OC**H**$_2$CH$_2$, noted as **c**); 2.20 (m, CH$_2$C**H**$_2$CH$_2$, noted as **d**); 4.10 (t, NC**H**$_2$CH$_2$, noted as **e**); 7.26 (s, N**H**$_2$, adenine heterocycle, noted as **g**); 8.15 (s, N=C**H**-N, adenine heterocycle, noted as **h**); 8.13 (s, N=C**H**-

N, adenine heterocycle, noted as **i**). ^{1}H NMR for *UrMA*, *Fig. S1 b* (400 MHz, DMSO-d_6) δ (ppm) = 6.01 (d, C**H**$_2$, noted as **a**); 5.58 (d, C**H**$_2$, noted as **a'**); 1.87 (s, C**H**$_3$, noted as **b**); 4.11 (t, C**H**$_2$CH$_2$, noted as **e**); 1.96 (m, CH$_2$C**H**$_2$CH$_2$, noted as **d**); 3.79 (t, C**H**$_2$CH$_2$, noted as **c**); 7.62 (d, C**H**=CH, uracil heterocycle, noted as **g**); 5.53 (d, CH=C**H**, uracil heterocycle, noted as **f**); 11.5 (s, N**H**, uracil heterocycle, noted as **h**).

Synthesis of Poly((3-(uracil-1-yl) propyl methacrylate) -stat-(2-ethyl thiomorpholine oxide methacrylate)) P(UrMA$_n$ -stat-THOXMA$_m$) and Poly(ethylene glycol)-b-Poly((3-(adenine-9-yl) propyl methacrylate) -stat-(2-ethyl thiomorpholine oxide methacrylate)) PEG$_{112}$-b-P(AdMA$_n$ -stat-THOXMA$_m$) by RAFT polymerisation

Statistical *P(UrMA$_n$ -stat-THOXMA$_m$)* copolymers and diblock *PEG$_{112}$-b-P(AdMA$_n$ -stat-THOXMA$_m$)* copolymers were obtained by following a previous protocol reported by our group. (ref. article 2) ^{1}H NMR for *P(UrMA$_n$ -stat-THOXMA$_m$)*, *Fig. S2 a* (400 MHz, DMSO-d_6) δ (ppm) = 1.8 (s, C**H**$_2$, polymerizable synthon, noted as **I$_b$**); 1.8 (m, C**H**$_2$, UrMA aliphatic linker, noted as **II$_b$**); 3.43 (d, C**H**$_2$, UrMA aliphatic linker, noted as **II$_a$** and **II$_c$**); 3.43 (d, C**H**$_2$, THOXMA aliphatic linker, noted as **II$_d$** and **II$_e$**); 2.62 (t, C**H**$_2$CH$_2$, thiomorpholine oxide cycle, noted as **III$_b$**); 3.87 (t, CH$_2$C**H**$_2$, thiomorpholine oxide cycle, noted as **III$_a$**); 0.87, 0.97, 1.1 (s, C**H**$_3$, noted as **I$_a$**); 7.57 (d, C**H**=CH, uracil heterocycle, noted as **i**); 5.87 (d, CH=C**H**, uracil heterocycle, noted as **h**); 11.5 (s, N**H**, uracil heterocycle, noted as **g**). ^{1}H NMR for *PEG$_{112}$-b-P(AdMA$_n$ -stat-THOXMA$_m$)*, *Fig. S2 b* (400 MHz, DMSO-d_6) δ (ppm) = 1.35 (s, C**H**$_2$, polymerizable synthon, noted as **I$_b$**); 1.35 (m, C**H**$_2$, Ad aliphatic linker, noted as **II$_b$**); 3.47 (m, C**H**$_2$, PEG, noted as **IV**); 3.96 (d, C**H**$_2$, AdMA aliphatic linker, noted as **II$_a$** and **II$_c$**); 3.96 (d, C**H**$_2$, THOXMA aliphatic linker, noted as **II$_d$** and **II$_e$**); 4.44 (t, C**H**$_2$CH$_2$, thiomorpholine oxide cycle, noted as **III$_a$** and **III$_b$**); 0.9 (s, C**H**$_3$, noted as **I$_a$**); 8.56 (s, N**H**$_2$, adenine heterocycle, noted as **g**); 8.97 (s, N=C**H**-N, adenine heterocycle, noted as **h**); 9.6 (s, N=C**H**-N, adenine heterocycle, noted as **i**).

Synthesis of Poly((3-(adenine-9-yl) propyl methacrylate) -stat-(2-ethyl thiomorpholine oxide methacrylate)) P(AdMA$_n$ -stat-THOXMA$_m$) by RAFT polymerisation

2-cyano-2-propyl benzodithioate (CTA, 1 eq.), AIBN (0.25 eq.), *adenine methacrylate (AdMA)* (x eq.) and *thiomorpholine oxide methacrylate THOXMA* ((y-x) eq.) were dissolved in a mixture of DMF/ aqueous phosphate buffer (pH 4, C_M = 4 M), in a volume ratio (DMF/buffer) of 2:1. The mixture was thoroughly degassed *via* 3 freeze–pump–thaw cycles, filled with nitrogen and immersed into an oil bath at 80 °C. At different time, an aliquot of the reaction mixture was

taken and analysed by ^{1}H NMR and SEC. After 7h, the reaction was stopped by exposure to air. The mixture was then dialysed against water (with a 1kDa MWCO membrane) for 3 days, followed by lyophilisation during 2 days. The resulting pink polymer powder was analysed by ^{1}H-NMR in DMSO-d_6 and DMF SEC. ^{1}H NMR, *Fig. S2 c* (400 MHz, DMSO-d_6) δ (ppm) = 1.35 (s, C**H**$_2$, polymerizable synthon, noted as **I$_b$**); 1.35 (m, C**H**$_2$, Ad aliphatic linker, noted as **II$_b$**); 3.96 (d, C**H**$_2$, AdMA aliphatic linker, noted as **II$_a$** and **II$_c$**); 3.96 (d, C**H**$_2$, THOXMA aliphatic linker, noted as **II$_d$** and **II$_e$**); 4.44 (t, C**H**$_2$CH$_2$, thiomorpholine oxide cycle, noted as **III$_a$** and **III$_b$**); 0.9 (s, C**H**$_3$, noted as **I$_a$**); 7.43 (s, N**H**$_2$, adenine heterocycle, noted as **g**); 8.2-8.5 (s, N=C**H**-N, adenine heterocycle, noted as **h** and s, N=C**H**-N, adenine heterocycle, noted as **i**).

Preparation of starting polymer solutions and of co-assembled formulations

The starting polymer solutions (noted as P1, P3 -uracil polymer solutions and P2, P4- adenine polymer solutions see *Table 2, Table S1*) were prepared in different buffers at pH 7.4 and pH 10 respectively, at a concentration of 5 g/L and stirred overnight at room temperature. Moreover, the co-assembled formulations were obtained by slowly adding the uracil solution to the adenine solution, the resulting mixture was then stirred for 2 days. For example, to prepare the System 1 (P1+P2, 1 mL), P1 solution (0.55 mL from a solution at concentration of 5 g/L, in buffer at pH 10, calculated as stated by Eq. S22.) was gently added by using a micropipette (15 min, 200 rpm) to P2 solution (0.46 mL from a solution at a concentration of 5 g/L, in buffer at pH 10, calculated according to Eq. S23.). Then, the solution mixture was stirred for 2 days (200 rpm, at room temperature). The solutions of starting polymers (P1, P2, P3, P4) were filtered through 0.2 μm pore size Waters filters (USA) prior to perform SLS, DLS and TEM characterisations. The absence of the concentration variation due to filtration was checked before further characterisation. Dilutions were made by adding the filtered solvent (through 0.2 μm filters) and then stirring the solution for 5 min.

Static light scattering

Static light scattering (SLS) measurements were performed using an LS spectrometer operating with a vertically polarized laser with wavelength λ = 660 nm. All measurements (including dilutions) were done at room temperature (25 °C), collected from 30° to 90° with an interval of 5°, from 90° to 110° with an interval of 10°, and up to 150° with an interval of 20°. Prior to measurements, filtered toluene and filtered buffer (through 0.2 μm pore size Waters filter membrane) were measured as reference and solvent respectively.

The Rayleigh ratio (R_θ) of the solution was determined following the Eq. 1. [26,27]

$$R_\theta = \frac{I_{solution}(\theta) - I_{solvent}(\theta)}{I_{toluene}(\theta)} \times \left(\frac{n_{solvent}}{n_{toluene}}\right)^2 \times R_{toluene} \text{ (Eq.1)}$$

where $I_{solution}$, $I_{solvent}$, and $I_{toluene}$ are the average intensities scattered by the solution, the solvent, and the reference (toluene) respectively, and $n_{solvent}$ = 1.333 (water) and $n_{toluene}$ = 1.496, and $R_{toluene} = 1.33 \times 10^{-5}$ cm^{-1} is the Rayleigh ratio of toluene for a wavelength λ = 660 nm.

At a given concentration C, R_θ is related to the apparent weight average molar mass of the scatterers (or apparent molecular weight), M_a, and to the structure factor, $S(q)$, which depends on the scattering wave vector, as shown by Eq. 2.[26,27] It is important to underline that M_a corresponds to the true molar mass (M_w) only in very dilute solutions, where the interactions between the scatterers can be neglected.[28,27] At high concentrations, interactions cause M_a to differ strongly from M_w. For this reason, in order to accurately evaluate the true M_a of the self-assemblies, SLS measurements were performed for concentrations ranging between 5 g/L and 1 g/L. Consequently, the curve representing each M_a corresponding to each tested concentration was fitted, in order to determine the real M_w of the self-assembled objects as the intercept.

$$R_\theta = K \times C \times M_a \times S(q) \text{ (Eq. 2.)}$$

with C the polymer concentration in g/L and K a constant:

$$K = \frac{4\pi^2 n_{solvent}^2}{\lambda^4 N_a}\left(\frac{\partial n}{\partial C}\right)^2 \text{(Eq. 3.)}$$

where N_a is Avogadro's number.

The aggregation number (N_{agg}) was expressed according to the Eq. 4. [26,27] :

$$N_{agg} = \frac{M_w}{M_u} \quad \text{(Eq. 4.)}$$

where N_{agg} is the aggregation number of particles, M_w is the average molar mass, and M_u is the molar mass of the unimer. M_u values were determined by multiplying their M_n (determined by ^{1}H NMR spectroscopy) by the corresponding M_w/M_n values determined by SEC. In the case of self-assembled structures, the aggregation number was evaluated by using the same equation, with an exception concerning the calculation of M_u. For self-assembled structures, the M_u was expressed as a sum between the weight ratio of each polymer multiplied by the $M_{polymer}$, according to the Eq. 5. $M_{polymer}$ was calculated by multiplying the M_n (determined by ^{1}H NMR spectroscopy) by the corresponding M_w/M_n values determined by SEC.

$$M_u = w_{polymer1} \times M_{polymer1} + w_{polymer2} \times M_{polymer2}$$ (Eq. 5.)

Dynamic Light Scattering

Particle size (Z_{ave}) of co-assembled polymers were determined by dynamic light scattering (DLS) (*Fig. S7*). The DLS instrumentation consisted of the same LS spectrometer used for SLS experiments. DLS measurements were performed at 25 °C with a He–Ne 630 nm laser module, at a detection angle of 150°.

Transmission Electron Microscopy

TEM assays were analysed by using a JEOL 1400+ instrument equipped with a numerical camera, operating with a 120 kV acceleration voltage at 25 °C. TEM samples were prepared by placing a drop (10.0 µL) of self-assembled polymers solution onto a carbon coated copper grid for 20 s, blotted with filter paper and then dried under ambient conditions.

Isothermal Titration Calorimetry

Thermodynamic data on H-bond interaction between adenine and uracil copolymers were obtained from isothermal titration calorimetry experiments at 25°C. By using a TAM III Thermostat, the measured heat flow was directly related with the extent of reaction taking place within the calorimetric cell. The setup contained a calorimetric cell and a syringe pump, which allowed the reagents to be introduced into the cell at given time periods and quantities. The homogeneity of the solution or suspension was ensured by a gold stirrer directly placed in the calorimetric cell (90 rpm). Measurements were made in the heat flow mode and in triplicate. The calorimetric cell was filled up with 800 µL of the solution of adenine copolymer *PEG_{112}-b-P($AdMA_n$ -stat-$THOXMA_m$)*, or *P($AdMA_n$ -stat-$THOXMA_m$)* respectively. The solution of uracil copolymer *P($UrMA_n$ -stat-$THOXMA_m$)* was placed in the syringe. When the thermal equilibrium had been reached, small amounts (10 µL) of the stock uracil solution were injected into the measuring cell. Injection speed was 10 s/min, and stabilization after each injection time was set at 200 min. A blank test for the dilution of each solution of uracil copolymer was carried out in the same way in order to remove the thermal influence of the dilution. Raw data were analysed using ITC software NanoAnalyze.

V. Results and Discussion

V. 1. Nucleobase-containing polymers

RAFT polymerisation was used to develop two families of water-soluble nucleobase containing polymers (*Scheme 1*), according to a previously published protocol by our group (ref. article 2). First, two uracil containing statistical copolymers *P(UrMA$_n$-stat-THOXMA$_m$)* (noted P1 and P3) were prepared. They presented the same degree of polymerisation (DP ~ 42), but different ratios of *UrMA co-monomer* (20 % and 50 %). Then, a statistical copolymer (DP ~ 100) made of *AdMA co-monomer* and *THOXMA co-monomer* using CPDT as CTA, *P(AdMA$_n$-stat-THOXMA$_m$)* (noted P4), was developed. In these polymers, the nucleobase units (uracil and adenine) are H-bond promoters, while THOX motifs provide a hydrophilic character to the macromolecular structure. Previous reports mentioned that piperazin-imidazole motif of adenine heterocycle could slightly decrease the water solubility of the statistical adenine copolymers compared to uracil copolymers.[29] Therefore, another copolymer of adenine (noted P2) was prepared containing a second block of PEG, *PEG$_{112}$-b-P(AdMA$_n$-stat-THOXMA$_m$)*. To this, PEG macro-CTA (with a DP of 112) was chain-extended with *AdMA* and *THOXMA* co-monomers, to reach an adenine containing block with a DP ~ 100. In this structure, PEG provides hydrosolubility and steric stabilisation[30] of the co-assembled formulations in water.

Table 1: Characterisation data of nucleobase polymers

	Polymer name	Experimental DP[a]	Experimental molar composition (%)[b]		Co-monomer conversion (%), by ^{1}H NMR[c]		M_n (g/mol), by ^{1}H NMR[d]	M_n (g/mol), by SEC[e]	Dispersity (Đ)[e]	Average number of nucleobases per polymer chain	M_{th} (g/mol)	Theoretical target DP[f]
			Nucleobase	THOXMA	Nucleobase	THOXMA						
P1	P(UrMA$_8$-*stat*-THOXMA$_{34}$)	42	20	80	85	92	10,000	10,430	1.21	8	11,840	50
P2	PEG$_{112}$-*b*-P(AdMA$_{30}$-*stat*-THOXMA$_{70}$)	104	30	70	72	88	30,200	32,100	1.32	30	29,400	100
P3	P(UrMA$_{22}$-*stat*-THOXMA$_{19}$)	41	53	47	81	90	10,500	11,200	1.1	22	11,950	50
P4	P(AdMA$_{14}$-*stat*-THOXMA$_{97}$)	111	13	87	83	85	26,300	30,000	1.25	14	29,320	100

a

Calculated by ^{1}H NMR performed in DMSO-d6, according to the Eq. S4., Eq. S9., Eq. S16.; [b] Calculated by ^{1}H NMR performed in DMSO-d6, according to the Eq. S5., Eq. S6., Eq. S12., Eq. S13. Eq. S19. and Eq. S20; [c] Calculated by ^{1}H NMR performed in DMSO-d6, according to the Eq. S1., Eq. S8. and Eq. S15.; [d] Calculated by ^{1}H NMR performed in DMSO-d6, according to the Eq. S7., Eq. S14. and Eq. S21.; [e] SEC analysis performed in DMF containing 0.1% LiCl and by using PMMA standards. [f]Calculated using the following equation DP_{target} = (([THOXMA]/[chain transfer agent]) x Conv $_{THOXMA}$) + (([AdMA or UrMA]/[chain transfer agent]) x Conv $_{AdMA\ or\ UrMA}$).

Each polymerisation was carried out for 7 h at 80 °C, in a mixture of DMF/ aqueous acid buffer at pH 4 (2:1 volume ratios). The acid buffer was used to prevent the undesired attack of the amine groups of nucleobases on the dithio- and trithio- moiety of the chain transfer agents. *Table 1* summarizes the characterization data of the obtained polymers. Proper corelation was observed between theoretical expected molecular weights, co-monomer ratios in copolymers and those experimentally determined by ^{1}H NMR (*Table 1*). SEC measurements revealed a narrow molecular weight distribution (Dispersity Đ ranging between 1.1 and 1.3, *see Table 1*), while the evolution of the molecular weight with conversion showed a linear relationship which illustrates that the polymerisation was controlled (*Fig. S3÷ S6.*). Overall, these results indicated that well defined nucleobase copolymers with controlled weight and ratios of co-monomers were obtained through RAFT polymerisation.

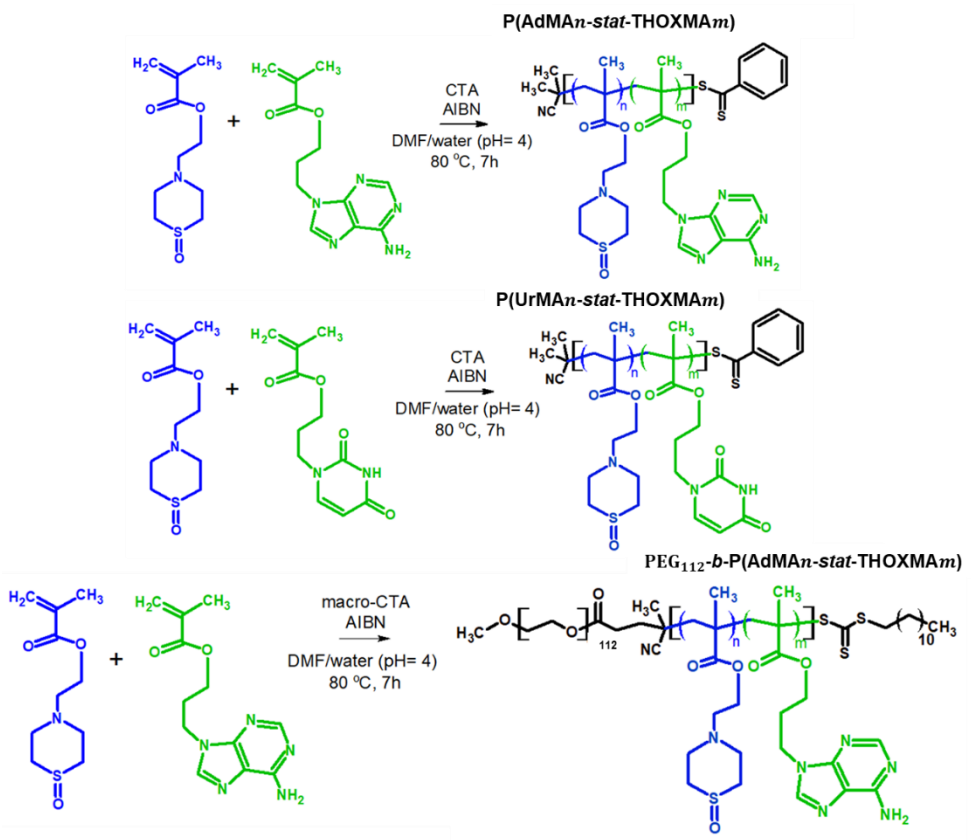

Scheme 1. Schematic representation of obtained nucleobase copolymers

V. 2. pH-responsive co-assembly with complex anisotropic morphologies

The co-assemblies were prepared as it follows. First, the starting polymer solutions (noted as P1, P3 -uracil polymer solutions and P2, P4- adenine polymer solutions see *Table 2*, *Table S1*) were separately dissolved in aqueous buffer at pH 7.4 and pH 10. Then, the co-assembled formulations were prepared by slowly adding the uracil solution to the adenine solution, in order to get 1:1 molar ratio between the molar equivalents of uracil and adenine units. After being stirred over 2 days, the formulations were analysed by SLS, DLS and TEM.

Switching the pH to 10 led to complex nano-objects with different physico-chemical properties, as illustrated in *Fig. 1*. Firstly, individual solutions of uracil polymers (P1: containing 8 Ur units, P3: containing 22 Ur units) and adenine polymers (P2: containing 30 Ad units, P4: containing 14 Ad units) were analysed by SLS, DLS and TEM at pH 10 (*Table S1*). Low particle sizes were noted by DLS for P1 (~20 nm) and P3 (~35 nm) uracil containing polymers (*Fig. 1, D*). In addition, low N_{agg} (~3 for P1 and ~7.1 for P3) were determined by SLS (*Fig. S8*, *Fig. S9*, *Table S1*). Similar results were assessed by TEM: herein, small particles were revealed for P1 (~26 nm, *Fig.2, H*) and P3 (~31nm, *Fig. 3, J-L*). Overall, these observations pointed out that individual uracil polymers had a soft tendency to self-assemble (low N_{agg}, particles with small size).

Then, the solutions of individual adenine polymers at pH 10, P2 and P4, were analysed by light scattering and transmission electron microscopy. PEG-containing adenine diblock copolymer *PEG_{112}-b-P($AdMA_n$-stat-$THOXMA_m$)* (P2) self-assembled in small particles (~38 nm, by DLS), as shown in *Fig. 1, D*. TEM captures showed small particle agglomerations (~42 nm *Fig. 2, E-F*). In addition, well-defined isolated particles with a denser core surrounded by a soft corona were revealed by TEM analysis (*Fig. 2, G*). Furthermore, the DLS analysis of *P($AdMA_n$-stat-$THOXMA_m$)* statistical copolymer (P4) showed the formation of particles with size around 110 nm (*Fig. 1, D*). Moreover, TEM representative pictures showed the presence of well-contoured particles that form well-defined agglomerations (~187 nm *Fig. 4, F-G*). The presence of large particles in P4 could be explained, as in the case of P2 polymer, by the $\pi - \pi$ interactions of stacked aromatic rings of adenine, leading to dense morphologies. Taken together, adenine containing polymers, P2 and P4, led to more aggregated structures at pH 10 compared to uracil containing copolymers (P1 and P3). The main difference between P2 and P4 consists in the presence of a hydrophilic PEG block (for P2). PEG is involved in the steric stabilisation of the obtained assembly, in consequence P2 shows particles with less dense morphology. Oppositely,

P4 is more hydrophobic, so the non-covalent interactions of the aromatic part of adenine resulted in the formation of dense particle aggregates.

Three co-assembly formulations, named System 1 (P1-P2), System 2 (P3-P2) and System 3 (P3-P4) were analysed by SLS, DLS and TEM at pH 10 (*Table 2*). In all three formulations, the molar ratio between the equivalents of complementary uracil and adenine units was 1:1 (*Fig. 1, C*). Complex q^{-3} or q^{-4} dependences of R/KC were observed over the whole q range by SLS, for all co-assembled formulations, at a concentration of 5 g/L (P1-P2, P3-P2 and P3-P4) (*Fig. 1, B*). This indicated that, at pH 10, very large co-assembled structures are formed. In SLS, M_{app} determination is only possible if $q \times R_g$ is lower than 1 and therefore it requires the existence of a plateau that correspond to a linear R/KC dependence.[32] Thus, at a concentration of 5 g/L, SLS did not allow the evaluation of N_{agg} of co-assemblies, since SLS plots were very sharp (q^{-3} or q^{-4}). Similar results were obtained when SLS experiments were performed at lower concentrations (from 3 g/L to 0.05 g/L) (*Fig. S14*). These results indicated that the concentration had no influence on the formation of co-assembled structures.

Table 2: Description of the related co-assembled formulations at pH 7.4 and pH 10

Formulation	**Description**	**Molar ratio between Ur/Ad units**	**pH**	**Aggregation number by SLS (N_{agg})[a]**	**Particle size by DLS (Z_{ave})[b]**	**Particle size by TEM (Z_{ave})[b]**
System 1	P1+P2	1:1	10	-	455	320
System 2	P3+P2	1:1	10	-	397	Long morphologies (900 nm long, 10 nm wide)
System 3	P3+P4	1:1	10	-	350	Long morphologies (920 nm long, 78 nm wide)
System 1a	P1+P2	1:1	7.4	315	130	150
System 2a	P3+P2	1:1	7.4	194	101	100

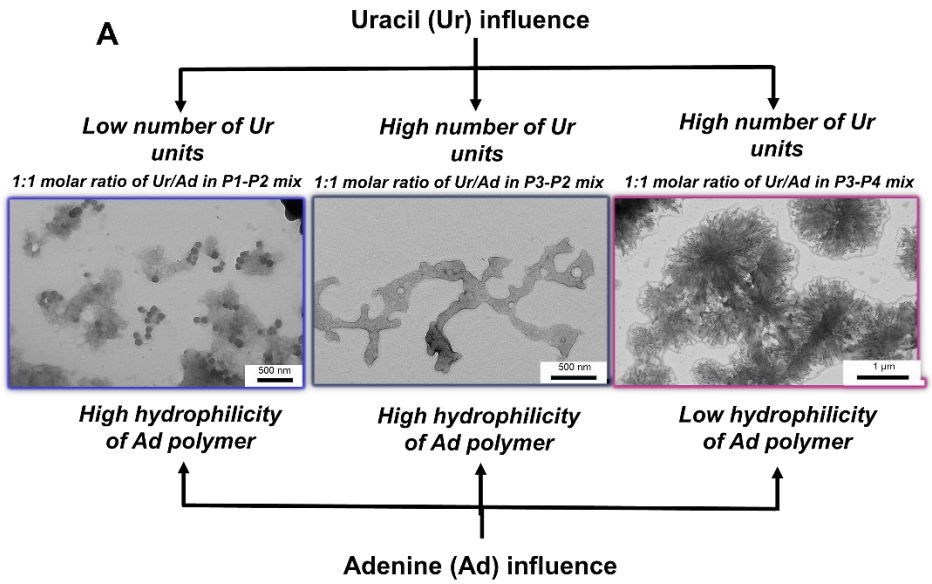

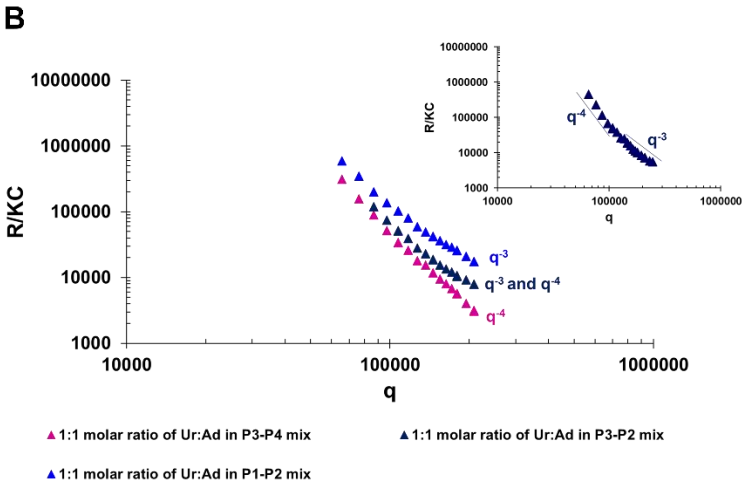

C

Composition	Ratio between molar equivalents of Ur and Ad	Number of uracil units in starting uracil polymer	Number of adenine units in starting adenine polymer
P1-P2	1:1	8	30
P3-P2	1:1	22	30
P3-P4	1:1	22	14

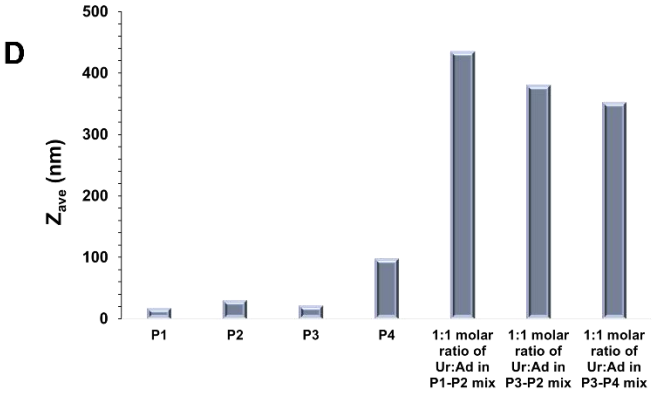

Fig. 1 (A) The influence of nucleobases on the morphological transitions at pH 10; (B) SLS analysis of co-assembled nucleobase polymers at pH 10; (C) Composition of co-assembled formulations; (D) DLS data of co-assembled structures at pH 10

Interesting morphological changes were depicted when the pH was switched from 7.4 to 10. In a previous study (ref. article 2), the System 1 (P1-P2, in *Table 2*, where P1 has 8 Ur units and P2 has 30 Ad units) was evaluated at pH 7.4 and formed spherical spheres with diffuse cores (*Fig. S10*, *Fig. S11*). At pH 10, well-defined spherical morphologies with fibrous internal microstructures were revealed by TEM (*Fig. 2, A-D*). The obtained morphologies had a size around 320 nm (by TEM). As shown in *Fig. 2. D*, the textured spheres had a tendency to coalesce which turns in very complex supramolecular architectures. A possible reason for the morphological transition between pH 7.4 and pH 10 could be an increase in the hydrophobicity of the system with the increase of the pH, which results in more complex and highly rigid architectures.[33]

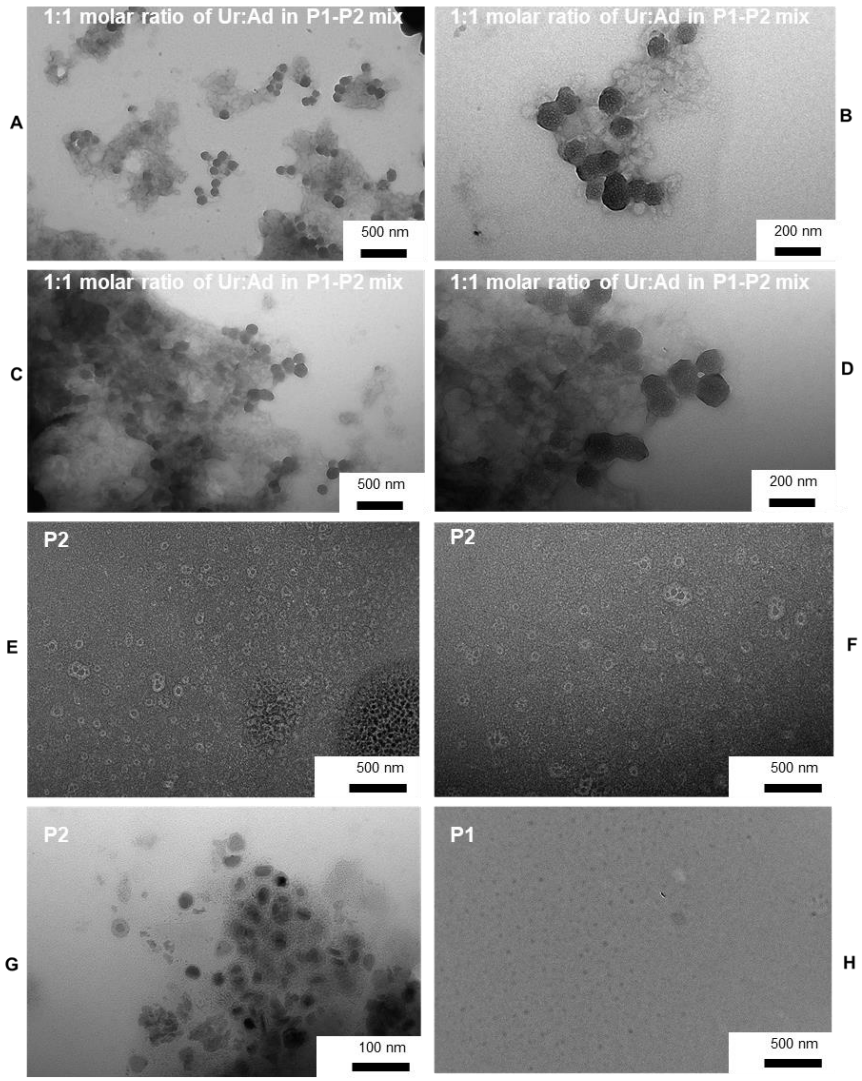

Fig. 2 Representative TEM images of P1-P2 system at pH 10 (noted as System 1). (A, B, C, D) 1:1 molar ratio of Ur:Ad in P1-P2 mix; (E, F, G) P2; (H)P1.

Moreover, we analysed the system composed on the same adenine-containing polymer (P2, 30 Ad units) and the uracil-containing polymer providing a high number of uracil units (P3, 22 Ur units). As reported in our previous study (ref. article 2), at pH 7.4, this system (noted as System 2a, *Table 2*, where P3 has 22 Ur units and P2 has 30 Ad units), formed spherical morphologies with a dense core, which were explained due to H-bond interactions between complementary nucleobases. Interesting transitions of the morphology were depicted for this system at pH 10. Respectively, the TEM analysis of this co-assembly (noted as System 2: P3-P2, *Table 2*, where P3 has 22 Ur units and P2 has 30 Ad units) revealed dendritic like morphologies (*Fig. 3*). These images showed clearly defined, rigid dendrites (~900 nm long and 10 nm diameter) that were assembled in long rigid networks (*Fig. 3, B and C*). As shown in *Fig. 3, G-H*, the texture of the dendrites seemed to be designed by the coalescence of spherical particles, and organized in elongated dendritic networks. The aggregation could be a consequence of hydrophobic interactions caused by alkyl spacer chains situated between the polymerizable backbone and the adenine groups, as well as by the aromatic stacking caused by adenine functions. Another example reporting fiber morphology was reported for nucleopeptides derivatives by Du *et al.* (2017).[34] Moreover, similar fiber and dendritic like morphologies were reported by Allain *et al.*[12] and were the result of the self-organisation of nucleolipids containing adenosine and uridine.[12] These complex morphologies were assigned to the hydrophobic non-covalent interactions of the lipid chains, as well as the complementary H-bonds promoted by the nucleic bases.

Then, long anisotropic morphologies (920 nm long and 78 nm wide) (*Fig. 4, A-E)* were observed for System 3 (P3-P4 in *Table 2*, where P3 has 22 Ur units and P4 has 14 Ad units). These snowflake-like morphologies were already reported by Tuyen Dao *et al.*[14,15] but were, to date, specific for peptide polymer self-assembly. According to the authors,[14,15] these morphologies originated from hydrophobic interactions between peptide aliphatic chains and from $\pi - \pi$ stacking between aromatic rings of the phenyl-alanine containing peptides. Similar observations were also depicted for nucleopeptides self-assembly.[34]

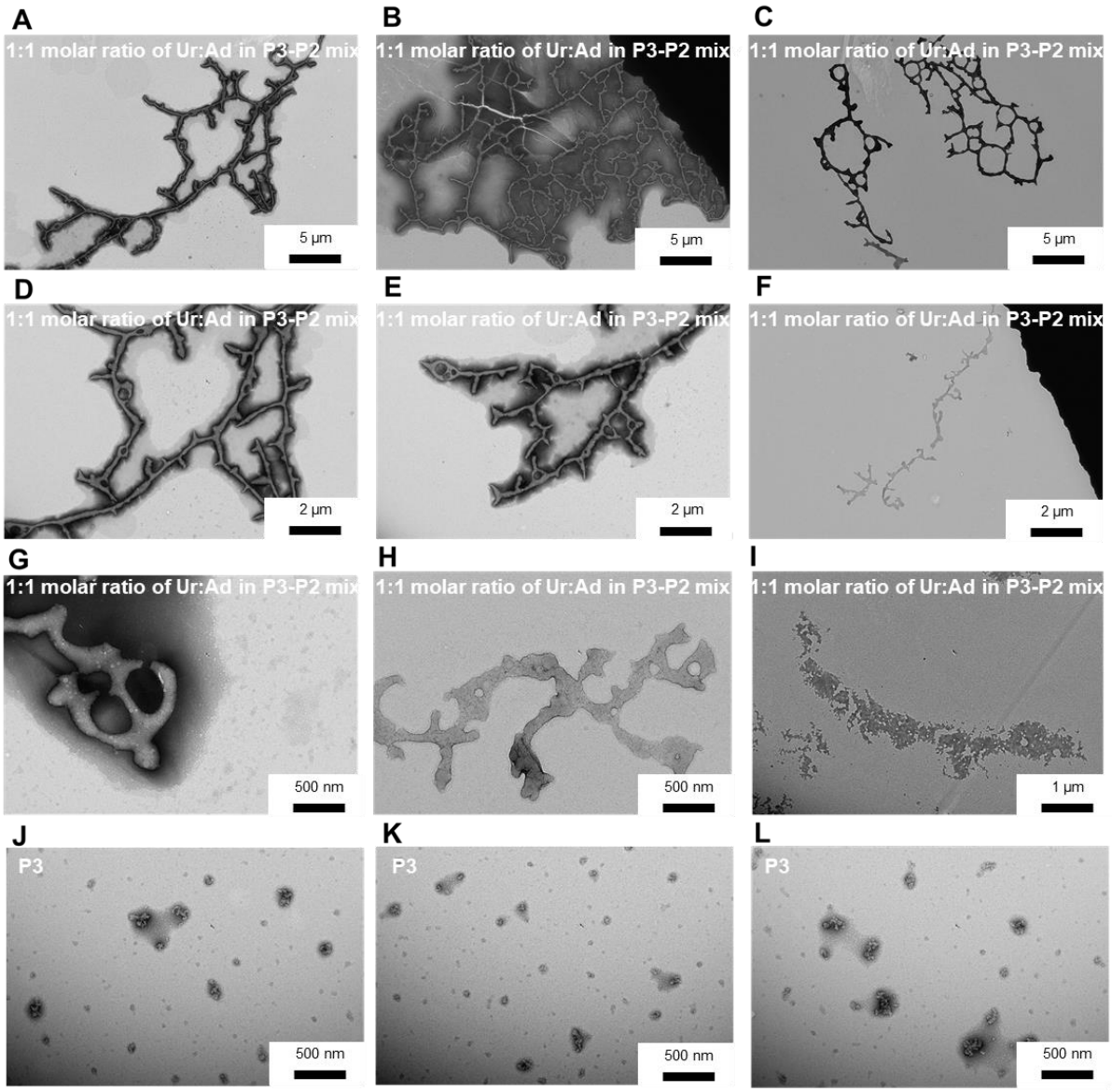

Fig. 3 Representative TEM pictures of P3-P2 system at pH 10 (noted as System 2). (A, B, C, D, E, F, G, H, I) 1:1 molar ratio of Ur:Ad in P3-P2 mix; (J, K, L) P3.

In the case of the System 3 the absence of hydrophilic PEG block in the design of adenine containing polymer induced a higher hydrophobicity and an absence of steric stabilisation. Therefore a correlation with the peptide system of the literature can be made and the aromatic ring of adenine enables similar $\pi - \pi$ transitions as for aromatic peptides. This snowflake-like morphology is probably induced by the stronger hydrophobic interactions of the adenine containing polymer at pH 10.

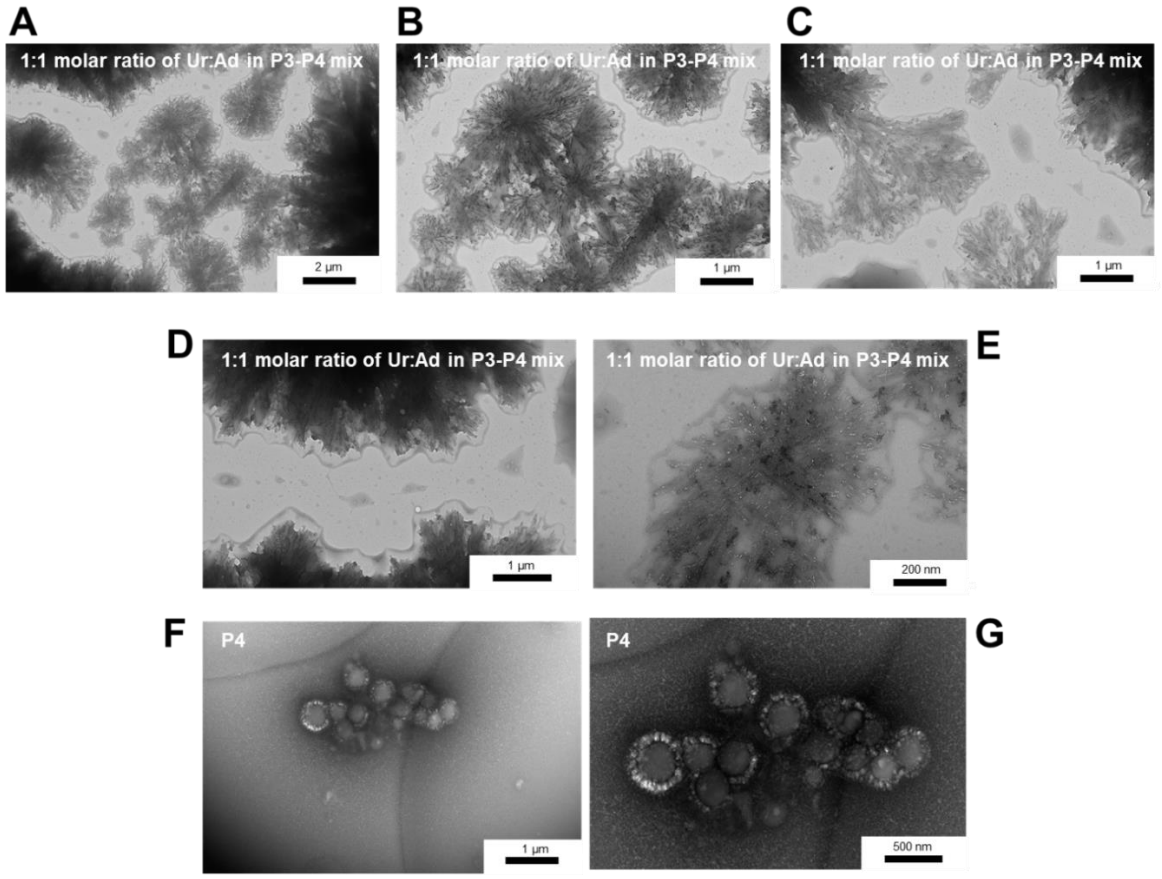

Fig. 4 Representative TEM pictures of P3-P4 system at pH 10 (System 3). (A, B, C, D, E) 1:1 molar ratio of Ur:Ad in P3-P4 mix; (F, G) P4.

V.3. Switching the pH: the key to obtain supramolecular platforms with different kinetics of co-assembly

So far, we showed that the aggregation and morphological properties of the obtained nucleobase containing co-assemblies obtained at pH 7.4 were a consequence of H-bond interactions between complementary nucleobases. (ref. article 2) On the other hand, complex morphologies obtained when increasing the pH at 10 were supposed to be a consequence of hydrophobic interactions. ITC experiments were conducted in order to investigate the impact of the type of supramolecular interactions (H-bonds/hydrophobic interactions) on the thermodynamic behaviour of co-assemblies at pH 7.4 and pH 10 (*Fig. 5, A and B*) and on the kinetics of co-assembly process. The ITC setup contained a calorimetric cell (filled with adenine containing polymer: P2 or P4) and a syringe pump (filled with uracil containing polymer: P1 or P3), which allowed the reagents to be introduced into the cell at given time periods and quantities.

ITC analysis of System 1a (P1-P2, where P1 has 8 Ur units and P2 has 30 Ad units) at pH 7.4 (*Fig. 5, A*, dark traces) revealed soft-width peaks (below 42 min) as well as broad peaks (above 42 min). The soft-width peaks denote a fast kinetics, while, after 42 min, the kinetics becomes slower, since the peak's broadness gives information about the time required by the system to reach the complete return to the baseline. Furthermore, the peak intensity increased proportionally with the molar ratio between Ur/Ad nucleobases, which indicates that the energy induced by the H-bond formation was gradually stronger when complementary uracil nucleobase was added.

Compared to the System 1a, System 2a (P3-P2, where P3 has 22 Ur units and P2 has 30 Ad units) (*Fig. 5, B*, grey doted traces) showed well-defined broad peaks over the complete time of analysis. The peaks of System 2a were broader over all the analysis than the peaks of System 1a which indicated that the kinetics of H-bond association between nucleobases was slower than in System 1a.

Furthermore, both systems at pH 7.4 showed an exothermic profile which is consistent with the creation of H-bonds between complementary nucleobases (uracil-adenine). The dilution of individual uracil polymer enabled an endothermic profile (*Fig. S13.*). The ITC results are consistent with the physico-chemical properties that were previously reported by our group (ref. article 2). Mainly, the use of low uracil ratios copolymer (*i.e.*, P1) (in System 1a) led to co-assemblies with fast kinetics that resulted in supramolecular organisations with high aggregation number (around 315). (ref. article 2) The increase of the ratio of uracil copolymer (*i.e.*, P3) (in System 2a) decreased the kinetics of H-bond association, probably because the system is richer in H-bonds. Since for both systems the same quantity of uracil was introduced for each injection, the variation of kinetics observed between System 1a and 2a are probably due to the greater difficulty (in the case of System 2a) to find a thermodynamic stable conformation that allows all uracil functions to interact with adenine functions.

Moreover, the evaluation of the molar enthalpy (*Fig. S15*.) at different Ur/Ad molar ratios reflected interesting results of the thermodynamic behaviour of the two systems. Mainly, the increase of complementary uracil units in the co-assemblies (System 1a *vs.* System 2a) shifted the enthalpy from -80 kJ/mol to -200 kJ/mol. These values are close to RNA type interactions reported previously by Rozners *et al*., illustrated for peptide nucleic acids (PNA).[35] In the literature, negative enthalpies suggest that the co-assembly is enthalpy driven and therefore that the H-bonds are involved in the association process.[36] In consequence, highly negative values

of the enthalpy suggest that the system release more energy as a result of H-bond nucleobase pairing. Previous reports of Thanasoullas *et al*. [37] on the investigation of the H-bond dynamics on nucleolipids showed lower enthalpies for supramolecular interactions between nucleobases. According to Thanassoulas *et al.*,[37] the low values of enthalpies were a consequence of the hydrophobicity induced by alkyl lipid chains. Contrary to these systems [37] our systems at pH 7.4 are mainly hydrophilic, which could explain the highly negative values of the enthalpy. Thus, these results confirmed that the H-bonds between complementary nucleobases drive the co-assembly process.

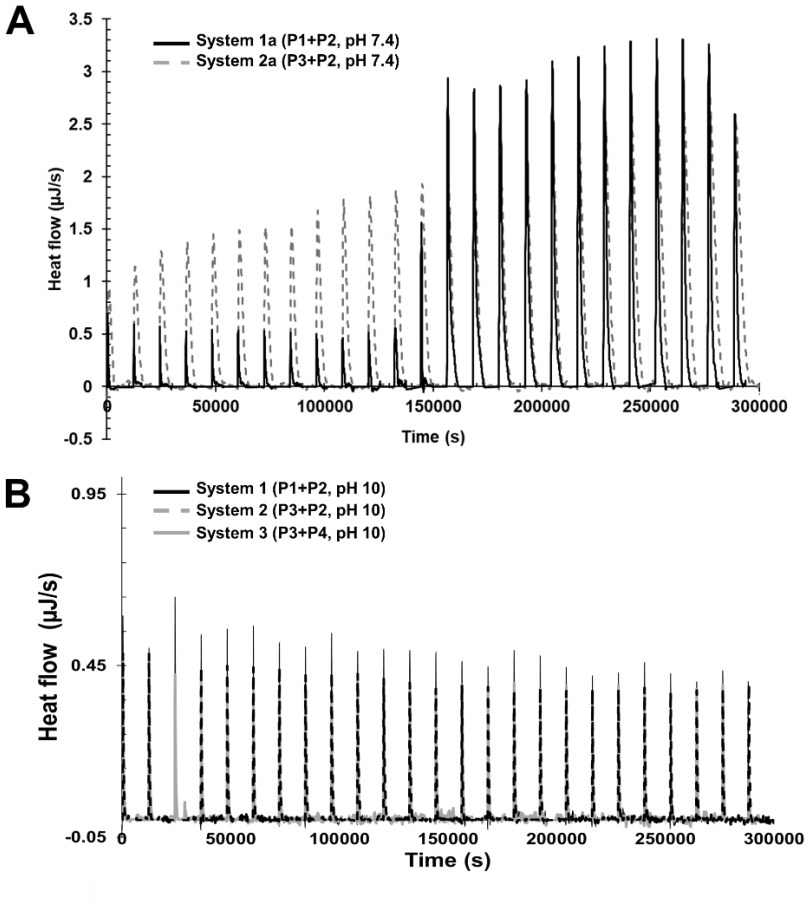

Fig. 5 ITC thermograms of co-assembled systems at pH 7.4 (A) and at pH 10 (B)

Since the pH changes from 7.4 to 10, led to strong differences of the morphologies of the co-assemblies, we were interested in investigating the thermodynamic origin of these variations. For this, ITC measurements were also conducted on the systems at pH 10 (noted as System 1, System 2 and System 3, *Table 2*) (*Fig. 5*, *B*), which exhibited a constant heat flow profile overtime, with sharp peaks of very low intensity. Since the intensity of the peaks is very low, there is almost no H-bond formation at the origin of co-assembly formation. Correlated with the previously TEM results (who indicated large anisotropic morphologies), our initial

hypothesis that the co-assembled architectures obtained at pH 10 are mainly governed by hydrophobic interactions is thus confirmed.

Overall, these results showed that the prepared co-assemblies were pH responsive and the switch of the pH was the key to achieve very complex morphologies, while investigating the supramolecular interactions which dominate the formation of co-assembly. Respectively, at physiological pH spherical shaped co-assemblies were mainly guided by H-bonds, while in alkaline conditions (pH 10) the anisotropic complex systems were formed as a result of hydrophobic interactions. Furthermore, these results possibly indicate that the co-assemblies were dynamic at pH 7.4 (since they were governed by H-bonds) and kinetically frozen at pH 10 (because they originated from hydrophobic interactions). However, further experiments (*e. g.*, Fluorescence Resonance Energy Transfer, FRET) are needed in order to prove the dynamic/frozen character of supramolecular co-assemblies, which are currently under investigation by our group.

VI. Conclusion

In summary, we designed co-assembled nucleobase copolymer architectures with tailorable morphologies under pH changes. Using RAFT polymerisation, a range of well-defined nucleobase containing polymers were synthesized, with various degrees of polymerisation and ratios in complementary uracil or adenine nucleobases. Then, a set of co-assemblies at pH 7.4 and pH 10 were prepared and their physico-chemical properties (evaluated by SLS, DLS, TEM) were compared. Noticeable morphological transitions were observed by switching the pH from 7.4 to 10. While at physiological pH (*i.e.*, 7.4) spherical particles with dense or diffuse cores were emphasized, the increase of the pH to 10 led to very complex anisotropic architectures that varied from micro-spheres with a fiber-like internal texture, to dendritic shapes and then to snowflake like morphologies. These large anisotropic morphologies were previously reported, in different organic solvents or water, in the case of self-assembled peptide polymers[14,15] and nucleolipids.[12] They mainly resulted from a combination of hydrogen bonds and hydrophobic interactions, with hydrophobic interactions as the main driving force of the assemblies. However, these morphologies have never been observed before in the case of co-assembled nucleobase containing polymers in water. Then, the influence of the pH on the thermodynamics parameters of the co-assembling process was studied by ITC. At pH 7.4 we concluded that the co-assembly was enthalpy driven ($\Delta H < 0$) and mainly due to H-bonds formation between complementary nucleobases. The kinetic of co-association was affected by the polymer composition in uracil. Oppositely, at pH 10, the co-assemblies were mainly driven by non-

covalent hydrophobic interactions. In addition, the supramolecular interactions responsible to the formation of co-assemblies were correlated to the observed morphologies. Thus, physiological pH (pH 7.4) was ideal to develop spherical shaped co-assemblies governed by complementary H-bonds between nucleobases, while high pH (pH 10) was appropriate to achieve complex anisotropic co-assemblies guided by hydrophobic interactions. On the basis of these results, we believe that the described pH responsive water soluble co-assembled nucleobase copolymer architectures with tailored morphologies and kinetics of co-assembly could find further use in the development of anisotropic drug delivery systems,[38] cellular transfection,[39] and various fields of biosciences.

VII. Acknowledgements

This research was funded by DAAD (German Academic Exchange Service) Research Grants-Short Term Grants 2022 (Funding program number: 57588366) as well as by the French Ministry of higher education and research.

VIII. References

1. R. Lanfranco, P. K. Jana, G. Bruylants, P. Cicuta, B. M. Mognetti and L. Di Michele, *Nanoscale*, 2020, **12**, 18616-18620.
2. M. Akashi, H. Takada, Y. Inaki and K. Takemoto, *J. Polym. Sci.*, 1979, **17**, 747–757.
3. J. Li, Z. Wang, Z. Hua and C. Tang, *J. Mater. Chem. B.*, 2020, **8**, 1576-1588.
4. C. G. Palivan, R. Goers, A. Najer, X. Zhang, A. Car and W. Meier, *Chem. Soc. Rev.* 2016, **45**, 377–411.
5. Z. Hua, R. Keogh, Z. Li, T. R. Wilks, G. Chen and R. K. O' Reilly, *Macromolecules* 2017, **50(9)**, 3662–3670.
6. Y. Kang, A. Lu, A. Ellington, M. C. Jewett, and R. K. O' Reilly, *ACS Macro Lett.*, 2013, **2(7)**, 581-586.
7. Y. Kang, A. Pitto-Barry, A. Maitland and R. K. O'Reilly, *Polym. Chem.*, 2015, **6**, 4984–4992.
8. Y. Kang, A. Pitto-Barry, M. S. Rolph, Z. Hua, I. Hands-Portman, N. Kirby and R. K. O'Reilly, *Polym. Chem.*, 2016, **7**, 2836–2846.
9. Z. Hua, T. R. Wilks, R. Keogh, G. Herwig, V. G. Stavros and R. K. O'Reilly, *Chem. Mater.*, 2018, **30(4)**, 1408-1416.
10. C-W. Huang, W-Y. Ji and S. W. Kuo, *Macromolecules*, 2017, **50**, 7091–7101.
11. H. Rosemeyer, *Chem. Biodivers.*, 2005, **2(8)**, 977–1063.
12. V. Allain, C. Bourgaux and P. Couvreur, *Nucleic Acids Res.*, 2012, **40**, 1891–1903.
13. G. B. Schuster, B. J. Cafferty, S. C. Karunakaran and N. V. Hud, *J. Am. Chem. Soc.*,

2021, **143**, 9279-9296.

14. T. P. Tuyen Dao, L. Vezenkov, G. Subra, M. Amblard, M. In, J-F. Le Meins, F. Aubrit, M-A. Moradi, V. Ladmiral and M. Semsarilar, *Macromolecules*, 2020, **53(16)**, 7034-7043.

15. T. P. Tuyen Dao, L. Vezenkov, G. Subra, V. Ladmiral and M. Semsarilar, *Polym. Chem.*, 2021, **12**, 113–121.

16. E. Largy and V. Gabelica, *Anal. Chem.*, 2020, **92(6)**, 4402-4410.

17. C. D. Bruce, M. M. Ferrara, J. L. Manka, Z. S. Davis, and J. Register, *JMR*, 2015, **28(5)**, 325-337.

18. M. Z. Brela, O. Klimas, M. Boczar, T. Nakajima and M. J. Wójcik, *Spectrochim. Acta A Mol. Biomol. Spectrosc.*, 2020, **237**, 118398-118408.

19. S. Pal, P. K. Maiti and B. Bagchi, *Chem. Phys.*, 2006, **125**, 234903-234913.

20. S. Catrouillet, C. Fonteneau, L. Bouteiller, N. Delorme, E. Nicol, T. Nicolai, S. Pensec and O. Colombani, *Macromolecules*, 2013, **46**, 7911-7919.

21. S. Catrouillet, L. Bouteiller, E. Nicol, T. Nicolai, S. Pensec, B. Jacquette, M. Le Bohec and O. Colombani, *Macromolecules*, 2015, **48(5)**, 1364-1370.

22. J. C. Brendel, J. Sanchis, S. Catrouillet, E. Czuba, M. Z. Chen, B. M. Long, C. Nowell, A. Johnston, K. A. Jolliffe and S. Perrier, *Angew. Chem. Int. Ed.*, 2018, **57(51)**, 16678-16682.

23. G. Mellot, J-M. Guigner, J. Jestin, L. Bouteiller, F. Stoffelbach and J. Rieger, *Macromolecules*, 2018, **51(24)**, 10214-10222.

24. Z. Hua, A. Pitto-Barry, Y. Kang, N. Kirby, T. R. Wilks and R. K. O'Reilly, *Polym. Chem.*, 2016, **7**, 4254–4262.

25. L. V. Arsenie, F. Hausig, C. Kellner, J. C. Brendel, P. Lacroix-Desmazes, V. Ladmiral and S. Catrouillet, *Molecules*, 2022, **27**, 4233-4248.

26. K. E. B. Doncom, A. Pitto-Barry, H. Willcock, A. Lu, B. E. McKenzie, N. Kirby and R. K. O'Reilly, *Soft Matter*, 2015, **11**, 3666–3676.

27. J. P. Patterson, M. P. Robin, C. Chassenieux, O. Colombani and R. K. O' Reilly, *Chem. Soc. Rev.*, 2014, **43**, 2412-2425.

28. R. Xu, *Particuology*, 2015, **18**, 11-21.

29. H. DeVoe and S. P. Wasik, *J. Solut. Chem.*, 1984, **13**, 51–60.

30. J. Thevenot, A-L.Troutier, L. David, T. Delair and C. Ladaviere, *Biomacromolecules*, 2007, **8**, 3651–3660.

31. C. H. Gorbitz, *Chem. Commun.*, 2006, **22**, 2332–2334.

32. K. E. B. Doncom, L. D. Blackman, D. B. Wright, M. I. Gibson and R. K. O'Reilly, *Chem. Soc. Rev.*, 2017, **46**, 4119–4134.

33. H. Wincel, *J. Am. Soc. Mass. Spectrom.*, 2016, **27(8)**, 1383–1392.

34. X. Du, J. Zhou, X. Li and B. Xu, *Interface Focus*, 2017, **7(6)**, 1-9.

35. T. Zengeya, M. Li and E. Rozners, *Bioorg. Med. Chem. Lett.*, 2011, **21**, 2121–2124.

36. E. Obert, M. Bellot, L. Bouteiller, F. Andrioletti, C. Lehen-Ferrenbach and F. Boué, *J. Am. Chem. Soc.*, 2007, **129(50)**, 15601-15605.

37. A. Thanassoulas, P. Barthelemy, L. Navailles and G. Sillaud, *J. Phys. Chem. B.*, 2014, **118(24)**, 6570-6585.

38. S. Bai, D. Jia, X. Ma, M. Liang, P. Xue, Y. Kang and Z. Xu, *Bioact. Mater.*, 2021, **6**, 2894–2904.

39. N. Semenova, M. Bosnjak, B. Markelc, K. Znidar, M. Cemazar and L. Heller, *Nucleic Acids Res.*, 2019, **47**, 10235–10246.

IX. Supplementary Information

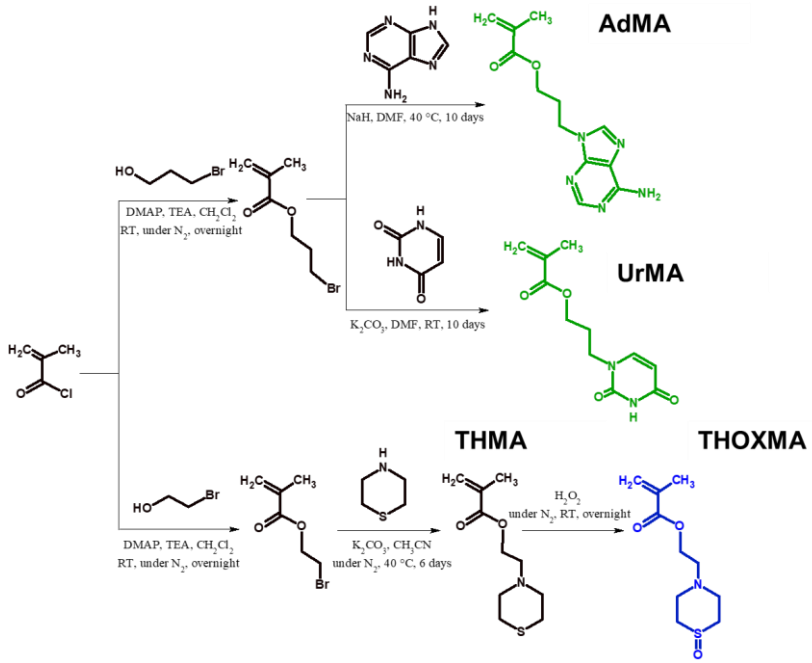

Scheme S1. Synthesis of adenine-containing monomer (AdMA), uracil-containing monomer (UrMA) and thiomorpholine-oxide (THOXMA) containing methacrylate monomer

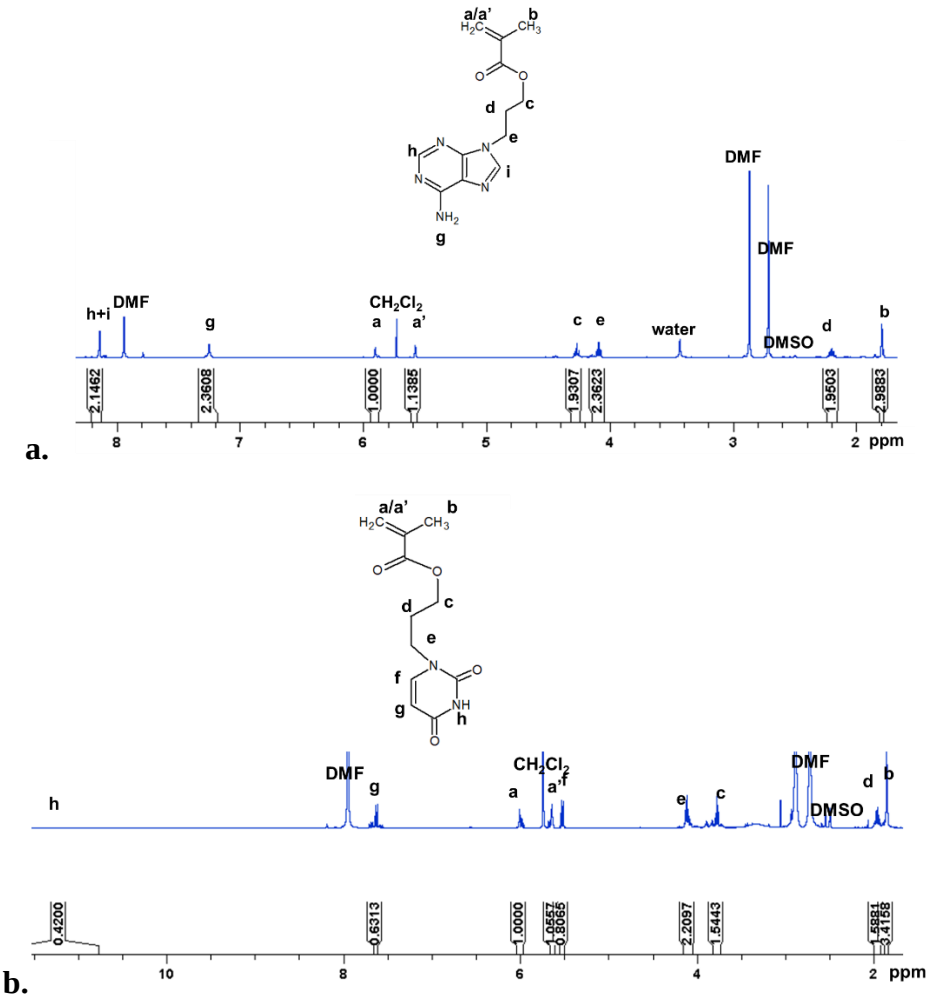

Fig. S1. ^{1}H-NMR spectrum of adenine(a) and uracil(b) containing monomers, performed in DMSO-d6

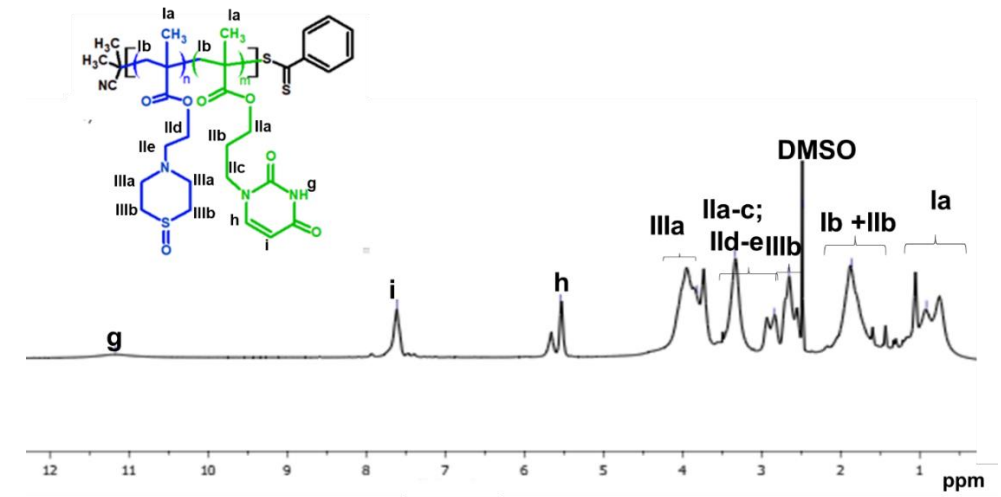

a.

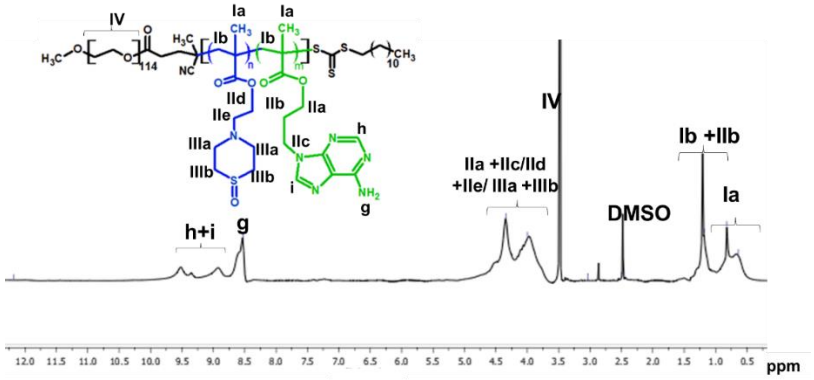

b.

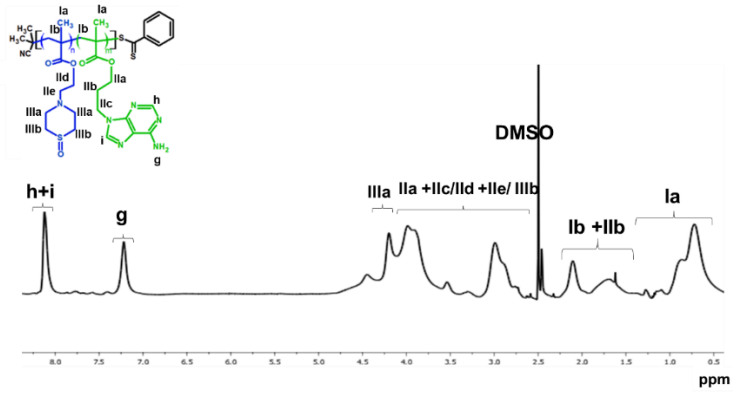

c.

Fig. S2. ^{1}H-NMR spectrum of uracil (a) and adenine (b,c) containing polymers, performed in DMSO-d6

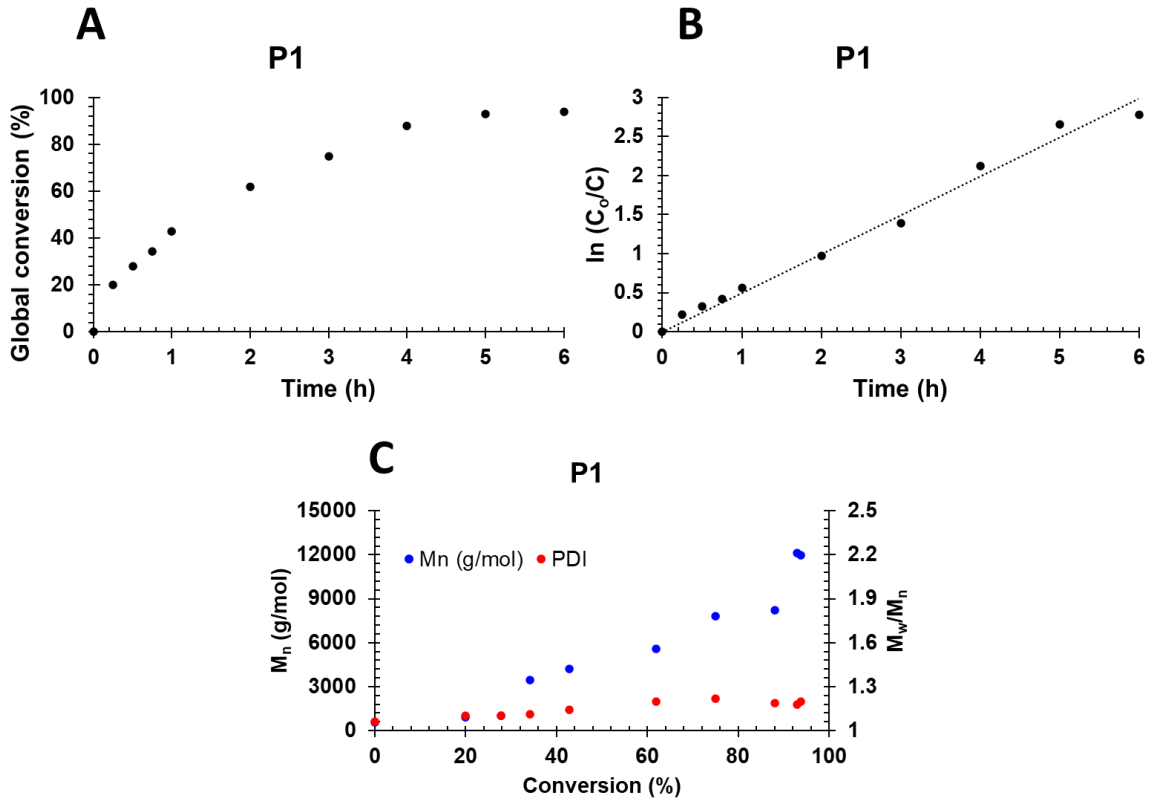

Fig. S3. Global conversion of uracil and thiomorpholine-oxide co-monomers, evaluated by ^{1}H-NMR (A); First order kinetic plot for RAFT statistical copolymerisation, evaluated by ^{1}H-NMR (B); Evolution of M_n and dispersity with conversion during the polymerisation evaluated by SEC (C). Results obtained for uracil containing polymer (P1).

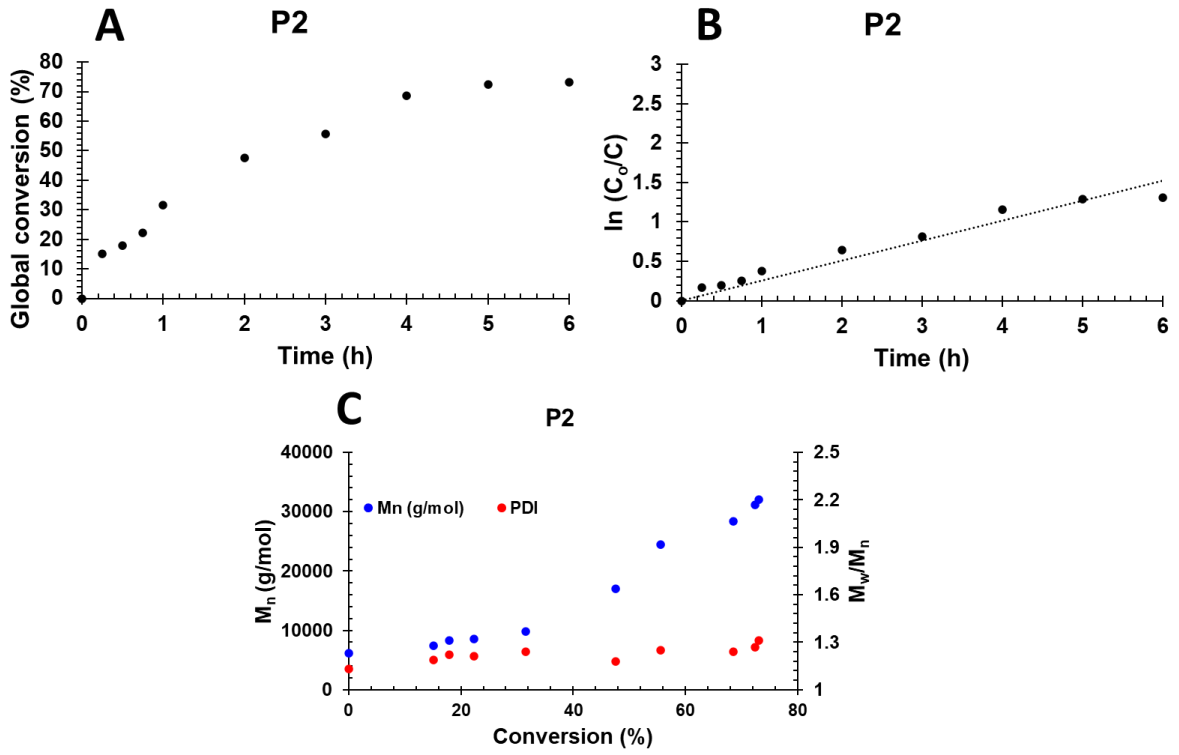

Fig. S4. Global conversion of adenine and thiomorpholine-oxide co-monomers, evaluated by ^{1}H-NMR (A); First order kinetic plot for RAFT statistical copolymerisation, evaluated by ^{1}H-NMR (B); Evolution of M_n and dispersity with conversion during the polymerisation evaluated by SEC (C). Results obtained for adenine containing polymer (P2).

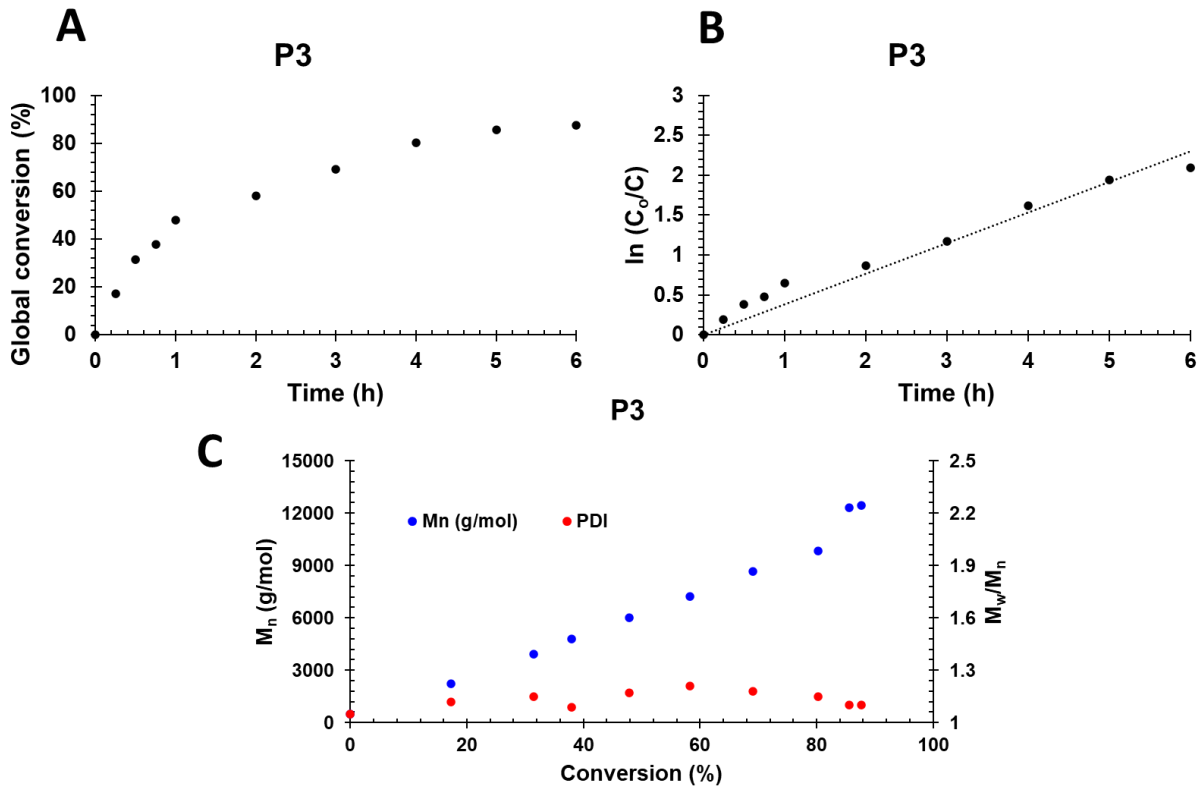

Fig. S5. Global conversion of uracil and thiomorpholine-oxide co-monomers, evaluated by ^{1}H-NMR (A); First order kinetic plot for RAFT statistical copolymerisation, evaluated by ^{1}H-NMR (B); Evolution of M_n and dispersity with conversion during the polymerisation evaluated by SEC (C). Results obtained for uracil containing polymer (P3).

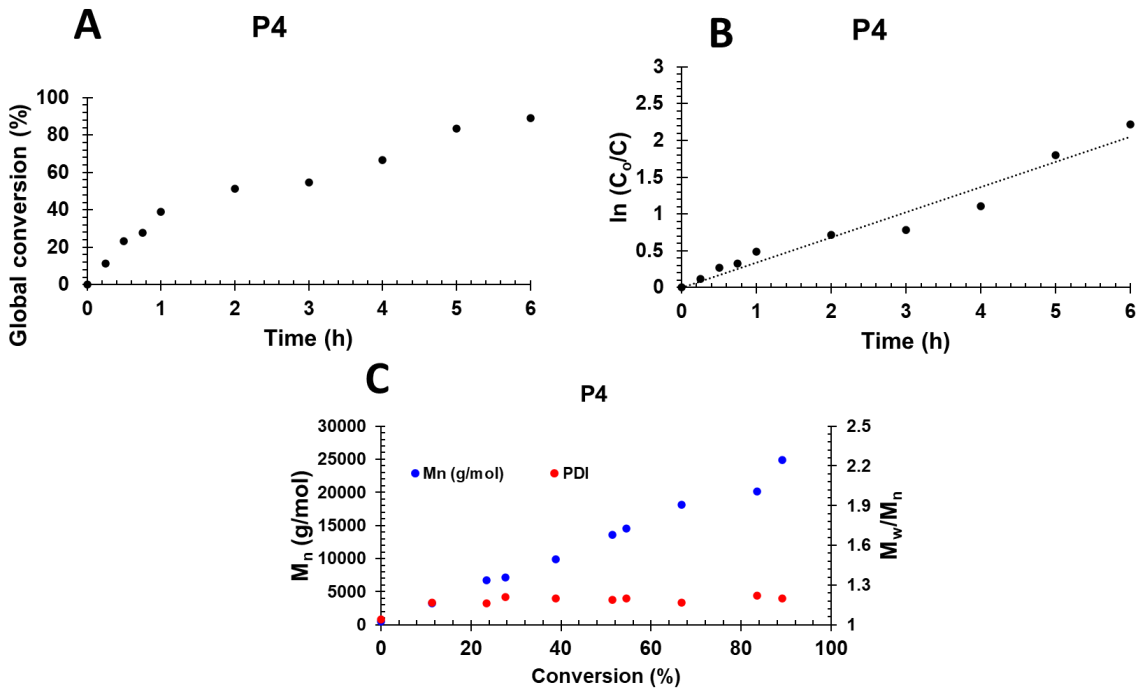

Fig. S6. Global conversion of adenine and thiomorpholine-oxide co-monomers, evaluated by ^{1}H-NMR (A); First order kinetic plot for RAFT statistical copolymerisation, evaluated by ^{1}H-NMR (B); Evolution of M_n and dispersity with conversion during the polymerisation evaluated by SEC (C). Results obtained for adenine containing polymer (P4).

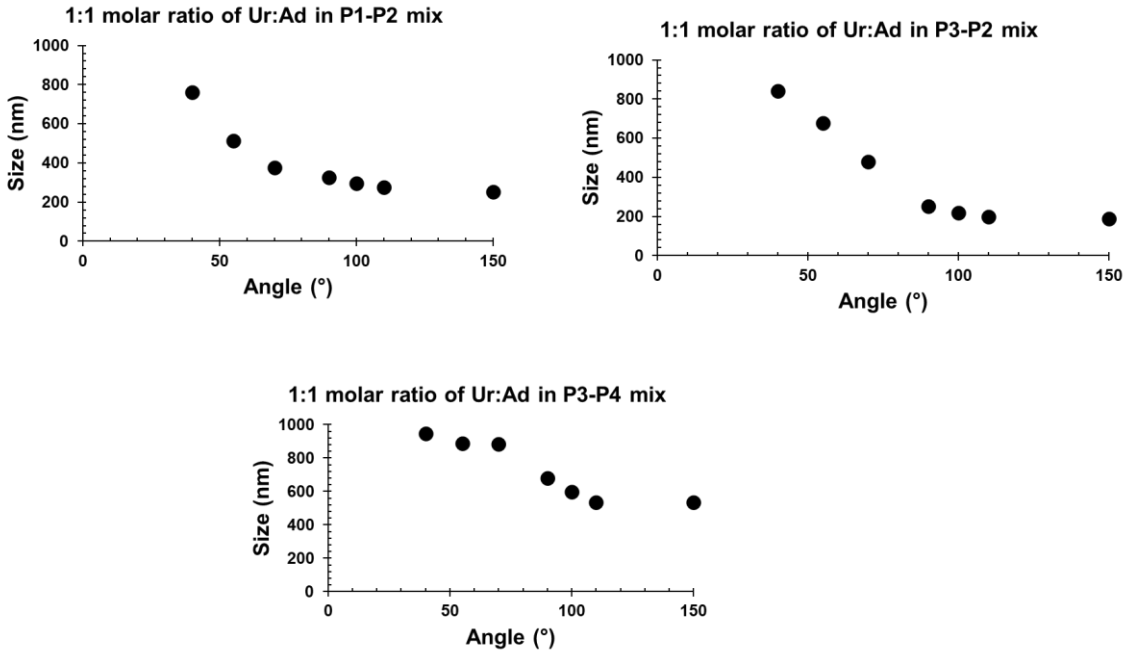

Fig. S7. Size(nm) of co-assembled formulations at different angles (evaluated by DLS) at pH 10

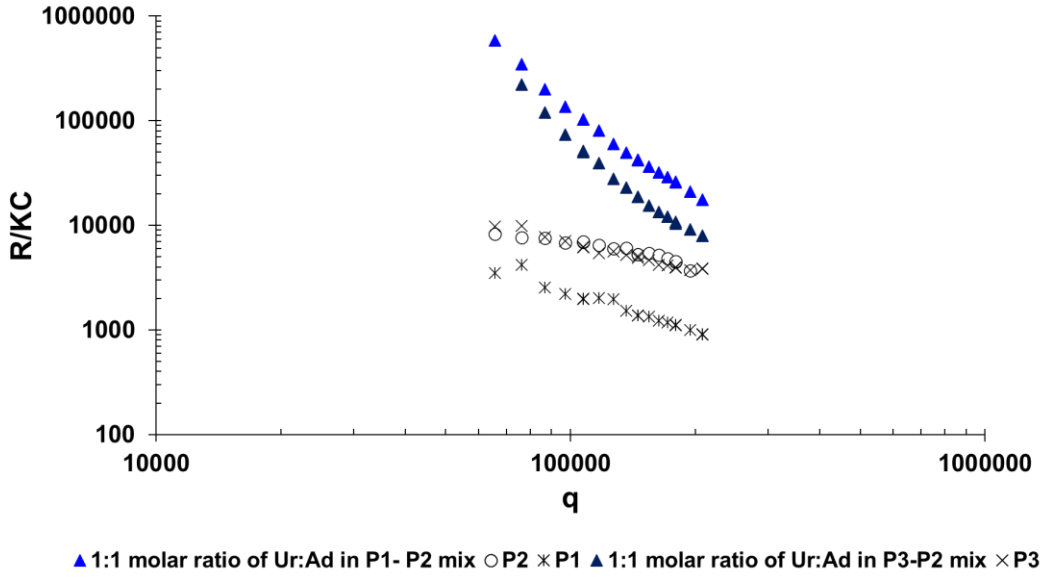

Fig. S8. SLS plots of P1-P2 mix, P3-P2 mix, and of individual polymer P1, P2, P3 at pH 10

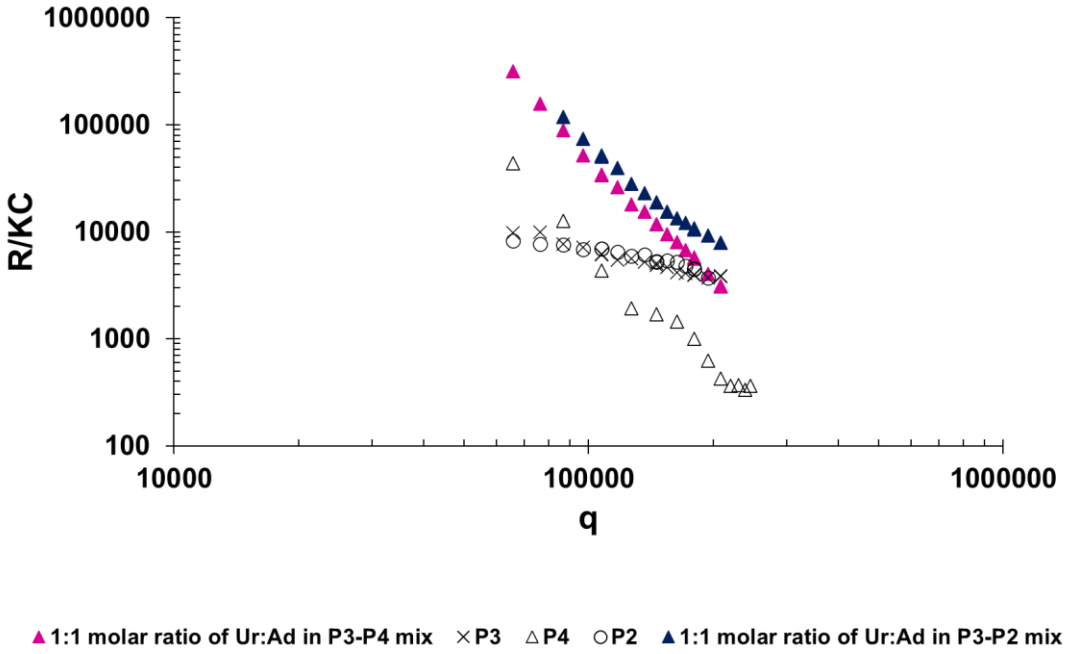

Fig. S9. SLS plots of P3-P2 mix, P3-P4 mix, and of individual polymer P2, P3, P4 at pH 10

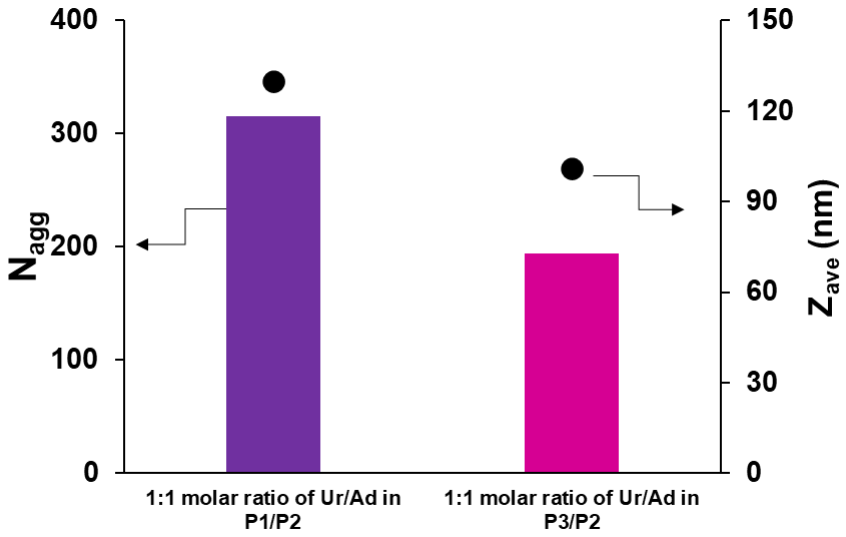

Fig. S10. N_{agg} (measured by SLS) and Z_{ave} (measured by SLS) of P1-P2 mix (at pH 7.4) and P3-P2 mix (at pH 7.4)

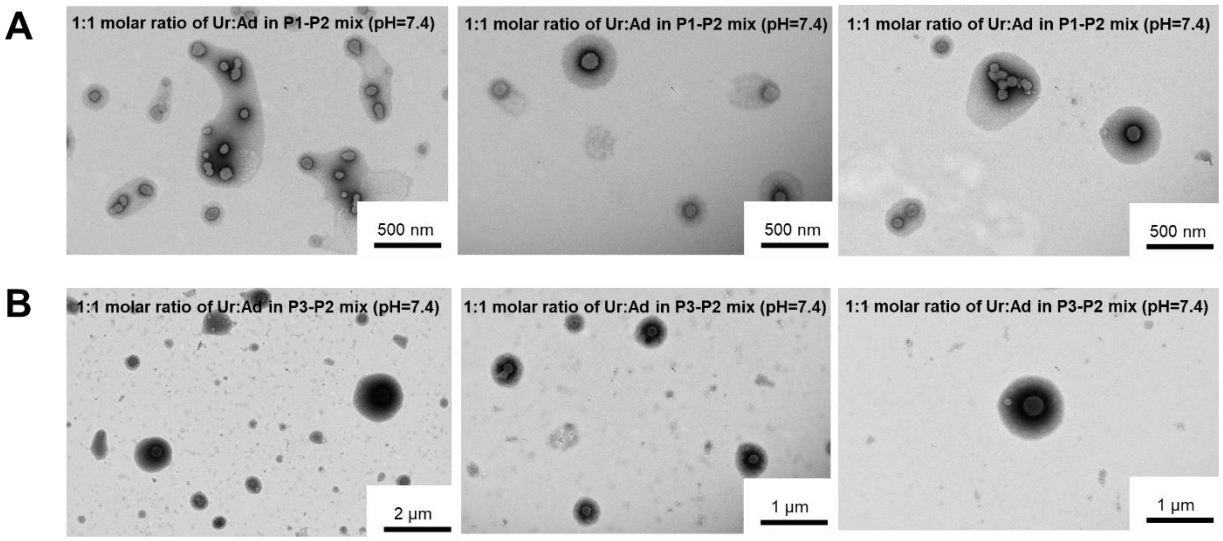

Fig. S11. TEM characterisation of P1-P2 mix (at pH 7.4) and P3-P2 mix (at pH 7.4)

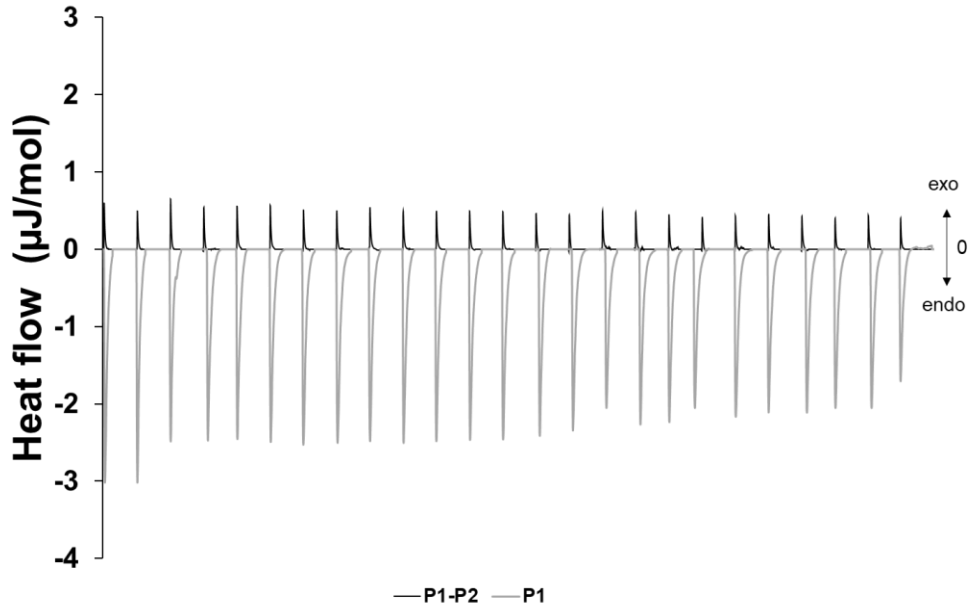

Fig. S12. ITC data at pH 10 for P1-P2 system (System 1) versus individual P1 polymer

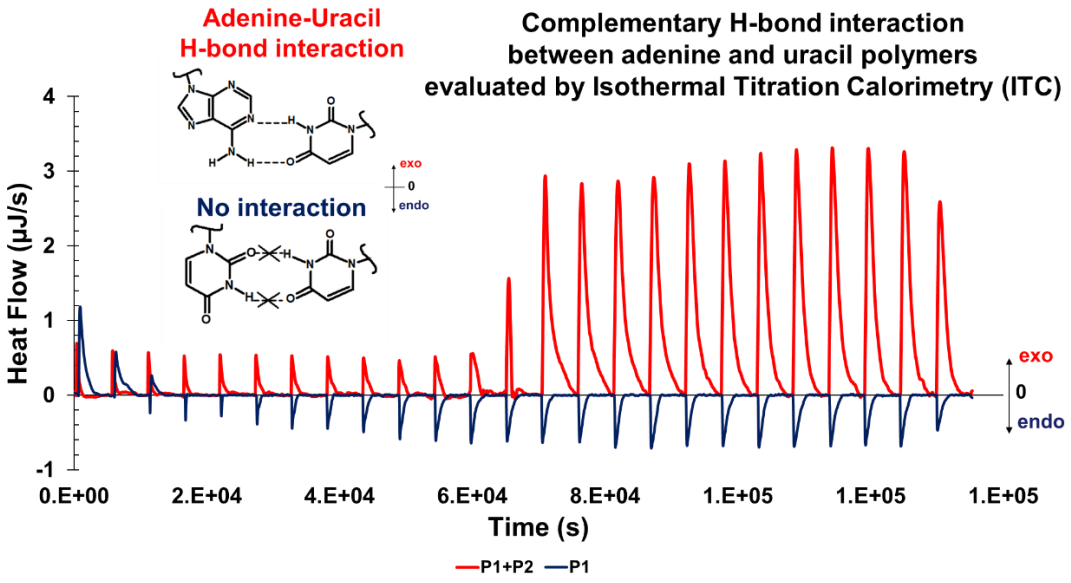

Fig. S13. ITC data at pH 7.4 for P1-P2 system (System 1a) versus individual P1 polymer

Table S1: Description of the related formulations at pH 7.4 and pH 10

Formulation	Description	Molar ratio between Ur/Ad units	pH	Aggregation number by SLS (N_{agg})[a]	Particle size by DLS (Z_{ave})[b]	Particle size by TEM (Z_{ave})[b]
Polymer solution	P1	-	7.4	2.5	11	-
Polymer solution	P2	-	7.4	7.5	20	-
Polymer solution	P3	-	7.4	3.3	13.2	-
Polymer solution	P1	-	10	3	20	26
Polymer solution	P2	-	10	8	38	42
Polymer solution	P3	-	10	7.1	35	31
Polymer solution	P4	-	10	-	110	187

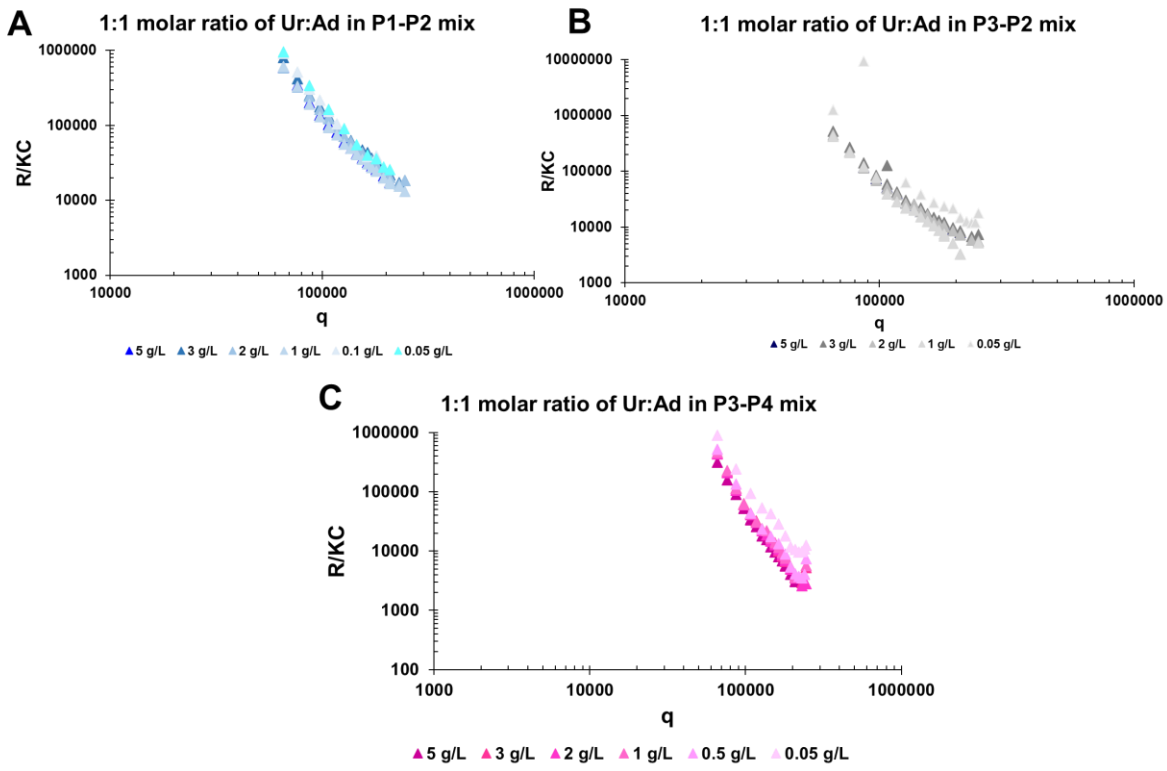

Fig. S14. SLS plots of co-assembled systems at pH 10 at different concentrations (A)1:1 molar ratio of Ur:Ad in P1-P2 mix; (B)1:1 molar ratio of Ur:Ad in P3-P2 mix; (C)1:1 molar ratio of Ur:Ad in P3-P4 mix.

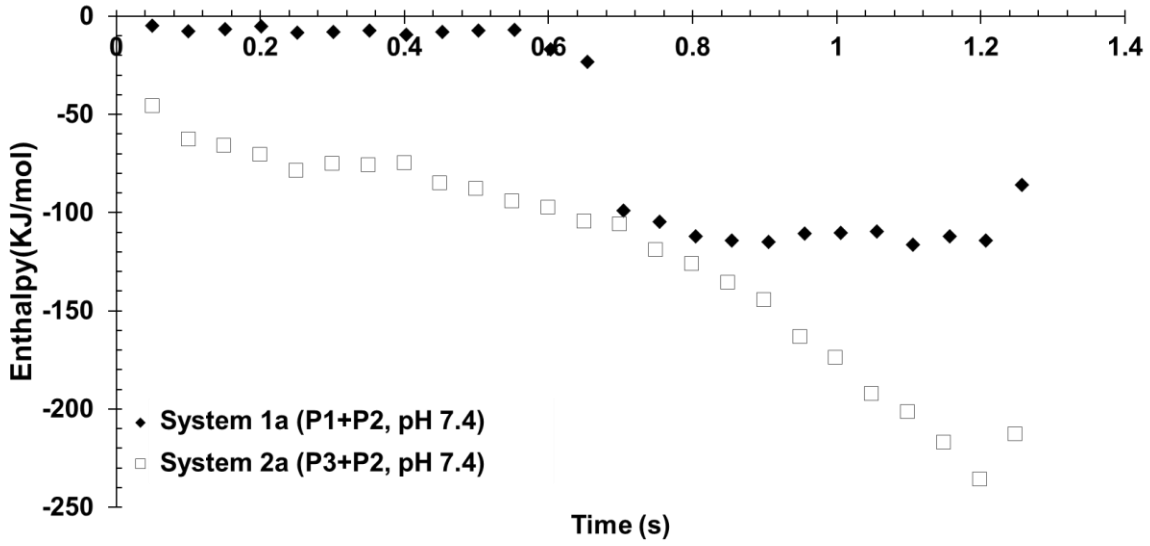

Fig. S15. Dependence of the enthalpy versus molar ratio, determined by ITC at pH 7.4, for P1-P2 mix (dark traces); P3-P2 mix (grey traces).

Equations used for polymer characterisation

A. Characterisation of P(UrMA$_n$ -stat-THOXMA$_m$) copolymers

- *Conversion of co-monomers*

The conversions of co-monomers were calculated by ^{1}H NMR (Eq. S1.), *via* the comparison of signal integrals of the CPDB (7.4-7.9 ppm) and of the protons of -C=C- double bond of *THOXMA* (6.06-5.68 ppm) and/or UrMA (5.99-5.73 ppm).

$$\text{Conversion (\%)} = \frac{(I_{0,vinyl\ function}/I_{0,CTA}) - (I_{t,vinyl\ function}/I_{t,CTA})}{(I_{0,vinyl\ function}/I_{0,CTA})} \times 100 \quad \text{(Eq. S1.)}$$

Where $I_{0,CTA}$ and $I_{t,CTA}$ are the values of the integrals of the signal of the aromatic protons of the chain transfer agent (between 7.4 ppm and 7.9 ppm) at t=0 and t respectively; $I_{0,vinyl\ function}$ and $I_{t,vinyl\ function}$ are the value of the integral of the signal of one of the protons of the vinyl group of methacrylate (5.68 ppm and 6.06 ppm for THOXMA, 5.73 ppm and 5.99 ppm for UrMA), at t=0 and t respectively.

- *Degree of polymerisation*

$DP_{\text{uracil copolymer}}$ was calculated as a sum between the number of UrMA (noted as $DP_{\text{UrMA synthons}}$) and THOXMA (noted as DP_{THOXMA}).

The number of UrMA was calculated considering the integral values at 5.56-5.58 ppm and 7.64 ppm that correspond to -C=C- double bond protons of uracil, compared to the two of the protons of CPBD (between 7.88 ppm and 7.9 ppm) as it follows (Eq. S2.):

$$DP_{UrMA} = \left(\frac{(I_1+I_2)/2}{I_{CTA}/2}\right) \text{ (Eq. S2.)}$$

Where I_1 is the value of the integral of the signal of the proton of double bond of uracil heterocycle (between 7.6 ppm and 7.83 ppm (H_i)), I_2 is the value of the integral of the other signal of the proton of double bond of uracil heterocycle (between 5.31 ppm and 5.71 ppm (H_h)), and I_{CTA} is the value of the integral of the signal of two of the aromatic protons of the chain transfer agent (between 7.88 ppm and 7.9 ppm).

The number of THOXMA were calculated according to Eq. S3.:

$$DP_{THOXMA} = \left(\frac{(I_3+I_4+I_5-2(I_1+I_2))/12}{I_{CTA}/2}\right) \text{ (Eq. S3.)}$$

The I_3 and I_4 are the values of the integrals of the proton signals in the field of 3.5 ppm-4.5 ppm and 2.52 ppm- 2.82 ppm respectively that correspond to the protons of thiomorpholine oxide cycle (**III_a and III_b**). I_5 is the value of the integral of the protons of UrMA aliphatic linker (**II_a and II_c)**, and the protons of THOXMA aliphatic linker (**II_d and II_e)** in the field of 2.82 ppm-3.48 ppm. To calculate the DP of THOXMA, the sum of integrals corresponding to these signals was assessed. Because this sum includes the integral of the protons of UrMA aliphatic linker, these values (I_1 and I_2) were subtracted in order to correctly evaluate the DP of THOXMA. However, it was impossible to determine exactly the region where the protons of UrMA aliphatic linker were situated, due to signal interferences. Since in UrMA4 protons of aliphatic linker are present in the field of 2.52 ppm- 4.55 ppm, the sum of integrals of uracil double bond protons (that correspond to 2 protons in UrMA) was multiplied by 2, to calculate the integral value of UrMA aliphatic linker protons. Then, this multiplied value (corresponding with the UrMA aliphatic linker) was subtracted and the result was divided by 12 (that correspond to the total of protons of thiomorpholine oxide cycle and THOXMA aliphatic linker).

Then, $DP_{uracil\ copolymer}$ was calculated (Eq. S4.):

$$DP_{uracil\ copolymer} = DP_{UrMA} + DP_{THOXMA} \text{ (Eq. S4.)}$$

- *Experimental molar percentage of co-monomers*

The molar percentage of UrMA and THOXMAwere calculated according to the equations:

% (molar) of *UrMA*= $(DP_{UrMA} \times 100) / DP_{uracil\ copolymer}$ (Eq. S5.)

% (molar) of *THOXMA* = $(DP_{THOXMA} \times 100) / DP_{uracil\ copolymer}$ (Eq. S6.)

- *Experimental M_n*

The experimental M_n of P($UrMA_n$-*stat*-$THOXMA_m$) copolymer was calculated as:

M_n = (% (molar) of UrMA $\times DP_{uracil\ copolymer} \times M_{th\ of\ UrMA}$) + (% (molar) of THOXMA $\times DP_{uracil\ copolymer} \times M_{th\ of\ THOXMA}$) + $M_{th,CTA}$ (Eq. S7.)

Where % (molar) of UrMA was calculated by Eq. S5., % (molar) of THOXMA was calculated by Eq. S6., $DP_{uracil\ copolymer}$ was calculated by Eq. S4. $M_{th,CTA}$ = 221.34 g/mol, $M_{th\ of\ THOXMA}$ = 231 g/mol, $M_{th\ of\ UrMA}$ = 238 g/mol.

B. Characterisation of PEG-*b*-P($AdMA_n$ -stat-$THOXMA_m$) copolymers

- *Conversion of co-monomers*

The conversions of co-monomers were calculated by ^{1}H NMR (Eq. S8.), *via* the comparison of signal integrals of the PEG region (noted as region IV) of the macro-CTA agent (3.48-3.58 ppm) and of the protons of -C=C- double bond of *THOXMA* (6.06-5.68 ppm) and/or AdMA (5.95-5.72 ppm).

Conversion (%) = $\frac{(I_{0,vinyl\ function} / I_{0,macro CTA}) - (I_{t,vinyl\ function} / I_{t,macro\ CTA})}{(I_{0,vinyl\ function} / I_{0,macro\ CTA})} \times 100$ (Eq. S8.)

Where $I_{0,macro\ CTA}$ and $I_{t,macroCTA}$ are the values of the integrals of the signal of the methylene protons of the PEG region of the macro-chain transfer agent (between 3.48 ppm and 3.58 ppm) at t=0 and t respectively; $I_{0,vinyl\ function}$ and $I_{t,vinyl\ function}$ are the value of the integral of the signal of one of the protons of the vinyl group of methacrylate (5.68 ppm and 6.06 ppm for THOXMA, 5.72 ppm and 5.95 ppm for AdMA), at t=0 and t respectively.

- *Degree of polymerisation of the adenine containing block*

$DP_{adenine\ containing\ block}$ was calculated as a sum between the number of AdMA (noted as DP_{AdMA}) and THOXMA (noted as DP_{THOXMA}).

The number of AdMA was calculated considering the integral values at 8.7-9.3 ppm and 9.48-9.56 ppm that correspond to the heterocycle protons of adenine (noted with h and i), compared to the methylene protons of the PEG region (region IV) of the macro-CTA (between 3.48 ppm

and 3.58ppm) as it follows (Eq. S9.). The DP of the macro-CTA is equal to 112, so it is assigned to 112 ethylene glycol units. Since 1 unit of ethylene glycol contains 4 protons, in the PEG region (with 112 ethylene glycol units) of macro-CTA we have 4x 112= 448 protons.

$$DP_{AdMA} = \left(\frac{(I_1+I_2)/2}{I_{macroCTA}/448}\right) \text{ (Eq. S9.)}$$

Where I_1 is the value of the integral of the signal of the first proton of adenine heterocycle (between 8.7 ppm and 9.3 ppm (H_h)), I_2 is the value of the integral of the other signal of the proton of double bond of uracil heterocycle (between 9.48 ppm and 9.56 ppm (H_i)), and $I_{macroCTA}$ is the value of the integral of the proton signals of PEG region the macro-chain transfer agent (between 3.48 ppm and 3.58 ppm).

The number of THOXMA were calculated according to Eq. S10.:

$$DP_{THOXMA} = \left(\frac{(I_3+I_4-2(I_1+I_2))/12}{I_{macroCTA}/448}\right) \text{ (Eq. S10.)}$$

The I_3 and I_4 are the values of the integrals of the proton signals in the field of 3.7 ppm-4.3 ppm and 4.31 ppm- 4.8 ppm respectively that correspond to the protons of thiomorpholine oxide cycle (**III_a and III_b**), the protons of AdMA aliphatic linker (**II_a and II_c)**, and the protons of THOXMA aliphatic linker (**II_d and II_e)**. To calculate the DP of THOXMA, the sum of integrals corresponding to these signals was assessed. Because this sum includes the integral of the protons of AdMA aliphatic linker, these values were subtracted in order to correctly evaluate the DP of THOXMA. However, it was impossible to determine exactly the region where the protons of AdMA aliphatic linker were situated, due to signal interferences. Since in AdMA 4 protons of aliphatic linker are present in the field of 3.7 ppm- 4.8 ppm, the sum of integrals of the protons of adenine heterocycle (that correspond to 2 protons in AdMA monomer) was multiplied by 2, to calculate the integral value of AdMA aliphatic linker protons. Then, this multiplied value (corresponding with the AdMA aliphatic linker) was subtracted and the result was divided by 12 (that correspond to the total of protons of thiomorpholine oxide cycle and THOXMA aliphatic linker).

Then, $DP_{\text{adenine containing block}}$ was calculated (Eq. S11.):

$$DP_{\text{adenine containing block}} = DP_{AdMA} + DP_{THOXMA} \text{ (Eq. S11.)}$$

- *Experimental molar percentage of co-monomers*

The molar percentage of AdMA and THOXMA were calculated according to the equations:

$$\%\text{ (molar) of } AdMA = (DP_{AdMA} \times 100) / DP_{adenine\ containing\ block} \text{ (Eq. S12.)}$$

$$\%\text{ (molar) of } THOXMA = (DP_{THOXMA} \times 100) / DP_{adenine\ containing\ block} \text{ (Eq. S13.)}$$

- *Experimental M_n*

The experimental M_n of PEG-*b*-P(AdMA$_n$ -stat-THOXMA$_m$) was calculated as:

M_n = (% (molar) of AdMA $\times DP_{\text{adenine containing block}} \times M_{\text{th of AdMA}}$) + (% (molar) of THOXMA $\times DP_{\text{adenine containing block}} \times M_{\text{th of THOXMA}}$) + $M_{n\ (\text{macro CTA})}$ (Eq.S14.)

Where % (molar) of AdMA was calculated by Eq. S12., % (molar) of THOXMA was calculated by Eq. S13., $DP_{\text{adenine containing block}}$ was calculated by Eq. S11. $M_{th,CTA}$ = 5400 g/mol, $M_{\text{th of THOXMA}}$ = 231 g/mol, $M_{\text{th of AdMA}}$ = 261 g/mol.

C. Characterisation of P(AdMA$_n$ -stat-THOXMA$_m$) copolymers

- *Conversion of co-monomers*

The conversions of co-monomers were calculated by ^{1}H NMR (Eq. S15.), *via* the comparison of signal integrals of the CPDB (7.4-7.9 ppm) and of the protons of -C=C- double bond of *THOXMA* (6.06-5.68 ppm) and/or AdMA (5.95-5.72 ppm).

$$\text{Conversion (\%)} = \frac{(I_{0,vinyl\ function}/I_{0,CTA}) - (I_{t,vinyl\ function}/I_{t,CTA})}{(I_{0,vinyl\ function}/I_{0,CTA})} \times 100 \quad \text{(Eq. S15.)}$$

Where $I_{0,CTA}$ and $I_{t,CTA}$ are the values of the integrals of the signal of the aromatic protons of the chain transfer agent (between 7.4 ppm and 7.9 ppm) at t=0 and t respectively; $I_{0,vinyl\ function}$ and $I_{t,vinyl\ function}$ are the value of the integral of the signal of one of the protons of the vinyl group of methacrylate (5.68 ppm and 6.06 ppm for THOXMA, 5.72 ppm and 5.95 ppm for AdMA), at t=0 and t respectively.

- *Degree of polymerisation*

$DP_{\text{adenine copolymer}}$ was calculated as a sum between the number of AdMA (noted as $DP_{\text{AdMA synthons}}$) and THOXMA (noted as DP_{THOXMA}).

The number of AdMA was calculated considering the integral values between 8.1 ppm and 8.4 ppm that correspond to the aromatic protons of adenine heterocycles, compared to the two of the protons of CPBD (between 7.88 ppm and 7.9 ppm) as it follows (Eq. S16.):

$$DP_{\text{AdMA}} = \left(\frac{(I_1+I_2)/2}{I_{CTA}/2}\right) \quad \text{(Eq. S16.)}$$

Where I_1 and I_2 are the values of the integrals corresponding to the protons of the adenine heterocycles (between 8.1 ppm and 8.4 ppm), and I_{CTA} is the value of the integral of the signal of two of the aromatic protons of the chain transfer agent (between 7.88 ppm and 7.9 ppm).

The number of THOXMA were calculated according to Eq. S17.:

$$DP_{THOXMA} = \left(\frac{(I_3+I_4+I_5-2(I_1+I_2))/12}{I_{CTA}/2}\right) \text{ (Eq. S17.)}$$

The I_3 and I_4 are the values of the integrals of the proton signals in the field of 3.5 ppm-4.5 ppm and 2.52 ppm- 3.49 ppm respectively that correspond to the protons of thiomorpholine oxide cycle (**III$_a$ and III$_b$**). I_5 is the value of the integral of the protons of AdMA aliphatic linker (**II$_a$ and II$_c$)**, and the protons of THOXMA aliphatic linker (**II$_d$ and II$_e$)** in the field of 2.52 ppm-3.49 ppm. To calculate the DP of THOXMA, the sum of integrals corresponding to these signals was assessed. Because this sum includes the integral of the protons of AdMA aliphatic linker, these values (I_1 and I_2) were subtracted in order to correctly evaluate the DP of THOXMA. However, it was impossible to determine exactly the region where the protons of AdMA aliphatic linker were situated, due to signal interferences. Since in AdMA, 4 protons of aliphatic linker are present in the field of 2.52 ppm- 4.55 ppm, the sum of integrals of adenine heterocycle protons (that correspond to 2 protons in AdMA) was multiplied by 2, to calculate the integral value of AdMA aliphatic linker protons. Then, this multiplied value (corresponding with the AdMA aliphatic linker) was subtracted and the result was divided by 12 (that correspond to the total of protons of thiomorpholine oxide cycle and THOXMA aliphatic linker).

Then, $DP_{adenine\ copolymer}$ was calculated (Eq. S18.):

$$DP_{adenine\ copolymer} = DP_{AdMA} + DP_{THOXMA} \text{ (Eq. S18.)}$$

- *Experimental molar percentage of co-monomers*

The molar percentage of AdMA and THOXMA were calculated according to the equations:

$$\%\text{ (molar) of } AdMA = (DP_{AdMA} \times 100) / DP_{adenine\ copolymer} \text{ (Eq. S19.)}$$

$$\%\text{ (molar) of } THOXMA = (DP_{THOXMA} \times 100) / DP_{adenine\ copolymer} \text{ (Eq. S20.)}$$

- *Experimental M_n*

The experimental M_n of P(AdMA$_n$-*stat*-THOXMA$_m$) copolymer was calculated as:

$$M_n = (\%\text{ (molar) of AdMA} \times DP_{adenine\ copolymer} \times M_{th\ of\ AdMA}) + (\%\text{ (molar) of THOXMA} \times DP_{adenine\ copolymer} \times M_{th\ of\ THOXMA}) + M_{th,CTA} \text{ (Eq. S21.)}$$

Where % (molar) of AdMA was calculated by Eq. S19., % (molar) of THOXMA was calculated by Eq. S20., $DP_{adenine\ copolymer}$ was calculated by Eq. S18. $M_{th,CTA}$ = 221.34 g/mol, $M_{th\ of\ THOXMA}$ = 231 g/mol, $M_{th\ of\ AdMA}$ = 261 g/mol.

Equations used for the preparation of co-assembled formulations

The volumes of uracil-containing copolymer solution (noted as V_1) and of adenine-containing copolymer solution (noted as V_2) were calculated according to the following equations (Eq. S22. and Eq. S23):

$$V_1 = \frac{R \times c_2 \times Number_{Ad} \times M_{Ur\ polymer}}{c_1 \times Number_{Ur} \times M_{Ad\ polymer} + R \times c_2 \times Number_{Ad} \times M_{Ur\ polymer}} \quad \text{(Eq. S22.)}$$

Where:

V_1 is the volume (in mL) of the uracil-containing copolymer solution; R is the molar ratio between the molar equivalents of the number of uracil groups and the number of adenine groups; $Number_{Ad}$ is the number of adenine groups in the copolymer; $Number_{Ur}$ is the number of uracil groups in the copolymer; c_1 is the concentration of uracil containing copolymer (in mg/mL); c_2 is the concentration of adenine containing copolymer (in mg/mL); $M_{Ur\ polymer}$ is the molecular weight of uracil containing copolymer (calculated by ^{1}H-NMR, according to the Eq. S7.) and $M_{Ad\ polymer}$ is the molecular weight of adenine containing copolymer (calculated by ^{1}H-NMR, according to the Eq. S14. or Eq. S21.).

$$V_2 = V_{total} - V_1 \quad \text{(Eq. S23.)}$$

Where: V_2 is the volume (in mL) of the adenine-containing copolymer solution and V_{total} is the total volume (in mL) of the formulation prepared by using uracil-containing and adenine-containing copolymers.

Conclusion Chapitre IV

Dans ce chapitre, nous avons présenté des co-assemblages de copolymères de nucléobases présentant à la fois des morphologies et une cinétique d'assemblages adaptables aux changements de pH.

Pour cela, des polymères contenant des nucléobases avec des architectures contrôlées ont été synthétisés par RAFT. Les propriétés physico-chimiques ainsi que les morphologies des co-assemblages issues de ces copolymères ont été étudiées à pH 7.4 et à pH 10 par SLS, DLS, et TEM. Des différences morphologiques notables ont été observés due au changement de pH. De plus, les analyses ITC ont montré que différents intéractions supramoléculaires sont à l'origine de la formation de ces auto-assemblages. Plus particulièrement, les particules sphériques obtenues en conditions physiologiques (pH 7.4) sont formées principalement grâce aux liaisons d'hydrogène complémentaires, tandis que les morphologies complexes anisotropes à pH 10 (de type sphères texturés, dendrites ou flocons de neige) sont causées majoritairement par des intéractions hydrophobes.

Ces résultats sont originaux par comparaison aux systèmes supramoléculaires formés à partir des copolymères contenant des bases azotées. Tout d'abord, ces systèmes sont obtenus dans l'eau (car les polymères de départ sont hydrosolubles), donc sans solvant organique, ce qui élargit leur accessibilité d'utilisation. Ensuite, nous sommes capables de développer une bibliothèque des morphologies supramoléculaires adaptables aux stimuli (dans ce cas, le pH), tout en maitrisant l'architecture des polymères de départ. Enfin, cette étude a abouti à tracer une corrélation entre les morphologies résultantes et le type d'intéraction supramoléculaire majoritaire qui est responsable d'apparition d'une telle morphologie. Dans son ensemble, ces travaux peuvent trouver de futures applications dans divers domaines des biosciences, comme par exemple le développement de systèmes d'administration de médicaments.

Chapitre V : L’intéraction des copolymères contenant des nucléobases avec différents types du matériel génétique

Chapitre V : L'intéraction des copolymères contenant des nucléobases avec différents types du matériel génétique

Introduction Chapitre V

Les chapitres précédents ont mis en évidence des architectures supramoléculaires originales réalisées à partir de copolymères contenant des nucléobases, solubles dans l'eau et présentant une cinétique d'modulable sous l'influence de différents stimuli tel que le pH ou la composition des copolymères. Ces systèmes sont originaux car ce sont les liaisons hydrogènes entre nucléobases complémentaires qui dirigent l'auto-assemblage à pH physiologique.

La reconnaissance moléculaire par liaisons hydrogène entre des nucléobases complémentaires étant un phénomène qui est à l'origine de la formation de l'ADN, notre objectif a ensuite été d'étudier comment les copolymères contenant des nucléobases interagissent avec le matériel génétique, dans la perspective d'évaluer leur potentiel utilisation comme vecteurs de l'ADN ou de l'ARN.

Les vecteurs artificiels du matériel génétique (ADN et/ou ARN) sont un sujet d'investigation continu depuis des dizaines d'années. Plus particulièrement, les vecteurs d'ARNm (ARN messager) ont connu un intérêt accru au niveau mondial suite au développement des vaccins contre le virus COVID-19. L'avantage des vaccins à ARNm est que le génome des cellules ne peut pas être modifié (contrairement aux thérapies traditionnelles avec siARN ou pADN qui peuvent présenter plus de risques). L'ARNm est traduit dans les cellules pour qu'elles produisent directement des protéines fonctionnelles avec un effet thérapeutique.

Les vecteurs artificiels du matériel génétique les plus connus sont les dendrimères cationiques, les lipides cationiques, ainsi que les polymères cationiques. La complexation de ces systèmes cationiques avec le matériel génétique (chargé négativement) se fait *via* des interactions électrostatiques. Malgré une complexation efficace avec l'ADN, ces systèmes induisent des interactions secondaires avec les protéines du sérum qui limitent l'efficacité de la transfection ainsi que la stabilité des complexes. De plus, des effets cytotoxiques sévères ont été observés

et associés à la présence d'une forte densité des charges positives dans la structure du vecteur artificiel.

Cependant, le remplacement total des interactions électrostatiques par des liaisons hydrogène complémentaires avec le matériel génétique n'a encore jamais été envisagé.

Dans le 3eme chapitre il a été mis en évidence que les copolymères de nucléobases ne sont pas cytotoxiques et qu'ils ne présentent pas d'effet hémolytique. Partant de ces résultats, nous nous sommes concentrés sur les copolymères polymétacrylates contenant des fonctions uracile et thiomorpholine oxide, P(UrMA$_n$-*stat*-THOXMA$_m$). Ces copolymères sont solubles à pH physiologique (pH 7.4) et présentent deux caractéristiques structurelles importantes. Premièrement, les fonctions thiomorpholine oxyde sont hydrophiles et neutres à pH 7.4. Deuxièmement, les groupes uracile peuvent former des liaisons hydrogène avec les unités d'adénine du matériel génétique.

Ce chapitre présente les propriétés de la complexation entre une série de copolymères P(UrMA$_n$-*stat*-THOXMA$_m$) et trois types de matériel génétique (ADN plasmidique, acide poly adénylique : polyA et ARN messager : ARNm). Alors que l'ADN plasmidique (ADNp) est un ADN circulaire double brin, le polyA et l'ARNm présentent des structures mono-brin. En ce qui concerne l'ARNm, sa structure mono-brin contient naturellement une terminaison par une chaine polyadénylée (polyA) qui améliore sa stabilité lors de la délivrance au noyau cellulaire pour effectuer la transfection cellulaire.

L'objectif majeur de ce travail est de vérifier si c'est possible de former des complexes *via* les liaisons hydrogène établies entre les fonctions uracile des copolymères et les unités adénine de la queue polyadenylée de l'ARNm, dans le but de protéger l'ARNm de la dégradation en milieu cellulaire et ensuite de réussir à le vectoriser. L'intérêt d'utiliser le polyA est que sa structure est proche de celle de l'ARNm. Ainsi il est possible d'étudier si la complexation des copolymères contenant de l'uracile est spécifique et sélective vis-à-vis des groupes adénines du matériel génétique à moindre cout.

Les résultats de ce chapitre sont résumés dans un article scientifique réalisé suite aux travaux que j'ai effectué lors d'un stage de recherche de 3 trois mois (01/03/2022-27/05/2022) dans le laboratoire IOMC (Iéna, Allemagne), sous la supervision du Dr. Anja Traeger et du Dr. Johannes Brendel. Cet article de recherche est en cours de validation par tous les co-auteurs, afin d'être soumis dans un journal scientifique dans les prochains mois.

Publication scientifique : Article de recherche numéro 4

Genetic material-neutral nucleobase copolymers assembly *via* H-bonds: a traditional concept of supramolecular chemistry applied to gene complexation

Laura Vasilica Arsenie,[1] Sylvain Catrouillet,[1] Vincent Ladmiral,[1] Anja Traeger,[2,*] and Johannes C. Brendel[2,*]

[1]ICGM, University of Montpellier, CNRS, ENSCM, Montpellier, France

[2]Laboratory of Organic and Macromolecular Chemistry (IOMC), Friedrich Schiller University Jena, Jena, Germany

I. Graphical abstract

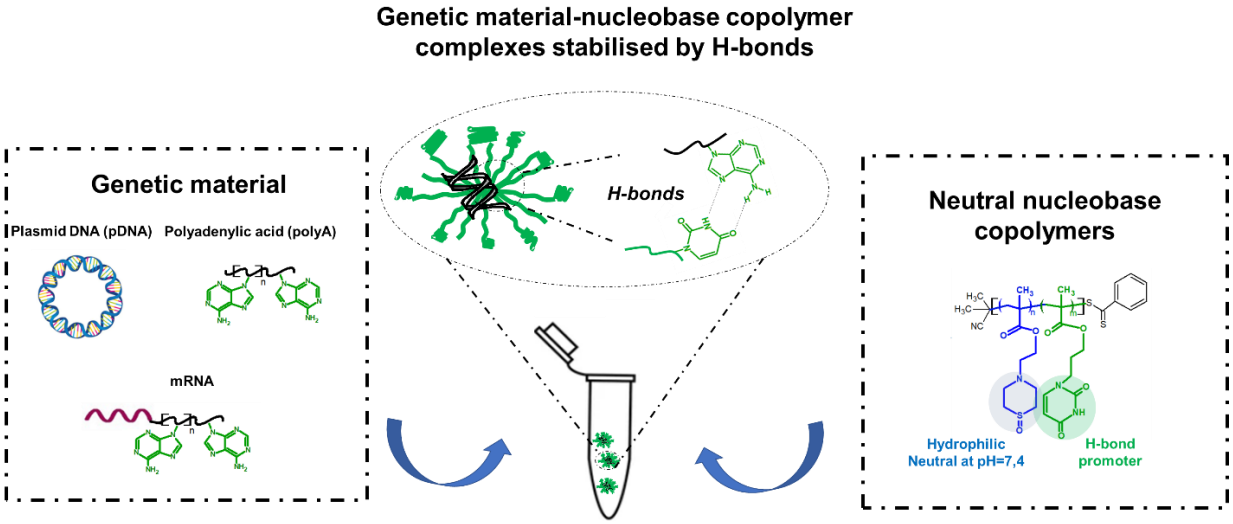

II. Abstract

Synthetic gene delivery vectors are based on cationic charged macromolecules such as cationic dendrimers or cationic polymers. Despite good transfection properties, cationic polymers showed side cytotoxic effects as well as adverse immunological reactions. Recent works emphasized that the use of neutral nucleobases attached to cationic dendrimers lowered the cytotoxicity and improved the cellular transfection properties. This study describes the complexation of genetic material with neutral nucleobase containing copolymers *via* complementary H-bond interactions. Nucleobase containing copolymers have never been explored before towards the complexation of DNA or RNA, mainly due to their difficult solubility in physiological conditions. Herein, well-defined statistical uracil containing

copolymers with different degrees of polymerisation and ratios between co-monomers, named P(UrMA$_n$-*stat*-THOXMA$_m$), were synthesized by RAFT polymerisation. These copolymers were soluble at physiological pH due to the presence of hydrophilic thiomorpholine oxide units, while the uracil groups promoted the H-bond recognition with adenine nucleobases of genetic material. The complexation between copolymers and three types of genetic material (plasmid DNA: pDNA, polyadenylic acid: polyA and mRNA) were investigated by gel electrophoresis, dynamic light scattering (DLS), and circular dichroism (CD). The complexation preferentially occurred with single strand genetic material (polyA, mRNA) due to the specificity of uracil-adenine H-bond recognition. Furthermore, the complexes were relatively stable in the presence of RNAse A and serum, which demonstrated that the H-bonds were stable enough to protect genetic material from degradation. Overall, these results open the gates towards new artificial gene delivery systems which may find further application in biological sciences.

III. Introduction

Continuous research efforts are devoted to find safer and more efficient gene vectors for various therapeutic approaches. In a large number of genetic diseases, the defective expression of certain genes leads to the absence of certain proteins that are vital to the proper functioning of the organism.[1] To overcome this issue, new gene therapy systems have been developed, that involve the delivery of functional genetic material into cells. Traditional delivery systems require the genetic material to be delivered into the nucleus in order to restore gene expression.[2] Messenger RNA (mRNA) is the key link in the translation of the genetic information of the DNA into instructions sequences which are used by cells to produce the proteins.[3] The delivery of mRNA doesn't require to reach the nucleus, as it is expressed in the cytoplasm of the cells. Hence, delivered mRNA is never in contact with the genome, it therefore can't modify the genome and induce genotoxicity (which is an issue in traditional transfection) contrary to traditional small interfering RNA (siRNA) or plasmid DNA (pDNA).[4]

The design of an ideal gene vector implies the complexation of genetic material (DNA or RNA) to protect it from degradation, a targeted delivery to the desired cells, and an efficient transfection. Low cytotoxicity and good stability in serum are mandatory in this context.[5] Natural delivery systems such as recombinant viruses demonstrate high transfection efficiencies, but they suffer from a limited cell specificity and adverse immunological reactions.[6]

Artificial gene delivery systems come as an improved alternative to the natural delivery systems, since they trigger fewer undesired biological reactions of the immune system and can selectively be modified to target specific cells via bound ligands.[7]

Among artificial gene delivery systems, mostly cationic dendrimers,[9] positively charged lipids[10] and cationic polymers[11] are described in literature. In these systems, the complexation with negatively charged genetic material occurs *via* electrostatic interactions. Despite the efficient gene complexation and good cellular uptake, these systems often induce secondary interactions with serum proteins limiting the transfection efficiency and stability of the complexes.[12] In addition, a high positive charge density in many of these artificial vectors cause severe cytotoxic effects. For these reasons, the development of an efficient artificial gene delivery is a challenging task.[8]

Many studies tried to reduce the positive charge density by attaching neutral polymers such as poly(ethylene glycol) (PEG) to the cationic structure of polyethyleneimine (PEI).[10,11] Another strategy to avoid the anionic protein corona formation around the cationic polymer was to develop PEG-aliphatic polycarbonate polymers containing protonated guanidinium frameworks.[13] According to the authors, the aliphatic polycarbonate disabled the serum protein attack on the gene complex, while the hydrophilic PEG and protonated guanidine in the polymers improved the complex formation with siRNA *via* H-bonds.[13] Another approach consisted in the functionalisation of polycationic dendrimers with neutral nucleobases, inducing a decreased cytotoxicity and highly improved cellular transfection properties.[14]

The full replacement of the electrostatic interactions by complementary H-bond *via* nucleobase modified polymers was, to the best of our knowledge, not considered in literature yet.

In a previous work (ref. article 2) we presented for the first time the synthesis of neutral nucleobase containing polymethacrylate copolymers containing uracil and thiomorpholine oxide units, P(UrMA$_n$-*stat*-THOXMA$_m$). These copolymers are soluble at physiological pH (pH 7.4) and show two significant structural features. First, they contain uracil groups which are involved in the formation of H-bonds with complementary adenine nucleobases (from genetic material). Second, the thiomorpholine oxide frameworks are hydrophilic and are neutral at pH 7.4.[15] Moreover, the thiomorpholine oxide groups in the copolymer have a pK_a ~5.6, as shown in a previous study of our group. [15] This property can be used to tailor the behaviour of the polymer in different biological environments such as endosome environment. The advantage of thiomorpholine oxide groups is that they could act as proton sponge frameworks

who facilitate the pH-induced endosomal escape, in order to protect the genetic material from degradation.

In this paper we design complexes formed *via* complementary H-bonds between neutral uracil containing copolymers and adenine groups from the genetic material. The use of supramolecular H-bonds interactions instead of electrostatic interactions aims to avoid the cytotoxicity and the undesired interactions with the anionic serum proteins, which are the main obstacles of cationic polymers, as mentioned before.

To this, RAFT polymerisation was used to obtain statistical P(UrMA$_n$-*stat*-THOXMA$_m$) copolymers with different degrees of polymerisation and ratios between co-monomers. The statistical type architecture was chosen to avoid the steric repulsions between crowded and voluminous co-monomers; second, to achieve a global disposition of H-bond promoting monomers and weak electrolytes on the entire hydrophilic structure. The *in-vitro* biocompatibility of obtained copolymers was evaluated through cytotoxicity and hemocompatibility assays. Then, the complexation of prepared copolymers was studied with three different genetic materials: plasmid DNA (pDNA), polyadenylic acid (polyA) and messenger RNA (mRNA). While pDNA is a circular, double stranded DNA (used traditionally in gene delivery), polyA and mRNA provide single strand structures. PolyA was chosen in order to study if the complexation of uracil containing copolymers is specific and selective to bind the adenine groups of genetic material. Furthermore, mRNA is naturally modified with polyadenine tails during nuclear processing.[16] This polyadenine tail provides a better stabilization of mRNA when it is delivered to the cytosol *via* the nucleus membrane.[16] In consequence, mRNA has also an interesting potential to be complexed by the uracil groups of the developed copolymers.

The complexation of copolymers with the different genetic material was studied by gel electrophoresis, whereas dynamic light scattering (DLS) was conducted to study the physico-chemical properties of the obtained complexes. Circular dichroism (CD) was additionally performed to get a deeper insight into the structural changes that occur during the complexation. Lastly, the *in-vitro* stability of complexes in the presence of RNAse A and physiological serum was evaluated in order to evaluate their further potential to be used in cellular transfection applications.

Table 1: Characterisation data of prepared nucleobase containing copolymers

	Polymer name	Experimental DP[a]	Experimental ratio of monomers(%)[b]		^{1}H-NMR	SEC[d]		Conversion of monomers(%)[e]		Number of nucleobases	M_{th} (g/mol)	Target DP[f]	Theoretical ratio of monomers(%)	
			Nucleobase	THOXMA	M_n (g/mol) [c]	M_n (g/mol) [d]	Dispersity (Đ) [d]	Nucleobase	THOXMA				Nucleobase	THOXMA
P1	P($UrMA_9$-*stat*-$THOXMA_{33}$)	42	21	79	9755	10430	1.21	85	92	9	11500	50	20	80
P2	P($UrMA_{22.4}$-*stat*-$THOXMA_{89.6}$)	112	20	80	26250	28950	1.18	86	89	22.4	22900	100	20	80
P3	P($UrMA_{15.6}$-*stat*-$THOXMA_{104.4}$)	120	13	87	28050	30200	1.2	88	90	15.6	23100	100	10	90

[a]Determined by ^{1}H-NMR performed in DMSO-d6, according to the (Eq. 8., SI); [b]Determined by ^{1}H-NMR performed in DMSO-d6, according to the (Eq. 9, Eq. 10., SI); [c]Determined by ^{1}H-NMR performed in DMSO-d6, according to the (Eq. 11., SI); [d]Performed in DMF containing 0.1% LiCl; [c]Determined according to the Eq. (see SI). [e]Determined by ^{1}H-NMR performed in DMSO-d6, according to the (Eq. 4., SI); [f]Calculated using the following equation DP_{target} = (([THOXMA]/[CPDB]) x Conv $_{THOXMA}$) + (([UrMA]/[CPDB]) x Conv $_{UrM}$

IV. Results and Discussion

IV.1. Characterisation of nucleobase-containing copolymers

Statistical copolymers containing uracil and thiomorpholine oxide frameworks P(UrMA$_n$-*stat*-THOXMA$_m$) were prepared by RAFT polymerisation (*Fig. 1. A.*), according to a previously published procedure by our group. (ref. article 2) The resulting copolymers were soluble at physiological pH (pH 7.4) due to hydrophilic thiomorpholine oxide motifs. In our previous work, (ref. article 2) we demonstrated that uracil containing polymethacrylate copolymers co-assemble at physiological pH *via* H-bonds with complementary adenine containing polymethacrylate copolymers. Thus, in this work, the complexation of uracil containing copolymers *via* H-bonds with adenine complementary nucleobases of genetic material will be investigated. To this, three copolymers were synthesised, respectively P(UrMA$_9$-*stat*-THOXMA$_{33}$) (noted as P1), P(UrMA$_{22.4}$-*stat*-THOXMA$_{89.6}$) (noted as P2) and P(UrMA$_{15.6}$-*stat*-THOXMA$_{104.4}$) (noted as P3). P1 and P2 contain the same molar ratio of UrMA containing co-monomer (~20%), but different degrees of polymerisation DP (P1: DP ~ 42, 8 units of Ur and P2: DP ~100, 22 units of Ur). P2 and P3 were present the same degree of polymerisation (DP~100), but different molar ratios of UrMA containing co-monomer (P2: ~20% UrMA, 22 units of Ur, P3: ~10% UrMA, 16 units of Ur). Copolymer length below 150 and molar ratios of UrMA below 30% were selected since at higher DP and higher molar ratios of UrMA, the copolymers presented a low solubility at physiological pH and formed big aggregates in solution (*Data not shown*).

Characterization data of the developed copolymers are summarized in *Table 1, Fig. S1.* and *Fig. S2*. The experimental molecular weights and co-monomer ratios of the copolymers determined by ^{1}H-NMR were close to the theoretical values (*Table 1*). SEC characterisation revealed overall narrow molecular weight distribution (Đ ≅ 1.2, *see Table 1*), while the evolution of molecular weight with conversion showed a linear relationship (*Fig. S2.*). These results confirmed that RAFT allowed the formation of well-defined nucleobase copolymers with controlled architectures.

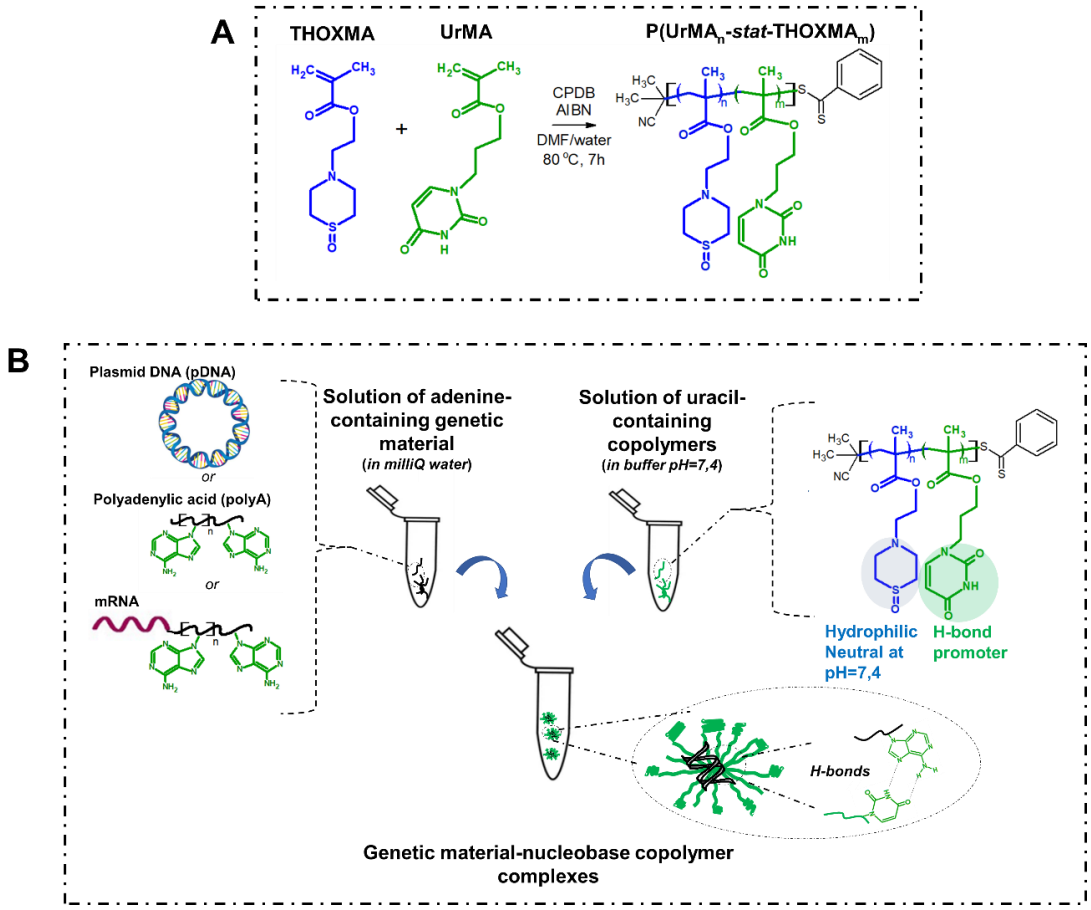

Fig. 1. Synthesis of uracil containing copolymers (A); Formulation of the genetic material-nucleobase copolymer complexes stabilised by complementary H-bonds (B).

IV.2. Biocompatibility of nucleobase-containing copolymers

The *in-vitro* biological properties (cytotoxicity, cellular aggregation assay and haemolytic activity) of obtained copolymers were investigated. Firstly, Resazurin-Alamar Blue cell viability assays were conducted at different concentrations of polymers (5 to 700 µg/mL), using L-929 mouse cell line, according to the procedure showed in Supplementary Information (SI). As illustrated in *Fig 2. A.*, an increased cellular viability (above 90%) underlined that the copolymers were not cytotoxic over the tested concentration range. Moreover, the aggregation behaviour of hematies in contact with the copolymers (*Fig. 2. B.*) was evaluated on human blood and compared to cationic branched bPEI (a polymer which provokes harmful aggregation of red cells),[17] according to the protocol illustrated in Supplementary Information (SI). Overall, the copolymers showed an aggregation rate below 1.3, which is coherent with an absence of aggregation effect of hematies in interaction with the polymers.[18] Moreover, the interaction of

the prepared copolymers with blood cell membrane was quantified by haemoglobin release assay (*Fig. 2. C.*). The haemolysis assay showed that very low amounts of haemoglobin (~ 1 %) were released after the treatment of red blood cells with the polymers, which means that the cellular membrane was not damaged by the polymers. Taken together, these results emphasize that the prepared nucleobase containing copolymers are biocompatible. Low values of released haemoglobin were recently reported in the case of nucleoside containing cationic phospholipids and were supposed to be a consequence of supramolecular H-bond interactions between the nucleoside and the proteins from blood which diminished the degradation of the cellular membrane compared to the simple cationic phospholipids.[19] Translated to our polymers, the neutral character at physiological pH of the copolymer structures might explain the obtained promising biocompatible properties.

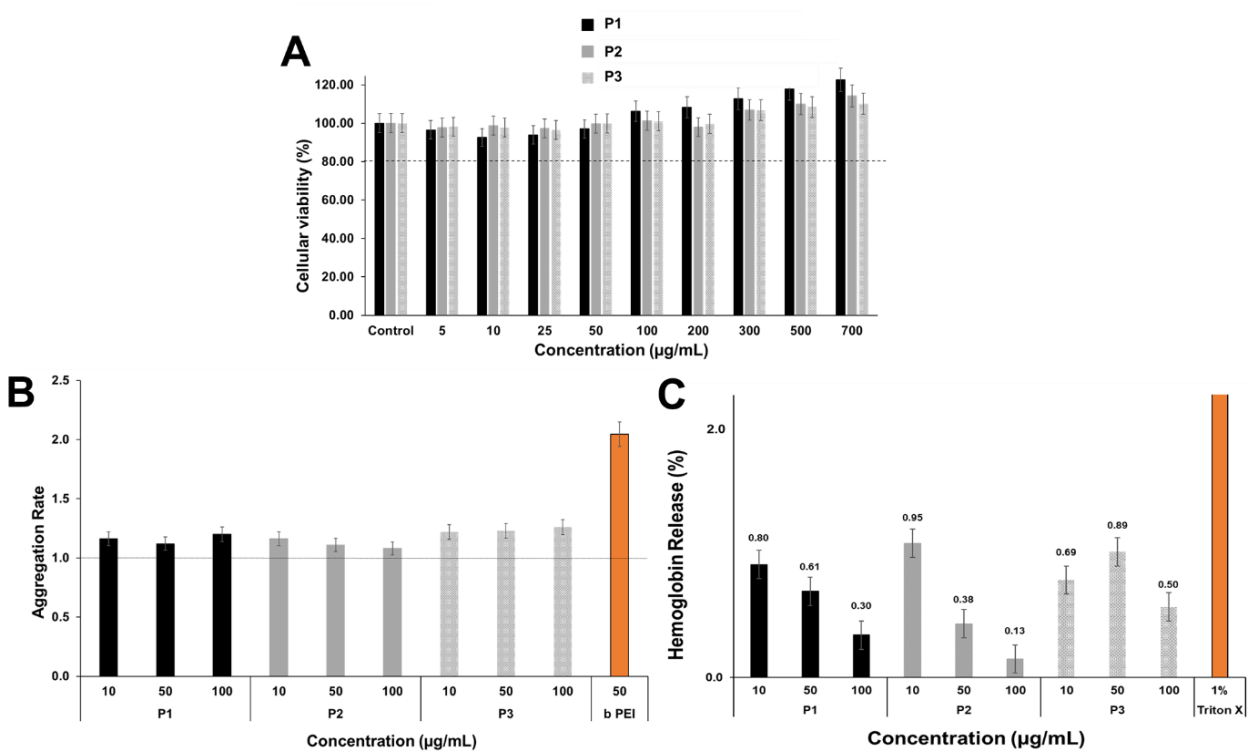

Fig. 2. In-vitro biological properties of uracil containing copolymers: cytotoxicity on L929 mouse cell line, pH 7.4 (A); aggregation rate of hematies evaluated on human blood, pH 7.4 (B) and the hemolysis properties evaluated on human blood, pH 7.4 (C).

IV.3. Complexation of nucleobase-containing copolymers with genetic material

An efficient binding of the genetic material is the first crucial step in the gene delivery process and it is required for protection and transport of the genetic material.[20] In this section, the main focus was to investigate the specific complexation *via* H-bonds of uracil containing copolymers with single strand RNA related genetic material. In this context, mRNA has recently received a particular attention in the field of cellular transfection and vaccine production. One big advantage of mRNA transfection is that it doesn't require an entrance of the mRNA inside the cell nucleus, nor to integrate the mRNA into the host genomic DNA.[4] However, mRNA is very unstable to the RNAses. For this reason, a polyadenylated tail (polyA tail) is naturally added during the mRNA transcription in order to increase the stability against the RNAses.[16] Considering the benefits of polyA tail in the structure of mRNA, we firstly aimed at investigating the complexation of uracil containing polymers with pure polyadenylic acid (polyA) which is a single stranded RNA, but is less expensive than mRNA and allowed us to optimise the experimental methodology involved in the complexation. The complexation was also investigated in the case of mRNA. Control experiments with plasmid DNA (pDNA) were performed in order to validate if the complexation occurs specifically with single stranded genetic material.

Gel electrophoresis (*Fig. 3.*), DLS (*Fig. S3.*) and circular dichroism (*Fig. S4.*) experiments were carried out to study the complexation of the nucleobase containing polymers with the three types of genetic material (polyA, mRNA and pDNA).

Since in this study, the main principle of genetic material complexation is assigned to the formation of H-bonds between adenine and uracil complementary nucleobases, gel electrophoresis experiments were performed at different ratios between the molar equivalents of uracil units in the copolymer and the molar equivalents of adenine units of genetic material. Individual P1, P2 and P3 polymers, as well as non-complexed genetic materials were used as controls.

The binding properties between nucleobase copolymers and polyadenylic acid (PolyA) are shown in *Fig. 3. B.* Polymers with low DP (*i.e.*, P1, DP~42, 20% of UrMA, 8 units of Ur) were not favourable to perform the complexation with polyA. In consequence, the bands

corresponding to the copolymer-polyA formulations developed by using P1 did not show significant differences compared to simple polyA. The increase of the DP, while keeping the same molar ratio in the UrMA co-monomer (*i.e.*, P2, DP~100, 20% of UrMA, 22 units of Ur), was favourable for the complexation with polyA. Respectively, it was noticed that for P2 containing formulations, the complexation with polyA was significantly increased when using high ratios in Ur/Ad. This observation is coherent since the increase of the amount of copolymer increased the number of H-bonds between uracil and adenine groups of the polyA which results in stronger complexation properties. Moreover, using copolymers with high DP, but with lower molar ratio of UrMA co-monomer (*i.e.*, P3, DP~100, 10% of UrMA, 16 units of Ur), gradually facilitates the complexation with polyA, even at low ratios in Ur/Ad. This behaviour could be explained by the statistical distribution of uracil groups in the copolymer structure. Copolymers providing high DP are supposed to coil their structure during the binding of genetic material, as suggested by previous studies.[21] However, high DPs are favourable to polyA they increase the probability to have several H-bonding sites on the same chain, and thus a stronger binding by H-bonds.[22] Moreover, the polyA containing formulations were evaluated by DLS which revealed the formation of particles with nanometric size in the range of 100-200 nm, which is compatible with cellular penetration (*Fig. S3*.). Then, CD measurements (*Fig. S4*.) showed that the introduction of nucleobase containing polymers led to the changes of the intensity of signals corresponding to the polyA backbone. This is an indication that an interaction between polymer and polyA occurred (as supported by gel electrophoresis), but no change of polyA conformation was induced by complexation.

Since the copolymers showed binding properties with polyA, further investigations were conducted to study the complexation properties between the copolymers and mRNA. As presented in *Fig. 3.C.*, the intensity of the bands is smoothly decreased when using high ratios in Ur/Ad, which is an indication that the nucleobase copolymers could bind the polyA tail of the mRNA. However, compared to the complexation with polyA, the complexation of copolymers with mRNA was less strong. One of the reasons is that the number of adenine groups of polyA tail is lower than in single polyA, so the number of H-bonds between uracil-adenine nucleobases is lower in the case of mRNA. Another reason might be the presence of other nucleotides in the structure of mRNA which are competitive towards H-bond interactions with the copolymer.

Lastly, control experiments were made with plasmid DNA (pDNA), a double stranded genetic material which is used in traditional gene delivery systems.[23] As illustrated in *Fig. 3. A.*, no specific complexation was observed between nucleobase containing polymers and pDNA.

Overall, gel electrophoresis experiments revealed that nucleobase copolymers, especially those with high DP, specifically interacted with adenine containing genetic material, respectively polyA and mRNA. This result is explained by the formation of H-bond between complementary nucleobases uracil and adenine which are at the origin of the complex formation.

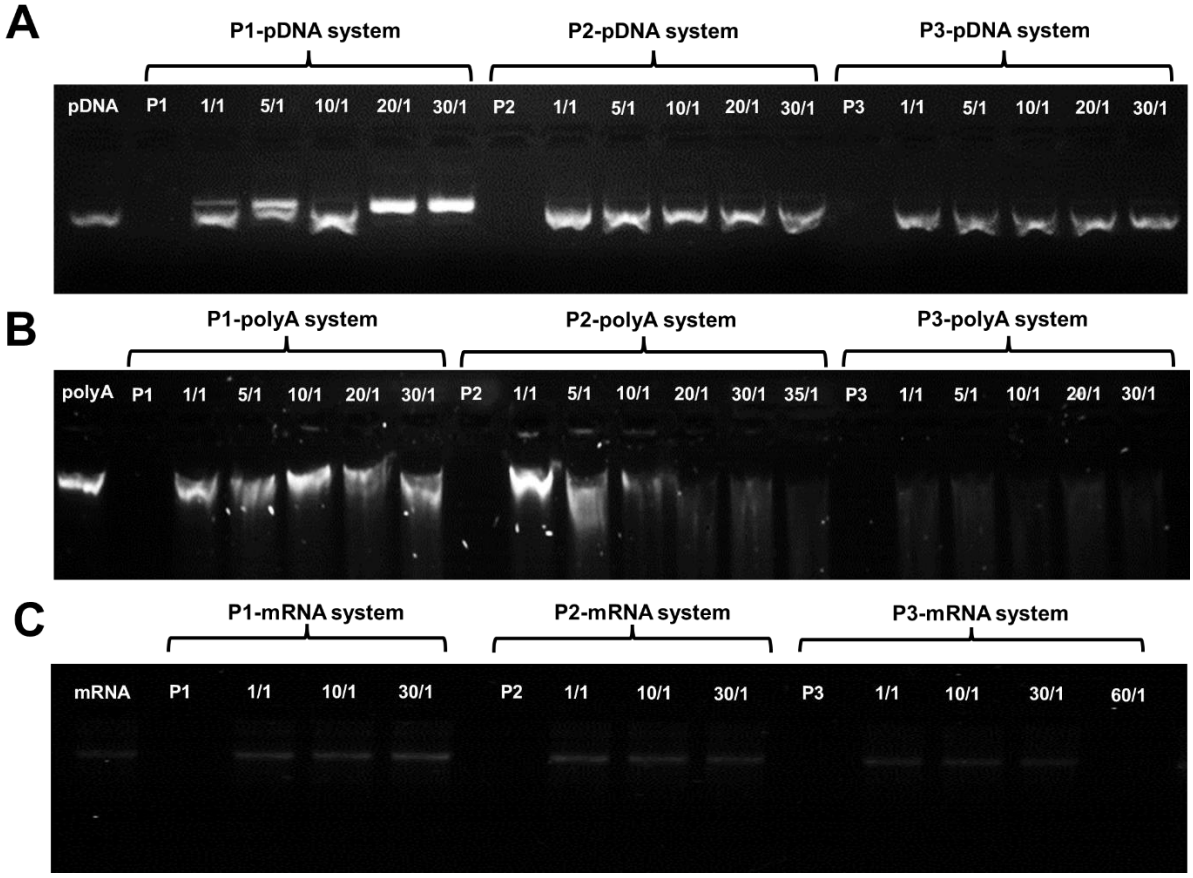

Fig. 3. Gel electrophoresis pages of the complexes performed by using neutral uracil containing copolymers and three different types of genetic material: pDNA (A); polyA (B) and mRNA (C).

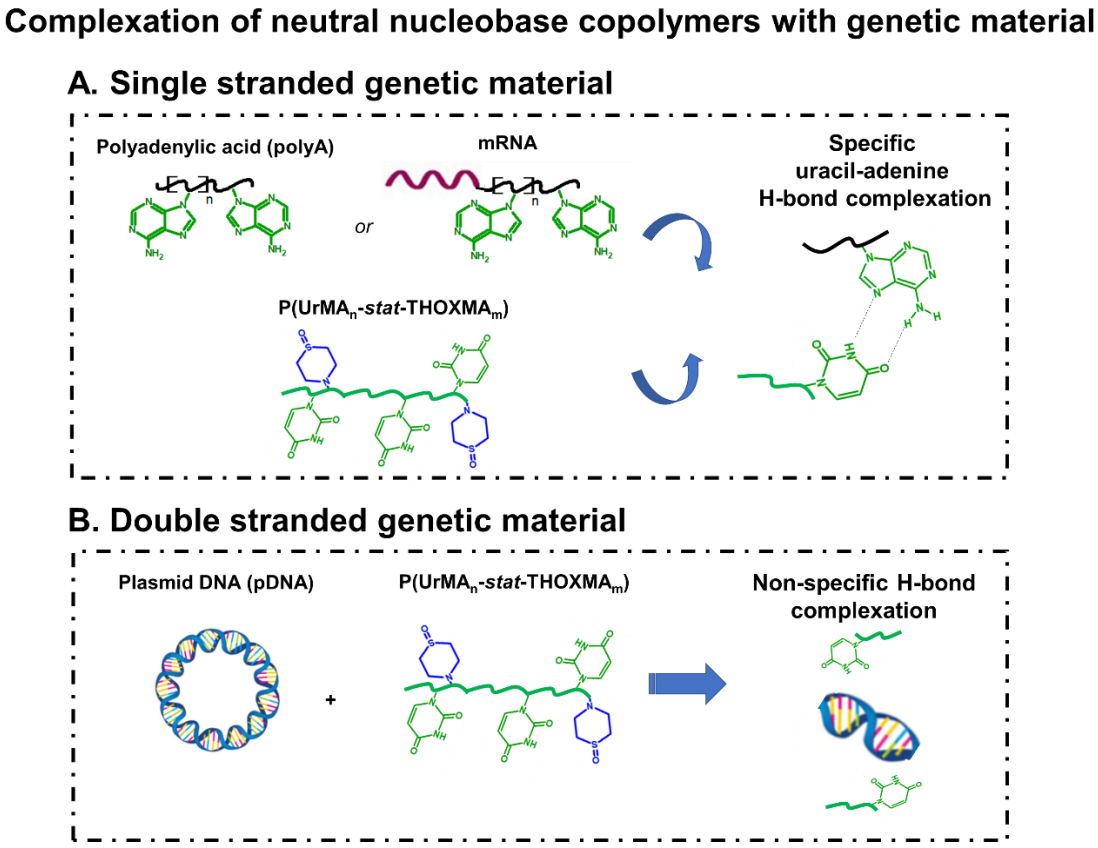

Fig. 4. Illustration of the selective genetic material binding by uracil containing nucleobase copolymers

IV.4. Behaviour of nucleobase-containing copolymers/ genetic material complexes in the presence of RNAses

RNAses are one of the first barriers of the immune system which remove the foreign genetic material in order to avoid infection. RNAses are therefore present and active in the entire vascular system and they represent one of the most significant difficulty to be overcome when performing gene transfection.[24] The metabolic stability of copolymer-polyA complexes to the digestion with RNAse A was evaluated by gel electrophoresis (*Fig. 5. A.*). In the case of pure PolyA, the characteristic band of single strand structure disappeared at high concentrations of RNAse A, which is consistent with the degradation of polyA (*Fig. 5. A.*). For nucleobase copolymers-polyA complexes the specific band still visible at low concentrations of RNAses, while at high concentrations of enzyme, the spots become more diffused. These results emphasize that, compared to the polyA, the copolymer-polyA complexes are more stables against RNAses at low and mild concentrations of enzyme. The increased stability of the

complexes compared to simple polyA are probably due to complementary H-bonds between uracil and adenine which stabilised the complex structure.

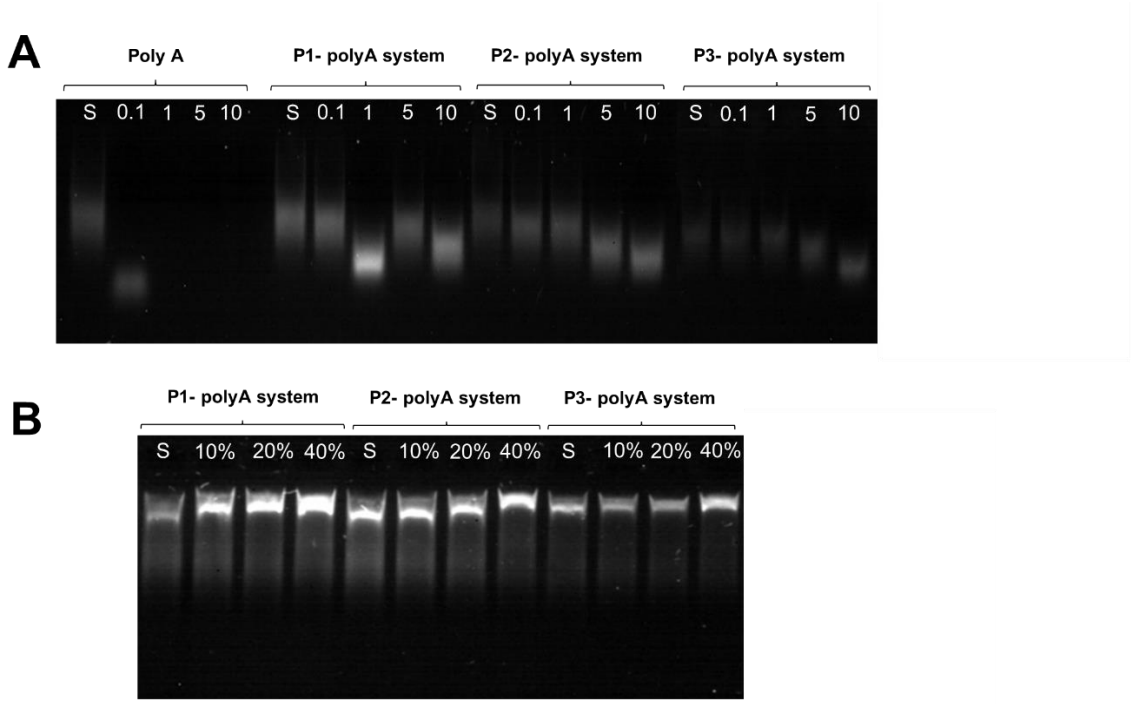

Fig. 5. Stability of polyA containing complexes evaluated by gel electrophoresis in the presence of various molar ratios of RNAse A (0.1 - 10) (A) and physiological serum (B)

IV.5. Behaviour of nucleobase-containing copolymers/ genetic material complexes in physiological serum

Although a positive charge in the case of traditional cationic polymers used for gene delivery has been associated with enhanced uptake *in vitro*, these cationic polymers also interact with negatively charged serum proteins *in vivo*, which further results in modification of cellular clearance and less effective transfection efficiency.[25] Since the developed nucleobase-copolymer/genetic material complexes are neutral charged at physiological pH, our idea was to investigate if the neutral behaviour could ameliorate the behaviour of these complexes in physiological serum. To this, the evaluation of the behaviour of polyA-containing complexes in the presence of serum was monitored by gel electrophoresis (*Fig. 5. B.*). As shown in *Fig. 5. B.*, the polyA-copolymer complexes were overall stable after 1h of exposure to physiological serum. However, at high ratios in serum, the intensity of bands increased, which could reveal

some supplementary interactions of the complexes with serum proteins. Nevertheless, it was noticed that the complexes prepared with P3 copolymer (*i.e.*, DP~100, 10% molar ratio of UrMA, 16 units of Ur), were the best candidates towards the stability in low and mild concentrations of serum.

V. Conclusion

In this study we designed neutral complexes formed at physiological pH *via* H-bond interactions between uracil containing copolymers and adenine groups of genetic material. The interactions involved in the formation of the complexes are H-bonds between complementary nucleobases instead of the traditional electrostatic interactions. This is a new concept which was barely explored so far. Based on our previous works on hydrophilic nucleobase copolymers, uracil and thiomorpholine oxide containing statistical copolymers P($UrMA_n$-*stat*-$THOXMA_m$) made by RAFT were chosen for the complexation with genetic material. These copolymers were hydrosoluble at physiological pH due to THOX groups, while uracil groups enabled the H-bond with adenine nucleobases of genetic material. The *in-vitro* evaluation revealed that the nucleobase containing copolymers were non-cytotoxic and blood compatible, compared to standard commercial cationic polymers (PEI), without emphasizing harmful degradation of the blood cellular membrane. These results were explained due to the neutral character of nucleobase copolymers which avoided the undesired interactions with anionic cellular membrane. Moreover, the complexation properties between nucleobase copolymers and genetic material were investigated. Gel electrophoresis revealed a specific affinity of copolymers to complex with single strand genetic material (polyA and mRNA), while no complexation was observed with double stranded DNA (plasmid DNA: pDNA). This result was expected because in the case of pDNA (which is double stranded) the adenine groups are already involved in H-bonds with the complementary DNA strand and thus the binding strength between complementary DNA strands is stronger than with uracil copolymers, so no complexation was observed. In contrast, in the case of polyA and mRNA (which are single stranded), the adenine groups are free and can therefore form H-bonds with the uracil copolymers. Furthermore, polyA complexes displayed a relative stability against RNAses and serum, which emphasize that complementary H-bonds were sufficiently strong to overcome genetic material degradation. Respectively, it was noticed that the copolymer providing the highest DP showed the most promising results in terms of complexation with single stranded

genetic material, stability against RNAse A, as well as resistance in physiological serum. Overall, this work underlines the advantage of using neutral charged nucleobase containing copolymers in order to complex specifically single strand genetic material by supramolecular H-bonds, which avoided the cytotoxicity issues of traditional cationic polymers used for this purpose. These results are very promising in order to further investigate the potential of these complexes as new gene delivery vectors. In this regard, current perspectives of this work concern the testing of the obtained complexes for cellular transfection.

VI. References

1. L. Ke, P. Cai, Y-L.Wu and X. Chen, *Adv. Ther.*, 2020, **3(6)**, 1-22.
2. C. H. Jones, C-K. Chen, A. Ravikrishnan, S. Rane and B. A. Pfeifer, *Mol. Pharm.*, 2013, **10(11)**, 4082-4098.
3. J. C. Burnett and J.J. Rossi, *Chem. Biol.*, 2012, **19**, 60–71.
4. U. Sahin, K. Karikó and O. Türeci, *Nat. Rev. Drug Discov.*, 2014, **13**, 759-780.
5. D. Luo and W. M. Saltzman, *Nat. Biotechnol.*, 2000, **18**, 33–37.
6. Y. K. Sung and S.W. Kim, *Biomater. Res.*, 2019, **23**, 1-7.
7. L. Peng and E.Wagner, *Biomacromolecules*, 2019, **20**, 3613–3626.
8. D. W. Pack, A. S. Hoffman, S. Pun and P. S. Stayton, *Nat. Rev. Drug Discov.*, 2005, **4**, 581–593.
9. S. C. De Smedt, J. Demeester and W. E. Hennink, *Pharm. Res.*, 2000, **17**, 113–126.
10. R. Ni, R. Feng and Y. Chau, *Life*, 2019, **9**, 1–28.
11. A. Kargaard, J. P. G. Sluijter and B. Klumperman, *J. Control. Release*, 2019, **316**, 263–291.
12. J. Zhou, J. Liu, C. J. Cheng, T. R. Patel, C. E. Weller, J. M. Piepmeier, Z. Jiang and W. M. Saltzman, *Nat. Mater.*, 2012, **11**, 82–90.
13. A. Frère, A. Baroni, E. Hendrick, A-S. Delvigne, F. Orange, O. Peulen, G. R. Dakwar, J. Diricq, P. Dubois, B. Evrard, K. Remaut, K. Braeckmans, S. C. De Smedt, J. Laloy, J-M Dogné, G. Feller, L. Mespouille, D. Mottet and G. Piel, *ACS Appl. Mater. Interfaces*, 2017, **9**, 2181–2195.
14. H. Wang, H. Wei, Q. Huang, H. Liu, J. Hu, Y. Cheng and J. Xiao, *Colloids Surf. B Biointerfaces*, 2015, **136**, 1148–1155.
15. L. V. Arsenie, F. Hausig, C. Kellner, J. C. Brendel, P. Lacroix-Desmazes, V. Ladmiral and S. Catrouillet, *Molecules*, 2022, **27**, 1–15.
16. C. R. Eckmann, C. Rammelt and E. Wahle, *Wiley Interdiscip. Rev. RNA*, 2011, **2**, 348–361.

17. D. Zhong, Y. Jiao, Y. Zhang, W. Zhang, N. Li, Q. Zuo, Q. Wang, W. Xue, Z. Liu, *Biomaterials*, 2013, **34**, 294–305.

18. C. Q. Lai, J. C. W. Shen, W. C. W. Cheng and C. H. Yap, *RSC Adv.*, 2016, **6**, 62451-62459.

19. F. Jia, X. Lu, X.Tan and K. Zhang, *Chem. Commun.*, 2015, **51**, 7843–7846.

20. J. I. Solomun, G. Cinar, P. Mapfumo, F. Riechter, E. Moek, F. Hausig, L. Martin, S. Hoeppener, I. Nischang and A. Traeger, *Int. J. Pharm.*, 2021, **593**, 120080-120095.

21. C. Chen, D. Y. Wah Ng and T. Weil, *Prog. Polym. Sci.*, 2020, **105**, 101241-101281.

22. C. J. Whitfield, M. Zhang, P. Winterwerber, Y. Wu, D. Y. W. Ng and T. Weil, *Chem. Rev.*, 2021, **121(18)**, 11030-11084.

23. N. P. Higgins and A. V. Vologodskii, *Microbiol. Spectr.*, 2015, **3(2)**, 1-49.

24. L. Lu, J. Li, M. Moussaoui and E. Boix, *Front. Immunol.*, 2018, **9**, 1-20.

25. S. Nimesh, *Ther. Deliv.*, 2012, **3(11)**, 1347–1356.

VII. Acknowledgements

This research was funded by DAAD (German Academic Exchange Service) Research Grants-Short Term Grants 2022 (Funding program number: 57588366) as well as by the French Ministry of higher education and research. The authors kindly thank Carolin Kellner (IOMC, Jena) who performed hemocompatible assays of uracil-containing copolymers.

VIII. Supplementary information

Table of contents

Materials

Methacryloyl chloride was acquired from Fluka (Switzerland) and distilled (50°C, 400 mbar) before use. 2-bromoethanol, and uracil (Ur) were purchased from Alfa Aesar (Germany). Thiomorpholine and 3-bromo-1-propanol were bought from Fluorochem (UK). Hydrogen peroxide (H_2O_2) solution (30% wt%) was received from Carlo Erba (France). 4-dimethylaminopyridine (DMAP), triethylamine (TEA), 2-cyano-2-propyl benzodithioate (CTA),_disodiumphosphate basic dodecahydrate ($Na_2HPO_4 \cdot 12H_2O$), potassium carbonate (K_2CO_3), and deuterated solvents (deuterated chloroform, $CDCl_3$, and hexadeuterodimethyl sulfoxide, DMSO-d_6) were provided by Sigma Aldrich. 2,2′-azobis(2-methylpropionitrile) (AIBN) was acquired from Sigma Aldrich (Germany) and recrystallised from methanol at 65°C before use. Sodium chloride (NaCl) and citric acid monohydrate ($C_6H_8O_7 \cdot H_2O$) were obtained from VWR Chemical. Sodium bicarbonate ($NaHCO_3$) was purchased from Fluka (France). Dimethylformamide (DMF) was acquired from Fisher Scientific (Belgium). HEPES (4-(2-hydroxyethyl)-1-piperazineethanesulfonic acid) buffered saline solution (20 mM) was acquired

from PromoCell (Germany). Agarose was provided by Roth (Germany). Poly adenylic acid (polyA) and RNAse A were achieved from Merck (Germany). β-galactosidase (β-gal) mRNA (c=1 mg/mL) was acquired from Tri Link Biotechnologies (France). Plasmid DNA (pDNA) encoding pKMyc were isolated from E. Coli using a Giga plasmid kit (Quiagen, Germany). Dry solvents (dichloromethane, CH_2Cl_2, and acetonitrile, CH_3CN) were purified using a PureSolv Micro solvent purification system purchased from Sigma Aldrich (USA). The dialysis membranes used for purification of polymers (Spectra/Por 7 Pretreated RC Dyalisis Tubing, MWCO= 1kDa, diameter 24mm, 4.6 mL/cm) were bought from Krackeler Scientific, USA.

Branched PEI (bPEI, M_w = 25 kg/mol) was obtained from Polysciences (U.S.). 1% ethidium bromide solution (EtBr) was obtained from Carl Roth (Germany). SYBR Gold Nucleic Acid Stain (10.000X concentrate in DMSO), SYBR Green II RNA stain (10.000X concentrate in DMSO) and Tris-Borate-EDTA (TBE) buffer (10X concentrate) were provided by Thermo Fisher Scientific (Germany). Green gel loading loading buffer was acquired from Jena Biosciences (Germany). 2 mM L-glutamine 100 U/mL penicillin, and 100 µg/mL streptomycin solutions were achieved from Biochrom. 10% fetal calf serum was bought from FCS, Capricorn Scientific. The PrestoBlue solution was obtained from Thermo Fisher, Germany. Human blood was provided by the Department of Transfusion Medicine from Jena University Hospital.

Instrumentation

^{1}H-NMR spectra were recorded on NMR Bruker Avance 400-MHz or NMR Bruker Avance III HD -400 MHz spectrometer using $CDCl_3$ or DMSO-d_6 as deuterated solvent. The chemical shifts of protons were relative to tetramethylsilane (TMS) at $\delta = 0$.

Size exclusion chromatography (SEC) data were obtained in DMF containing 0.1 wt. % LiCl, with a flow rate of 0.8 mL min^{-1} at 40°C by using TE36 Whatman PFTE-supported membrane filter paper (0.45 µm, 47 mm diameter). The data were calibrated using polymethyl methacrylate (PMMA) standards.

Dynamic light scattering (DLS) experiments were performed by using Malvern Instrument. Transmission electron microscopy (TEM) assays were conducted on JEOL 1200 EXII-120 kV instrument.

Gel electrophoresis imaging was performed by using the Alpha Innotech Gel Imaging System (Germany).

The cells incubation for the cytotoxicity tests was performed in a 96 well plate acquired from VWR, Germany. The fluorescence measurements used to determine the cell viability were assessed using an Infinite M200 PRO microplate reader (Tecan, Germany). The haemoglobin release measurements and the cell aggregation rate were performed using a plate reader from Tecan (Männedorf, Switzerland).

Methods

Synthesis of 2-ethyl thiomorpholine oxide methacrylate

2-ethyl thiomorpholine oxide methacrylate was synthesized by oxydation of 2-ethyl thiomorpholine methacrylate, following a previously published procedure.[1]

Synthesis of 3-(uracil-1-yl)propyl methacrylate

3-(uracil-1-yl)propyl methacrylate was synthesized according to a previously published procedure. (ref. Article 2)

Synthesis of Poly((3-(uracil-1-yl) propyl methacrylate) -stat-(2-ethyl thiomorpholine oxide methacrylate)) P(UrMA$_n$ -stat-THOXMA$_m$) by RAFT polymerisation

In a typical protocol, 2-cyano-2-propyl benzodithioate (CTA, 1 eq.), AIBN (0.25 eq.), *uracil monomer (UrMA)* (x eq.) and *thiomorpholine oxide monomer THOX*MA((y-x) eq.) were dissolved in a mixture of DMF/ aqueous buffer (pH 4, $C_{M\,=}$4 M). The mixture was thoroughly degassed *via* 3 freeze–pump–thaw cycles, filled with nitrogen and immersed into an oil bath at 80 °C. At different time, an aliquot of the reaction mixture was taken and analysed by ^{1}H-NMR and SEC. After 7h the reaction was stopped by exposure to air. The mixture was then dialysed against water (with a 1kDa MWCO membrane) for 3 days, followed by lyophilisation during 2 days. The resulting pink polymer powder was analysed by ^{1}H-NMR in DMSO-d$_6$ and DMF SEC. For example, to obtain P(UrMA$_8$-*stat*-THOXMA$_{34}$), the quantities of reagents used were: CTA (1eq., 8 mg, 0.036 mmol), AIBN (0.25 eq., 1.5 mg, 0.009 mmol), *uracil monomer UrMA* (10 eq., 82 mg, 0.36 mmol), *thiomorpholine oxide monomer THOXMA* (40 eq., 332 mg, 1.44 mmol), dissolved in DMF (2 mL)/ aqueous buffer (pH=4, $C_{M\,=}$4 M, 60 eq., 0.54 mL). ^{1}H-NMR, *Fig. S1*. (400 MHz, DMSO-d$_6$) δ (ppm) = 1.8 (s, C**H**$_2$, polymerizable synthon, noted as **I$_b$**); 1.8 (m, C**H**$_2$, UrMA aliphatic linker, noted as **II$_b$**); 3.43 (d, C**H**$_2$, UrMA aliphatic linker, noted as **II$_a$** and **II$_c$**); 3.43 (d, C**H**$_2$, THOXMA aliphatic linker, noted as **II$_d$** and **II$_e$**); 2.62 (t, CH$_2$C**H**$_2$, thiomorpholine oxide cycle, noted as **III$_b$**); 3.87 (t, CH$_2$C**H**$_2$, thiomorpholine oxide cycle, noted

as **III$_a$**); 0.87, 0.97, 1.1 (s, C**H**$_3$, noted as **I$_a$**); 7.57 (d, CH=C**H**, uracil heterocycle, noted as **i**); 5.87 (d, C**H**=C**H**, uracil heterocycle, noted as **h**); 11.5 (s, N**H**, uracil heterocycle, noted as **g**).

Preparation of solutions of complexes between uracil containing copolymers and genetic material

The genetic material-uracil containing copolymer complexes were prepared in HBG buffer (pH 7.4). HBG buffer consisted of 20 mM 4-(2-hydroxethyl) piperazine-1-ethanesulfonic acid (HEPES) containing 5 % (w/v) glucose. Genetic material containing solution was added to the polymer solution (stock solution concentration: 5 mg/mL), to give the final formulation. The formulations were prepared in different molar ratios between the molar equivalents of uracil (Ur) units of the copolymer and the molar equivalents of adenine (Ad) units from the genetic material (Ur/Ad ratio). Immediately after combination, the genetic material-polymer mixtures were vortexed for 30 s at 1500 rpm and incubated at room temperature for 30 min to ensure complex formation.

Dynamic Light Scattering

Particle size (Z_{ave}) of co-assembled polymers were determined by dynamic light scattering (DLS). The DLS instrumentation consisted of the same LS spectrometer used for SLS experiments. DLS measurements were performed at 25 °C with a He–Ne 630 nm laser module, at a detection angle of 150°.

Circular Dichroism

The circular dichroism (CD) spectra were recorded on a JASCO J-815 spectropolarimeter. The formulations (prepared with a constant concentration of 150 nM of genetic material) were loaded into a 1 mm quartz cuvette. The spectra were obtained at 37°C from 190 nm to 400 nm with 0.1 nm step, 0.5 nm bandwidth, and 100 nm/min scanning speed.

Cytotoxicity of uracil containing copolymers

Cytotoxicity studies were performed using the mouse fibroblast cell line L929, as recommended by ISO10993-5. L929 cells were cultured in Dulbecco's modified eagle's medium prepared with 2 mM L-glutamine supplemented with 10% fetal calf serum, 100 U/mL penicillin, and 100 µg/mL streptomycin at 37 °C under a humidified 5% (v/v) CO_2 atmosphere. Cells were seeded at 10^3 cells/mL in a 96 well plate and then incubated for 24 h. No cells were seeded in the outer wells. The medium was changed to fresh cell culture medium 1 h prior to treatment. The cold

polymer solutions prepared in 20 mM HEPES (4-(2-hydroxyethyl)-1-piperazineethanesulfonic acid) were added to the cells in different concentrations (from 5 to 700 μg/mL), and then incubated for 24 h. The control cells were incubated with fresh culture medium containing the same amount of HEPES as the treated cells. Furthermore, the medium was replaced by a mixture of a fresh culture medium and the resazurin-based solution PrestoBlue (prepared according to the manufacturer's instructions). After further incubation for 45 min at 37 °C under a humidified 5% (v/v) CO_2 atmosphere, the fluorescence was measured at λ_{ex} = 560 nm/λ_{em} = 590 nm with gain set to optimal, with untreated cells on the same well plate serving as negative controls. The negative control was standardized as 0% of metabolism inhibition and referred to as 100% viability. Cell viability below 70% was considered to be indicative of cytotoxicity. Experiments were conducted in triplicate, including blanks and negative controls.

Erythrocyte aggregation in the presence of uracil containing copolymers

Red blood cells were treated with the polymer solutions under physiological conditions in human blood (pH 7.4). Erythrocyte suspensions in PBS (at pH 7.4) values were prepared and mixed 1:1 (volume: volume ratio) with the polymer solutions. After incubation at 37 °C for 2 h, the aggregation of erythrocytes was measured at 645 nm. As positive and negative assay controls erythrocytes were treated with 50 μg/mL of 25 kDa branched poly(ethylene imine) (bPEI) solution at pH 7.4. The aggregation activity of the polymer at different concentrations is given as an aggregation rate calculated as follows (Eq. 2.):

$$Aggregation\ rate = \frac{1}{\mathrm{A(sample)}} \qquad \text{(Eq. 2.)}$$

Here, $A_{(sample)}$ is the mean absorbance of a given sample.

Hemolysis assay

The membrane damaging properties of the polymer were quantified by analysing the release of hemoglobin from erythrocytes. Human blood was centrifuged at 4 500g for 5 min. The pellets were washed three times with PBS (pH 7.4) by centrifugation at 4 500g for 5 min. Erythrocytes were suspended in PBS at pH 7.4 to resemble physiological conditions in blood/cytoplasm. The polymer solutions were prepared by dissolving the polymer in cold 20 mM HEPES (4-(2-hydroxyethyl)-1-piperazineethanesulfonic acid) buffer at a concentration of 1 mg/mL. Cold polymer solutions were mixed 1:1 (volume: volume ratio) with cold erythrocyte suspensions

and were incubated at 37°C for 1 h. Erythrocyte suspensions were centrifuged at 2 400g for 5 min. The release of hemoglobin in the supernatant was determined at 544 nm. The absorbance was measured using a plate reader. Concurrently, determinations were conducted with washed erythrocytes either lysed with 1% Triton X-100, as well as erythrocytes suspended in PBS, which were used as reference. The hemolytic activity of the polymer was calculated as follows (Eq. 3.):

$$Hemolysis\ \% = \left(\frac{\mathrm{A(sample)-A(PBS)}}{\mathrm{A(Triton\ X-100)}}\right) \times 100 \qquad \text{(Eq. 3.)}$$

Here, $A_{(sample)}$, $A_{(PBS)}$, and $A_{(Triton\ X\text{-}100)}$ are the absorbance of erythrocytes incubated with a respective sample, suspended in PBS, and erythrocytes lysed with Triton X-100, respectively. The analysis was repeated in triplicate.

Complexation of genetic material by gel electrophoresis assay

Gel preparation occurred as it follows: agarose powder was suspended in 1X TBE buffer (pH 8.3) and heated until it was completely dissolved. For pDNA and polyA experiments, the gel concentration used was 1%, whereas for mRNA the experiment was conducted at a concentration of 2% of agarose gel. Then, 15µL of nucleic acid stain (EtBr: for pDNA experiment /SYBR Gold: for polyA experiment/ SYBR Green II: for mRNA experiment) was added to the gel, and then the gel was poured into a gel tray with a suitable comb. After 1h, the gel was placed in the electrophoresis bath filled with 1X TBE buffer (pH 8.3). To prove the complexation of genetic material with uracil containing copolymers, 40 µL of the complex solution (polymer + genetic material) were mixed with 10 µL of the gel loading dye, and then were added in each pocket. The electrophoresis was run at RT, at 80 V, for 60 min.

Stability of polyA containing complexes in the presence of RNAse A

The stability of polyA containing complexes in the presence of RNAse A was evaluated by gel electrophoresis. The gel preparation was made as described previously, by using a concentration of agarose gel of 1%. The preparation of the formulations used for this assay was made as it follows: the complex solution (polymer + polyA) was mixed with RNAse A solution (stock solution concentration: 1 mg/mL) in different molar ratios (0.1:1, 1:1, 5:1 and 10:1), in order to get at the end 40 µL of formulation. The ratios used for this assay refers to the molar ratios between the molar equivalents of adenine units of polyA and the molar equivalents of

RNAse A. Then the formulations were incubated for 1h at 37°C. After the incubation period, 40 µL of formulation was mixed with 10 µL of the gel loading dye, and then added in each pocket. The electrophoresis was conducted at RT, at 80 V, during 60 min.

Stability of polyA containing complexes in the presence of serum

The stability of polyA containing complexes in the presence of serum medium was assessed by gel electrophoresis. The gel preparation was performed as described previously, by using a concentration of agarose gel of 1%. The formulations used for this assay were prepared as it follows: the complex solution (polymer + polyA) was combined with different volume percentages of serum (10%, 20% and 40%, calculated compared to the final volume of formulation i.e. 40 µL), in order to obtain at the end 40 µL of formulation. The resulted formulations were incubated for 1h at 37°C. After the incubation time, 40 µL of formulation was mixed with 10 µL of the gel loading dye, and then added in each pocket of the gel. The electrophoresis was conducted at RT, at 80 V, during 60 min.

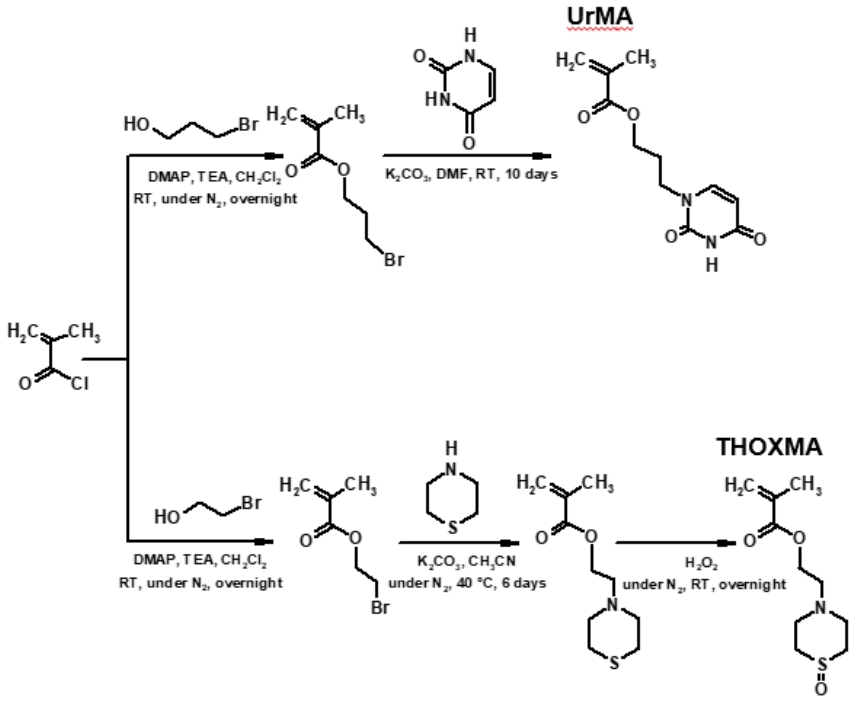

Scheme S1. Synthesis of uracil-containing monomer (UrMA) and thiomorpholine-oxide containing monomer (THOXMA)

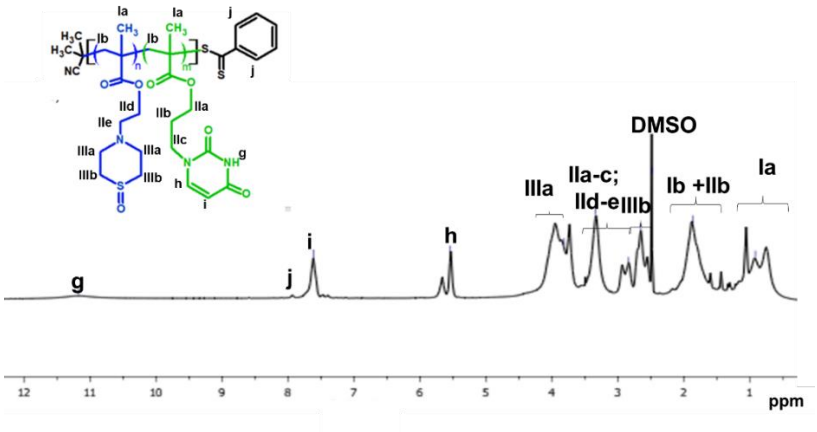

Fig. S1. ^{1}H-NMR spectrum of uracil containing copolymers, performed in DMSO-d6

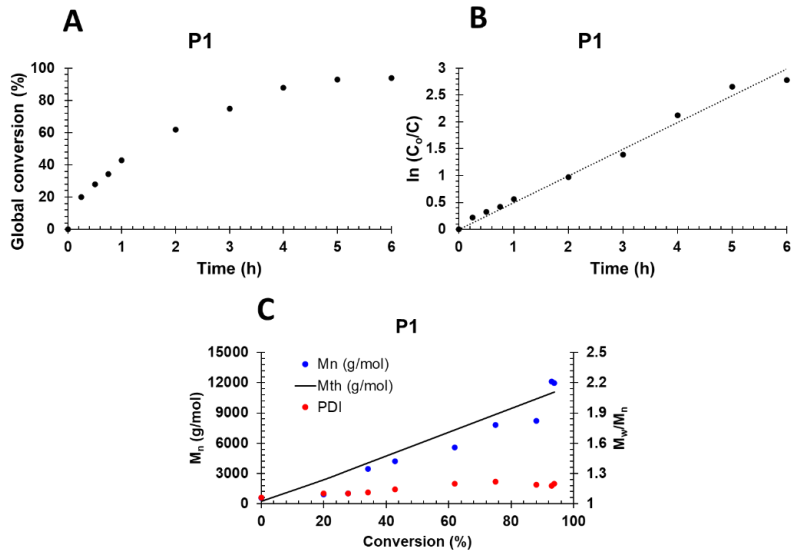

Fig. S2. Global conversion of uracil and thiomorpholine-oxide co-monomers, evaluated by ^{1}H-NMR (A); First order kinetic plot for RAFT statistical copolymerisation, evaluated by ^{1}H-NMR (B); Evolution of M_n and dispersity with conversion during the polymerisation evaluated by SEC (C). Results obtained for uracil containing polymer (P1).

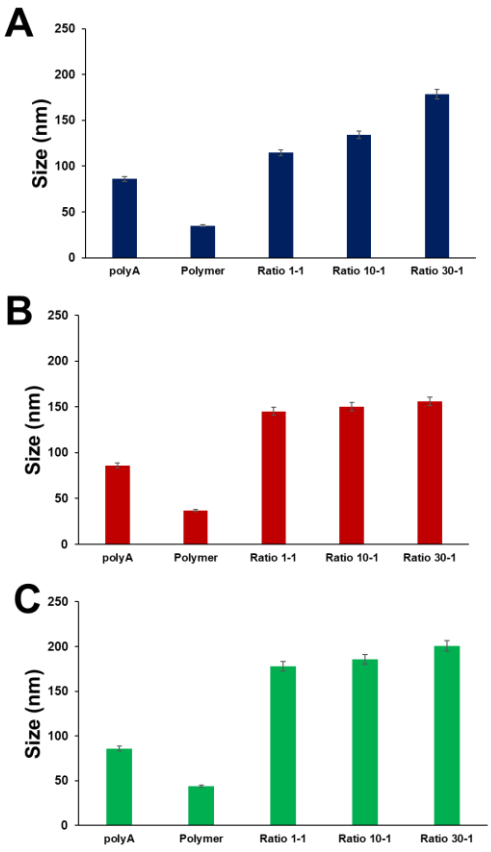

Fig. S3. Hydrodynamic size (Z_{ave}) evaluated by DLS of polyA-copolymer complexes: (A) with P1 copolymer; (B) with P2 copolymer and (C) with P3 copolymer

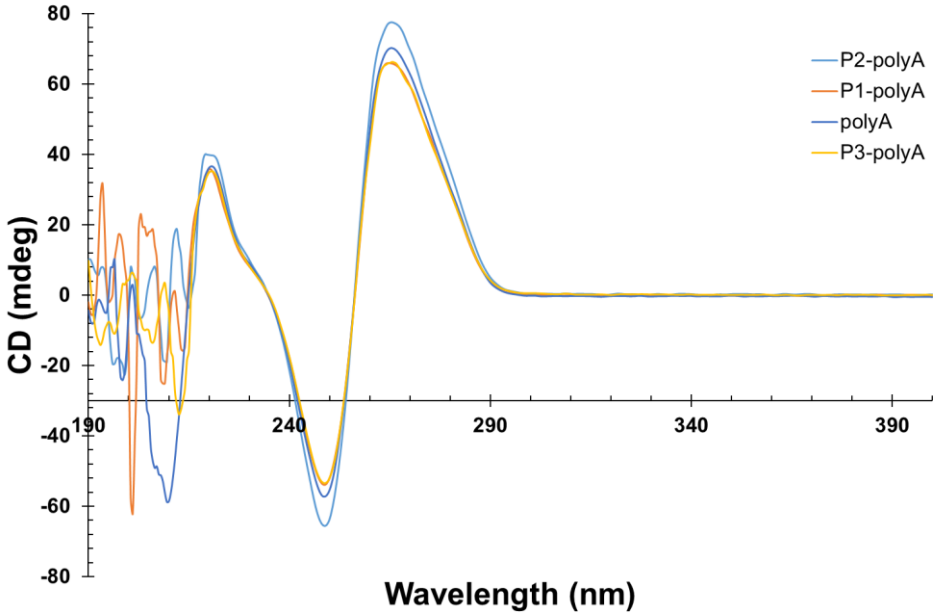

Fig. S4. Circular dichroism (CD) measurements for polyA-copolymer complexes performed at 37˚C in HEPES buffer (pH 7.4)

Equations used for polymer characterisation

- *Conversion of co-monomers*

The conversions of co-monomers were calculated by ^{1}H-NMR (Eq. 4.), *via* the comparison of signal integrals of the CPDB (7.4-7.9 ppm) and of the protons of -C=C- double bond of *THOXMA* (6.06-5.68 ppm) and/or UrMA (5.99-5.73 ppm).

$$\text{Conversion (\%)} = \frac{(I_{0,vinyl\ function}/I_{0,CTA}) - (I_{t,vinyl\ function}/I_{t,CTA})}{(I_{0,vinyl\ function}/I_{0,CTA})} \times 100 \quad \text{(Eq. 4.)}$$

Where $I_{0,CTA}$ and $I_{t,CTA}$ are the values of the integrals of the signal of the aromatic protons of the chain transfer agent (between 7.4 ppm and 7.9 ppm) at t=0 and t respectively; $I_{0,vinyl\ function}$ and $I_{t,vinyl\ function}$ are the value of the integral of the signal of one of the protons of the vinyl group of methacrylate (5.68 ppm and 6.06 ppm for THOXMA, 5.73 ppm and 5.99 ppm for UrMA), at t=0 and t respectively.

- *Degree of polymerisation*

$DP_{\text{uracil copolymer}}$ was calculated as a sum between the number of UrMA based synthons (noted as $DP_{\text{UrMA synthons}}$) and THOXMA containing synthons (noted as $DP_{\text{THOXMA synthons}}$).

The number of UrMA synthons was calculated considering the integral values at 5.56-5.58 ppm and 7.64 ppm that correspond to -C=C- double bond protons of uracil, compared to the two of the protons of CPBD (between 7.88 ppm and 7.9 ppm) as it follows (Eq. 6.):

$$DP_{\text{UrMA synthons}} = \left(\frac{(I_1+I_2)/2}{I_{CTA}/2}\right) \quad \text{(Eq. 6.)}$$

Where I_1 is the value of the integral of the signal of the proton of double bond of uracil heterocycle (between 7.6 ppm and 7.83 ppm (H_i)), I_2 is the value of the integral of the other signal of the proton of double bond of uracil heterocycle (between 5.31 ppm and 5.71 ppm (H_h)), and I_{CTA} is the value of the integral of the signal of two of the aromatic protons of the chain transfer agent (between 7.88 ppm and 7.9 ppm).

The number of THOXMA synthons were calculated according to Eq. 7:

$$DP_{\text{THOXMA synthons}} = \left(\frac{(I_3+I_4+I_5-2(I_1+I_2))/12}{I_{CTA}/2}\right) \text{(Eq. 7)}$$

The I_3 and I_4 are the values of the integrals of the proton signals in the field of 3.5 ppm-4.5 ppm and 2.52 ppm- 2.82 ppm respectively that correspond to the protons of thiomorpholine

oxide cycle (**III_a and III_b**). I_5 is the value of the integral of the protons of UrMA aliphatic linker (**II_a and II_c)**, and the protons of THOXMA aliphatic linker (**II_d and II_e)** in the field of 2.82 ppm-3.48 ppm. To calculate the DP of THOXMA synthons, the sum of integrals corresponding to these signals was assessed. Because this sum includes the integral of the protons of UrMA aliphatic linker, these values (I_1 and I_2) were subtracted in order to correctly evaluate the DP of THOXMA synthons. However, it was impossible to determine exactly the region where the protons of UrMA aliphatic linker were situated, due to signal interferences. Since in the UrMA monomer 4 protons of aliphatic linker are present in the field of 2.52 ppm- 4.55 ppm, the sum of integrals of uracil double bond protons (that correspond to 2 protons in UrMA monomer) was multiplied by 2, to calculate the integral value of UrMA aliphatic linker protons. Then, this multiplied value (corresponding with the UrMA aliphatic linker) was subtracted and the result was divided by 12 (that correspond to the total of protons of thiomorpholine oxide cycle and THOXMA aliphatic linker).

Then, $DP_{uracil\ copolymer}$ was calculated (Eq. 8.):

$$DP_{uracil\ copolymer} = DP_{UrMA\ synthons} + DP_{THOXMA\ synthons} \quad \text{(Eq. 8.)}$$

- *Experimental molar percentage of co-monomers*

The molar percentage of UrMA and THOXMA monomers were calculated according to the equations:

$$\%\ \text{(molar) of } Ur \text{ monomer} = (DP_{UrMA\ synthon} \times 100) / DP_{uracil\ copolymer} \quad \text{(Eq. 9.)}$$

$$\%\ \text{(molar) of } THOX \text{ monomer} = (DP_{THOXMA\ synthon} \times 100) / DP_{uracil\ copolymer} \quad \text{(Eq. 10.)}$$

- *Experimental M_n*

The experimental M_n of P($UrMA_n$-*stat*-$THOXMA_m$) copolymer was calculated as:

$$M_n = (\%\ \text{(molar) of UrMA monomer} \times DP_{uracil\ copolymer} \times M_{th\ of\ UrMA\ monomer}) + (\%\ \text{(molar) of THOXMA monomer} \times DP_{uracil\ copolymer} \times M_{th\ of\ THOXMA\ monomer}) + M_{th,CTA} \quad \text{(Eq. 11.)}$$

Where % (molar) of UrMA monomer was calculated by Eq. 9., % (molar) of THOXMA monomer was calculated by Eq. 10., $DP_{uracil\ copolymer}$ was calculated by Eq. 8. $M_{th,CTA}$ = 221.34 g/mol, $M_{th\ of\ THOXMA\ monomer}$ = 231 g/mol, $M_{th\ of\ UrMA\ monomer}$ = 238 g/mol.

References

1. L. V. Arsenie, F. Hausig, C. Carolin, J. C. Brendel, P. Lacroix-Desmazes, V. Ladmiral and S. Catrouillet, *Molecules*, 2022, **27**, 1-15.

Conclusion Chapitre V

Ce chapitre a permis de mettre en évidence le très grand potentiel des copolymères contenant des nucléobases pour la conception des vecteurs artificiels du matériel génétique. Comme les vecteurs du matériel génétique mono brin (surtout ARNm) sont actuellement au cœur de la recherche biomédicale mondiale, suite à l'apparition des vaccins anti-COVID19, il y a une énorme demande de développer des nouveaux systèmes capables de cibler et vectoriser l'ARNm.

Pour ceci, une nouvelle approche de la complexation du matériel génétique a été envisagée en utilisant des liaisons d'hydrogène. Les liaisons d'hydrogène formés entre des nucléobases complémentaires s'avère être une alternative aux interactions électrostatiques traditionnellement utilisées pour complexer le matériel génétique avec des polymères, car elles n'ont pas d'effets cytotoxiques *in-vitro*.

Un prémier aspect innovateur de ces travaux est que les liaisons d'hydrogène formées entre les fonctions uracile du polymère et les groupements adénine du matériel génétique ont été la clé pour développer des complexes obtenus spécifiquement avec le matériel génétique de type mono brin (polyA et ARNm). Une deuxième particularité innovatrice de ces systèmes est qu'elles présentent une stabilité raisonnable contre les RNAses, ainsi que dans le sérum, par comparaison aux systèmes cationiques contenant des nucléobases illustrés dans la littérature. Ceci souligne que les liaisons d'hydrogène complémentaires sont suffisamment fortes pour empêcher la dégradation du matériel génétique. De plus, le caractère neutre des polymères nous a permis d'éviter les problèmes de cytotoxicité, qui sont souvent retrouvés dans le cas des polymères cationiques traditionnels utilisés pour ces applications.

Dans son ensemble, ce travail met en évidence l'avantage d'utiliser des copolymères contenant des nucléobases pour complexer spécifiquement le matériel génétique simple brin par des liaisons d'hydrogène, dans le but de concevoir nouveaux vecteurs artificiels du matériel génétique. La perspective principale de ces travaux concerne l'évaluation des complexes obtenus pour la transfection cellulaire.

Conclusions générales

Conclusions générales

Les polymères contenant des nucléobases présentent un intérêt certain pour le développement d'architectures supramoléculaires originales et inspirées de la structure du matériel génétique.

Les groupements nucléobases trouvés dans ces polymères permettent la formation de liaisons hydrogène complémentaires qui conduisent aux co-assemblages supramoléculaires. Pourtant, les copolymères contenant des nucléobases signalées jusqu'à présent dans la littérature sont globalement hydrophobes et sont solubles uniquement dans des solvants organiques (DMF, DMSO, ou $CHCl_3$). Cette insolubilité dans l'eau limite les applications possibles, en particulier en biologie, des co-assemblages formés à partir des copolymères contenant des bases nucléiques.

Quant aux co-assemblages obtenues à partir de ces copolymères, ceux-ci présentent différentes morphologies (sphères, cylindres ou vésicules), qui sont obtenues soit dans des solvants organiques, soit dans des mélanges solvant organique/ eau. Ces morphologies sont dues à des interactions supramoléculaires (liaisons hydrogène, forces van der Waals, interactions $\pi - \pi$). Même si ces travaux précédents ont été centrées sur le développement des objets supramoléculaires à partir des copolymères à bases nucléiques, aucune investigation n'a pas été menée précédemment dans le but de savoir quelles sont les interactions supramoléculaires majoritaires (liaisons hydrogène ou interactions hydrophobes) qui contrôlent la formation de ces co-assemblages. Or, maitriser le type d'interaction à l'origine des co-assemblages obtenues (*i.e.*, liaisons d'hydrogène complémentaires ou interactions hydrophobes) est importante afin d'étudier la cinétique de co-association des copolymères à bases nucléiques.

L'objectif global de cette thèse consistait à déverrouiller les verrous majeurs suivant des co-assemblages des copolymères de nucléobases :

- Développer une plateforme supramoléculaire composée de polymères synthétiques à liaison hydrogène dont la structure moléculaire et la conception peuvent être facilement ajustées ;
- Evaluer la sensibilité aux stimuli de la plateforme supramoléculaire ;
- Contrôler la dynamique de co-assemblage d'une plateforme supramoléculaire ;
- Etudier le potentiel des polymères de nucléobases comme vecteurs du matériel génétique

Ce travail a donc été organisé sur cinq chapitres (*Fig. 0-1.*), qui correspondent à six publications scientifiques (respectivement deux revues de littérature et quatre articles de recherche) déjà publiées, en processus de Peer-Review dans des journaux scientifiques, ou en cours de finalisation pour soumission.

Lors du premier chapitre de la thèse, nous avons présenté un état de l'art sur les autoassemblages des polymères contenant des nucléobases et les paramètres qui ont influencé la formation de ces architectures supramoléculaires. Cette revue de la littérature a été organisée en deux parties : 1) la mise à jour et les caractéristiques des copolymères synthétiques contenant des nucléobases et 2) l'étude des différents paramètres (structuraux, solvant, pH, température) sur la variété des morphologies issues du co-assemblage de ces polymères, en corrélation avec les interactions supramoléculaires (liaisons hydrogène/ interactions hydrophobes) qui sont responsables de l'apparition de ces architectures. L'information majeure apportée par ce chapitre a été que les polymères contenant des nucléobases peuvent s'auto-assembler dans des architectures supramoléculaires avec des morphologies très variées sous l'action des paramètres tel que la structure des polymères de départ, le pH ou le solvant. Néanmoins, l'insolubilité de ces polymères en milieu aqueux reste une problématique majeure à débloquer.

Tout d'abord, l'un des objectifs de cette thèse a été de synthétiser un nouveau monomère hydrosoluble de type métacrylate. Ces études ont fait partie du 2eme Chapitre. Dans la première partie de ce chapitre, nous avons réalisé une revue de recherche portant sur les nombreuses applications des polymères contenant de la morpholine (dans l'immunologie, dans la transfection cellulaire ou dans la délivrance des principes actifs, etc.). Comme présenté dans cette revue, il s'est avéré que les polymères à base de la morpholine constituent des alternatives aux dérivées de PEG utilisés classiquement en biologie. Pourtant, peu de travaux ont étudié les propriétés physico-chimiques des polymères contenant de la thiomorpholine ou bien de la thiomorpholine oxydée, ainsi que leurs propriétés biologiques. C'est pourquoi, nous avons développé un nouveau monomère contenant de la thiomorpholine oxydée, ainsi que son homopolymère qui sont décrits dans la deuxième partie de ce chapitre 2. Cet homopolymère a montré une LCST variable selon le pH. Ainsi la structure originale de cet homopolymère présente un caractère hydrophile ainsi qu'un caractère neutre à pH physiologique (pK_a ~ 5.6), ce qui explique ses propriétés hémocompatibles supérieures aux dérivés cationiques de type PEI.

Fig. 0-1. Représentation des chapitres inclus dans la thèse

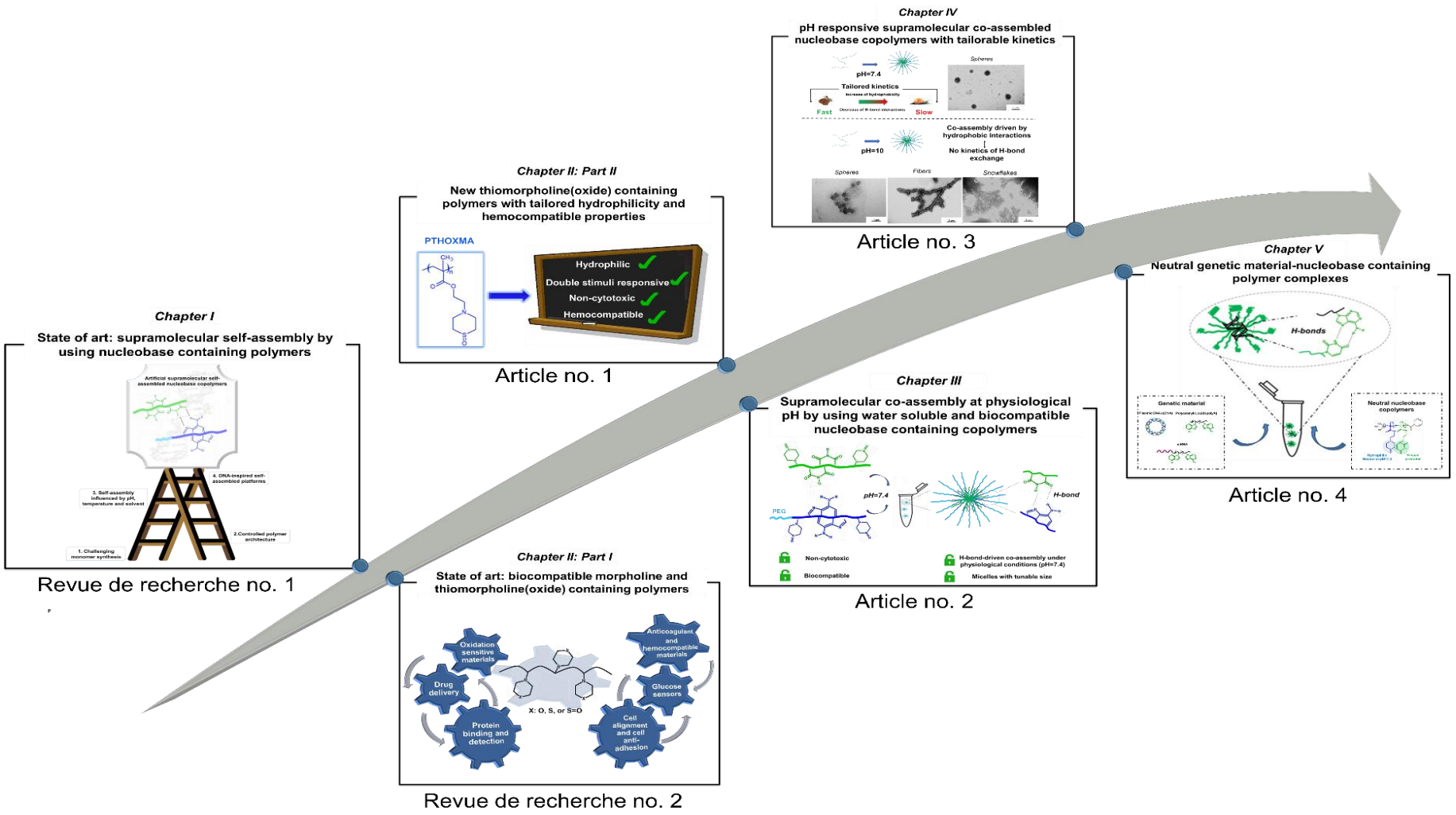

Le monomère contenant de la thiomorpholine oxydée développé dans le chapitre précédent a ensuite été utilisé pour obtenir des copolymères hydrophiles statistiques et/ou à bloc contenant des nucléobases. Dans le troisième chapitre, les structures originales de ces copolymères ont été caractérisés. Grace à la polymérisation RAFT, nous avons pu contrôler l'architecture de ces copolymères (dégrée de polymérisation, divers ratios entre les co-monomères, etc.), ce qui nous a conduit à obtenir diverses structures macromoléculaires. La nouveauté des copolymères obtenues par rapport à ceux présentés dans la littérature est qu'ils sont solubles à pH physiologique (pH 7.4). Par la suite, les co-assemblages issues de ces co-polymères à pH 7.4 ont été étudiés par diffusion de la lumière (SLS/DLS) et par microscopie électronique en transmission (TEM). Globalement, la structure des copolymères de départ a eu une influence majeure sur la modulation de la taille des nano-objets obtenues. Particulièrement, les degrés de polymérisation (DP) élevés du bloc d'adénine ont été propices à la formation de co-assemblages avec des nombres d'agrégation (N_{agg}) élevés, tandis que des DP faibles sont moins favorables aux assemblages. Les copolymères d'uracile ont principalement fait varier la taille des particules obtenues. L'aspect innovant de ces co-assemblages est, qu'ils ont majoritairement été formées grâce aux liaisons hydrogène entre des nucléobases complémentaires, ce qui les rapprochent des systèmes naturels tel que l'ADN. Enfin, l'évaluation des copolymères contenant des nucléobases en biologie a montré que ces copolymères étaient hémocompatibles. Ces travaux ont montré pour la première fois le développement des co-assemblages à pH physiologique à partir des copolymères comportant des nucléobases avec une haute biocompatibilité *in-vitro.*

Le quatrième chapitre de cette thèse porte sur l'élaboration des co-assemblages à partir de copolymères de nucléobases qui présentent une dynamique d'échange par liaisons hydrogène modulable par le pH. Dans cette partie de thèse, nous avons montré que l'augmentation du pH (de 7.4 à 10) a conduit à des co-assemblages supramoléculaires présentant des morphologies anisotropes (sphères denses texturés, dendrites ou flocons de neiges). Les morphologies obtenues sont similaires à celles des co-assemblages de peptides et de nucléopeptides, mais elles ont été observées pour la première fois dans le cas de copolymères de nucléobase. Ces transitions morphologiques sont liées aux changements de la cinétique de formation des liaisons hydrogène entre les polymères de nucléobases complémentaires, qui a été évaluée par titrage calorimétrique isotherme (ITC). Globalement, lorsque les liaisons hydrogène (entre les fonctions uracile-adénine) sont l'interaction principale dirigeant la formation des co-

assemblages, une cinétique rapide et modulable et des morphologies sphériques avec une taille variable à pH physiologique sont observées. D'autre part, les morphologies complexes anisotropes apparaissent lorsque les interactions purement hydrophobes deviennent prédominantes. Cependant, aucune dynamique d'échange *via* liaisons hydrogène n'a été mise en évidence par ITC. Donc, la nouveauté de cette étude est que les copolymères contenant des bases nucléiques sont un choix intéressant pour développer des co-assemblages supramoléculaires sensibles aux stimuli, avec une cinétique d'association adaptable et une gamme variée de morphologies.

Enfin, le 5eme chapitre a été centré sur l'étude de l'interaction des copolymères contenant des bases azotées avec différents types de matériel génétique. En particulier, une complexation sélective des copolymères de nucléobases avec le matériel génétique mono brin (acide polyadénylique : polyA et ARN messager : ARNm) a été noté et expliqué grâce aux liaisons hydrogène complémentaires entre l'uracile et l'adénine (retrouvée dans le matériel génétique). Cependant, aucune complexation spécifique n'a pu être observée avec le matériel génétique double brin (ADN plasmidique). Ceci a été expliqué par la structure plus élaboré de l'ADN plasmidique qui rend la complexation avec le polymère moins accessible au niveau stérique. Dernièrement, les complexes copolymère-polyA ont montré une résistance effective satisfaisante en présence de RNAses et du sérum. De plus, ces complexes sont non-cytotoxiques et hémocompatibles *in-vitro*, à pH physiologique (pH 7.4).

Pour conclure, cette thèse a validé chacun de ses objectifs. Dans ces travaux, nous avons présenté le développement d'une plateforme supramoléculaire soluble dans l'eau, en utilisant des copolymères synthétiques contenant des nucléobases. Ces co-assemblages ont globalement été dirigés par des liaisons hydrogène à pH physiologique. De plus, les systèmes obtenus sont sensibles aux changements du pH. Plus particulièrement, l'augmentation du pH nous a permis d'obtenir des architectures avec des morphologies anisotropes complexes lorsque les interactions hydrophobes deviennent prédominantes. Par contre, la formation d'objets anisotropes lorsque les liaisons hydrogènes étaient les intéractions supramoléculaires prédominantes n'a pas été possible.

Les copolymères contenant des bases nucléiques ainsi que les co-assemblages issues de ces polymères ont présenté un potentiel notable d'utilisation en biologie. Tout d'abord, ces polymères ont présente une forte biocompatibilité à pH physiologique. De plus, cette thèse a

ouvert la possibilité d'utiliser ces systèmes comme potentiels vecteurs de gènes, en proposant une nouvelle manière de complexer le matériel génétique mono brin (de type polyA, ARNm) qui s'est avérée être très prometteuse. Cependant, des études complémentaires sont nécessaires et sont en cours de réalisation, pour mettre en évidence l'efficacité de ces systèmes sur tous les aspects requis pour développer un vecteur de matériel génétique.

Perspectives

Perspectives

Grâce au potentiel très prometteur de l'utilisation des co-assemblages formées avec des polymères contenant des bases azotées en sciences biologiques, les perspectives issues de ces travaux sont très nombreuses. Dans ce contexte, des perspectives à court terme, ainsi qu'à long terme sont proposées :

- **Perspectives à court terme**

Les perspectives à court terme sont organisées sur deux axes :

1ere axe : étude du caractère dynamique des co-assemblages des copolymères contenant des nucléobases

Dans le quatrième chapitre de cette thèse on a montré par titrage calorimétrique isothèrme (ITC) que les co-assemblages issues des copolymères contenant des bases nucléiques ont présenté une cinétique d'auto-association dépendante du pH. De plus, nos travaux ont montré une corrélation entre la cinétique d'assemblage, les intéractions supramoléculaire majoritairement impliqués dans le co-assemblages (liaisons hydrogène/ intéractions hydrophobes) et les morphologies des co-assemblages obtenus.

Ces résultats, surtout ceux à pH physiologique, peuvent nous permettre d'étudier plus en détail la dynamique (réversibilité) d'assemblage de ces systèmes. Maitriser la dynamique du co-assemblage supramoléculaire est intéressant afin de trouver des nouvelles applications de ces systèmes en biologie, par exemple dans de nouveaux matériaux de l'auto-régéneration tissulaire[1] (où on a besoin des systèmes dynamiques), la délivrance des substances actives[2] (ou on a besoin des systèmes dynamiques/ figées en fonction du type du médicament), etc.

Cependant, il existe très peu de techniques permettant de mettre en évidence le caractère dynamique supramoléculaire. Dans le cas des co-assemblages de polymères à bases azotées, le caractère dynamique n'a jamais été démontré auparavant dans la littérature. Quelques travaux réalisés auparavant dans le groupe du Professeur Perrier ont montré par FRET (Transfert d'Energie par Résonance de Fluorescence) la dynamique des systèmes supramoléculaires des peptides cycliques.[3] En partant de ces travaux, on envisage d'appliquer la technique FRET dans

le but d'étudier le caractère dynamique/figé des assemblages crées à pH physiologique et à pH basique. Des expériences sont menées actuellement afin de modifier les polymères contenant des bases nucléiques avec des fluorophores, pour réaliser ensuite des expériences de FRET sur nos systèmes.

2eme axe : utilisation des copolymères contenant des nucléobases dans la transfection cellulaire

Dans le dernier chapitre de cette thèse nous avons montré que les copolymères contenant des uraciles ont spécifiquement complexé le matériel génétique monobrin (l'acide polyadénylique polyA et l'ARN messager ARNm). La nouveauté de cette étude a été que les complexes obtenus ont été formées par des liaisons hydrogène entre l'adénine et l'uracile, et non par des interactions électrostatiques comme dans le cas des polyplexes classiquement utilisés en transfection cellulaire. Ces complexes ont présenté une résistance contre l'attaque des RNAses, ce qui représente un énorme avantage dans la conception de nouveaux vecteurs du matériel génétique, ainsi qu'une stabilité raisonnable en milieu physiologique qui est une conséquence du caractère neutre.

La spécificité de ces polymères pour complexer le matériel génétique monobrin peut être exploitée pour trouver des nouveaux alternatives thérapeutiques (à long terme) basées sur l'ARNm.[4] Actuellement, des études sont menées au sein du laboratoire IOMC (Iéna, Allemagne) afin de tester les polymères contenant des nucléobases dans la transfection cellulaire. Ceci fera l'objet d'un cinquième article de recherche qui sera préparé et publiée dans les prochains mois en collaboration avec le laboratoire allemand.

- **Perspectives à long terme**

Les perspectives à long terme sont centrées sur plusieurs thématiques :

La synthèse de copolymères avec une architecture contrôlée contenant de la cytosine et de la guanine pour le développement des hydrogels supramoléculaires biomimétiques avec des propriétés d'auto-réparation

Les systèmes supramoléculaires développés pendant cette thèse ont été formés à partir des copolymères contenant de l'adénine et de l'uracile. La cytosine et la guanine sont l'autre couple de nucléobases complémentaires de l'ADN. En comparaison du couple adénine-uracile, qui

forment deux liaisons hydrogène entre elles, la cytosine et la guanine forment trois liaisons hydrogène.

Cependant, il existe très peu d'information sur les matériaux supramoléculaires obtenues à partir de copolymères contenant de la cytosine et de la guanine, principalement due à une forte difficulté de la synthèse organique des monomères de départ.[5] Malgré les difficultés synthétiques, ces polymères pourront offrir de nombreuses et riches opportunités de travaux innovants sur ce sujet presque vierge.

Notre hypothèse est que les copolymères contenant de la cytosine et de la guanine pourraient constituer des matériaux de départ intéressants pour développer des hydrogels biomimétiques avec des propriétés d'auto-réparation. Leur avantage majeur est que, par co-assemblage, ces polymères peuvent générer des réseaux supramoléculaires avec une densité élevée des liaisons hydrogène, favorable à la formation d'un gel.[5,6,7] Cependant, les liaisons hydrogènes sont sensibles aux stimulus tels que le pH ou la température, ce qui pourrait rendre ces systèmes dynamiques et donc auto-réparables sous l'action de certains stimuli. De plus, la capacité des nucléobases à interagir par liaisons hydrogène avec des peptides spécifiques pourrait être développée, en incluant un peptide au sein des gels, dans le but d'offrir des propriétés spécifiques de réparation tissulaire à ces matériaux.

La conception d'une plateforme supramoléculaire biomimétique en utilisant les polymères contenant de l'adénine/uracile et des synthons avec des groupements phosphate, pour l'application dans la transfection cellulaire

Des études récentes ont montré un intérêt particulier concernant l'utilisation des polymères anioniques dans la transfection cellulaire, dans le but de limiter les réactions adverses avec les protéines plasmatiques.[8]

Les polymères à bases azotées développées dans cette thèse ont montré un potentiel attractif vis-à-vis du ciblage spécifique du matériel génétique. Dans une approche biomimétique, il pourrait être intéressant de synthétiser un polymère qui se rapproche de la structure du matériel génétique. Pour cela, nous proposons de développer des polymères (statistiques et/ou à bloc), formés à partir des monomères contenant la thiomorpholine oxide et l'uracile (synthétisés lors de la thèse) et des monomères incluant des unités phosphates (qui sont les fragments anioniques du matériel génétique).

Ces polymères présentent l'avantage de former des complexes avec le matériel génétique grâce aux liaisons hydrogènes entre des nucléobases complémentaires, tandis que les unités phosphates se rapprochent de la structure du polymère à celle du matériel génétique. Ces polymères peuvent présenter des propriétés intéressantes de complexation avec le matériel génétique, dans le but de concevoir de nouveaux vecteurs artificiels.

Références bibliographiques :

1. Z. Alvarez, A. N. Kolberg- Edelbrock, I. R. Sasselli, J. A. Ortega, R. Qiu, Z. Syrgiannis, P. A. Mirau, F. Chen, S. M. Chin, S. Weigand, E. Kiskinis, S. I. Stupp, *Science*, 2021, **374**, 848-856.
2. B. T. Ledford, A. W. Akerman, K. Sun, D. C. Gillis, J. M. Weiss, J. Vang, S. Willcox, T. D. Clemons, H. Sai, R. Qiu, M. R. Karver, J. D. Griffith, N. D. Tsihlis, S. I. Stupp, J. S. Ikonomidis, M. R. Kibbe, *ACS Nano*, 2022, **16(5)**, 7309-7322.
3. J. Y. Rho, H. Cox, E. D. Mansfield, S. H. Ellacott, R. Peltier, J. C. Brendel, M. Hartlieb, T. A. Waigh, S. Perrier, *Nat. Commun*., 2019, **10**, 1-9.
4. A. I. S. van der Berg, C-O. Yun, R. M. Schiffelers, W. E. Hennick, *J. Control. Rel*., 2021, **331**, 121-141.
5. X. Zhang, D. Wang, H. Liu, L. Yue, Y. Bai, J. He, *Eur. Pol. Journal*, 2020, **133**, 109741-109750.
6. L. Peng, M. You, Q. Yuan, C. Wu, D. Han, Y. Chen, Z. Zhong, J. Xue, W. Tan, *J. Am. Chem. Soc*., 2012, **134(29)**, 12302-12307.
7. H. Yang, W. Xi, *Polymers*, 2017, **9**, 666-691.
8. F. Richter, K. Leer, L. Martin, P. Mapfumo, J. I. Solomun, M. T. Kuchenbrod, S. Hoeppener, J. C. Brendel, A. Traeger, *J. Nanobiotechnol*., 2021, **11**, 292-307.

Production scientifique

Production scientifique

Participation aux conférences

1. **L.V. Arsenie**, V. Ladmiral, S. Catrouillet, *New methacrylate-derived monomers for the design of hydrophilic polymer blocks in artificial-DNA inspired materials*, 16eme Edition des Journées Scientifiques et Industriels organisées par le Groupe Français de Polymères (GFP) section Méditerranée, 9-10 Mars **2020**, Alès, **France** (**poster en Anglais**)
2. **L.V. Arsenie**, V. Ladmiral, S. Catrouillet, *New nucleobase derived polymers for selfassembled DNA-inspired architectures*, Conférences Balard, 15-18 Juin **2021**, Montpellier, **France** (**poster en Anglais**)
3. **L.V. Arsenie**, V. Ladmiral, S. Catrouillet, *Self-assembly of nucleobase copolymers in distinct architectures inspired by nature*, Journées des Etudes des Polymères (JEPO), 03-08 Octobre **2021**, Ile de Porquerolles, **France** (**communication orale en Français**)
4. **L. V. Arsenie**, V. Ladmiral, S. Catrouillet, *Development of new self-assembled architectures in water by using complementary nucleobase copolymers*, Journées Méditerranéenes des Jeunes Chercheurs (JMJC), 28-29 Octobre **2021**, Montpellier, **France** (**communication orale en Anglais**)
5. **L. V. Arsenie**, V. Ladmiral, M. Semsarilar, A. Geneste, B. Prelot, P. Lacroix-Desmazes, S. Catrouillet, *Bioinspired self-assembled nucleobase polymers: from self-assembly formulation to description of dynamic properties*, JCF Früehjahrssymposium, 23-26 Mars **2022**, Hannover, **Allemagne** (**poster en Anglais**)
6. **L. V. Arsenie**, V. Ladmiral, M. Semsarilar, A. Geneste, B. Prelot, S. Catrouillet, *Dynamic self-assembled nucleobase copolymers in water: new stimuli-responsive platforms for future biological applications*, Bordeaux Polymer Conference, 13-16 Juin **2022**, Bordeaux, **France** (**communication orale en Anglais**)
7. **L. V. Arsenie**, V. Ladmiral, M. Semsarilar, A. Geneste, B. Prelot, S. Catrouillet, Supramolecular water soluble self-assembled nucleobase copolymers: new synthetic platforms towards biomimetic materials, European Polymer Federation Congress, 26 Juin-1 Juillet **2022**, Prague, **République Tchèque** (**communication orale en Anglais**)

Publications scientifiques

1. L. V. Arsenie, S. Catrouillet, P. Lacroix-Desmazes and V. Ladmiral, *Nucleobase-polymer architectures controlled by supramolecular interactions: the key to achieve biomimetic platforms with various morphologies* – **revue de literature publiée dans le journal Polymer Chemistry (IF: 5.582)**

2. L. V. Arsenie, S. Catrouillet, P. Lacroix-Desmazes and V. Ladmiral, *Morpholine and thiomorpholine derived polymers: multifunctional platforms for biological applications* **– revue de literature en cours de soumission dans Polymer Chemistry (IF: 5.582)**

3. L. V. Arsenie, F. Hausig, C. Kellner, J. Brendel, P. Lacroix-Desmazes, V. Ladmiral, S. Catrouillet, *Stimuli-responsive thiomorpholine oxide derived polymers with tailored hydrophilicity and hemocompatible properties*– **article de recherche publié dans le journal Molecules (IF: 4.927)**

4. L. V. Arsenie, M. Semsarilar, P. Lacroix-Desmazes, J. C. Brendel, V. Ladmiral and S. Catrouillet, *Supramolecular hydrosoluble self-assembled nucleobase copolymers: bioinspired synthetic platforms towards new biomimetic materials* **– article de recherche publié dans le journal Polymer Chemistry (IF: 5.582)**

5. L. V. Arsenie, M. Semsarilar, P. Gonzales, A. Geneste, B. Prelot, P. Lacroix-Desmazes, V. Ladmiral and S. Catrouillet, *Switchable pH-responsive dynamics of co-assembled nucleobase polymers***– article de recherche en cours de finalisation/validation par tous les auteurs, journal prévu : Macromolecules (IF : 6.057).**

6. L. V. Arsenie, S. Catrouillet, V. Ladmiral, A. Traeger and J. C. Brendel, *Genetic material-neutral nucleobase copolymers assembly via H-bonds : traditional concept of supramolecular chemistry applied to gene complexation* **– article de recherche en cours de finalisation/validation par tous les auteurs, journal prévu : Angewandte ou ACS Nano.**

Bourse de financement des projets scientifiques et des congrès

1. **Bourse DAAD** (Office Allemand d'échanges universitaires) pour le financement des projets de recherche de courte durée en collaboration avec un institut de recherche allemand, obtenue pour la période 01/03/2022-31/05/2022. Intitulé du projet: ***Complexation of mRNA by non-ionic nucleobase polymers through complementary hydrogen bonds.*** Ce stage de recherche a été effectué au sein du laboratoire d'accueil IOMC, de l'Université Friedrich Schiller, Iéna, Allemagne.
2. **Bourse GFP (Groupe Français des Polymères-Section Méditerranée)** pour financer la participation à un congrès international avec une communication orale. Cette bourse m'a permis de présenter mes travaux de recherche à la conférence internationale Bordeaux Polymer Conference (BPC) entre 13/06/2022-16/06/2022.
3. **Bourse EDSCB (Ecole Doctorale Sciences Chimiques Balard)** pour financer la participation à un congrès international avec une communication orale. Cette bourse m'a permis de présenter mes travaux de recherche au congrès international European Polymer Federation Congress (EPF) qui a eu lieu à Prague (République Tchèque) entre 26/06/2022-01/07/2022.

Activités d'enseignement

Travaux pratiques en chimie analytique (18h), effectuées à l'Université de Montpellier entre 01/03/2021-01/04/2021.

Prix obtenus lors des congrès

Prix pour le Meilleur Poster de la section Matériaux pour la santé, obtenu dans le cadre des Conférences Balard, 2021, France

Résumés de la thèse

Plateforme d'assemblages supramoléculaires de copolymères synthétiques promoteurs de liaisons hydrogènes

Dans le vivant, les liaisons hydrogène sont à l'origine des structures secondaires et tertiaires des enzymes (protéines) mais aussi de la structure à double hélice de l'ADN. Les composants de base à l'origine de la formation des liaisons hydrogène dans l'ADN sont les bases azotées (connues aussi sous le nom de nucléobases) : Cytosine (C), Guanine (G), Adénine (A), Thymine (T) (et Uracile pour l'ARN)). Le co-assemblage des bases complémentaires est favorisé par rapport aux autres combinaisons possibles (A-T > A-A, AG ou AC dans le cas de l'adénine par exemple). Dans une approche biomimétique, certains groupes ont étudié la synthèse de polymères porteurs de nucléobases. Cependant, les polymères contenant des nucléobases présentés jusqu'à présent dans la littérature sont insolubles dans l'eau, ce qui limite leur potentielle utilisation en sciences biologiques. Pourtant, les systèmes précédemment obtenus à partir des copolymères contenant des nucléobases forment des auto-assemblages supramoléculaires dont la morphologie est adaptable et influencée par l'architecture des copolymères de départ (le degré de polymérisation, le nombre de nucléobases dans le polymère), ainsi que par la balance hydrophile/hydrophobe du système. Ainsi, quelques travaux ont montré la dépendance des morphologies formées en fonction du solvant due à leur capacité à former ou à limiter la formation des liaisons hydrogène. Globalement, les exemples illustrés dans la littérature ont montré que ces morphologies résultent des équilibres entre les interactions supramoléculaires (liaisons hydrogènes, forces de Van der Waals, interactions $\pi - \pi$) et sont influencés par les paramètres structuraux des polymères. Ces premiers travaux apportent une preuve de concept sur l'autoassemblage des copolymères contenant des bases nucléiques, mais ils n'ont pas étudié précisément les paramètres qui influent sur ces co-assemblages, ni leurs limites. La connaissance de l'origine des autoassemblages obtenues (*i.e*., liaisons d'hydrogène complémentaires ou interactions hydrophobe) est d'une importance majeure pour maitriser la dynamique d'auto-assemblage : obtenir des auto-assemblages réversibles ou irréversibles, et pour contrôler la cinétique d'auto-association. Néanmoins, l'investigation de la cinétique ou de la dynamique d'auto-association n'a jamais été explorée auparavant dans le cas des autoassemblages des copolymères contenant des nucléobases. En pratique, la maitrise de la cinétique d'association/dissociation des liaisons hydrogène peut-être un outil précieux dans des applications comme des vecteurs de substances actives ou de matériel génétique. Le premier objectif de cette thèse a été de développer des polymères hydrosolubles contenant des nucléobases et d'étudier les co-assemblages de ces polymères dans des conditions physiologiques, ainsi que la biocompatibilité *in-vitro* de ces polymères. Le deuxième objectif de ce projet a été d'étudier les propriétés des co-assemblages supramoléculaires des polymères comportant des nucléobases sensibles aux changements de pH et avec une cinétique d'assemblage contrôlable. Enfin, le but de ce projet a été de trouver une potentielle applicabilité aux polymères de nucleobases en biologie, en étudiant la complexation *via* des liaisons hydrogène entre les polymères comportant des nucléobases et différents types de matériels génétiques, pour la conception de vecteurs d'ARNm.

Mots clés : polymères nucléobases, auto-assemblage, chimie supramoléculaire, liaisons hydrogène, matériel génétique

Platform of supramolecular assemblies of hydrogen bonding synthetic copolymers

The hydrogen bonds (H-bonds) are at the origin of the secondary and tertiary structures of enzymes (proteins), but also of the double helix structure of the DNA. The nucleobases are the main active frameworks which are at the origin of H-bond formation in genetic material: Cytosine (C), Guanine (G), Adenine (A), Thymine (T) (and Uracil for RNA)). The co-assembly of complementary nucleobases is favored over other possible combinations (A-T > A-A, AG or AC in the case of adenine for example). In a biomimetic approach, some groups have investigated the synthesis of polymers containing nucleobases. However, the nucleobase-containing polymers presented so far in the literature are insoluble in water, which limits their potential use in biological sciences. However, the systems previously obtained in the literature from nucleobase-containing copolymers form supramolecular self-assemblies. Their morphology is adaptable and is mainly influenced by the architecture of the starting copolymers (the degree of polymerization, the number of nucleobases in the polymer), and thus, by the hydrophilic/hydrophobic balance of the system. Overall, the examples of the literature have shown that these morphologies result from equilibria between supramolecular interactions (hydrogen bonds, van der Waals forces, π-π interactions) and are influenced by the structural parameters of the polymers. These studies provided a proof of concept on the self-assembly of nucleobase-containing copolymers, but did not specifically investigate the parameters that influence these co-assemblies, nor their limitations. The knowledge of the type of supramolecular interactions that are at the origin of the resulting self-assemblies (*i.e.*, complementary hydrogen bonds or hydrophobic interactions) is of significant importance in order to modulate the dynamics of self-assembly (to obtain reversible or irreversible self-assemblies), as well as to control the kinetics of H-bond association. Nevertheless, the investigation of the kinetics or dynamics of H-bond association has never been explored before in the case of self-assembled nucleobase-containing copolymers. As a perspective, the control of the kinetics of association/dissociation of hydrogen bonds can be a valuable tool in applications such as delivery systems of active substances and/or genetic material. The first axis of this thesis included the development of water-soluble nucleobase containing copolymers, the investigation of the properties of resulting co-assemblies at physiological conditions, as well as the *in-vitro* evaluation of biocompatibility of these polymers. The second objective of this project was to investigate the properties of supramolecular co-assemblies of nucleobase-containing polymers under pH changes, in order to design supramolecular systems with tuneable kinetics of H-bond association. Finally, the aim of this project was to find a potential applicability of nucleobase containing copolymers in biology. To this, we investigated the complexation *via* hydrogen bonds between nucleobase-containing polymers and different types of genetic material in order to design a future platform for mRNA artificial vectors.

Keywords: nucleobase polymers, self-assembly, supramolecular chemistry, H-bonds, genetic material